

International Atomic Energy Agency

INDC(NDS)-114/GT

---

**INDC**

---

---

**INTERNATIONAL NUCLEAR DATA COMMITTEE**

---

PROCEEDINGS OF THE IAEA CONSULTANTS' MEETING

ON

NEUTRON SOURCE PROPERTIES

Debrecen, Hungary, 17 - 21 March 1980

Edited

by

K. Okamoto

June 1980

---

**IAEA NUCLEAR DATA SECTION, WAGRAMERSTRASSE 5, A-1400 VIENNA**



PROCEEDINGS OF THE IAEA CONSULTANTS' MEETING

ON

NEUTRON SOURCE PROPERTIES

Debrecen, Hungary, 17 - 21 March 1980

Edited  
by  
K. Okamoto  
June 1980



## **DISCLAIMER**

**Portions of this document may be  
illegible in electronic image products.  
Images are produced from the best  
available original document**

## FOREWORD

In view of the considerable improvement in the accuracy and consistency of the properties of neutron sources relevant to neutron metrology achieved in recent years, the International Nuclear Data Committee at its recent meetings\*) recommended that a meeting on Neutron Source Properties be held in 1980. In response to this recommendation, the IAEA Nuclear Data Section, with the support of the Hungarian authorities, in co-operation with the Institute of Experimental Physics of the Kossuth Lajos University acting as the host, convened a Consultants' Meeting on "Neutron Source Properties" during the week 17-21 March 1980 in Debrecen, Hungary.

The meeting was attended by 29 scientists and more than 10 observers from 13 Member States.

The main objectives of the meeting, in addition to high-lighting current important developments in this field were:

- to review the requirements and status of all properties and data on neutron sources such as mono-energetic neutron-producing reactions, white source neutron spectra, spontaneous fission neutron spectra, gamma-neutron and alpha-neutron sources, filtered neutron beams and thermal and epi-thermal pile neutron beams. The neutron energies to be covered extend from thermal to 40 MeV and above. Plasma neutron sources are not to be included,
- to identify the uncertainties in the properties of neutron sources and the corrections needed to improve the accuracy and consistency of neutron measurements, and
- to formulate specific technical recommendations for future work and its coordination.

The proceedings contain the review papers, the abstracts of the contributed papers presented at the meeting as well as the introduction and report on the summary conclusions and recommendations of the meeting related to the following subjects:

1. Radioactive Be( $\alpha$ ,n), photoneutron and spontaneous fission sources;
2. White neutron sources and filtered beams; and
3. Mono-energetic neutron sources from charged particle reactions.

The assistance of the Hungarian Government, the Hungarian Atomic Energy Commission, the Hungarian Academy of Sciences, the Kossuth Lajos University, and, in particular, its Institute of Experimental Physics, in the organization and conduct of the Meeting is most gratefully acknowledged.

K. Okamoto  
Editor  
Nuclear Data Section

\*) 10th INDC Meeting in October 1978 (INDC-31/L appendix XI.C. p.5)



CONTENTS

	Page
FOREWORD . . . . .	iii
AGENDA . . . . .	ix
INTRODUCTION (A. B. Smith) . . . . .	1
SUMMARY CONCLUSIONS and RECOMMENDATIONS	
Working Group 1 (Radioactive ( $\alpha$ ,n) Photoneutron and Spontaneous Fission Sources) . . . . .	5
Working Group 2 (White Neutron Sources and Filtered Beams) . . . . .	7
Working Group 3 (Monoenergetic Neutron Sources from Charged Particle Reactions) . . . . .	13
REVIEW PAPERS	
R-1 Neutron Sources in Perspective . . . . . A. B. Amith (Session I)	19
R-2 Radioactive Be( $\alpha$ ,n) and Be( $\gamma$ ,n) Neutron Sources . . . . . K. W. Geiger (Session I)	43
R-3 Neutron Energy Spectra of Spontaneous Fission Sources . . . . . M. V. Blinov (Session I)	79
R-4 Thermal and Epi-Thermal Reactor Neutron Beams and Fields . . . . . W. G. Alberts (Session II)	107
R-5 Accelerator - based White Neutron Sources S. Clerjacks (Session II) - not available -	
R-6 White Source Use in a Neutron Standards Laboratory . . . . . C. D. Bowman et al. (Session II)	119
R-7 Reactor - and Accelerator - based Filtered Beams . . . . . A. J. Mill, J. R. Harvey (Session II)	135
R-8 Production of Fast Monoenergetic Neutrons by Charged Particle Reactions Among the Hydrogen Isotopes. Source Properties, Experimental Techniques and Limitations of the Data . . . . . M. Drosz (Session III)	201
R-9 Properties of Monoenergetic Neutron Sources from Proton Reactions with Nuclei Other than Tritons . . . . . M. Drosz (Session III)	241



	Page
R-10 Production of 14 MeV Neutrons by Low Voltage Accelerators . . . . .	265
J. Csikai (Session IV)	

# ABSTRACTS OF CONTRIBUTED PAPERS

## Session I

C-1 Emission Rate and Neutron Spectrum Measurements for Be( $\alpha$ ,n) Sources . . . . .	295
H. Kluge, H. W. Zill	
C-2 Radioisotope Neutron Sources . . . . .	296
Glenn F. Knoll	
C-3 Radioactive Neutron Source Measurements at the National Physical Laboratory, England . . . . .	297
A. G. Bardell	
C-4 Properties and Applications of Radioactive Photoneutron Sources . . . . .	298
Friedrich Bensch	
C-5 Absolute Calibration of $^{252}\text{Cf}$ Sources and Effective Half-Life . . . . .	299
W. G. Alberts, W. Mannhart, M. Matzke	
C-6 Measurement of the Neutron Activity of a $^{252}\text{Cf}$ Source Relative to $V_p$ for the Spontaneous Fission . . . . .	300
J. Fréhaud, M. Beau	
C-7 $^{235}\text{U}$ Cavity Fission Neutron Field Calibration via the $^{252}\text{Cf}$ Spontaneous Fission Neutron Field . . . . .	301
V. Spiegel, C. M. Eisenhauer, D. M. Gilliam, J. A. Grundl, E. D. McGarry, I. G. Schröder, W. E. Slater and R. S. Schwartz	
C-8 The Fast Neutron Emission Spectrum of $^{252}\text{Cf}$ . . . . .	302
Friedrich Bensch and Hans Jasicek	
C-9 Note on the Prompt-Fission-Neutron Spectra of $^{233}\text{U}$ , $^{235}\text{U}$ , $^{239}\text{Pu}$ and $^{240}\text{Pu}$ Relative to that of $^{252}\text{Cf}$ . . . . .	303
A. Smith, P. Guenther, G. Winkler and R. McKnight	
C-10 A Radiative Neutron Source with an Effective Energy of 500 eV . . . . .	304
J. R. Harvey and A. J. Mill	
C-11 The Measurement of the Average Number of Prompt Neutrons and the Distribution of Prompt Neutron Numbers for $^{252}\text{Cf}$ Spontaneous Fission . . . . .	305
Zhang Huan Qiao, Liu Zu-Hua	

	Page
C-12 Measurement of Prompt Neutron Energy Spectrum for Spontaneous Fission of $^{252}\text{Cf}$ . . . . . Mon Jiang-shen, Bai Xi-xiang, Zhang Bai-shen, Hwang Sheng-nian	306
Session II	
C-13 The Current Status of Accelerator Produced Neutron Fluence Standards at the National Physical Laboratory, England . . . . . A. G. Bardell	307
C-14 Neutron Yields from Proton, Deuteron and Alpha Bombardment of Beryllium . . . . . M. A. Lone	308
C-15 Flux Density Measurements in the FMRB Filtered Neutron Beams . . . . . W. G. Alberts, K. Knauf, H. Lesiecki	309
C-16 Examples of Theoretical and Experimental Determinations of Neutron Yield from $(\alpha, n)$ Reactions in the Light Elements . . . . . A. Capgras	310
Session III	
C-17 Production of Monoenergetic Neutrons with Energies Between a Few Hundred KeV and 40 MeV . . . . . G. Haouat and M. Cance	311
C-18 Neutron Production in the Energy Range 7 to 12 MeV Using a Gas-Target . . . . . S. Mittag, W. Pilz, D. Schmidt, D. Seeliger and T. Streil	312
C-19 Limitations in the Use of Deuterium Gas Targets . . . H. Klein, H. J. Brede	313
C-20 Multipurpose Intense 14 MeV Neutron Source at Bratislava: Design Concept . . . . . J. Pivarc, S. Hlavác, J. Král, P. Oblozinský, I. Ribanský and I. Turzo	314
C-21 Monoenergetic Neutron Sources in the Energy from 10 keV to 20 MeV for Dosimetry Experiments . . . . M. Cosak, S. Guldbakke, H. Klein	315
C-22 Neutron Sources for the Medical Use . . . . . K. Tsukada	316
C-23 Neutron Source Investigations in Support of the Cross Section Program at the Argonne Fast-Neutron Generator. . James W. Meadows and Donald L. Smith	317

	Page
C-24 Limits of Application of the Method of Recoil Protons in Neutron Spectrometry Using a NE 213 Organic Scintillator . . . . .	318
A. Capgras	
C-25 Performance of Gas Target Using D(d,n) Reactions as a Fast Neutron Source . . . . .	319
Lian Tun-chi, Ye Jine-ping, Sa Dren	

## APPENDICES

Appendix 1: Other papers (Abstracts) . . . . .	323
0-1 : Measurements and Calculations of Neutron Spectra from 35 MeV Deuterons on Thick Lithium for the FMIT Facility D. L. Johnson and F. M. Mann	
0-2 : Measurements of Neutron Spectra from 35 MeV Deuterons on Thick Lithium for the FMIT Facility (Updated version of 0-1) D. L. Johnson and F. M. Mann	
0-3 : Radioactive Neutron Source Spectra from <sup>9</sup> Be( $\alpha$ ,n) Cross Section Data K. W. Geiger and L. Van der Zwan	
0-4 : Résumé on Neutron Yields from $\alpha$ -Particle Bombardment of Light Elements K. W. Geiger	
Appendix 2: List of Participants . . . . .	325

Consultants' Meeting on Neutron Source Properties

Debrecen, Hungary, 17-21 March 1980

ADOPTED MEETING AGENDA

Monday, 17 March

Morning (10:00):

Opening  
Election of Chairman  
Adoption of Agenda  
Announcements  
Introductory Address  
(J.J. Schmidt, IAEA and A.B. Smith, ANL, Argonne)

Session I:

Radioactive Neutron Sources

[Be( $\alpha$ ,n) and ( $\gamma$ ,n) and Spontaneous fission sources  
with emphasis on Cf-252]

[Review Paper]

1. Be( $\alpha$ ,n) and Be( $\gamma$ ,n) Neutron Sources  
(K.W. Geiger, NRC, Ottawa)

[Contributed Paper]

2. Emissionrate measurements and neutron  
spectrum considerations for Be( $\alpha$ ,n) sources  
(W.G. Alberts, PTB, Braunschweig)

" "

3. Radioisotope neutron sources  
(G.F. Knoll, Univ. Michigan, Michigan)

" "

4. Radioactive neutron source measurements  
at the National Physical Laboratory  
(A.G. Bardell, NPL, Teddington)

Afternoon:

[Contributed Paper]

5. Properties and applications of radioactive  
photoneutron sources  
(F. Bensch, Atominst., Vienna)

" "

6. • Radioactive neutron source with an effective  
energy of 500 eV  
(A.J. Mill, CEGB, Berkeley, Gloucestershire)

[Review Paper]

7. Neutron energy spectra of spontaneous  
fission sources  
(M.V. Blinov, R.I.V.G. Khlopina, Leningrad)

[Contributed Paper]

8. Absolute calibration of Cf-252 sources  
and effective half-life  
(W.G. Alberts, PTB, Braunschweig)

" "

9. Measurement of the neutron activity of a Cf-252  
source relative to  $\bar{\nu}_p$  for the spontaneous fission  
(J. Fréhaut, CEN, Bruyères-le-Châtel)

---

• Contributed paper but not presented

- [Contributed Paper]
10.  $^{235}\text{U}$  cavity fission neutron field calibration via the  $^{252}\text{Cf}$  spontaneous fission neutron field (V. Spiegel, NBS, Washington)
  - " " 11. The fast neutron emission spectrum of  $^{252}\text{Cf}$  (F. Bensch, Atominst., Vienna)
  - " " 12. Note on the prompt-fission-neutron spectra of U-233, U-235, Pu-239 and Pu-240 relative to that of Cf-252 (A.B. Smith, ANL, Argonne)
  - " " 13. • The measurement of the average number of prompt neutrons and the distribution of prompt neutron numbers for Cf-252 spontaneous fission (Zhang Huan-Qiao and Liu Zu-Hua, Inst. Atomic Energy, Peking)
  - " " 14. • Measurement of prompt neutron energy spectrum for spontaneous fission of Cf-252 (Mon Jiang-shen, Bai Xi-Xiang, Zhang Bai-Shen, Hwang Sheng-nian, Inst. Atomic Energy, Peking)

Tuesday, 18 March

Morning (9:00):

Session II:

White Neutron Sources

[Thermal and epithermal reactor beams and fields  
Accelerator-based white source  
Filtered beam]

[Review paper]

1. Introductory remarks on thermal and epithermal reactor beams and fields (W.G. Alberts, PTB, Braunschweig)
- " " 2. Accelerator-based white neutron sources (S. Cierjacks, KFK, Karlsruhe)
- " " 3. White source use in a neutron standard laboratory (C.D. Bowman, NBS, Washington)

[Contributed Paper]

4. <sup>a</sup> The current status of accelerator produced neutron fluence standards at the National Physical Laboratory (A.G. Bardell, NPL, Teddington)

Afternoon:

[Contributed paper]

5. Neutron yields from proton, deuteron and alpha bombardment of beryllium (M.A. Lone, AECL, Chalk River)

---

• Contributed Paper but not presented

<sup>a</sup> Note: The paper was presented at the Session because of the inclusion of thermal neutron facility. However, most parts are of Monoenergetic Neutron Sources (Session III).

- [Contributed Paper] 6. • Some examples of theoretical and experimental determinations of yields ( $\alpha, n$ ) reaction on the light elements  
(A. Capgras, LMRI.CEA, Saclay)
- [Review Paper] 7. Reactor and accelerator-based filtered beams  
(A.J. Mill, CEEB, Berkeley, Gloucestershire)
- [Contributed Paper] 8. Flux density measurement at the FMRB filtered neutron beams  
(W.G. Alberts, PTB, Braunschweig)
- Evening: Visit to the ATOMKI (Institute of Nuclear Research of the Hungarian Academy of Sciences)

Wednesday, 19 March

Morning (9:00):

Session III:

Monoenergetic Neutron Sources from Charged Particle Reactions

- [Review Paper] 1. Production of fast monoenergetic neutrons by charged particle reactions among the hydrogen isotopes. Source properties, experimental technique and limitation of data  
(M. Drosz, LASL/Univ. Vienna)
- " " 2. Properties of monoenergetic neutron sources from proton reactions with nuclei other than triton  
(M. Drosz, LASL/Univ. Vienna)
- " " 3. Production of 14 MeV neutrons by low voltage accelerators  
(J. Csikai, Kossuth Univ., Debrecen)
- Afternoon:
- [Contributed Paper] 4. Production of monoenergetic neutrons with energies between a few hundred keV and 40 MeV  
(G. Haouat, CEN, Bruyères-le-Châtel)
- " " 5. Neutron production in the energy range 7 to 12 MeV using a gas target  
(D. Seeliger, presented by H. Helfer, TU, Dresden)
- " " 6. Limitations in the use of deuterium gas targets  
(H. Klein, PTB, Braunschweig)
- " " 7. Multipurpose intense 14 MeV neutron source at Bratislava; Design concept  
(J. Pivarč, Inst. Phys. SAS, Bratislava)

---

• Contributed Paper but not presented

- [Contributed Paper]
8. Monoenergetic neutron sources in the energy range from 10 keV to 20 MeV for dosimetry experiments  
(H. Klein, PTB, Braunschweig)
- " " 9. Neutron sources for the medical use  
(K. Tsukada, Nihon Univ., Tokyo)
- " " 10. Neutron source investigations in support of the cross-section programme at the Argonne fast-neutron generator  
(J.W. Meadows and D.L. Smith, presented by A.B. Smith, ANL, Argonne)
- " " 11. • Limits of application of the method of recoil protons in neutron spectrometry using a NE 213 organic scintillator  
(A. Capgras, LMRI CEA, Saclay)
- " " 12. • Performance of gas target using D(d,n) reactions as a fast neutron source  
(Lian Tun-Chi, Ye Jine-ping, Sa Dren, Inst. Atomic Energy, Peking)
- Evening: Visit to the Institute of Experimental Physics, Kossuth Lajos University

Thursday, 20 March

Morning and Afternoon:

Session IV:

Working Group Sessions

Preparations for the Conclusions and Recommendations

Working Group 1 (Session I)

Chairman/Co-Chairman: I.M. Blinov/K.W. Geiger

Working Group 2 (Session II)

Chairman/Co-Chairman: C.D. Bowman/W.G. Alberts

Working Group 3 (Session III)

Chairman/Co-Chairman: H. Klein/M. Drosz

Evening:

Informal meeting on the Intense Neutron Source Programme in Hungary

Friday, 21 March

Morning:

Session V:

Concluding Session

Reports by the Chairmen of the three Working Groups

Summary of conclusions and recommendations

(Final Summary by A.B. Smith, ANL, Argonne)

Closing

Excursion to Hortobágy (40 km from Debrecen)

---

• Contributed Paper but not presented

## INTRODUCTION

For nearly half a century neutron sources have been of high interest in both basic and applied contexts; extending from the very low energies primarily relevant to condensed-matter studies to the very high energies associated with elementary-particle interactions. A diversity of neutron-source types are involved ranging, for example, from small sources implanted in human tissue to the very largest of accelerator-based research facilities. The primary application of neutron sources is now energy related, particularly associated with the provision of the basic physical parameters underlying the utilization of both fusion- and fission-energy systems. Neutron sources are also widely applied in other fields; for example geological and bio-medical. The requirements for neutron data, and neutron-source properties generally, have shifted from a qualitative to the present very quantitative status; often reflecting very large cost and/or safety impact. In many cases very small parameter variations can be decisive. The interest in and utilization of neutron sources is world wide though the character, the application, and the magnitudes may be very different.

Considerations of the above nature have resulted in a continued and high international interest in neutron sources that is reflected in considerations of the International Nuclear Data Committee over an extended period of time. As a result of this continuing assessment that Committee felt that a timely review of the neutron-source field by a small group of selected specialists was now warranted and this meeting is the result of that recommendation. The objective is the wide-scope technical assessment of the status of neutron sources with emphasis on their relevance to and use in neutron-associated applications. The energy range of interest extends from sub-thermal to 50 MeV and above. A wide range of source types are relevant including; those based upon natural activities, mono-energetic sources (e.g. accelerator based, filtered beams, etc.), white sources (e.g. reactors, accelerators, etc.), and reference neutron fields particularly employed for calibration purposes. The assessments should include not only the properties of the sources themselves but also aspects of their practical utilization. Projections as to future trends in both large and small source contexts are sought. Comparative evaluations should identify both strengths and weaknesses of the various source types. From these deliberations should emerge definitive guidance for future efforts with particular attention to cooperative endeavors.

A. Smith  
Argonne National Laboratory  
March 1980





## Summary Conclusions and Recommendations

### Working Group 1

#### Radioactive ( $\alpha$ ,n), Photoneutron and Spontaneous Fission Sources

Chairman: M. V. Blinov, Radievj Institute V.G. Khlopina.

Co-Chairman: K. W. Geiger, National Research Council of Canada

#### Utilization

Radioactive neutron sources as well as fission-neutron sources are of low cost and normally easily obtainable. They are used as neutron standards and as calibration sources for instruments, in particular dosimeters. Furthermore they are suited to special applications notably as probes in geological exploration. For these probes Be( $\alpha$ ,n) sources are of particular interest because relatively hard spectra are required. Radioactive ( $\gamma$ ,n) sources are particularly useful for the precise absolute measurement of neutron cross sections at reference energies, notably activation and fission cross sections. Because of their high specific emission rates  $^{252}\text{Cf}$  sources are widely used in activation analysis, neutron radiography and as instrument-intensity and energy standards. In addition  $^{252}\text{Cf}$  sources have found application in medical therapy.

#### Recommendations

##### Be( $\alpha$ ,n) and Photo-neutron Sources

1) Above energies of 2 MeV the neutron spectra of Be( $\alpha$ ,n) sources are well known in the context of their applications. Below 2 MeV better spectrum measurements are needed. The low-energy range is important in neutron dosimetry calibration and in the determination of corrections involved in the precise calibration of Be( $\alpha$ ,n)-source intensities using  $\text{MnSO}_4$  bath methods.

2) Present inconsistencies in the stopping power data for He and Be need to be resolved. These uncertainties strongly affect the calculated yield from Be( $\alpha$ ,n) sources.

3) For photo-neutron sources, the relationship between calculated yield, measured yield and photoneutron cross section should be further investigated. Such results could provide a mechanism for obtaining more accurate ( $\gamma$ ,n) cross-section data than available at present.

4) A catalog of essentially mono-energetic ( $\gamma$ ,n) sources, listing all pertinent source parameters, should be made.

5) Modifying the Sb-Be( $\gamma$ ,n) source spectrum by filtering and moderation allows the production of spectra with average energies down to  $\sim 0.5$  keV. Application of such methods could provide sources of various energies complementing those available at larger laboratories using filtered reactor or accelerator beams.

6) The published neutron fluence-to-kerma conversion factors should be reviewed in the light of the present improved knowledge of  $(\alpha, n)$  and  $(\gamma, n)$  source spectra.

#### $^{252}\text{Cf}$ Spontaneous Fission Sources

1) A new evaluation of the experimental results on the spectra should be made using the latest data. This should include full statements on the evaluation error.

2) The  $^{252}\text{Cf}$  spectrum can be assumed to follow a Maxwellian shape with temperature  $T \approx 1.42$  MeV in the energy interval 10 keV to 10 MeV. However, this representation is only a first approximation as deviations from the Maxwellian shape were reported in several papers. What is needed now is more experimental work using a variety of detectors with well known neutron detection efficiency, good energy resolution and reliable energy calibrations.

3) The error goal in spectral measurements is  $\pm 3\%$  from 0.2 to 8.0 MeV increasing at the extremes of the energy range to  $\pm 10\%$  at 0.001 MeV and 15 MeV. These accuracy goals reflect both the important requirements for spectrum-shape information and experimental capabilities for determining such information.

4) Measurements of  $\bar{\nu}$  for  $^{252}\text{Cf}$  show discrepancies of  $\lesssim 1\%$  which are frequently associated with the measurement method, particularly considering the  $\text{MnSO}_4$  bath method versus liquid scintillation counting. These discrepancies should be resolved.

5) Because  $^{252}\text{Cf}$  is widely used as a standard, not only the half life but the isotopic composition of the samples should be well known as well. The chemical composition of the samples should also be carefully specified as chemical impurities may affect the spectrum by  $(\alpha, n)$  reactions.

6) We appreciate the efforts of the International Bureau of Weights and Measures in arranging intercomparisons of absolute source calibrations and we encourage participation on the part of additional countries.

7) We recommend that  $^{252}\text{Cf}$  sources be utilized as standards for  $\bar{\nu}$  and for the prompt-fission-neutron spectrum.

## Summary Conclusions and Recommendations

### Working Group 2

#### White Neutron Sources and Filtered Beams

Chairman: C. D. Bowman, National Bureau of Standards

Co-chairman: W. G. Alberts, Physikalisch Technische Bundesanstalt

#### 1) Accelerator-based White-Neutron Sources

As neutron-based technology has grown so have the methods for neutron production. The rate of development has increased and now we are probably on the threshold of significantly larger source intensities and improved measurement methods for use in neutron research and applications. It is expected that the reactor will continue to hold a firm position particularly in material studies. Further development of reactor intensities will probably be limited due to the large energy release per available neutron ( $\sim 200$  MeV/neutron). The accelerator-based sources are not near such a barrier and thus a variety of accelerator concepts are under study for the provision of neutron sources of increased intensity. In addition there are engineering and management advantages to the accelerator source (e.g. ease of control and reduced residual activity), and accelerator reliability may be approaching that of a reactor. The accelerator-source advantages are most sharply drawn at the highest intensity levels but many of the advantages remain true at more modest intensities.

Accelerator systems used for white neutron source production can be qualitatively characterized as follows:

- Spallation Sources,  $>200$  MeV
- Electron linacs, 30-150 MeV
- Ion accelerators,  $<200$  MeV
- Electron linacs, 10-15 MeV
- Electrostatic accelerators,  $<5$ -10 MeV.

These categories are only general guide lines as other considerations, such as the particular application, may be governing factors.

The advantage of the spallation source is the low energy release per emitted neutron ( $\sim 25$  MeV/neutron) which is an important consideration in target-heat-dissipation capability and accelerator-energy efficiency (i.e. energy cost). The accelerator concepts involved have been largely proven in high-energy research facilities. For these reasons the accelerator-spallation source has considerable development potential beyond current concepts. Additional advantages are; comparatively low  $\gamma$ -flash, flexibility including pulsed and continuous-mode operation, spectral options extending from fast to cold neutrons, and the capability for multiple research stations. A disadvantage of the spallation source is the presence of a high-energy neutron component which is difficult to shield against and which may perturb experimental measurements. Experience also indicates the presence of high-energy proton and meson backgrounds that are not always easily removed from the measurement systems. Though efficient systems are involved, power costs

can be a concern. The usefulness of the spallation source in both steady state and pulsed modes is broad as indicated by the qualitative comparative chart of Table 1.

Electron linacs are the most intense presently available accelerator-driven neutron sources. Even though less energy efficient than the spallation source these devices have proven very successful and should remain so into the future. However, it is not clear that new facilities of this type should be built except, perhaps, to meet special objectives. For example, a major area for improvement is in shorter pulses (e.g.  $\sim 50$  psec) which are particularly promising in some experiments. This type of source also offers ideal capability for activation analyses by the  $(\gamma, n)$  method complementing thermal-reactor activation methods.

Proton or deuteron accelerators of  $< 200$  MeV have been productively utilized as white sources. They are not truly spallation sources and are less neutron efficient than the spallation source but they have advantages. The pulse width is characteristically  $\sim 1$  nsec. The neutron beam is strongly forward peaked making the source particularly useful for radiation damage and therapy. Duty cycles are inherently high and reduced repetition rates may significantly curtail the average beam currents. In various modes, the application of this type of source is broad as outlined in Table 1. This type of source again has a high-energy neutron-spectrum component that is a liability in some applications. The heat is more localized in the target than for the spallation source and the beam currents are characteristically higher than in spallation sources thus placing more burden on beam handling and diagnostic systems.

10-12 MeV electron beams can be used for neutron production with an efficiency approaching that of a 100 MeV beam by using  $Ta(e^-, \gamma)$  converters and Be or D  $(\gamma, n)$  radiators. Recent technological advances permit a trade-off between beam current and energy for nearly the same neutron production efficiency as for the 100 MeV electron beam. The high-current low-energy option has some significant advantages. The neutron spectrum is free of high energy components. Shielding requirements are less resulting in reduced costs and space and better experimental fluxes. The accelerators are simplified single-section units and the induced radioactivity is relatively small. With existing technology, the total neutron production with conventional units remains less than that of a 100 MeV facility, but induction-linac technology, with the promise of 1000 ampere beams, may alter this situation. The applicability of the concept is outlined in Table 1. The disadvantages of the concept are the absence of neutrons with energies above  $\sim 4$  MeV, e.g. as needed for radio-therapy purposes, and less source brightness.

The final category is the low-energy electrostatic accelerator which, with thick targets, offers selected opportunities for specialized white-neutron-source work with comparatively high intensity. Optimum utilization of the method requires a solution to the target power dissipation problem in order to utilize available beam power. The method is particularly useful in neutron data measurements in the keV and low MeV energy ranges where good results can be obtained with modest facilities and costs.

In summary, a wide range of options is available for improved accelerator-based neutron white-source studies leading to further development of neutron research and neutron based technology.

## 2) Calibrated Beams and Fields from Reactors and Accelerators

Calibrated neutron beams and fields include; those produced by various filter applications (primarily at reactors), thermal reactor beams, neutron fields driven by thermal neutrons and fields driven by accelerators. The accuracy and quality of these beams and fields was discussed including their use in cross section measurements, instrument calibration, bio-medical applications and for other purposes.

Filtered beams have been developed for a wide range of energies using reactor sources and, to a lesser extent, accelerator sources. The filtered beam, first introduced by the MTR group, has been a very useful tool in both basic and applied studies particularly where the object is high accuracy.

The most widely considered filter energies are;

2.35	MeV;	$^{16}\text{O}$
144.	keV,	Si
55.	keV;	Si
24.	keV,	Fe
2.	keV,	Sc
186.	eV,	$^{238}\text{U}$ .

The filtered beams are particularly valuable at energies of  $<30$  keV, where other methods are difficult, but they are also applicable at higher and selected energies. Neutron spectroscopy is generally not the primary purpose of these filtered beams. Thus the availability of such beams at decade intervals below 200 keV is probably adequate with possibly one well-defined energy per decade. With this assumption the primary shortfall is in the 20-50 eV energy range. This low-energy range is difficult as, already, the 186 eV ( $^{238}\text{U}$ ) beam is subject to background problems. Beam purity remains a problem, particularly due to higher-energy perturbations, and attention should be given to alternate material combinations (e.g. the use of other windows in  $^{238}\text{U}$ ), isotopic filters and careful selection of filter materials. At low energies (e.g. less than 2 keV) better methods of characterizing the beam are desired. At present the beams obtained from the reactor are very stable. This and their steady-state nature is a strong advantage in many applications (e.g. dosimetry). The use of neutron filters in conjunction with a pulsed-white source results in a background reduction in time-of-flight experiments while in some cases intensities are comparable with those obtained with a reactor (e.g. the  $^{16}\text{O}$  filter at 2.35 MeV is approximately of equivalent intensity at an accelerator and reactor). Generally, what is obtained is a pulsed mono-energetic beam with its advantages in some types of measurements (e.g. neutron scattering studies). In other usage there is an advantage to the pulsed and filtered beam provided by a small accelerator. The potential of small electrostatic accelerators, filtered beams and thick targets (e.g.  $^7\text{Li}(p,n)$ ) should be examined. Similarly, research with the objective of producing intense monoenergetic beams via thermal-neutron de-excitation of isomeric atoms, molecules or nuclei was encouraged.

Energies in the low-keV region are particularly important in personnel dosimetry as they contribute significantly to typical neutron fields of nuclear power stations. Below ~2 keV a better calibration field would be very helpful. Biological and medical applications are interested in the results of neutrons incident on Cd and  $^{10}\text{B}$  implanted in human tissue both in diagnostic and therapy contexts. In either case, keV neutrons are used to achieve deep tissue penetration not available with thermal neutrons. Generally, the basic physics of neutron damage to biological specimens is not clearly understood and it is reasonable to expect filtered beams to help resolve the issues.

Calibrated thermal neutron beams from reactors provide a further energy range for instrument calibrations and  $(n,\gamma)$  work. Standard neutron fields with broad energy distributions play an important role in nuclear power development. They are frequently derived by placing  $^{235}\text{U}$  fission sources in a cavity within a reactor thermal column. Appropriate use of moderators and/or absorbers tailors the cavity spectrum to that of the particular need (frequently a fast-reactor spectrum). The cavity-field geometries are simple and the spectrum calculated to accuracies of ~5% at intensities of  $\sim 10^9$  n/cm<sup>2</sup>-s and tested by selected benchmark measurements. An accelerator - based white source offers an alternate method for the provision of standard fields when the emphasis is on accuracy and a tailored energy spectrum. The use of a pulsed source and drift tube provides further spectral definition and reasonable intensity (e.g.  $10^8$  n/sec). The use of calibrated fields should be improved by the implementation of a variety of complimenting methods and approaches.

Table 1. Comparative Utilization of Accelerator-based White-neutron Sources.<sup>†</sup>

Source Category	Type of Utilization										Radiation Damage
	Solid State	Medium Energy Phys.	Nucl. Phys.	Neutrino Phys.	Nucl. Data	Bio-Research	Isotope Production	Act-Analysis	Neut. Radiography	Cancer Therapy	
Spallation Sources, $E_p$ or $d \geq 700$ MeV	•	•	•	•	•	•	•	•	•	•	•
Electron Beams 30-150 MeV	•	-	•	-	•	•	•	•	•	-	-
Ion Accelerators <200 MeV, No Storage ring	•	-	•	•	•	•	•	•	•	•	•
Electron Beams 10-12 MeV	•	-	•	-	•	•	-	•	•	-	-
Electrostatic Accelerators, Thick Targets	-	-	•	-	•	•	-	-	•	-	-

<sup>†</sup>The degree of applicability depends on the details of the method.





## Summary Conclusions and Recommendations

### Working Group 3

#### Monoenergetic Neutron Sources from Charged-particle Reactions

Chairman: H. Klein, Physikalisch Technische Bundesanstalt

Co-Chairman: M. Drosch, Inst. für Experimentalphysik, University of Wien

Various applications of monoenergetic sources have been discussed by this working group (~15 members) of the IAEA consultant's meeting. These considerations are divided into topical sections as follows:

#### 1) Monoenergetic neutron sources in the energy range 30 keV to 60 MeV

For basic and applied physical research, calibration purposes and neutron dosimetry over the energy range 30 keV to 60 MeV several of the reactions of Table 1 are suitable. In that context the following recommendations and requirements are set forth as referenced to that table.

1A) Reasonable energy resolution of ~10% for 30 keV neutrons can be achieved at low yield. The development of a high intensity target is required and source-associated cross section measurements are needed in this energy range including attention to the structure of the reaction cross section.

1B) Excellent energy resolutions have been achieved using monoenergetic sources in studies of inelastic-neutron scattering with excitation energies up to ~400 keV (e.g. ~10 keV for a 3 MeV incident neutron energy) and in similar studies involving reaction-product spectroscopy. Associated  $\gamma$ -ray techniques can be applied in neutron-flux-intensity measurements above ~700 keV.

1C) These sources may be useful in both relative and absolute calibrations to accuracies of ~5%. However, the application is limited by the relatively low reaction cross section.

1D) The application of tritium is largely limited to use in solid-state metal-implanted targets (e.g. absorbed in titanium) or gas targets. The advantages of a triton beam will, unfortunately, not be utilized at most installations due to safety regulations. Here continued development of low background  $T_2$  - gas targets is required (e.g. employing  $^{58}\text{Ni}$  entrance foils and  $^{58}\text{Ni}$  or  $^{28}\text{Si}$  backing).

1E) This is the most practical source in this energy region, providing high neutron fluxes. The signal-to-noise ratio can be improved by using Mo entrance foils and Ta backings. The background due to  $D_2$  self-buildup in the target can be reduced by decreasing projectile energies over the period of target use. The neutron angular distributions at incident deuteron energies of 5 to 6 MeV are recommended as secondary calibration standards.

An evaluation of all available d-breakup measurements is required for use in many applications (e.g. neutron scattering, angle-integral cross section measurements, correction calculations, etc.).

1F) This reaction may be used up to ~30 MeV neutron energy but above ~20 MeV the background problems increase rapidly.

1G) Here cross section measurements should be extended up to ~60 MeV neutron energy. Complete neutron energy spectra are required for the interaction of protons with  $^7\text{Li}$  and  $^9\text{Be}$ .

For all of these neutron producing reactions the compilation of the relevant measured source-reaction data is required so as to permit the quantitative use of improved data in further evaluations (e.g. for the evaluation of the p-t reaction at ~3 MeV and the p- $^7\text{Li}$  reaction near 5 MeV).

## 2) High Intensity Neutron Sources at ~14 MeV

High intensity neutron sources are of special interest in many fields of application; e.g. basic nuclear research, nuclear data measurements, solid-state physics, particle-damage studies, chemical analysis, bio-medical uses, neutron radiography, neutron-shielding studies, etc.

It is recommended that laboratories working in the 14 MeV area cooperate in the design and construction of intense-neutron-source facilities, particularly where involving rotating Ti(t) and other special high-intensity targets, and in the development of intense deuteron ion sources suitable for use at ~400 keV accelerators in either DC or pulsed (~nsec) modes.

Multiple scattering of deuterons in thick Ti(t)- targets has to be calculated to determine the angular dependence of the neutron energy distribution. For this purpose the d-t cross section at projectile energies of <10 keV is required. The influence of structural material should be included in such calculations (e.g. by means of monte-carlo simulation). The results of these calculations should be verified by means of high-resolution time-of-flight spectroscopy.

In addition to common (or standardized) source configurations common (or standard) experimental setups should be developed for:

The measurement of neutron flux intensity (e.g. proton-recoil telescope, Al(n,  $\alpha$ ) activation, etc.).

The determination of mean neutron energy (e.g. proton-recoil telescope).

The use of secondary-reference scatterers (e.g. C, Bi, Fe instead of, or complementing, CH<sub>2</sub>).

The operation of these new high-intensity neutron sources will make possible more complex experiments (e.g. particle-angle correlation measurements) providing more detailed understanding of the basic reaction mechanisms.

### 3) Special-purpose Monoenergetic Sources

There are a number of reactions, in addition to those identified in Table 1, that are very good monoenergetic neutron sources in particular experimental contexts. Notable of these are a number of (d,n) and ( $\alpha$ ,n) reactions on light targets (e.g.  $^7\text{Li}$ ,  $^9\text{Be}$ ) having well defined neutron groups, useful intensities and often positive Q-values. The working group acknowledges their importance but due to their specialized nature and application does not deal with them here.

### 4) General Considerations

A number of aspects of the use of monoenergetic neutron sources involve computing codes many of which can be made operable on modest computational equipment. It is recommended that, where possible, these codes be standardized, documented, and made generally available particularly with respect to:

Calculation of neutron-detector efficiencies (e.g. liquid scintillators and proton-recoil telescopes).

Corrections to scattering measurements due to geometry, flux attenuation and multiple events.

Such codes should operate on small computers (e.g. 16K bit words, 32K storage). The NDS-IAEA provides a suitable mechanism for the acquisition and distribution of such special-purpose codes. The development, careful test and documentation should be the responsibility of the originator and not of the compilation and distribution entity.

Table 1. Recommended "Monoenergetic" Neutron Sources

<u>No.</u>	<u>Reaction</u>	<u>Neutron Energy range, zero deg.</u>	<u>Remarks</u>
1A	Sc(p,n)	5.5 keV-53 keV	Low intensity
1B	$^7\text{Li}(p,n)$	Threshold-5 MeV	Monoenergetic to ~0.7 MeV Second kinematic group present near threshold
1C	$^{11}\text{B}(p,n)$ $^{12}\text{C}(d,n)$	90 keV-2.39 MeV 14 keV-2.7 MeV	Low intensity
1D	T(p,n)	0.5-14 MeV	Also useful to higher energies
1E	D(d,n)	Threshold-14 MeV	Background and breakup problems above ~6 MeV
1F	T(d,n)	~15-30 MeV	Background problems for $E_n \gtrsim 20$ MeV
1G	T(p,n) $^7\text{Li}(p,n)$ $^9\text{Be}(p,n)$	25-60 MeV	Accelerator energies of 25-60 MeV required. Backgrounds a problem in many cases.
2A	T(d,n)	~14 MeV	High intensity source.
3A	Variety of (d,n) and ( $\alpha$ ,n) reactions	up to 20 MeV and above	Sources are "monoenergetic" only in context of par- ticular application

## ***REVIEW PAPERS***



NEUTRON SOURCES IN PERSPECTIVE\*

A. B. Smith  
Argonne National Laboratory  
Argonne, Illinois 60439, USA

I. INTRODUCTORY REMARKS

It has often been said that the problem of experimental neutron physics is intensity. The axiom remains true but there are mitigating circumstances; the character of the source, specific brightness, and the canonical variables space, time, energy and momentum.

This meeting should sharpen the understanding of a wide range of complementary neutron sources, many within the scope of modest resources. Strengths and weaknesses should be identified and innovative applications and techniques put forth. Specific technical recommendations with the objective of improved quality and utilization are sought with the emphasis on modest-facility applications. On a larger scale, major source facilities are of interest in a cooperative regional and international context and technical recommendations toward encouraging such cooperative use are sought.

The following remarks have the objective of setting the stage in the areas of: monoenergetic accelerator based neutron sources, white neutron sources, neutron sources based upon natural activities, reactor-based neutron sources, and neutron sources employing a variety of filter concepts.

II. NATURAL RADIOACTIVE SOURCES<sup>+</sup>

Fermi and coworkers used sources of this type to study neutron-induced activity and, probably, unknowingly observed fission. These sources remain useful due to their stability which makes them good intensity and spectral reference standards and to their isotropy of emission which makes them particularly suitable for the provision of standard fields and the application of the sphere-transmission and similar special techniques. The sources are frequently relatively simple to use and of low cost. The limitations are associated with spectral coverage and definition (or lack thereof), high levels of radioactivity and practical problems associated with fabrication.

---

\*Prepared for the IAEA Consultants' Meeting on Neutron Source Properties; Debrecen, Hungary, 17-21 March 1980.

<sup>+</sup>Professor G. F. Knoll was kind enough to provide the author with a pre-print of an extensive review which stimulated many of the following remarks.



#### A. (alpha,n) Sources

Early sources of this type were primarily based upon radium (and product) activities. The radium source still is one of the basic intensity standards, known to fractional-percent accuracies in the best cases. More recently trans-uranium activities have been widely used. The latter provide convenient half-lives, good yields and relatively low backgrounds. Illustrative examples of such sources are given in Table 1. Most of these sources employ an essentially infinitely thick beryllium target for neutron production via the  $\alpha + {}^9\text{Be}$  reaction. As a consequence all of the spectra are continuously distributed in energy up to  $\sim 10$  MeV and above as illustrated in Fig. 1. The spectra are moderately dependent upon the underlying activity and the details of fabrication. None can be considered a "monoenergetic source" and thus the use is primarily as an intensity standard in a wide spectrum of applications (e.g. bath and dosimetry calibrations). The gamma-ray emission is generally of approximately the same intensity as the neutron emission. Alternate and softer spectral distributions can be obtained by using conversion materials other than Be, e.g. B, C or Li, as illustrated in Fig. 2. In doing so there is a sacrifice in intensity similar to that encountered in the use of the same (alpha,n) reactions at monoenergetic accelerator facilities.

#### B. (gamma,n) Sources

The primary advantage of these sources is their stable and well defined spectral distributions which can approach those of a monoenergetic source. Thus these sources are useful as both intensity and energy-reference standards. The disadvantages are the very large gamma-ray intensities, the often relatively short half-lives, and the practical problems of producing and handling very intense radioactive samples. In practice, the use of these sources often implies the availability of a modest sized research reactor. The conversion radiator is usually Be ( $Q = -2.226$  MeV) or deuterium ( $Q = -1.666$  MeV) and, from the point of view of the gamma-ray, the radiators are "thin". The sources are not thin to the emitted neutrons and secondary-reaction yields must be carefully considered. With these two radiators, a range of gamma-ray sources provide a number of reasonably monoenergetic and isotropic neutron sources distributed over the neutron energy range of approximately 1 keV to 2.5 MeV as illustrated in Table 2. Yields can vary by several orders of magnitude and half-lives from minutes to days. The sources are monoenergetic to within 10-20% as illustrated by the distributions of Fig. 3. That resolution is generally larger than provided by the well filtered beam or the monoenergetic accelerator sources. In addition there are perturbations resulting in long tails that must be carefully considered in precision measurements. However, with care some very precise reference-cross-section values have been obtained using relatively simple methods.

#### C. Spontaneous-fission Sources

By availability and half-life these are, in practice, confined to Pu-240 and Cf-252. Only the latter has a wide applicability and is of concern here. Cf-252 is recognized as the basic fission-source reference but it, perhaps, remains the most-under exploited of all natural neutron sources.

The neutron intensities available with the Cf-252 source can range up to  $\lesssim 10^{10}$  n/sec and be accurately known. The neutron-emission spectrum is reasonably known over the region of appreciable intensity (0.1 - 10.0 MeV). Moreover, this spectrum is favorably distributed, from the point of view of many microscopic measurements. On a velocity scale and on an energy scale it is closely similar to the common actinide fission-neutron spectra of high applications importance. The time of neutron emission is readily determined to within  $\approx 1$  nsec making possible the application of the associated particle technique with all its advantages. The fission- and alpha-decay half-lives are both well known and in a useful range (5). This source can provide a readily transferable standard-reference field that is far more attractive than the transfer instrument concept.

The Cf-252 source has been used to a limited extent for instrument calibration purposes (6). It is the primary nu-bar reference (7) but has been relatively unused in microscopic cross section measurements. Where the latter have been attempted the results have been encouraging (8). The source provides a standard-reference field largely free of environmental perturbations without any requirement for a major facility (e.g. without the need for a reactor). Only now is the source assuming a proper place in the context of a standard-reference field for integral validations, e.g. for integral tests of cross sections and macroscopic properties such as age to indium resonance (9).

There are basic problems associated with the Cf-252 source. It is an international concern that nu-bar is known to no better than 0.7%; though even that value is very good in the context of the knowledge of the intensities of other sources (7). The delayed neutron yield is uncertain but small (10). There are questions as to the presence of short-lived fission-product isomers and these can be a concern in some applications. The spectral knowledge over the range of appreciable intensity is probably no better than 3-5%. The spectrum observations are generally consistent with a maxwellian shape and a temperature of  $\sim 1.42$  MeV (11). However, the latter value and recent measurements raise questions with respect to the fission-neutron spectra of the common actinides (e.g. U-235 and Pu-239) (12). At low energies the exact nature of the spectrum remains uncertain and that is a concern in some applications despite the relatively small intensities involved.

Applications problems are less serious but significant. Cf-252 stock material is reasonably available at most major institutions and can be of good purity. It is not clearly so at the smaller installations. Fabrication remains a problem both in the context of encapsulated sources and thin films suitable for fragment detection. Fragment detection can be simple and achieve good results as illustrated by the time-of-flight-spectrum measurement of Fig. 4. However, in such measurements attention must be given to dead-time and time-zero determination and, more generally, to fragment detection efficiency. The latter is not trivial and can be deceptive as careful studies indicate that counting losses and spectral perturbations can occur in otherwise apparently properly functioning detection systems (12). Such losses may be a factor in some fission-cross-section measurements.

### III. WHITE ACCELERATOR-BASED SOURCES

#### A. Major-accelerator-based Facilities

These sources are the premium tools for high-resolution neutron-resonance spectroscopy. They are based upon  $(\gamma, n)$  and  $(X, n)$  reactions involving large electron or positive-ion (proton or deuteron) accelerators.  $(\gamma, n)$  targets are conventionally thick heavy metals designed for power capabilities of  $\geq 20$  kW and very short bursts (13).  $(X, n)$  targets are again usually heavy metals and also Beryllium with deuterium beams (14). Incident beam energies are 10's of MeV to  $\sim$  GeV and the emitted neutron spectra a continuum distribution similar to a hard fission spectrum. The energy distribution is frequently shifted by moderation and the intensity enhanced by the use of fissile boosters (which in the extreme become pulsed reactors). Pulse rates and durations vary widely but most fast-neutron resonance studies employ burst widths of 1-50 nsec. Some indication of the diversity of these devices is given in Table 3. Even this extensive representation is an understatement for there are a number of subjective judgments involved in assessing relative merit. There are, however, some overall qualitative features.

All the spectra are "white" with emission well defined in time. Essential to use as a spectrometer is the determination of primary beam velocity. This has the advantage of precise time determination and multichannel efficiency. However,  $\frac{\Delta E}{E} \sim \frac{\Delta t}{L} E^{1/2}$  with the implication of long flight path ( $L$ ) and correspondingly high intensities for optimum resolution. Dimensional limitations and neutron velocities put practical restrictions on burst duration ( $\Delta t$ ). The technology is such that this method can provide experimental resolutions finer than the underlying physical structure in wide (and primarily low) neutron energy ranges.

The method inherently denies one canonical variable (time) to the secondary (or emitted-particle) detection system. This is an unfortunate limitation as the velocity spectra of emitted particles can not be readily determined and alternate neutron-spectroscopic techniques are notoriously difficult.

The method is troubled with background perturbations. Only at very low energies can backgrounds be solidly determined (e.g. using black resonance methods). The source itself introduces serious perturbations; for example, the intense flash from the  $(\gamma, n)$  reaction or a variety of high energy particle effects using  $(p, n)$  processes (15).

It is clear that the method places a premium on intensity. It is not only inherent in the method of measurement but also in the dimensionality of the source and measurement systems.

Over about a decade intensity levels have grown by about an order of magnitude to something in excess of the distributions shown in Fig. 5. Work already in progress (e.g. LASL-WNR, Ref. (15)) promises a similar order of magnitude improvement in the coming 10 years based primarily on spallation reactions. Perhaps a question is whether or not the relevant physical problem areas warrant such continued growth of these massive facilities.

The question is highlighted by what appears to be a curtailment of programs at some of the most powerful of these facilities. This suggests that the smaller institution interested in relevant experimental efforts would be well advised to pursue them in concert with one of the existing major facilities. It is noted that such cooperative programs have been very successful on a regional and national basis. It is further noted that these large facilities are very prolific data producers and that the overall limitation is often not the measurements themselves but the analysis; which can be carried out elsewhere.

#### B. Modest e<sup>-</sup>-based Neutron Sources

The above major facilities involve large capital and operating costs. However, modest e<sup>-</sup>-based neutron sources can be productive in basic and applied neutron research.

Consider the 10-12 MeV electron facility underlying the photo-neutron research program of Jackson and Holt (16). This linear-accelerator facility is currently equipped with 10 m and 20 m flight paths and an electron gun providing 35 psec bursts at 200-amp levels. The result is a very good measurement capability as illustrated in Fig. 6. These very nicely resolved neutron groups from the  $^{208}\text{Pb}(\gamma, n)$  reaction show the power of the method. They also illustrate the axiom that neutrons are rather slow and the practical instrumentation of finite dimension. As a consequence the overall time resolution is fractional nsec despite the burst of 35 psec.

Recently it has been suggested by Bowman (17) that modest e<sup>-</sup> accelerators have a neutron-research potential rivaling that of the larger installations if Be or deuterium converters are employed. It is estimated that neutron yields with 10 MeV e<sup>-</sup>-beams and Be or D converters are equivalent to those at 100 MeV using typical tungsten converters and equivalent beam power. The concept has not been exploited, the neutron energies will be  $\leq 10$  MeV and there remain questions as to e<sup>-</sup>-beam technology (particularly with respect to beam power as a function of current and voltage).

#### C. Damage Sources

Development of fusion-energy concepts based upon the (d,t) reaction have stimulated material-damage studies particularly of structural materials associated with plasma containment. The dose levels projected for the practical device are very large ( $10^{17}$ - $10^{25}$  nvt) primarily at neutron energies of 8-14 MeV. Engineering feasibility may be governed by these radiation-damage effects.

Monoenergetic (d,t) source facilities can provide 14 MeV point neutron sources with intensities of  $10^{12}$ - $10^{13}$  n/s (18). Such intensities are useful in damage studies but  $\sim 4$  orders of magnitude below that desired and even then are available in relatively small volumes. An alternative is a 35-40 MeV deuteron beam incident on thick lithium targets. The emitted neutron spectrum is angle dependent but can be selected to provide an average neutron energy of  $\sim 14$  MeV with intensities of  $\sim 10^{16}$  n/s. The implied deuteron-beam intensities are within accelerator technology and molten-metal lithium targets with requisite power-handling capability are under development (19). In the US such a

concept is being implemented as the Fusion Materials Irradiation Test (FMIT) facility with design parameters as outlined in Table 4. The FMIT facility represents an advanced engineering application of white-source technology at extreme intensity levels. It is not a modest concept technically or fiscally.

In passing, it should be noted that intense white neutron sources developed in the context of fusion energy may have a future applicability in a far wider scope; e.g. pellet fusion, the dense-plasma focus, etc. It should also be remembered that there are other pulsed white sources that have been used with varying degrees of success; e.g. burst or pulsed reactors, explosive devices, etc. These diverse sources are beyond the scope of the present remarks.

#### IV. MONOENERGETIC NEUTRON SOURCES

##### A. Overview

Since the advent of the electrostatic accelerator (20) and the discovery of the neutron (21) nearly half a century ago, the light-particle monoenergetic neutron sources have played a major part in experimental fast neutron physics. The attributes of these sources remain great. They provide control of all canonical variables (energy, time, space and momentum) and, in certain classes of experiments, this characteristic places these sources in a uniquely favorable position (e.g. processes involving residual activities and/or secondary timing). The neutron yields are prolific and, in optimum configurations at modest facilities, comparable with those of the very large white-source facilities. Most of the reactions are truly monoenergetic over only limited energy ranges. Characteristically, there are secondary and/or minority neutron groups and the curve of binding energy dictates troublesome multi-particle breakup a few MeV above the primary threshold. The challenges are the selection of the source in the context of the problem and facility, the innovative ability of the experimenter and his mastery of practical technology.

There are three monoenergetic neutron source categories.

1) The primary "big-4" (22).

$T(p,n)^3\text{He}$	$Q = - 0.763 \text{ MeV}$
$T(d,n)^4\text{He}$	$Q = +17.590 \text{ MeV}$
$D(d,n)^3\text{He}$	$Q = + 3.270 \text{ MeV}$
$^7\text{Li}(p,n)^7\text{Be}$	$Q = - 1.644 \text{ MeV}$

2) The secondary group.

$^9\text{Be}(d,n)^{10}\text{B}$	$Q = + 4.361 \text{ MeV}$
$^7\text{Li}(d,n)^8\text{Be}$	$Q = +15.031 \text{ MeV}$
$^{51}\text{V}(p,n)^{51}\text{Cr}$	$Q = - 0.331 \text{ MeV}$
+ various other d + and $\alpha$ + light target reactions.	

3) Advanced or developmental sources exemplified by, for example, those induced by tritium beams.

Our attention is primarily on the "big-4" as they constitute 90+% of the sources used in programs at, particularly, smaller facilities. The secondary group is of interest in specialized contexts. The "advanced and developmental" sources can be very powerful but often involve serious facility considerations (e.g. tritium activities) that make them difficult.

## B. The "big-4"

Over the applicable energy ranges the zero-deg. neutron yields of these sources can vary by an order of magnitude as illustrated in Fig. 7. None is ideal over the 10-14 MeV range important to fusion technology. All but one ( ${}^7\text{Li}(p,n)$ ) inherently involve gaseous targets.

### 1. The $T(p,n)$ reaction

The inherent advantages of this source are: a relatively low-energy threshold, a very wide monoenergetic range (0.1-8.0 MeV), and a simple reaction mechanism relatively free of background effects (e.g. no associated gamma-ray). Multi-particle breakup is a problem only at relatively high energies. There are inherent and practical limitations. The very light system makes the reaction sensitive to kinematic effects. There is some uncertainty associated with the absolute yields but the relative angular distributions and polarizations are reasonably known (23). Best yields are obtained with gas targets--and with associated health hazards. Power handling capabilities are approximately 10 w/mm<sup>2</sup>. The limitation is the gas-cell window usually of nickel, molybdenum or tungsten. The power capability can be somewhat improved through the use of multiple and cooled windows or supporting and cooled grids. Windowless cryogenetic or hypersonic gas cells have been proposed and even tested. However, they remain complex developmental devices that have not found wide application. There are backgrounds associated with contaminants and the beam stop. The latter is subject to hydrogen inclusion resulting in the well known blistering phenomena even in heavy metals. Use of special low-background stops (e.g. Si-28) is limited by material availability and fabrication problems. Yields from gas-absorbed metal foils (e.g. titanium) are inferior, target life is limited and target thickness difficult to control. However, the foils are easier to use and the health hazards reduced. The kinetics of the reaction make it attractive from the point of view of the associated-particle calibration technique despite the low energies frequently involved. This capability is illustrated by the low energy results of Mier et al. (24) shown in Fig. 8. These were obtained using gas loaded titanium foils and form a part of an extensive program for the provision of precisely known neutron fields.

### 2. The $T(d,n)$ Reaction

The large positive Q-value, the good yield at low incident energies, the near isotropy of neutron emission and a relatively high three-particle breakup threshold make this a particularly attractive reaction for studies employing small accelerators. Such measurements are now of considerable technological importance due to the key part the same reaction plays in fusion-energy concepts. The yield is maximum at very low incident energies and relatively simple gas-absorbed metal targets are conventionally

employed. These have limited power handling capability but that can be greatly increased by rapid physical motion as at the Lawrence Livermore Laboratory RTNS facility (25). However, at higher powers target life is short and there is a considerable release of tritium. This source is, perhaps, the optimum reaction for the application of associated particle techniques; for example, as used to high accuracy by Genier et al. (26). In view of the contemporary technological importance of this source it is odd that many major institutions have no research capability in this area. There remains a dearth of accurate non-elastic cross sections at 14 MeV to the detriment of precise evaluation. There are relatively few determinations of 14 MeV neutron induced neutron emission spectra as illustrated, for example, by the work of the Dresden Group. And yet, technologically, it is relatively simple to produce very intense nsec bursts near 14 MeV (27). Macroscopic 14 MeV benchmark neutron measurements have been largely confined to the work of one group (28) and yet they provide critical tests of evaluated neutronic files. It is only recently that higher intensity versions of this source have been used to provide a good understanding of radiation damage in materials of fusion interest (25). Certainly, this source offers basic and applied research opportunities for the smaller facility.

### 3. The D(d,n) Reaction

This reaction has many of the attributes and problems of the T(p,n) and T(d,n) reactions, above. The yield is large and well known (23) (see Fig. 7) both at a zero-degree reaction angle and as a function of angle. The Q-value is positive and the source attractive at modest facilities. The health hazards involved with the source are relatively modest. The reaction is widely used in applications of the associated-particle technique (24). The primary liability is a relatively low threshold for three-particle breakup (4.98 MeV) and a large breakup yield as illustrated in Fig. 9. At an incident energy of 10 MeV the breakup yield accounts for approximately half the neutron yield and severely limits the usefulness of the source (29). Here, as in the use of the above two reactions, practical applications using either gas-cell or metal-film techniques involve background determinations that can be significant. Many of these are of a contaminant nature.

### 4. The $^7\text{Li}(p,n)$ Reaction

This is the only inherently metallic target of the "big-4". This characteristic provides for a control of target performance and ease of fabrication not enjoyed with the above three alternates. The reaction Q-value is negative and relatively large making necessary a few-MeV accelerator. The source is truly mono-energetic over only a rather narrow range (0.1-0.6 MeV) with the threshold for the second and minority neutron group at 2.38 MeV. There is a residual-product activity that has been exploited in absolute source-strength determinations (30). The second-neutron-group yield can be both a sin and a blessing. It provides a mechanism for the accurate determination of the energy of the primary group (31) and the associated gamma-ray emission can be used for accurate flux determinations (32). More serious is the breakup reaction ( $n + ^3\text{He} + ^4\text{He}$ ) with its relatively low threshold (3.68 MeV) and its rapidly increasing yield with energy (see Fig. 10) (33). There are extensive compilations of total and partial yields but uncertainties remain particularly where associated with the secondary yields (34). The source is polarized, an often ignored

factor in some experiments. There are practical considerations in target fabrication and use. Lithium metal is not a good heat conductor, has a low melting point and is chemically active. In conventional applications the power handling capability seems to be limited to  $50 \text{ w/mm}^2$ . The use of molten metal targets has been explored but not widely employed. Backing materials are a concern from the point of view of heat dissipation and background contributions. However the widely used vacuum deposition techniques employed in fabrication remain simple.

### C. The Secondary Group

There are a number of these reactions that can be productively used in special applications at monoenergetic facilities. Typical examples are:

#### 1. The V(p,n) Reaction

This reaction has a relatively low Q-value ( $-0.33 \text{ MeV}$ ) and a nearly isotropic yield. The intensity is weak and the reaction follows a relatively sharp energy-dependent structure. The primary advantage is in absolute intensity measurements based upon the well known residual activity (Cr-51) (35).

#### 2. The Pseudo-white and White Sources, ${}^7\text{Li}(p,n)$ , ${}^7\text{Li}(d,n)$ and ${}^9\text{Be}(d,n)$

It is not generally realized that these reactions can be very productive at even rather modest monoenergetic facilities. They are bright sources and have been used in the pulsed mode with flight paths of more than 100 m with consequent very good resolutions. They can provide a very good knowledge of energy scales through the use of various techniques relative to precisely determined frequencies and the velocity of light (36) and, if properly utilized, can provide energy resolutions comparable to those of the most intense white source facilities (37). In view of these capabilities at rather modest facilities it is odd that these sources have not been more exploited.

### D. Energy Scales

The underlying source-reaction Q-values are generally well known. However, the neutron energy scale in many monoenergetic applications is dependent upon the precise calibration of the facility. There are a number of (p,n) and (p,gamma) reactions that are known to the requisite accuracies (38). It is not clear that they are always carefully used nor that they are readily available in a compiled format suitable for wide and competent use.

### E. Reaction Theory

Our present knowledge of monoenergetic neutron sources is largely a numerical construction from experimental observations. The underlying nuclear structure is often at relatively high excitations (e.g.  $\sim 17 \text{ MeV}$  for the  ${}^7\text{Li}(p,n)$  reaction). However, the structure is relatively simple and there is hope of physical understanding. Reaction theory combined with experimental structure knowledge, may have the potential for substantive theoretical interpretation of measured source reactions in a manner similar to that pursued in other



neutron-reaction contexts. Such interpretations might improve accuracies and remove some of the present numerical and experimental artifacts. The requisite structure studies and interpretations have been long neglected yet they remain within the province of modest capabilities.

#### F. Calculational Capability

Inherent to the precise use of monoenergetic neutron sources, and neutron sources generally, are detailed corrections associated with the source, its environment and the detection system. Often these are pursued using monte-carlo or other extensive numerical calculations. Such calculations are demanding of calculational time but often not of storage and I/O capability. The problems can be readily and economically handled on small and low-cost computational machines and thus are well within the capabilities of the small institution. The wide availability of small, fast and low cost computational equipment is a technological advance of profound impact that is underestimated and underutilized.

### V. FILTERED BEAMS

#### A. At reactors

More than a decade ago the MTR group recognized that the familiar  $\ell = 0$  resonance-potential interference patterns could be utilized to obtain intense fast-neutron beams of well known energy and stability at a reasonably powerful research reactor by means of neutron transmission through well defined "windows" in a number of materials (40). Since that time the concept has been used in both basic and applied research endeavors; for example at BNL, NBS and the University of Missouri (41,42,43). The usefulness of the concept has been augmented by the concurrent development of precise neutron-flux- and spectrum-measurement techniques applicable to the low energy region (44,45). There are problems associated with the concept. The beams are not truly monoenergetic and all have some secondary-energy components. Backgrounds can be a problem both in the context of secondary neutron groups and of residual gamma-radiation. Performance is sensitive to isotopic and chemical impurity and consequently material availability. Consideration of these factors has led to the selection of three primary beam filters; Sc-45 (2 keV), Fe-56 (25 keV) and Si-28 (144 keV). A wide range of alternate filters have been employed to a lesser extent over the energy range  $<1$  keV -  $>2.5$  MeV. Each has a deep resonance interference minimum at the respective energy. Only Sc-45 is mono-isotopic in the elemental form. Minor isotopic contributions degrade the performance of both Fe-56 and Si-28 filters. Secondary and composite filter systems have been employed for special purposes as illustrated by the extensive capture gamma-ray studies of Bollinger et al. (46) but these are not of general usefulness.

The iron filter is perhaps in widest use and its application well illustrates the power and the problems of the method. The Fe-56 total cross section is known to display a very deep minimum (8-9 mb) at 24.5 keV as illustrated in Fig. 11 (41). This minimum value can increase by factors of 4-5 with very small chemical impurities. In elemental iron the corresponding minimum value is nearly two orders of magnitude larger. Clearly, filter thickness must be

carefully considered and there is motivation for very good isotopic and chemical purity with the associated problem of material availability. There are characteristically a number of higher-energy satellite windows. The satellite windows are largely "closed" by judicious selection of additional components in the filter. When properly done 99+% of the transmitted intensity falls within a few keV of the primary 25 keV window as illustrated in Fig. 12. In this particular example the performance is achieved with elemental iron of reasonably available purity. The intensity in the window is approximately  $10^5$  n/cm<sup>2</sup> when using a 5-10 megawatt reactor. Improved spectral performance and a two order of magnitude increase in intensity can be achieved by using an isotopic filter and a more powerful reactor. The variation of spectral distribution with filter thickness is shown in Fig. 13. Backgrounds and spectral distributions can be improved by attention to the configuration of the primary neutron source within the reactor core as illustrated in Fig. 14. In this example, rather than looking directly at the primary fission source, a titanium scattering source is used with the resulting reduction in gamma-ray background and satellite components, all-be-it at some compromise of intensity.

The above concepts, illustrated by the iron example, can be directly extended to the Sc-45, Si-28 and other applications (44). Again, careful attention to filter composition and the primary source results in beam spectra with approximately 99% of the intensity in a very narrow and well defined energy band.

These filtered beam sources are very stable and very reproducible. They provide excellent standard fields of good intensity in an energy region difficult to address by other means. The beams are nearly monoenergetic and steady state. The number of high-quality energies is limited. Secondary-reaction-spectroscopy requires a spectral sensitive detector. Recent advances in the GeLi detection of gamma-rays and the measurement of neutron spectra by proton recoil counters have greatly increased the power of the filtered beam concept in both gamma- and neutron-spectroscopy.

#### B. At pulsed white-source accelerators

Filters, particularly of iron, have been effectively used at pulsed white-source accelerators, notably at RPI and ORNL (41,48). Beyond the well known energy, the advantage of the method is increased intensity (primary flight path is no longer an essential concern) and a well known time of burst. What is achieved is essentially a pulsed monoenergetic source whose intensity often exceeds that available with the conventional monoenergetic facility. The method has been used at very large white-source facilities with pulse durations of 5-25 nanoseconds. However, there seems to be no inherent limitation to productive use at much smaller facilities and with time scales in the fractional nanosecond range.

#### C. Inverse filters, or the bright-line detector

One can make use of the filter principle in an inverse manner using very modest monoenergetic facilities. A detector response can be obtained with good resolution at a well known energy where other techniques are difficult. For example, the prominent 89 keV resonance in Mg-24 has been used

to obtain a scattered-neutron-detector response with a resolution of about 5 keV. Such a detector is being employed in inelastic-scattering measurements involving heavy and deformed actinides. It provides a degree of resolution not easily obtained in this low energy region using other methods.

## VI. PILE-NEUTRON SOURCES

### A. Large Reactors

About 30 years ago Arthur Snell reviewed neutron sources and concluded that a reactor was a costly research-neutron factory (49). The conclusion was prophetic. By 1966, at the INS Conference (50) it was clear that the trend was toward pulsed neutron sources for fast-neutron research purposes, while the steady-state reactor remained promising for condensed-matter studies. That position has been eroded in the intervening 15 years. Several large reactors (e.g. BNL and Grenoble Franco-German) have come into use, primarily for condensed-matter work, but a number of other similar projects have been aborted. New projects, under construction or recently commissioned (e.g. ANL-IPNS, Rutherford Laboratory, Harwell-linac and Dubna-IBR-II), are pulsed devices; either accelerator driven, pulsed reactors, or both. It is difficult to avoid the conclusion that the large steady-state research reactor is a costly source approaching a technological intensity limit thus restricting future utility in neutron-nuclear research and there are similar considerations in the area of condensed matter studies. Certainly, such devices are far too costly and specialized to be implemented by any but the most affluent.

### B. Reference Fields

Certain technological applications make wide use of standard fast-neutron reference fields. These fields are provided by cavities introduced in moderate-sized (few MW) reactor thermal columns. The fast-neutron spectral distribution is determined by the configuration and composition of the cavity lining always including a fissile material. With care, the spectrum can be made to closely approach that of technological interest (e.g. a fast-fission-reactor spectrum). Computational and experimental techniques can be used to determine the exact spectral character. Illustrative of such a reference cavity and its associated field is the ISNF facility at the National Bureau of Standards shown in Fig. 15 (51).

### C. Modest Source Reactors

Very modest reactors can be exceedingly useful ancillary neutron sources supporting measurement programs over a wide scope. They can, for example, provide precise calibrations of cross sections at thermal, prepare standard-reference activities and undertake materials assay using activation techniques. The devices are simple, relatively cheap and safe. A number already exist throughout the world. Illustrative of this type of reactor is the ANL-Argonne Thermal Source Reactor (ATSR) shown in Fig. 16. This light-water-moderated reactor first ran at the 1958 Geneva Conference and since then has been in routine use at powers of up to 10 kW. Thermal- and fast-neutron fluxes are readily available to levels of  $\sim 10^{12}$  n/cm<sup>2</sup>. There are also facilities for fast sample transfer (rabbit) and beam extraction. These capabilities have long met many requirements at a large laboratory involving both microscopic

and macroscopic neutron research. Operation is on a "on demand" basis. Fuel life is practically infinite and radioactivity encountered during and after use is modest.

#### VII. A CONCLUDING REMARK

In the beginning it was pointed out that source intensity is often considered the essential factor in neutron physics.

In the end it is suggested that the paramount consideration is system effectiveness, of which the source is only one factor. One cannot help but wonder what would have happened if the resources that have gone into some large-source developments had been devoted to creative physical concepts and their experimental investigation. It remains true that the creative and innovative concepts very often occur and can be exploited in modest circumstances. It is hoped that this gathering will stimulate such accomplishments.

#### ACKNOWLEDGEMENTS

The author is indebted to a host of able men who have tutored him on neutron physics (often without success) over many years. Particularly notable are Dr. Alexander Langsdorf Jr., Professor H. W. Newson and members of the Applied Nuclear Physics Section (AP-ANL).

#### REFERENCES

1. E. Anderson and R. Neff, Nucl. Instr. and Methods, 99 231 (1972).
2. E. Lorch, Inter. Journal of Applied Radiation and Isotopes, 24 585 (1973).
3. K. Geiger and L. VanderZwan, Health Physics, 21 120 (1971).
4. G. F. Knoll, private communication (1980).
5. Properties of Cf-252 spontaneous-fission source.  $t_{1/2} = 2.65$  yrs,  $\bar{\nu} \sim 3.75$  n/f, Ave. energy  $\sim 2.14$  MeV.
6. A. Smith, P. Guenther and R. Sjoblom, Nucl. Instr. and Methods, 140 397 (1977).
7. J. Boldeman, National Bureau of Standards Pub., NBS-493 (1977); see also R. Spencer et al., Oak Ridge National Lab. Report, ORNL/TM-6805 (1979) and ORNL/TM-7148 (1980).
8. For example, L. Green et al., Proc. Conf. on Nuclear Cross Sections and Technology, 325 (1971).
9. J. Grundl and C. Eisenhauer, National Bureau of Standards Pub., NBS-425 (1975); See also V. Spiegel, private communication (1975).
10. S. A. Cox, Argonne National Laboratory Report, ANL/NDM-5 (1974).

11. J. Boldeman, D. Culley and R. Cawley, Proc. Inter. Conf. on Nuclear Physics and Nuclear Data for Reactors and Other Applications, Harwell (1978).
12. A. Smith, P. Guenther, G. Winkler and R. McKnight, Argonne National Laboratory Report, ANL/NDM-50 (1980).
13. J. Salome and K. Böckhoff, Bull. Am. Phys. Soc., 24 7 (1979).
14. S. Cierjacks, Proc. Inter. Conf. on the Interaction of Neutrons with Nuclei, CONF-760715-P2 (1976).
15. G. Auchampaugh, Bull. Am. Phys. Soc., 24 7 (1979).
16. R. Holt and H. Jackson, Private Comm. (1980).
17. C. Bowman, Bull. Am. Phys. Soc., 24 7 (1979).
18. R. Booth, Lawrence Livermore Laboratory Report, UCRL-70183 (1967).  
See also Nucl. Instr. and Methods, 99 1 (1974).
19. D. Johnson et al., Jour. Nucl. Materials, 85 467 (1979).
20. J. Cockroft and E. Walton, Proc. Roy. Soc., A136 619 (1932).
21. J. Chadwick, Nature, 129 312 (1932).
22. All Q-values calculated from The Table of Isotopes, 7th Edition, C. Lederer and V. Shirley editors, John Wiley and Sons, Inc., Pub. New York (1978).
23. H. Liskien and A. Paulsen, Nucl. Data Tables, 11 569 (1973).
24. M. Mier, National Bureau of Standards Publication, NBS-493 (1977).
25. R. C. Haight, Sym. on Neutron Cross Sections from 10-40 MeV, Brookhaven National Laboratory Report, BNL-NCS-50681 (1977).
26. G. Grenier, 3rd Sym. on Neutron Dosimetry in Biology and Medicine, Munich (1977).
27. P. Stelson et al., Nucl. Phys., 68 97 (1965).
28. J. Kammerdiener, Lawrence Livermore Laboratory Report, NCRL-51232 (1972).
29. D. Smith and J. Meadows, Argonne National Laboratory Report, ANL/NDM-9 (1974).
30. R. Taschek and A. Hemmendinger, Phys. Rev., 74 373 (1948).
31. J. Davis et al., Phy. Rev., C4 1061 (1971).
32. J. Brandenberger, National Bureau of Standards Publication, NBS-493 (1977).

33. J. Meadows and D. Smith, Argonne National Laboratory Report, ANL-7938 (1972).
34. H. Liskien and A. Paulsen, Atomic Data and Nuclear Data Tables, 15 57 (1975).
35. P. Byerly Jr., Fast Neutron Physics, Eds. J. Marion and J. Fowler, Interscience Publishers, New York (1963).
36. A. Smith, P. Guenther, D. Haveland and J. Whalen, Argonne National Laboratory Report, ANL/NDM-29 (1977).
37. G. Auchampaugh, S. Plattarel and N. Hill, Nucl. Sci. and Eng., 69 30 (1979).
38. J. B. Marion, Rev. Mod. Phys. 38 660 (1966).
39. J. Meadows and D. Smith, elsewhere in these proceedings.
40. O. Simpson, J. Smith and J. Rodgers, Proc. Sym. on Neutron Standards and Flux Normalization, AEC Sym. Series #23 (1971).
41. R. E. Chrien et al., National Bureau of Standards Pub., NBS-493 (1977).
42. E. McGarry and I. Schroder, National Bureau of Standards Pub., NBS-493 (1977).
43. F. Tsang and R. Brugger, private communication (1976).
44. I. Schroder, R. Schwartz and E. McGarry, National Bureau of Standards Pubs., NBS-493 (1977).
45. E. Bennett, private communication (1980).
46. L. Bollinger et al., Exp. Neutron Resonance Spectroscopy, Editor, J. Harvey, Academic Press, New York (1970).
47. R. C. Block et al., CONF-720901, Vol. 2 p. 1107 (1972), See also J. Nucl. Sci. and Tech. 12 1 (1975).
48. R. Greenwood, R. Chrien and K. Rimawi, Proc. Conf. on Nucl. Cross Sections and Technology, NBS-425 (1975).
49. A. H. Snell, Physics Today, 9 7 (1954).
50. Proc. Seminar on Intense Neutron Sources, CONF-660925 (1966).
51. C. Eisenhauer, J. Grundl and A. Fabry, National Bureau of Standards Pub., NBS-493 (1977).

Table 1. Illustrative Be( $\alpha$ ,n) Neutron Sources

Source	Half-life	$E_{\alpha}$ (MeV)	Neutron Yield per $10^6$ Primary Alphas		Percent Yield with $E_n < 1.5$ MeV	
			Calculated <sup>a</sup>	Experimental	Calculated	Experimental
$^{239}\text{Pu}/\text{Be}$	24000y	5.14	65	57	11	9-33
$^{241}\text{Am}/\text{Be}$	433 y	5.48	82	70	14	15-23

<sup>a</sup>Calculated values from G. Knoll et al.Table 2. Illustrative ( $\gamma$ ,n) Neutron Sources

Gamma Ray Emitter	Half- Life	Gamma Energy (MeV)	Target	Neutron Energy (keV)	Neutron Yield, n/s for $10^{10}$ Bq activity
$^{24}\text{Na}$	15.0 h	2.7541	Be	967	340 000
		2.7541	D	263	330 000
$^{124}\text{Sb}$	60.2 d	1.6910	Be	23	210 000

Table 3. Specifications of Accelerator-Based Pulsed Neutron Facilities as Taken from Ref. 14.

Accelerator	Part.	Target	Energy (MeV)	Peak Current (mA)	Instant Neutron Intensity*	Repet. Rate (pps)	Average Neutron Intensity*	Pulse Duration (nsec)	Flight Path Length (in Meters)	Best Nominal Resolution (nsec/m)
Upgraded Geel Linac	e	U	120	10,000	$4 \cdot 10^{18}$	900	$1 \cdot 10^{13}$	3	30-400	0.008
				600	$2.5 \cdot 10^{16}$	900	$4.5 \cdot 10^{14}$	2,000		
Existing Harwell Linac	e	U	45	1,000	$2 \cdot 10^{17}$	500	$1 \cdot 10^{12}$	10	100	0.1
		U-booster	42	500	$5 \cdot 10^{17}$	500	$2.5 \cdot 10^{13}$		5-300	0.3
Scheduled New Harwell Linac	e	(U Ta)	120	6,000	$2 \cdot 10^{18}$	2,000	$2 \cdot 10^{13}$	5	5-400	0.01
			80	1,000	$3 \cdot 10^{17}$	300	$2 \cdot 10^{14}$	2,000		
		U-booster	110	1,000	$3 \cdot 10^{18}$	300	$1 \cdot 10^{14}$	100		
Kurchatov Linac	e	U	60	1,000	$3 \cdot 10^{17}$	50	$8 \cdot 10^{11}$	50	10-300	0.16
				1,000	$3 \cdot 10^{17}$	150	$2.5 \cdot 10^{14}$	5,500		
Above-Ground NBS-Linac	e	Ta	120	4,000 <sup>+</sup> )	$8 \cdot 10^{17}$	720	$3 \cdot 10^{12}$	5	20-200	0.025
			100	300	$6 \cdot 10^{16}$	200	$1 \cdot 10^{13}$	1,000		
								0.05		(0.003) <sup>++</sup> )
Livermore Linac	e	Ta	115	10,000	$2 \cdot 10^{18}$	1,440	$1.5 \cdot 10^{13}$	5	7-250	0.02
			100	350	$7 \cdot 10^{16}$	360	$8 \cdot 10^{13}$	3,000		
Oak Ridge Linac	e	Ta	140	15,000	$4 \cdot 10^{18}$	1,000	$1.2 \cdot 10^{13}$	3	10-200	0.01
			140	500	$1 \cdot 10^{17}$	1,000	$1 \cdot 10^{14}$	1,000		
RPI Linac	e	Ta	80	7,000	$7 \cdot 10^{17}$	720	$5 \cdot 10^{12}$	10	10-250	0.04
			45	900	$5 \cdot 10^{16}$	360	$8 \cdot 10^{13}$	4,500		
Harwell Synchrocycl.	p	W	150	3,000	$3 \cdot 10^{19}$	800	$1 \cdot 10^{14}$	4	8-100	0.04
Columbia Synchrocycl.	p	Ta	600	6,600 <sup>+++</sup> )	$3.2 \cdot 10^{20}$	300	$1 \cdot 10^{15}$	10	35-200	0.05
Karlsruhe Isochr. Cycl.	d	U	50	1,000	$7 \cdot 10^{18}$	20,000	$2 \cdot 10^{14}$	1.5	10-200	0.008
					$7 \cdot 10^{17}$	200,000	$2 \cdot 10^{14}$			
Kiev Isochr. Cyclotron	d	U	60	2,000	$1.7 \cdot 10^{18}$	20,000	$3.4 \cdot 10^{14}$	1	200	0.005
Los Alamos WNR Fac.	p	W	800	340	$2 \cdot 10^{19}$	120	$7 \cdot 10^{11}$	5	4-200	0.02
						120	$1 \cdot 10^{15}$	6,000		

\*neutrons/sec; <sup>+</sup>)with the new gun a peak current of 20,000 mA is expected; <sup>++</sup>)See text; <sup>+++</sup>)Assuming that the present design goal of 25  $\mu$ A average beam current is met, presently only 1  $\mu$ A is realized.



Table 4. Fusion Materials Irradiation Test Neutron Source

---

Characteristics	
Continuous Output	$2 \times 10^{16}$ Neutrons/sec
Mean Neutron Energy	14 MeV
Peak Neutron Flux	Near $10^{15}$ n/cm <sup>2</sup> - sec
Primary Test Volume	1 Liter
Deuterium Beam	
Current	0.1 A
Energy	35 MeV
Lithium Target	
Flow Velocity	12 Meters/sec
Average Temperature Rise	50°
Target Size	1 x 10 x 2 cm

---

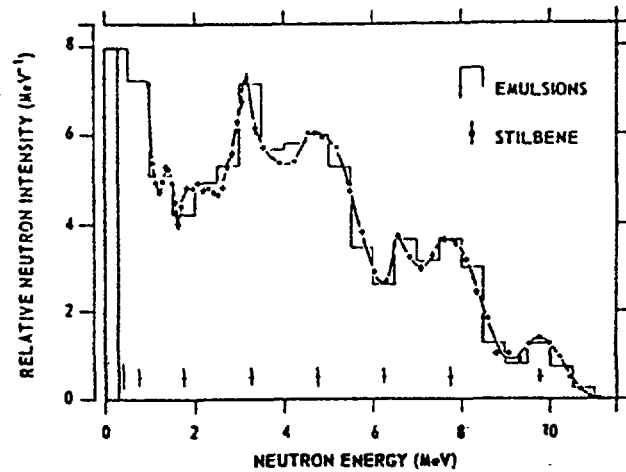


Fig. 1. Illustrative neutron energy spectrum from a Pu-239/Be source (1).

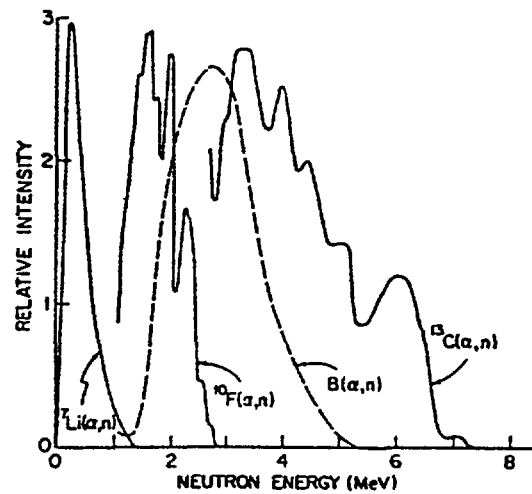


Fig. 2. Illustrative neutron spectra obtained using the (α,n) reaction and "alternate" radiators (2,3).

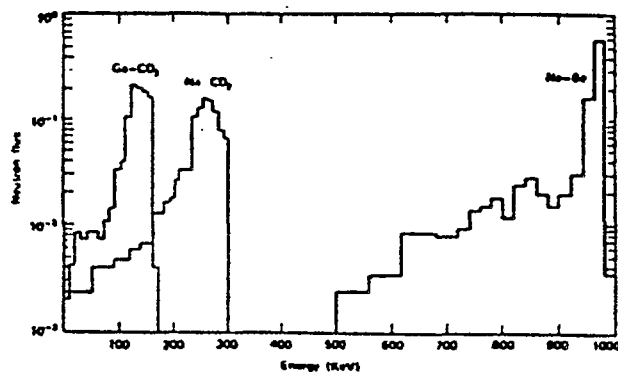


Fig. 3. Illustrated neutron spectra from three (γ,n) sources as calculated by Knoll et al. (4).

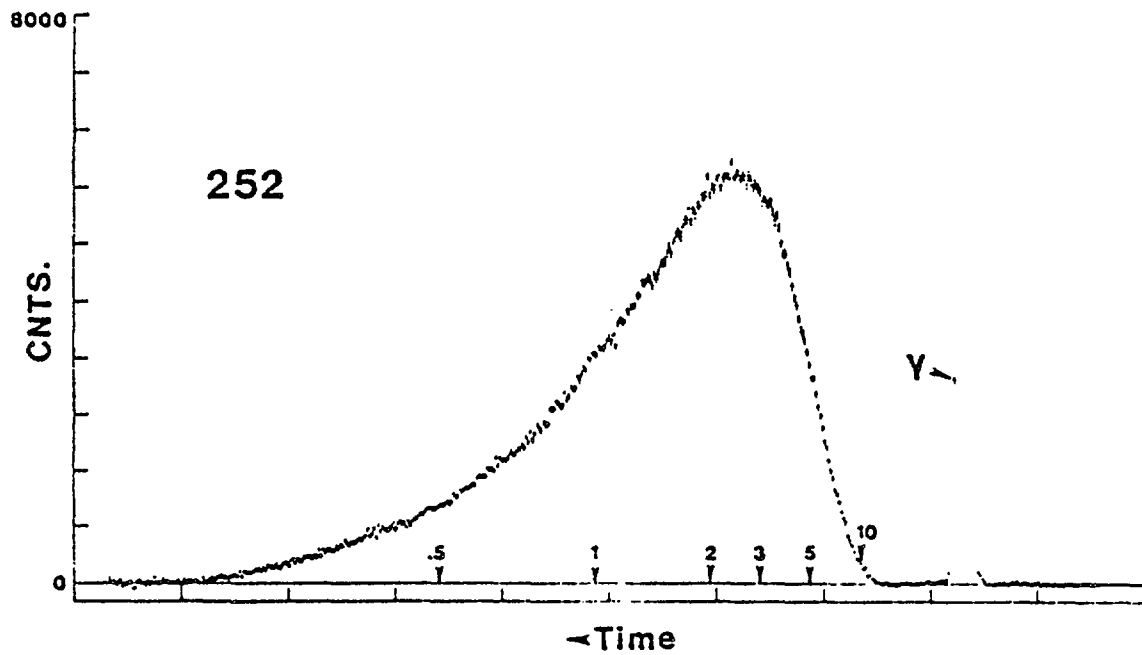


Fig. 4. Illustrative measured velocity spectrum of Cf-252 fission neutrons (8).

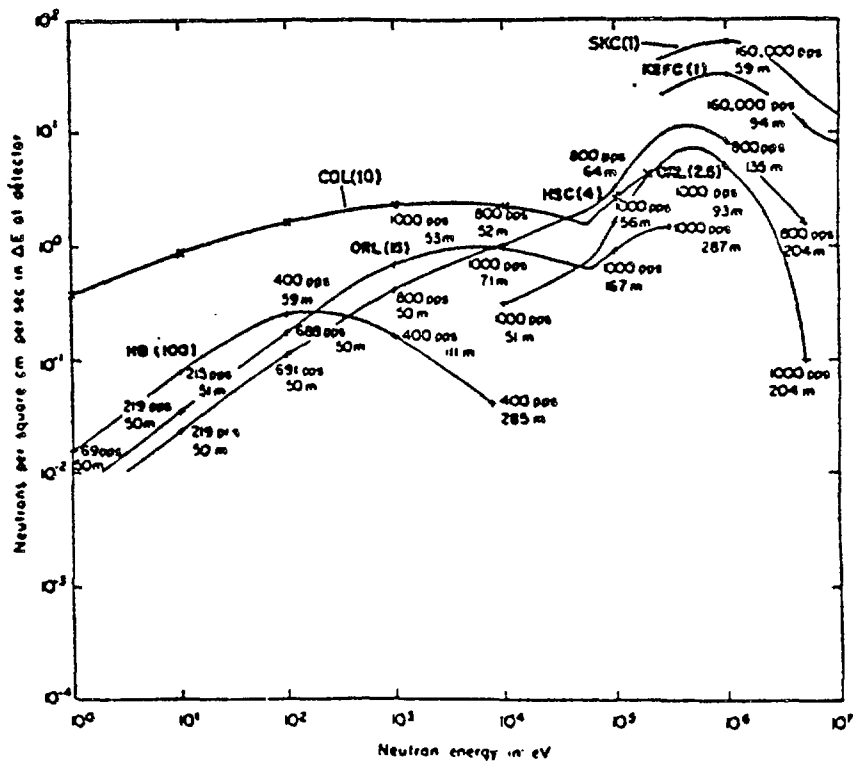


Fig. 5. Illustrative intensities for a variety of large pulsed-accelerator sources (taken from Ref. 14).

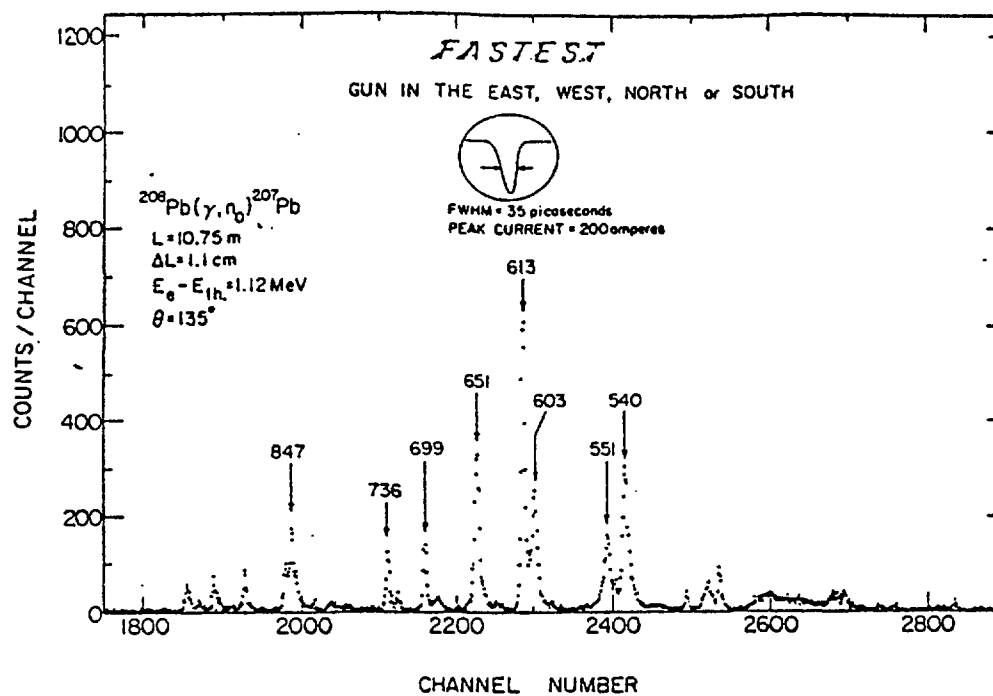


Fig. 6. Illustrative  $^{208}\text{Pb}(\gamma, n)$  spectra obtained using a modest facility (16).

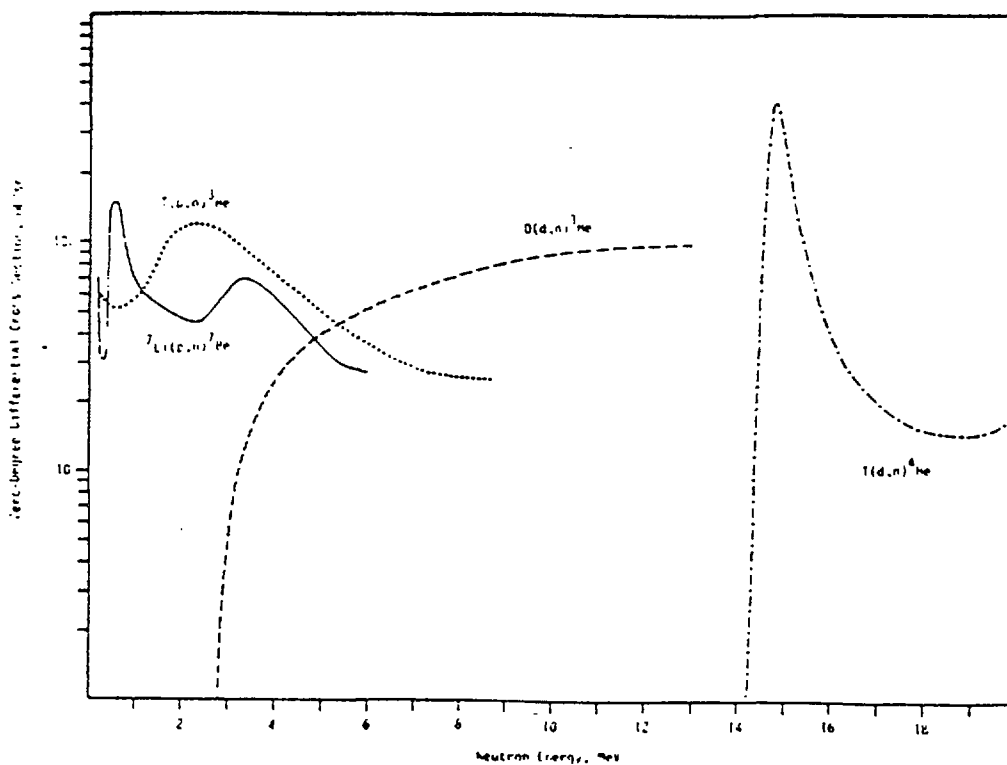


Fig. 7. Neutron yields for the "big-4" taken from Ref. 39.

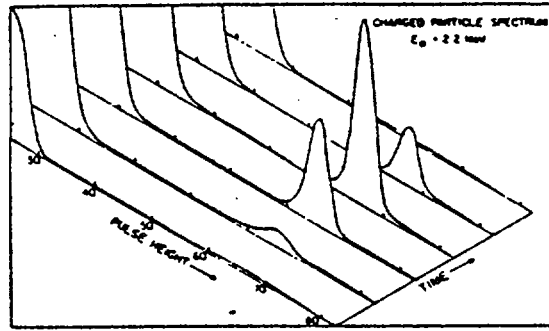


Fig. 8.  $^3\text{He}$  particles from the  $\text{T}(\text{p},\text{n})$  reaction at a proton energy of 2.25 MeV (24).

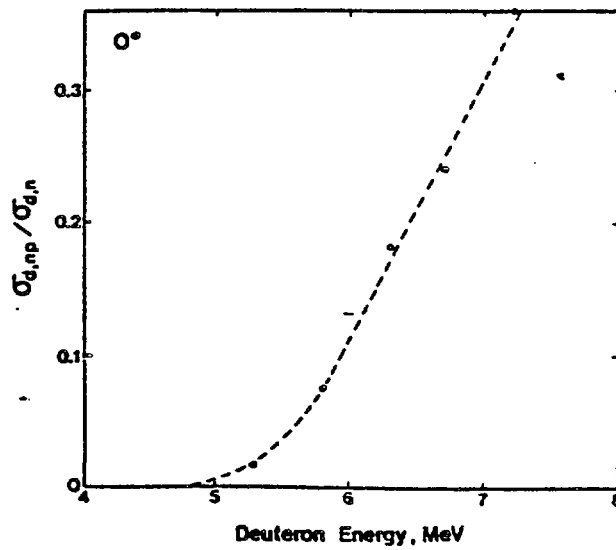


Fig. 9.  $(\text{d},\text{np})/(\text{d},\text{n})$  neutron yields as function of  $E_d$ , Ref. 39.

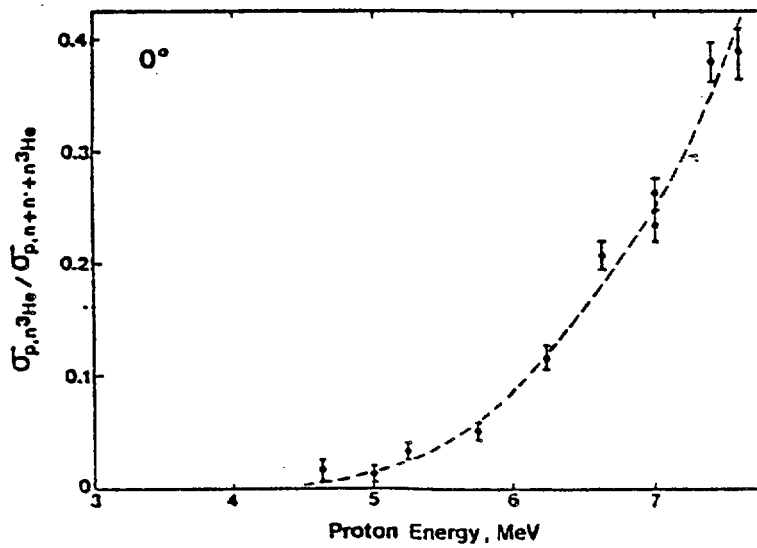


Fig. 10. Breakup fraction observed using  $^7\text{Li}(\text{p},\text{n})$  target, Ref. 20.

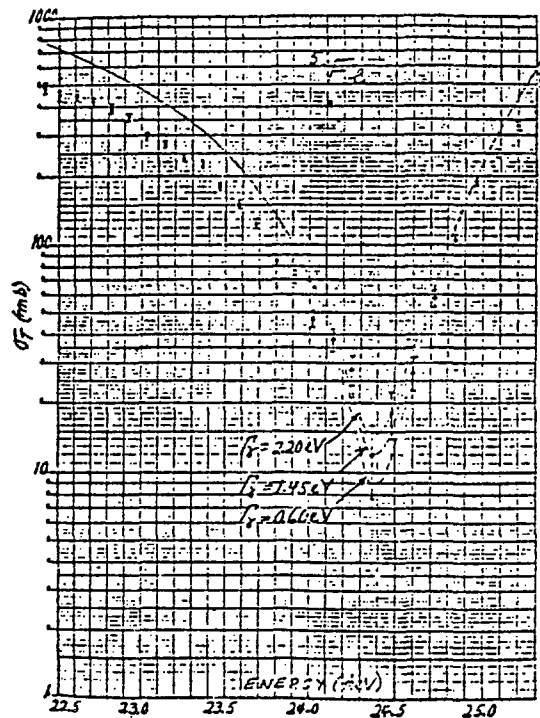


Fig. 11. 24.5 keV window in the neutron total cross section of iron-56 (41).

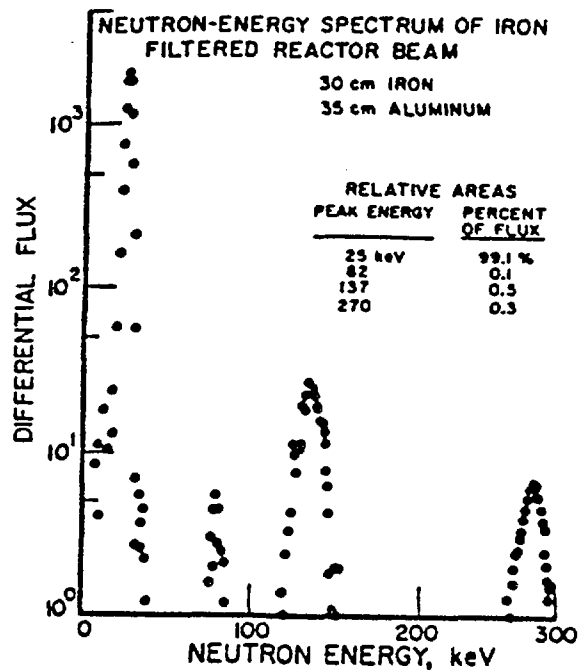


Fig. 12. Iron-filtered beam using composite filter construction (42).

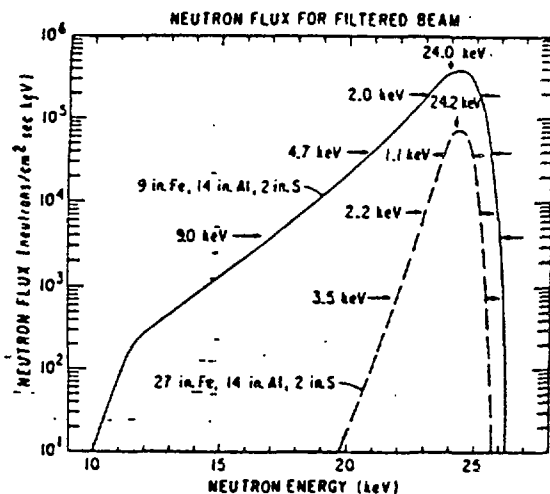


Fig. 13. Calculated flux through two thicknesses of composite iron filter (48).

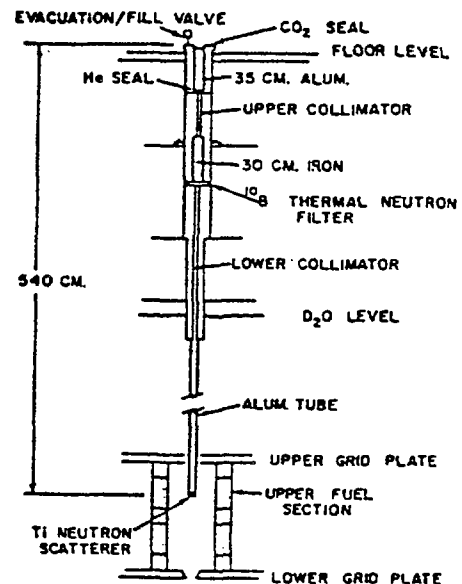


Fig. 14. Filtered-beam configuration using a titanium-scattering source (48).



November 29, 1979

Résumé on neutron yields from  $\alpha$ -particle bombardment of light elements

K.W. Geiger, Division of Physics, National Research Council, Ottawa,  
Canada K1A 0R6

1. Introduction

The thick target neutron yield which results from  $\alpha$ -particle bombardment of light elements is important for environmental considerations in the spent fuel technology. The yield can also serve as an additional parameter in chemical analysis. Actinide  $\alpha$ -emitters are produced by successive neutron capture when burning the fuel in a reactor. Inevitably these  $\alpha$ -emitters come into contact with light elements, either by chemical processing or because the fuel itself has a light element component when, for instance, it consists of  $\text{UO}_2$  or UC. The spent fuel will, in addition to spontaneous fission neutrons, exhibit neutron emission through  $(\alpha, n)$  reactions. To evaluate such complex actinide plus light element system one needs to know the thick target  $(\alpha, n)$  yields as a function of incident  $\alpha$ -energy.

2. Thick target  $(\alpha, n)$  neutron yields

The yields can be measured directly by using a positive ion generator, capable of producing  $\alpha$ -particles of up to 8 MeV and thick targets of those elements which emit significant numbers of neutrons. On the other hand, the yields can be calculated from existing  $(\alpha, n)$  total neutron cross section data combined with the stopping powers for the respective target element. References 1 to 4 are the principal papers which deal with the problem.

In the first two papers, yields are calculated using cross section data for Li, Be, B, C, N, O, Ne, Mg, Si and  $\text{UO}_2$ . Uncertainties are approximately  $\pm 30\%$ . For the rather important element fluorine, no appropriate cross section data are available. For magnesium, a rather old excitation curve by Halpern (1949) was used in ref. 2. The  $^{26}\text{Mg}(\alpha, n)$  cross section only was used in ref. 1. For this reason, Dr. Van der Swan and myself have just begun a  $^{25}\text{Mg}(\alpha, n)$  study at this laboratory. The most abundant  $^{26}\text{Mg}$  does not contribute to the neutron yield.

Actual thick target measurements were carried out in ref. 3 and 4, using a Van de Graaff generator and a  $4\pi$  detector surrounding the target. This detector needs to have an efficiency which is independent of neutron energy. This can never quite be achieved and presents a major difficulty. Even if the efficiency variation with energy is known, it is often impossible to apply the correction since low energy neutron groups populate excited states of the product nucleus. Relative intensities for various neutron groups are frequently unknown. In addition to the elements listed earlier, yields for F, Al, Fe and UC were determined.





Fig. 1 shows a comparison between yields of ref. 2 and 3. Good agreement between measurement and calculation is obtained, except for Si and  $\text{UO}_2$ , where differences of up to a factor of two occur. I believe this is caused mostly by poor input data for the calculations. The effect of input data is illustrated well

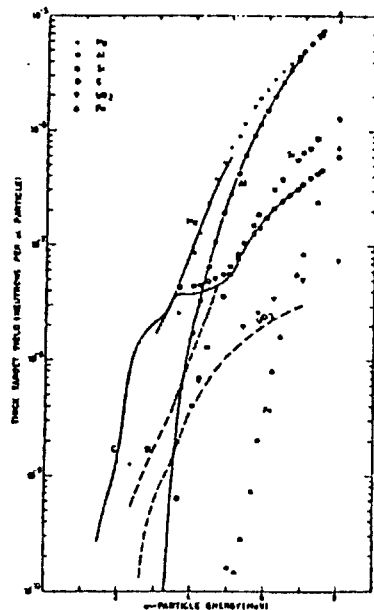


Fig. 1. The points show experimental values for thick target ( $\alpha, n$ ) neutron yields<sup>3</sup>). The lines represent the calculated yields of ref. 2. The figure is taken from ref. 3.

for the case of beryllium, where a number of measurements and calculations are available, see table 1.

Table 1.  $\text{Be}(\alpha, n)$  yield at 5.5 MeV  $\alpha$ -energy

Method	Ref.	Yield per $10^6$ $\alpha$ -particles
Thick target measurement	4	$65 \pm 4$
$Y = 0.95 \times 0.152 E_{\alpha}^{3.65}$	quoted in 5	61
Max., Po-Be source	6	$69 \pm 2$
Calculated	6	$61 \pm 2$
"	2	$86 \pm 25$
"	5	$73 \pm 7$

It should be noted that the measurement (first entry in the table) does not include a correction of about +5% to take care of the fall-off in detector sensitivity with neutron energy and of the  $\text{Be}(n, 2n)$  reaction within the target. The last two entries use the same nuclear cross section data<sup>5</sup>) but different atomic stopping cross sections for beryllium<sup>7,8</sup>). The Be nuclear cross section data are known better than for any of the other elements.

### 3. Conclusions

In an intimate mixture of target material and  $\alpha$ -emitting actinides, such as in spent fuel, the  $\alpha$ -particles are slowed down and may interact at any energy, from the maximum available. Also the  $\alpha$ -particles travel into all directions. Therefore, the distinct neutron spectrum, otherwise found with thin targets, is very much broadened. Because the spectra have lost most of their identity, I believe it would only be possible in rare cases to obtain a chemical analysis from a measured neutron spectrum. The neutron spectrum is further degraded when it passes through the material. However, the measured neutron intensity itself is clearly a further parameter to be considered when combined with other methods of chemical analysis.

### References:

1. E.H. Tsentser and A.B. Silin, *Atomnaya Energiya* 19, 914 (1965)
2. H. Liskien and A. Paulsen, *Atomkernenergie* 30, 59 (1977)
3. D. West and A.C. Sherwood, OECD Conf. Harwell "Neutron Physics and Nuclear Data" p. 610 (1978)
4. J.K. Bair and J. Gomez del Campo, *Nucl. Sci. Eng.* 71, 18 (1979)
5. K.W. Geiger and L. Van der Zwan, *Nucl. Instr. Meth.* 131, 315 (1975)
6. H.E. Anderson and M.R. Hertz, *Nucl. Sci. Eng.* 44, 437 (1971)
7. J.F. Ziegler and W.K. Chu, *Atomic Data and Nuclear Data Tables* 13, 463 (1974); C.F. Williamson, J.-P. Boujot and J. Picard, Report CEA-R 3042 (1966)
8. M. Bader, R.E. Pixley, F.S. Mozer and E. Whaling, *Phys. Rev.* 105, 32 (1956).



Radioactive Be( $\alpha$ ,n) and Be( $\gamma$ ,n) neutron sources

K.W. Geiger  
Division of Physics, National Research Council of Canada  
Ottawa, Canada K1A 0R6

March 17, 1980

1. Introduction

The neutron was discovered in 1932 by Chadwick as a product of the Be+ $\alpha$  reaction. Since then, radioactive Be( $\alpha$ ,n) and Be( $\gamma$ ,n) sources have found widespread use because of their smallness and hence their easy portability. The variation of neutron emission rate with time is predictable. Therefore such sources serve as laboratory standards for instrument calibration, in particular of neutron protection instrumentation. Thermal neutron flux density standards contain these sources for the same reason. Industrial applications include their use in soil moisture meters and in other small probes for the study of geological formations. Disadvantages are the broad neutron spectrum of ( $\alpha$ ,n) sources and the  $\gamma$ -rays which accompany  $\alpha$ -emission.

For activation analysis and for neutron radiography these sources have in the last decade been replaced by  $^{252}\text{Cf}$  fission sources which have much higher neutron emission rates per unit source weight and only few accompanying  $\gamma$ -rays. Their disadvantage is the relatively short half-life of 2.6 years. Nevertheless, for neutron emission rates of up to  $10^6 \text{ s}^{-1}$ , Be( $\alpha$ ,n) and Be( $\gamma$ ,n) sources are often the most suitable ones. A discussion of their properties is timely since during recent years, new results became available on measured and calculated spectra. It is essential to know the shape of these spectra accurately for dosimeter calibration so as to be able to make the appropriate fluence to kerma conversion.

## 2. Experimental Be( $\alpha$ ,n) source spectra

To understand the formation of the neutron spectrum from radioactive Be( $\alpha$ ,n) sources, let us first consider the thin target situation where, because of the energy conservation law, a line spectrum is obtained. Fig. 1 shows the energy level diagram. Neutron groups  $n_0$  to  $n_3$  are expected, populating the well known states in  $^{12}\text{C}$ . An example of a thin target spectrum is given in fig. 2. Except for the  $n_0$  group which is outside the dynamic range of the stilbene spectrometer used, the groups  $n_2$  to  $n_3$  are clearly visible. But note the neutron continuum below 3.5 MeV. This might partly be caused by broad levels in  $^{12}\text{C}$  above 9.6 MeV but the main contribution is caused by the break-up reaction



involving the 1.67, 2.43 and 3.06 MeV levels of  $^9\text{Be}$  (OBS72). This interpretation was already put forward in 1938, see AMA59. We will later discuss the continuum in more detail.

Let us now look at what happens when we replace the thin Be layer by a target thicker than the range of the incoming  $\alpha$ -particle beam (fig. 3). The bombarding energy is 5.48 MeV, corresponding to the  $\alpha$ -particle energy from  $^{241}\text{Am}$ . Since we now have a continuous distribution of  $\alpha$ -energies within the target we get a broadening of the lines but not as yet an overlap. Because of the recoil given to

the compound nucleus, the neutron energy in the laboratory system changes with the angle of observation. After weighting the spectra with the appropriate solid angle, their sum will simulate the spectrum of an  $^{241}\text{Am}$ -Be source shown on top of fig. 3. In a radioactive neutron source we have an intimate mixture of Be and  $\alpha$ -emitter. Not only is a continuous  $\alpha$ -energy distribution present, but also the observation occurs at all angles, leading to further broadening of the spectra.

A typical source capsule for radioactive ( $\alpha$ ,n) sources is shown in fig. 4. To obtain a nearly equal neutron fluence rate into all directions, it is desirable to make the source as spherically symmetrical as possible. For the more usual cylindrical shape, length and diameter should be about equal and the inner capsule should be inverted. The source material may either be a pressed pellet, a sintered pellet or an alloy, such as  $\text{AmBe}_{13}$  in a Be matrix. For a high relative source yield an excess of Be is needed. For a neutron standard, the alloyed source is the preferred one because the alloy ensures that no physical change takes place during the lifetime of the source.

Until the beginning of the last decade the results of the spectra measurements were quite varied and inconsistent. An example for  $^{210}\text{Po}$ -Be is given in fig. 5. The spectrum by Whitmore and Baker (WHI50) is noteworthy: It is based on the analysis of 7000 proton recoil tracks in emulsion and it will be seen later that the shape comes close to the expected one. A more recent spectrum by MED62 is of similar shape. The situation for  $^{241}\text{Am}$ -Be is given in fig. 6, which also lists the various spectrometers used. The word "barrel" applies to a spectrometer where a barrel shaped hydrogenous

foil is placed around the axis between source and proton recoil detector in such manner that the scattering angle becomes independent of the scatter location.

### 3. The calculation of spectra from Be( $\alpha$ ,n) sources

These large discrepancies which were also seen in sources like Ra-Be, Pu-Be etc., prompted L. van der Zwan and myself to calculate the spectra from known differential Be( $\alpha$ ,n) cross sections (GEI75). By 1974 sufficient cross section data were available, including those for the break-up of  $^9\text{Be}$  which produces the neutron continuum. The low energy component had rarely been measured directly on sources but needs to be known well when calculating the kerma produced by a source spectrum.

Obst et al. (OBS72) measured the angular dependence of the cross section responsible for the continuum in great detail by the time of flight method. As an example, a series of these spectra at  $E_\alpha = 5.38$  MeV is shown in fig. 7. The authors were also able to establish from which of the excited states of  $^9\text{Be}$  the neutrons originated (fig. 8). The low energy limit of the time of flight method was 0.5 MeV but Werle et al. (WER73) were able to extend the energy range down to 0.1 MeV using proportional counters. Again, an example is seen in fig. 9. Combining these data we obtained the thin target, angle integrated cross sections shown in fig. 10. As there were no measurements available extending below 0.1 MeV neutron energy, the curves were extrapolated to zero intensity at  $E_n = 0$ . These cross section curves are identical to the thin target continuum spectra when observed from all angles.

For the  ${}^9\text{Be}(\alpha, n){}^{12}\text{C}$  reaction cross section the published data were carefully evaluated, appropriately averaged and smoothed. The compilation is given in GEI76. The data had been adjusted to a certain extent to follow the direct measurement of the total neutron production by GIB65 as seen in fig. 11. The uncertainties in "SUM" are estimated to be  $\pm 8\%$  whereas for the individual neutron groups they are somewhat larger. The relative angular distributions have an uncertainty of  $\pm 5\%$  for the  $n_0$ ,  $n_1$  and  $n_2$  groups.

The neutron spectra can now be calculated. We consider at the moment an idealized source where the  $\alpha$ -particles are slowed down only in the Be matrix and not in the  $\alpha$ -emitter itself. Then, for  $\alpha$ -particles of an energy between  $E_\alpha$  and  $E_\alpha + \Delta E_\alpha$  the distribution of neutrons per unit energy interval is

$$F(E_n) = \sigma(\theta) \frac{2\pi \sin \theta d\theta}{dE_n} \frac{\Delta E_\alpha}{\epsilon} \quad (1)$$

where  $\sigma(\theta)$  is the c.m. differential cross section for neutron production and  $\epsilon$  the stopping cross section for beryllium at  $E_\alpha$ . The neutron energy in the laboratory system may be expressed as a function of the c.m. angle in the form (MAR68)

$$E_n = a + b \cos \theta. \quad (2)$$



This allows rewriting of eq. 1 in terms of  $E_n$ :

$$F(E_n) = \sigma(E_n) \frac{4\pi}{E_n(\theta=0) - E_n(\theta=\pi)} \frac{\Delta E_\alpha}{\epsilon} \quad (3)$$

where  $E_n(\theta=0)$  and  $E_n(\theta=\pi)$  are the maximum and minimum neutron energies kinematically possible. The neutron energy distributions for a particular  $\alpha$ -energy are therefore simply proportional to the c.m. differential cross section expressed as function of neutron energy, see fig. 12. Note that an isotropic angular distribution in the c.m. system results in a neutron spectrum of rectangular shape. A graphical approach used by LEH68 further illustrates the method (fig. 13). Fig. 14 shows the addition of such partial spectra. We have actually added the spectra in steps of  $\Delta E_\alpha = 0.05$  MeV up to the maximum  $\alpha$ -energy available and our results are shown in figs. 15 and 16 which include the break-up component. For a  $^{239}\text{Pu}$ -Be source, the various neutron groups remain still quite distinguishable. The peaks in the spectra near 3 and 5 MeV are caused by the back and forward peaking in the angular distribution for the  $n_1$  group.

Errors in the shape of the spectra depend mostly on the angular distributions and are estimated to be  $\pm 5\%$  above 2.5 MeV, increasing to  $\pm 10\%$  below 2 MeV. It is unlikely that further supplementary cross section information would change the shape significantly for  $E_n > 2$  MeV. The yields are proportional to the total cross section (uncertainty  $\pm 8\%$ ) and inversely proportional to the stopping cross section ( $\pm 3.5\%$ ).

#### 4. Comparison of calculated with measured source characteristics

The calculations can now be compared with measured spectra as shown in fig. 17 for Am-Be. The match at higher energies can be considered excellent but at lower energies the shapes differ although the actual number of neutrons is nearly equal for  $E_n < 1.5$  MeV. Fig. 18 shows a calculation by Kumar (KUM77b). Not much is known about his input cross sections but it appears they are less complete than ours. Also note the good agreement of the measurement by WHI50 (fig. 7) with our calculations.

Important parameters for a number of source types, namely the total yield, the yield for  $E_n < 1.5$  MeV and the average neutron energy are listed in table 1. The yield in column 5 is calculated from (RUN56):

$$Y = 0.95 \times 0.152 E_\alpha^{3.65} \text{ neutrons per } 10^6 \alpha\text{-particles} \quad (4)$$

where  $E_\alpha$  is the  $\alpha$ -energy of the emitter in MeV and the factor 0.95 takes care of a more recent calibration of the neutron standard used to establish this formula. The variation in yield is more easily seen graphically (fig. 19). Our calculated yields lie somewhat above the curve given by the experimental points of RUN56 but a measurement on a specifically prepared Po-Be source (AND71) is in good agreement.

TABLE 1  
Characteristics of Be( $\alpha$ ,n) sources.

Source	$E_\alpha$ (MeV)	Yield per $10^6$ alphas			Fraction with $E_n < 1.5$ MeV		$\bar{E}_n$	
		This work	Maximum experimental	$Y$ from eq. (4)	This work (%)	Literature (%)	This work (MeV)	Literature (MeV)
1	2	3	4	5	6	7	8	9
$^{238}\text{Pu}-\text{Be}$	5.14	$65 \pm 6$	$57 \pm 3^{18)}$	57	$11 \pm 2$	$9^{22)}$ $33^{21)}$	4.59	$4.2^{13)}$ $4.7^{22)}$
$^{210}\text{Po}-\text{Be}$	5.30	$73 \pm 7$	$69 \pm 2^{20)}$	64	$13 \pm 2$	$12^{23)}$	4.54	$4.3^{23)}$
$^{241}\text{Am}-\text{Be}$	5.48	$82 \pm 8$	$70 \pm 3^{18)}$	72	$14 \pm 2$	$15^{25)}$ $23^{21)}$	4.46	$3.9^{27)}$ $4.3^{20)}$
$^{244}\text{Cm}-\text{Be}$	5.79	$100 \pm 9^a$		88	$18 \pm 3$	$29^{24)}$	4.31	$3.55^{24)}$
$^{242}\text{Cm}-\text{Be}$	6.10	$118 \pm 10$	$106 \pm 5^{18)}$	106	$22 \pm 3$	$26^{21)}$	4.16	
$^{226}\text{Ra}-\text{Be}$	7.69, 6.00, 5.49, 5.30 (50%), 4.77	$502 \pm 50$		$491^b$	$26 \pm 3$	$33^{25)}$ $38^{21)}$	3.94	$2.75^{27)}$ $3.6^{23)}$
$^{227}\text{Ac}-\text{Be}$	7.365, 6.71 6.56, 5.90, 5.65	$702 \pm 60$		$683^b$	$28 \pm 3$	$38^{26)}$	3.87	$3.14^{26)}$

<sup>a</sup> This does not include a 4% contribution from spontaneous fission of  $^{244}\text{Cm}$ . <sup>b</sup> Summed over all five emitters.

Columns 7 and 9 give experimental values. Where two values are listed, only the largest and smallest values published are given. References: 18 RUN56; 20 AND71; 21 PAU72; 22 AND72; 25 KLU69. The other references as listed in GEI75.

The yields for the low energy component with  $E_n < 1.5$  MeV are displayed in fig. 20, together with the spread of published data. The threshold detector activation results of PAU72 are particularly high. It is worth noting that PET73 and FOM70b found lower values by this method. Most of the other determinations are based on a comparison of the total source emission rate determined in a  $\text{MnSO}_4$  bath and the emission rate found by neutron spectroscopy for  $E_n > 1.5$  MeV only (e.g. KLU69). The values for the average neutron energy, fig. 21, include the low energy component. Note that for fig. 20 and 21 the data for  $^{226}\text{Ra}$  and  $^{227}\text{Ac}$  should not be related to the  $\alpha$ -energy axis since these two isotopes with their daughters emit  $\alpha$ -particles covering a broad range (table 1).

### 5. Time dependence of emission rate and deformation of spectra

We have so far considered "ideal" sources, without taking into account variations of neutron emission with time or modifications in the spectrum caused by interactions of neutrons within the source.

Half life corrections can easily be dealt with in the usual way. Some problems may be encountered for  $^{239}\text{Pu}$ -Be sources because commercial  $^{239}\text{Pu}$  is usually admixed with small quantities of  $^{240}\text{Pu}$  and  $^{241}\text{Pu}$ . It is necessary to know the exact isotopic composition and to consider their parent-daughter relationships for appropriate decay and growth corrections (AND68). Similar considerations apply to  $^{226}\text{Ra}$ -Be sources. The last  $\alpha$ -emitting daughter in the decay chain,  $^{210}\text{Po}$ , grows slowly into the source because of its  $^{210}\text{Pb}$  parent having a half life of 22.3 y. Taking account of the relative neutron contribution caused by  $^{210}\text{Po}$  through equation 4, the neutron emission  $Q_t$  at the time  $t$  becomes

$$Q_t = Q_0 (1.138e^{-\lambda_1 t} - 0.138 e^{-\lambda_2 t}) \quad (5)$$

where  $\lambda_1$  and  $\lambda_2$  are the decay constants for Ra and  $^{210}\text{Pb}$  respectively. The emission rate  $Q_0$  relates to the time  $t = 0$  when the radium had last been purified and the source was made. Actually,  $Q_0$  should be determined one month after fabrication when the 3.8 day radon daughter has completely grown into the source.

The physical composition and mass of a neutron source modifies its calculated yield and spectrum to some extent. What happens experimentally can be seen in fig. 22 where Tyufyakov et al. (TYU73) measured the spectrum from a single Po-Be source and from an assembly of 10 such sources. We notice a considerable softening of the spectrum. It will now be necessary to consider the various causes which deform the spectra:

- 1) Elastic and inelastic neutron collisions within the source.
- 2) Neutron induced fission within the  $\alpha$ -emitter.
- 3) The  ${}^9\text{Be}(n,2n)$  reaction.
- 4) The  ${}^9\text{Be}(\gamma,n)$  reaction. Occurs only with  ${}^{226}\text{Ra}$  and can be estimated from the data given in Chapter 8.
- 5) Reduction of the effective  $\alpha$ -energy by slowing down of the  $\alpha$ -particle within the  $\alpha$ -emitting cluster.

For sources not exceeding 2 cm in capsule dimensions, the first three causes do not deform the spectrum by more than the error for the spectrum calculation. For larger sources, the neutron spectrum can be expressed as follows:

$$\begin{aligned} \phi(E) = & \phi_0(E) + \phi_{1s}(E) + \phi_{2s}(E) \dots \dots \dots \\ & + \phi_{1f}(E) + \phi_{2f}(E) \dots + \phi_{1n}(E) + \phi_{2n}(E) \end{aligned} \quad (6)$$

where  $\phi_0$  is the uncollided spectrum.  $\phi_{1s}$ ,  $\phi_{2s}$  refer to the single, double, etc., scattering collisions and similarly  $\phi_{1f}$  and  $\phi_{1n}$  to collisions producing fission and  $n,2n$  reactions. The long, 24000 year half life of  ${}^{239}\text{Pu}$  requires physically large sources to obtain adequate neutron emission. These sources therefore become

particularly susceptible to these corrections. For a 10 Ci source, Monte Carlo calculations for the various spectral components have been carried out by KUM77a and are shown in fig. 23. Note the logarithmic scale. The uncollided spectrum is designated as "1". After adding the components, the source emission spectrum "total" is obtained. Considerable softening occurs, mainly caused by single scattering events on Be. Earlier experimental studies by AND72 on four  $^{239}\text{Pu}$ -Be sources of various sizes show a similar trend, namely a slight broadening of peaks and an increase in low energy neutrons.

Spectral distortion by the last of the five causes listed above is not a function of source size and can be almost eliminated by proper care in the fabrication of a source. The  $\alpha$ -emitting clusters must be made very small in relation to the  $\alpha$ -particle range. Cluster effects in alloyed sources were studied experimentally by RUN56. Path length distributions of  $\alpha$ -particles within spherical clusters and their energy losses were calculated by a Monte Carlo technique (VDZ68). The energy distribution of the  $\alpha$ -particles leaving the clusters could thus be obtained. Spectral deformations are noticeable when the clusters consist of Po but are very small even for quite large clusters of Pu-Be<sub>13</sub> or Am-Be<sub>13</sub> in the beryllium matrix (fig. 24). Neutron yields are much more severely affected than the spectra (fig. 25). Since the theoretical yield of a source is known (table 1), the source emission rate is a measure of clustering and therefore of the quality of source fabrication.

## 6. Helium stopping power in beryllium

In source spectrum calculations, the shape and even more so the yield are affected by the value of  $\epsilon$ , the stopping cross section for beryllium (equation 3). Recommended values are given by Ziegler in his recent compilation (ZIE77) and are shown in fig. 26. The author adjusted the theoretical curve to fit the experimental data of CHU69 which are only available up to  $E_{\alpha} = 2$  MeV. However, for source calculations accurate stopping power data are needed for  $E_{\alpha}$  from 2 to 8 MeV, the  $\alpha$ -particle range from which most of the neutron yield originates. For the calculations carried out in Chapter 3 we decided therefore to use instead the experimental proton stopping power data by BAD56 and to convert these to  $\alpha$ -stopping powers which we assumed could be done with negligible additional error. These data are shown in the upper curve of fig. 26. Since then however new direct measurements on Be by Santry et al. (SAN78, SAN79) became available. Their results are about 8% below the curve of BAD56. This is now a matter of some concern since, although the new data would not noticeably change the calculated spectra, the source yields would increase by 8%, pushing measured and calculated yields further apart than seen in fig. 19.

## 7. Other ( $\alpha, n$ ) neutron sources

To conclude the review of  $\alpha$ -induced neutron sources it appears worthwhile to briefly mention ( $\alpha, n$ ) reactions on other elements and to show some source spectra. A number of different sources is commercially available. Table 2 shows approximate neutron yields with various elements when using  $^{210}\text{Po}$  as  $\alpha$ -emitter. Beryllium gives the highest neutron yield by far, followed by  $^{18}\text{O}$  and  $^{11}\text{B}$ . Some of the elements listed can not be incorporated directly into a source. It is for instance necessary to use compounds, such as  $\text{H}_2^{18}\text{O}$  or  $\text{CaF}_2$  as source material with an equivalent decrease in neutron yield. Examples of spectra for four different source types are given in fig. 27. The  $\text{LiH}(\alpha, n)$  source is of particular interest because of the low average neutron energy. The B and  $\text{H}_2^{18}\text{O}$  source simulate to some extent a spontaneous fission spectrum which is nowadays more easily produced by  $^{252}\text{Cf}$ .

Table 2 ( $\alpha, n$ ) Reactions on Light Nuclei

Target	Q-Value	Yield per $10^6$ alphas
$^7\text{Li}$	-2.79	2.6
$^9\text{Be}$	5.70	80
$^{10}\text{B}$	1.06	13
$^{11}\text{B}$	0.16	26
$^{13}\text{C}$	2.22	10
$^{18}\text{O}$	-0.70	29
$^{19}\text{F}$	-1.95	12

(Data of Roberts 1947, as quoted in BEC 64)



#### 8. Be( $\gamma$ ,n) photoneutron sources

Sources using the Be( $\gamma$ ,n) reaction are less commonly used because of their extremely intense  $\gamma$ -emission which imposes severe restrictions on the choice of the neutron detector. They do, however, have their special applications. Photoneutron sources containing a radium capsule in the center of a 4 cm diameter beryllium sphere are the primary standards at the national laboratories of the United States and the Soviet Union (CUR49, FOM70a). These sources can be built in a reproducible manner and emit, with 1 g radium in their center, about  $10^6$  neutrons per second. Another advantage is the absence of the Po growth correction. The spectrum consists of several neutron groups with energies of up to 670 keV. Depending on the  $\gamma$ -energy of the isotope used, other Be( $\gamma$ ,n) sources emit quasi-monoenergetic neutrons at energies from 23 to 1000 keV (table 3). These sources are therefore often used to determine absolute activation or fission cross sections at these energies.

It is also possible to obtain average neutron energies as low as 0.5 keV by surrounding the neutron source with appropriate moderators and absorbers (HAR76). This is a particularly interesting energy range occurring around nuclear reactor shielding for which the response of neutron rem-meters has not as yet been fully explored.

Table 3 Data on Be( $\gamma$ ,n) Photoneutron Sources

$\gamma$ - emitter	$T_{1/2}$	$\gamma$ - energy	line strength $\epsilon$	Average neutron energy		Yield ( $\mu \times 10^{-4}$ )
		(keV)		calc. (keV)	meas. (keV)	
$^{124}\text{Sb}$	60.2d	1691.03 RYV71	.49	$22.8 \pm 0.6$ RYV71	$26.0 \pm 1.3$ LAL70	12.4
		2091.0	.06	378	$363 \pm 15$ LAL70	
$^{116}\text{In}$	54.1m	2112.1	.15	397.3	$399 \pm 10$	0.94
$^{140}\text{La}$	40.3h	2522.0	.04	761.7	$765 \pm 15$	0.20
		2899.8	.001	1097.5	$1099 \pm 30$	
$^{24}\text{Na}$	15.0h	2752.9	1.0	966.9	$971 \pm 18$	10.8
$^{226}\text{Ra}$	1599y	6 lines	varies	21 to 670		7 MAR60

For In, La and Na the energies listed are from MUE73.  
 Except for Ra, the yields were measured by BEN69  
 The yield  $\mu$  is expressed in  $\text{cm}^2\text{g}^{-1}\text{s}^{-1}\text{Ci}^{-1}$

Because the  $\gamma$ -radiation in photoneutron sources does not lose energy in beryllium in the same way as  $\alpha$ -particles do, spectrum calculations are simplified. Again, in first approximations the neutron energy is of the general form of equation (2):

$$E_n = a + b \cos\theta \quad (2)$$

In a photoneutron source, all neutron emission angles occur. For monochromatic  $\gamma$ -rays of energy  $E_\gamma$  the neutron energy is therefore not strictly monochromatic. Then the full equation reads as follows (BEC64):

$$E_n = \frac{A-1}{A} (E_\gamma - |Q|) \pm E_\gamma \sqrt{\frac{2(A-1)(E_\gamma - |Q|)}{931 A^3}} \quad (6)$$

where the energies and the  $Q$  values of the  $\text{Be}(\gamma, n)$  reaction ( $Q = 1.665$  MeV) are expressed in MeV;  $A$  is the atomic weight of Be. Because the center of mass movement of the  $\text{Be} + \gamma$  system is small (this contrasts with a deuterium photoneutron source) the resulting neutron line width is quite narrow, for instance  $\pm 1.4$  keV for the 23 keV line from a  $^{124}\text{Sb}$ -Be source.

Table 3 shows the properties of some  $\text{Be}(\gamma, n)$  sources. The short half life of the isotopes emitting energetic  $\gamma$ -rays is a major impediment. Also, the presence of weak higher energy  $\gamma$ -lines, producing supplementary high energy neutrons is of disadvantage, particularly for dosimetry calibrations. The kerma factor is increasing nearly proportionally with the neutron energy making the evaluation of the dosemeter response often uncertain. The calculated and measured neutron energies are given in the table, as well as the yield  $\mu$  which would be obtained for 1g of Be located 1 cm away from a 1 curie source. This yield  $\mu$ , also called the Wattenberg constant, is then defined by

$$Q = \mu DM/r^2 \quad (7)$$

where  $Q$  is the emission rate,  $D$  the activity in curies of the radioactive isotope,  $M$  the Be target mass in gram and  $r$  the effective distance between  $\gamma$ -emitter and the Be target.

By appropriate integration and by taking self-shielding of  $\gamma$ -rays within the Be into account, Bensch and Vesely (BEN69) could express the relationship between  $\mu$  and the emission rate of a spherical source with the  $\gamma$ -emitter in its center. The emission rates of such sources were measured by activation of a manganese sulphate bath. The results for the yield constant  $\mu$  are listed in the last column of table 3.

Similarly to equation 7 one can also define the neutron emission rate from a thin Be target in terms of the  $\text{Be}(\gamma, n)$  cross section:

$$Q = 3.7 \times 10^{10} DfN\sigma_{\gamma n}/(4\pi r^2) \quad (8)$$

By comparison with equation 7 it follows that

$$\mu = 3.7 \times 10^{10} fN\sigma_{\gamma n}/(4\pi) \quad (9)$$

where  $N$  is the number of Be nuclei per gram and  $f$  is the fractional intensity of the  $\gamma$ -ray responsible for the neutron production. Since this fraction  $f$  is generally not too well known and weak additional  $\gamma$ -lines producing neutrons may be present, BEN69 did not attempt to derive  $\text{Be}(\gamma, n)$  cross sections from their yield determinations.

Cross sections have been measured directly using the bremsstrahlung difference method. Results are given in figs. 28 and 29. The errors are much larger than those found for the constant  $\mu$ . It therefore seems valuable to study the relation between  $\sigma$  and  $\mu$  in the future.

Measurements of photoneutron source spectra have been made with proportional counters. Pulse shape discrimination was needed to discriminate against the intense  $\gamma$ -radiation. Furthermore, lead shielding was required and the effect of different shielding configurations was studied as shown for the upper three spectra in fig. 30 (LAL70). The bottom spectrum is particularly significant as it shows that the authors were actually able to detect the weak higher energy neutron lines. An intensity ratio of  $I(363 \text{ keV})/(26 \text{ keV}) = (5.1 \pm 1.0)\%$  was found. The upper spectra in fig. 30 were now fitted to Monte Carlo transport calculations for neutrons in lead and in the source material which permitted to derive the primary photoneutron spectrum shown on top of fig. 31. Below, computed spectra for various source configurations are shown. The source used for the experiment was the homogenous, cylindrical source, consisting of a 30 g mixture of Sb and Be powder in a thin aluminium capsule.

The average energy of the measured primary spectrum is  $(26.0 \pm 1.3) \text{ keV}$  (table 3). Ryves and Robinson (RYV71) made elaborate determinations of the  $^{124}\text{Sb}$   $\gamma$ -line energy and calculated an average neutron energy of  $(22.8 \pm 0.6) \text{ keV}$ . This discrepancy is not understood and needs further investigation.

## 9. Conclusions and recommendations

- 1) For the neutron energy range between 2.5 MeV and the maximum, the agreement between measured and calculated spectra of  $\text{Be}(\alpha, n)$  sources is now within the expected errors.
- 2) Below 2.5 MeV discrepancies still exist. More cross section data for the break-up neutron production are needed. The proportional counter method needs further refinement. It appears to be the only technique which has been applied at low energies for cross section as well as for spectrum measurements. Are other suitable techniques available?
- 3) When measuring source spectra, the effect of source material and capsule should always be considered when making comparisons with calculations.
- 4) The present inconsistency in the stopping power data for beryllium needs to be resolved.
- 5) The reason for the difference between the calculated and measured average neutron energy for  $\text{Sb-Be}(\gamma, n)$  needs to be explained.
- 6) The relationship between photoneutron source yields obtained through the constant  $\mu$  and through  $(\gamma, n)$  cross sections should be investigated.
- 7) For many source types, neutron fluence-to-kerma conversion factors have been published. These papers should be reviewed in the light of the present knowledge about spectra and a new comprehensive list of these factors should be made.

## References

### General

- AMA59 E. Amaldi in Handbuch der Physik, Vol. 38/2 edited by S. Flügge, Springer-Verlag  
AUG71 Neutron Sources and Applications, Proceedings of ANS National Topical Meeting, Augusta, Georgia, DuPont de Nemours & Co.  
KNO79 G.F. Knoll, Radiation Detection and Measurement, J. Wiley  
MAR60 Fast Neutron Physics, Part I, edited by J.B. Marion and J.L. Fowler, Interscience  
BEC64 K.H. Beckurts and K. Wirtz, Neutron Physics, Springer-Verlag.

### Specific

- AND68 M.E. Anderson, Nuclear Applications, 4, 142  
AND71 M.E. Anderson and M.R. Hertz, Nucl. Scie. Eng. 44, 437  
AND72 M.E. Anderson and R.A. Neff, Nucl. Instr. Meth. 99, 231  
BAD56 M. Bader, R.E. Pixley, F.S. Mozer and W. Whaling, Phys. Rev. 103, 32  
BEN69 F. Bensch and F. Vesely, J. Nucl. Energy 23, 537  
CHU69 W.K. Chu and D. Powers, Phys. Rev. 187, 478  
CUR49 L.F. Curtiss and A. Carson, Phys. Rev. 76, 1412  
FOM70a V.I. Fominykh and I.A. Yaritsyna, Izmeritel'naya Tekhnika 11,80  
FOM70b V.I. Fominykh, Atomnaya Energiya 28, 59  
GEI70 K.W. Geiger and L. van der Zwan, Int. J. Apl. Rad. Isotopes 21, 193  
GEI71 K.W. Geiger and L. van der Zwan, Health Physics 21, 120  
GEI75 K.W. Geiger and L. van der Zwan, Nucl. Instr. Meth. 131, 315  
GEI76 K.W. Geiger and L. van der Zwan, National Research Council of Canada, Report PXNR-2404  
GIB65 J.H. Gibbons and R.L. Macklin, Phys. Rev. 137, B1508  
HAR76 J.R. Harvey and R.C. Bending, Phys. Med. Biol. 21, 85  
HUG75 R.J. Hughes, R.H. Sambell, E.G. Muirhead and B.M. Spicer, Nucl. Phys. A238, 189  
JAK61 M.J. Jakobson, Phys. Rev. 123, 229  
KHA59 A.G. Khabakhpashev, Atomnaya Energiya 7, 71  
KLU69 H. Kluge, Z. Naturforsch. 24a, 1289  
KUM77a A. Kumar and P.S. Nagarajan, Nucl. Instr. Meth. 140, 175  
KUM77b A. Kumar and P.S. Nagarajan, Nucl. Instr. Meth. 141, 145  
LAL70 M. Lalovic and H. Werle, J. Nucl. Energy 24, 123  
LEH68 R.L. Lehman, Nucl. Instr. Meth. 60, 253  
LOR73 E.A. Lorch, Int. J. Apl. Rad. Isotopes 24, 585  
MAR68 J.B. Marion and F.C. Young, Nuclear Reaction Analysis, J. Wiley  
MED62 L. Medveczky, Atomnaya Energiya 13, 583  
MUE73 K. Mueck and F. Bensch, J. Nucl. Energy 27, 857  
NOT62 S. Notarrigo, R. Parisi, R. Ricamo and A. Rubbino, Nucl. Phys. 29, 507

- OBS72 A.W. Obst, T.B. Grandy and J.L. Weil, Phys. Rev. C5, 738  
PAU72 H. Pau and A.H.W. Aten Jr., Health Physics 22, 511  
PET73 G. Pető, J. Csikai, G.M. Shuriet, I. Józsa and V. Asztalos, Acta  
Physica Scient. Hung. 33, 363  
RUN56 O.J.C. Runnalls and R.R. Boucher, Can. J. Phys. 34, 949  
RYV71 T.B. Ryves and J.C. Robertson, J. Nucl. Energy 25, 557  
SAN78 D.C. Santry and R.D. Werner, unpublished  
SAN79 D.C. Santry and R.D. Werner, Nucl. Instr. Meth. 159, 523  
TYU73 N.D. Tyufyakov, L.A. Trykov and A.S. Shtan, Atomnaya Energiya 34,  
349  
VDZ68 L. van der Zwan, Can. J. Phys. 46, 1527  
VDZ70 L. van der Zwan and K.W. Geiger, Nucl. Phys. A152, 481  
WER73 H. Werle, L. van der Zwan and K.W. Geiger, Z. Physik 259, 275  
WHI50 B.G. Whitmore and W.B. Baker, Phys. Rev. 78, 799  
ZIE77 J.F. Ziegler, He Stopping Powers and Ranges in all Elemental  
Matter, Pergamon Press



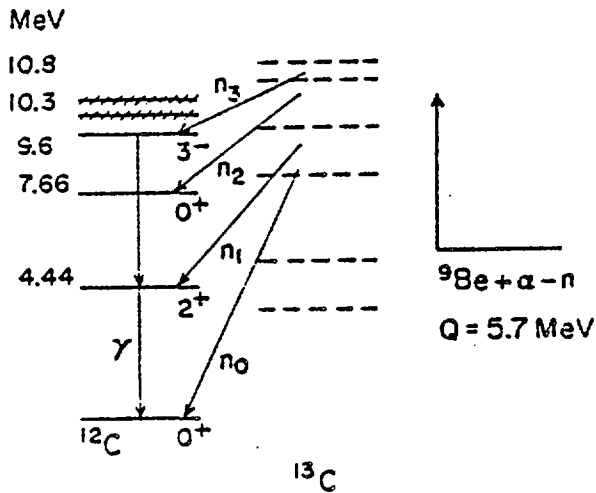


Fig. 1 The  $^9\text{Be}(\alpha, n)^{12}\text{C}$  reaction.

Fig. 3 Thick target neutron spectra at various emission angles for an incident energy of  $E_\alpha = 5.48 \text{ MeV}$ . The uppermost spectrum is composed so as to simulate an  $^{241}\text{Am}$ -Be source spectrum. From GEI70.

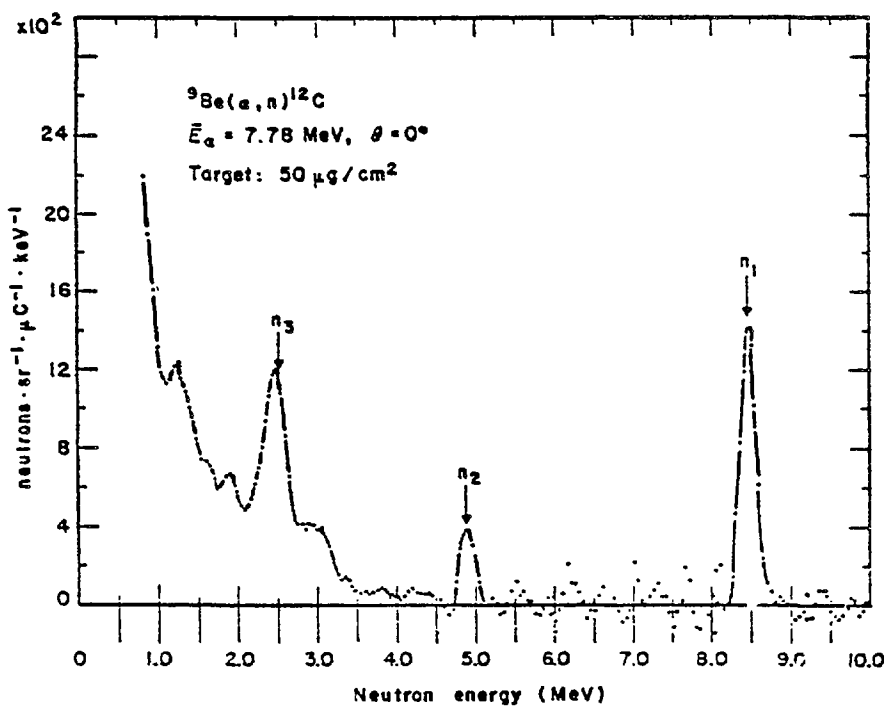
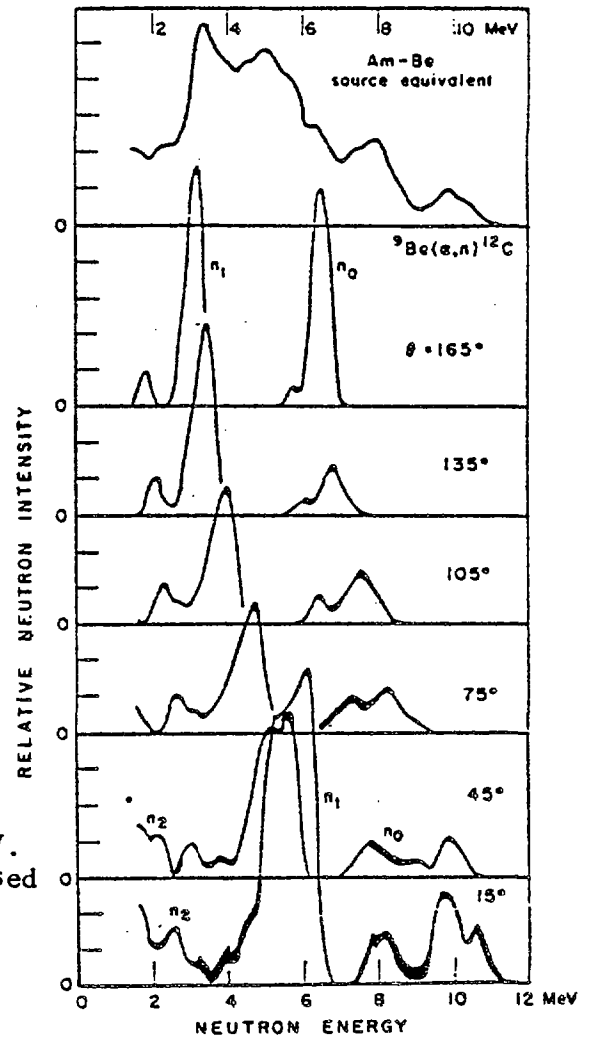


Fig. 2 Thin target neutron spectrum. The low energy continuum is caused by the break-up of  $^9\text{Be}^*$ . From VDZ70.

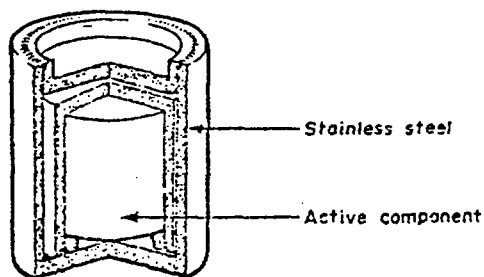


Fig. 4  
Typical double walled source capsule for radioactive ( $\alpha$ ,n) sources. From KNO79.

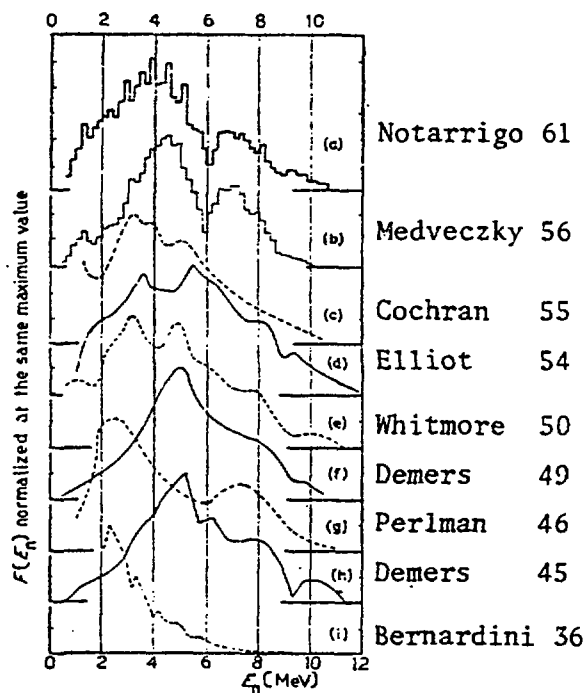


Fig. 5  
Some measured neutron energy spectra from  $^{210}\text{Po}$ -Be sources. See NOT62 for references.

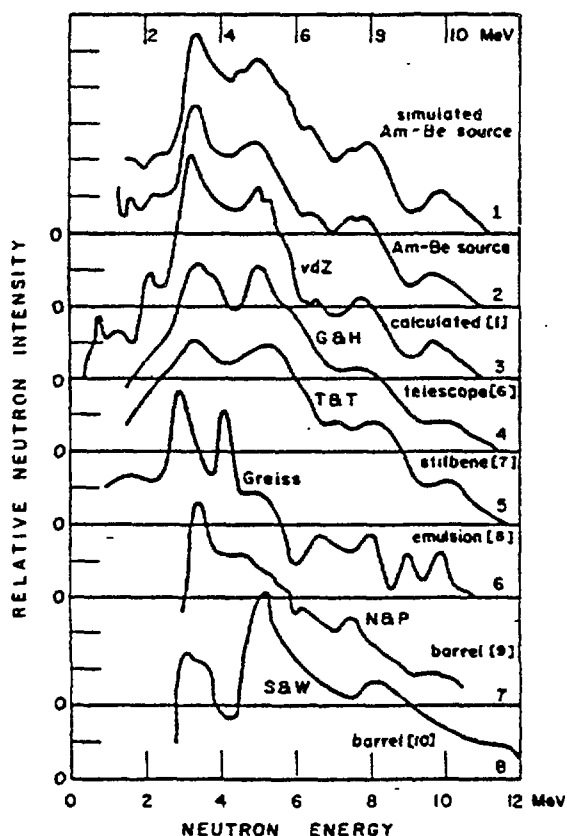


Fig. 6  
Some  $^{241}\text{Am}$ -Be source spectra. See GEI70 for references.

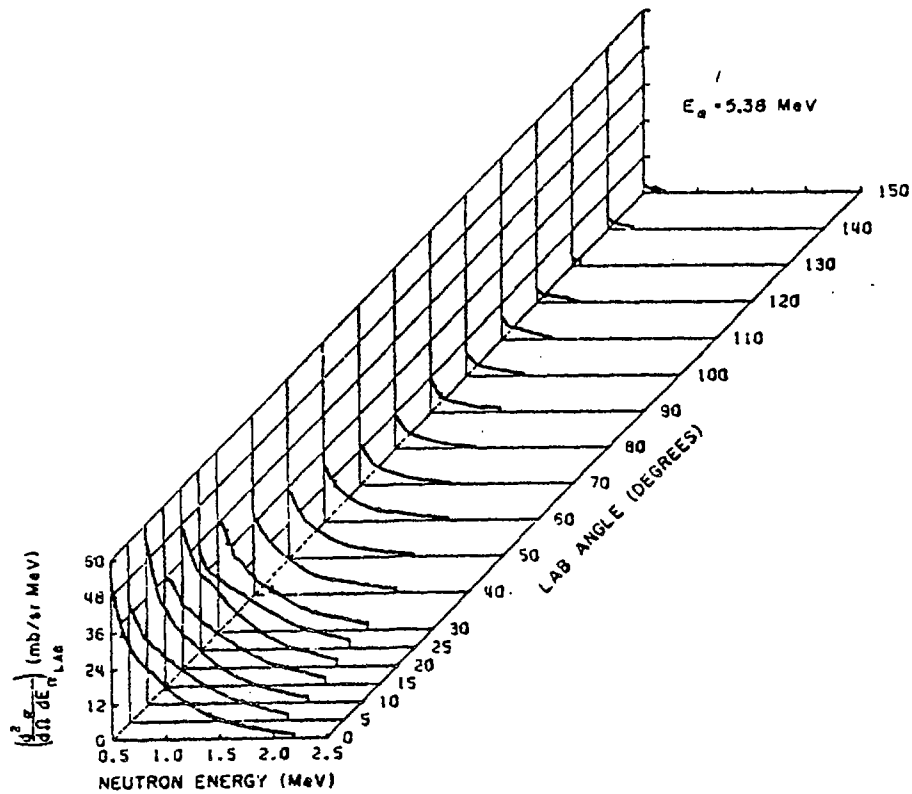


Fig. 7  
Angular distribution of the neutron continuum at  $E_\alpha = 5.38$  MeV for the Be+ $\alpha$  thin target reaction. From OBS72.

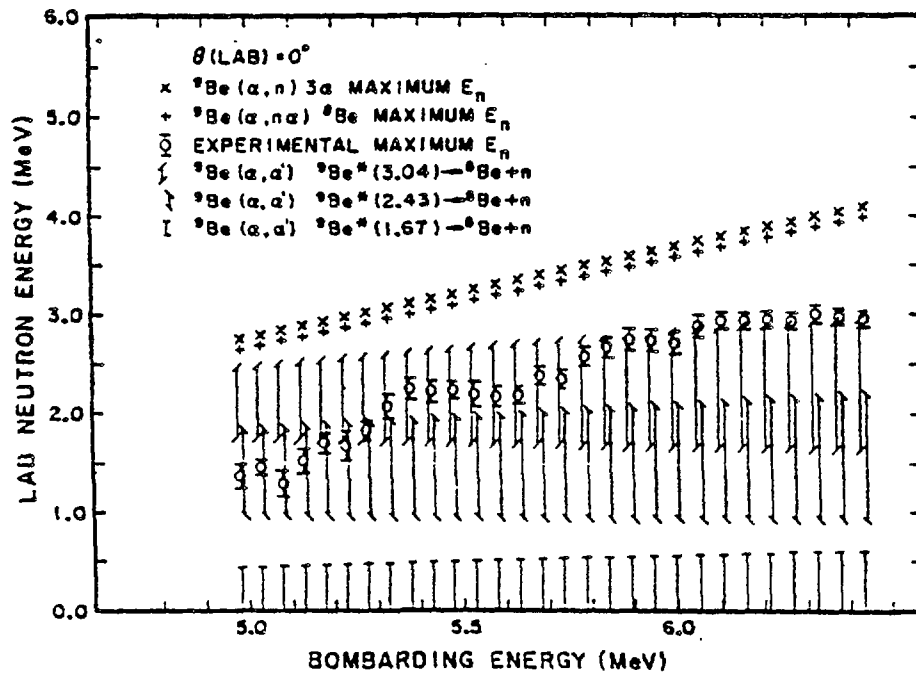


Fig. 8  
Neutron energy limits as function of the bombarding energy for the possible break-up reactions. From OBS72.

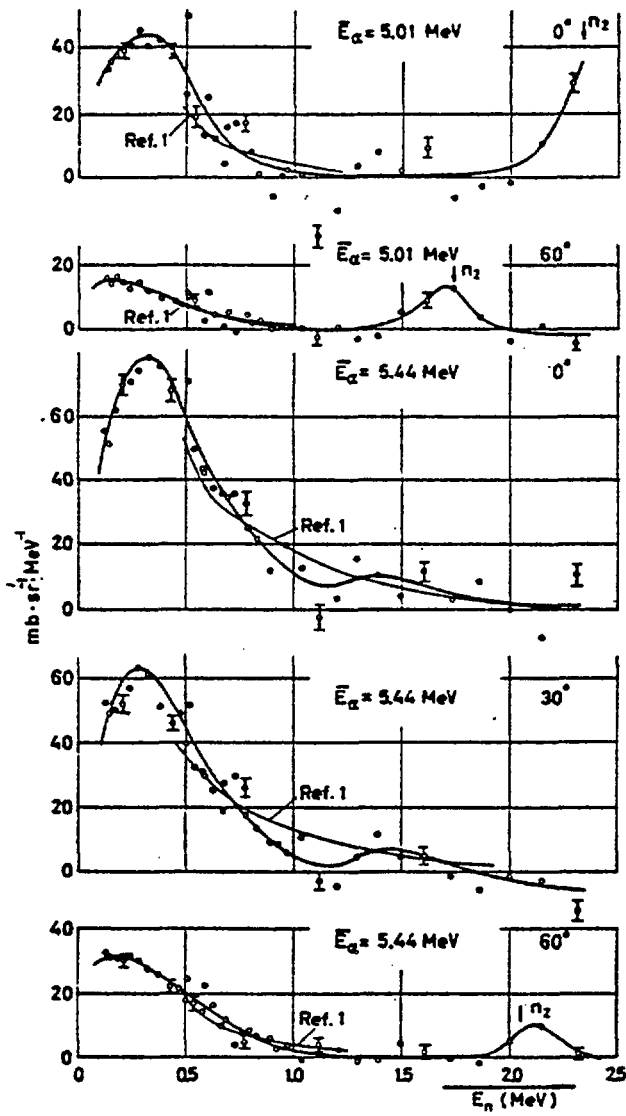


Fig. 9  
Continuum spectra extended to lower energies. Ref. 1 refers to OBS72.  
From WER73.

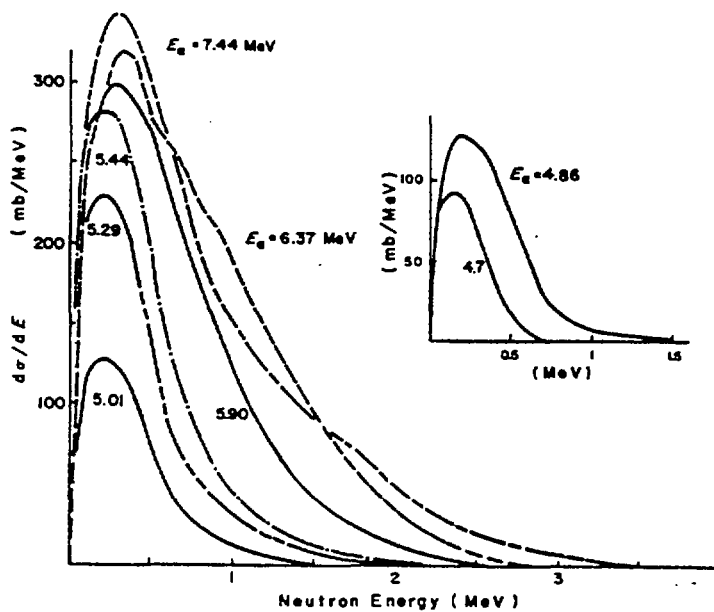


Fig. 10  
Angle integrated break-up spectra.  
From GEI76.

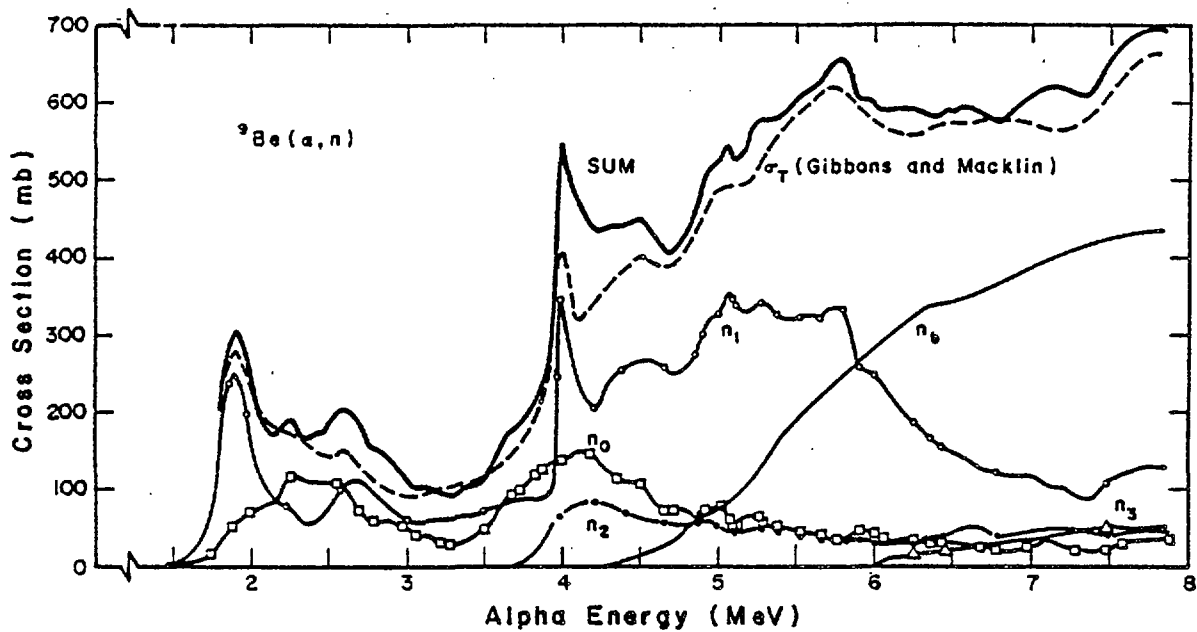


Fig. 11  
Evaluated neutron production cross sections from GEI76. The dashed curve has been measured by GIB65 using a  $4\pi$  neutron detector. The break-up cross section is  $n_b$ .

Fig. 12  
Examples of angular distributions drawn as functions of laboratory neutron energy. The circles indicate  $15^\circ$  steps in the c.m. system. The back angle,  $\theta = 180^\circ$ , corresponds to the lowest neutron energy. From GEI71,  ${}^6\text{Li}(\alpha, n)$  reaction.

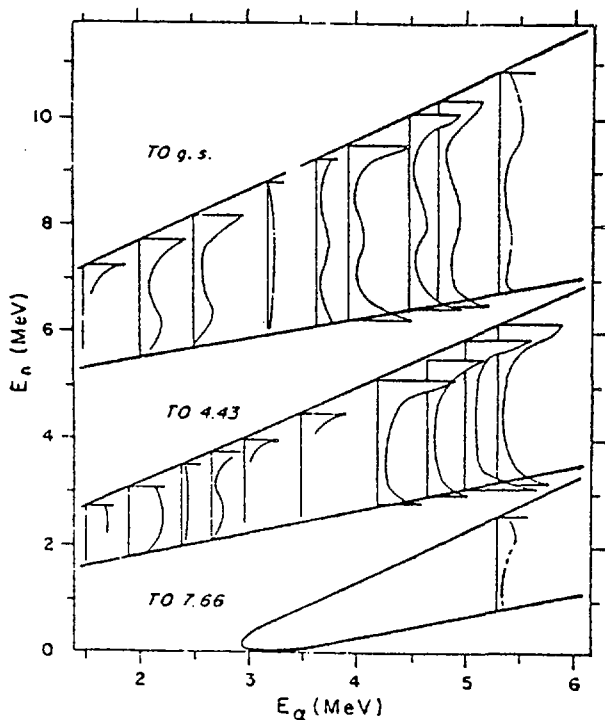
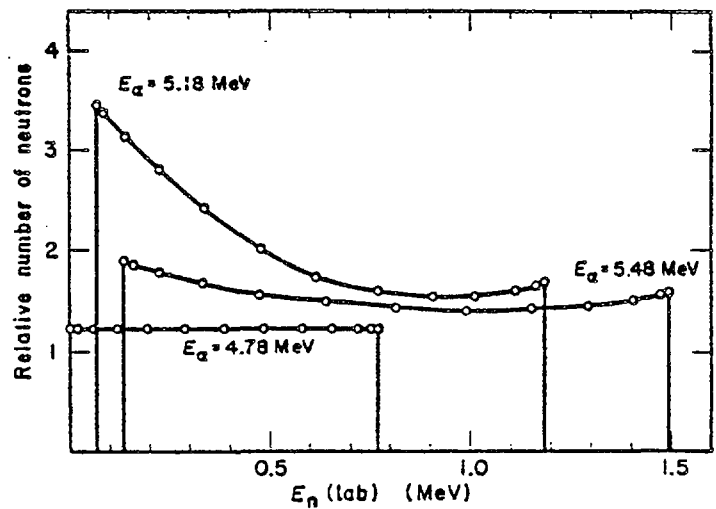


Fig. 13  
Reaction diagram for the  ${}^9\text{Be}(\alpha, n)$  reaction showing neutron spectra. Graphical method of LEH68.

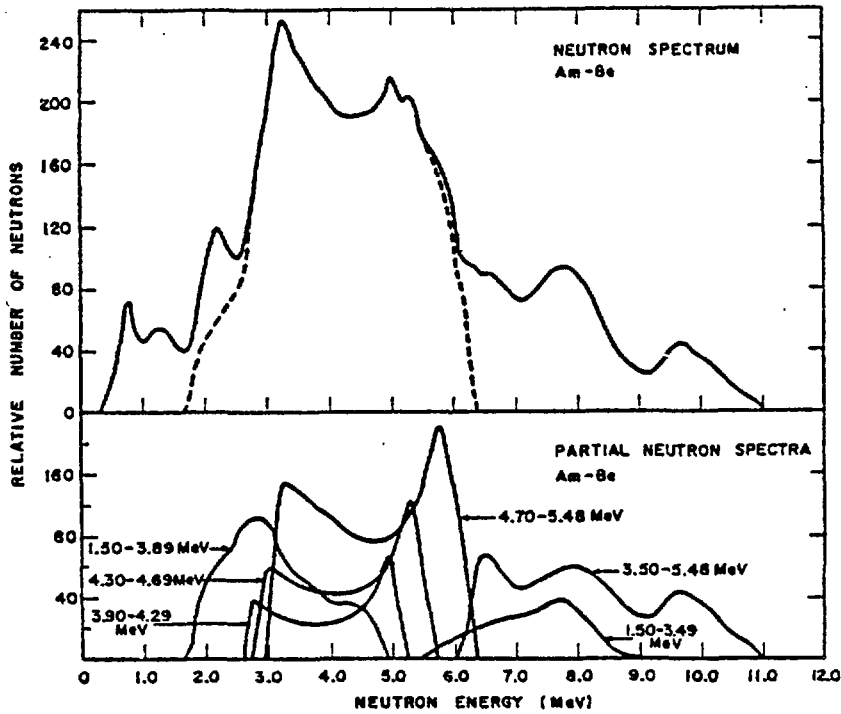


Fig. 14  
How partial neutron spectra  
sum up to result in the  
spectrum from an Am-Be  
source. From VDZ68.

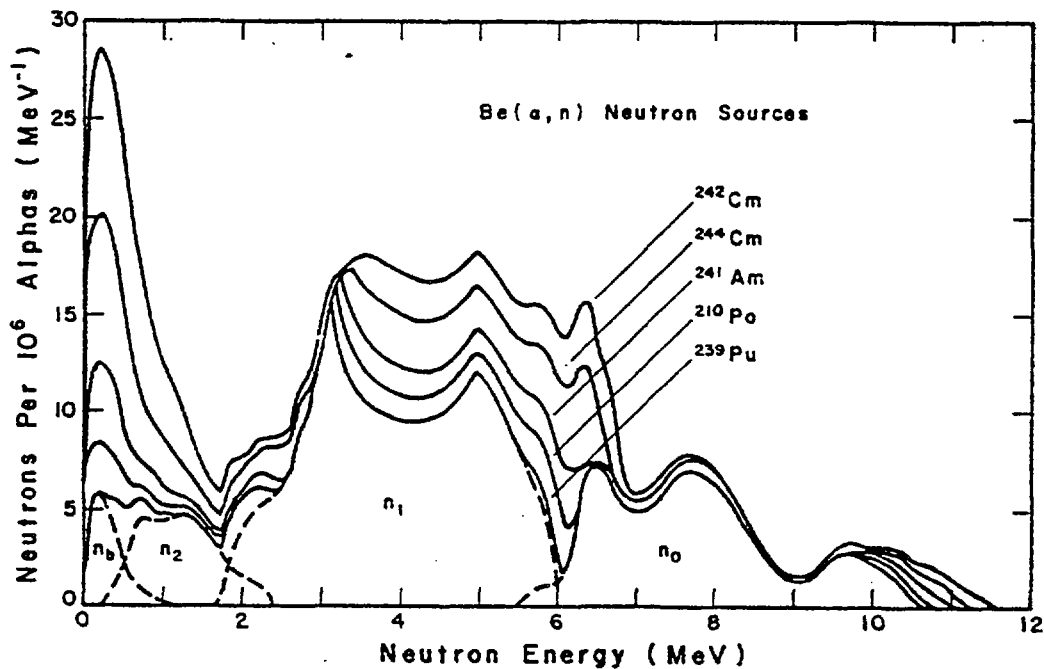


Fig. 15  
Source spectra calculated from the most recent compilation  
of cross section data. From GEI75.

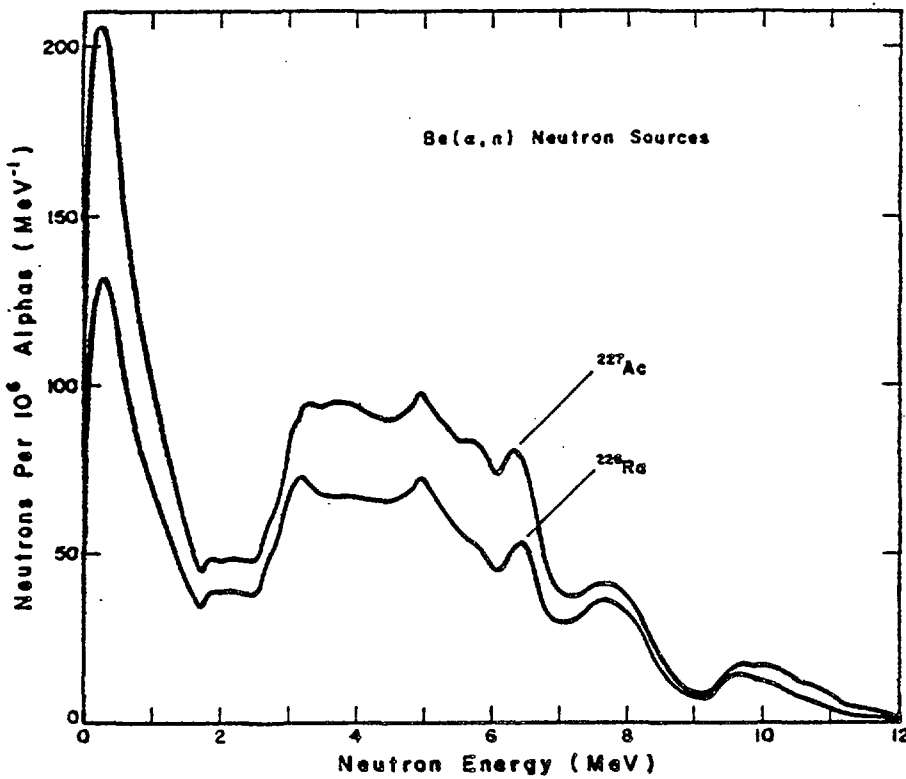


Fig. 16  
Source spectra with  
multiple radioactive  
 $\alpha$ -emitters.

Fig. 17  
Comparison with measured  
spectra. Proportional counter  
data from WER73, stilbene data  
from GEI70.

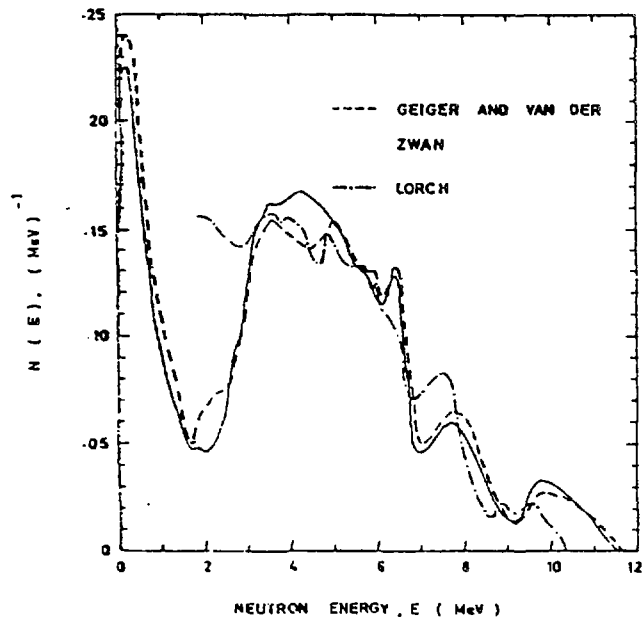
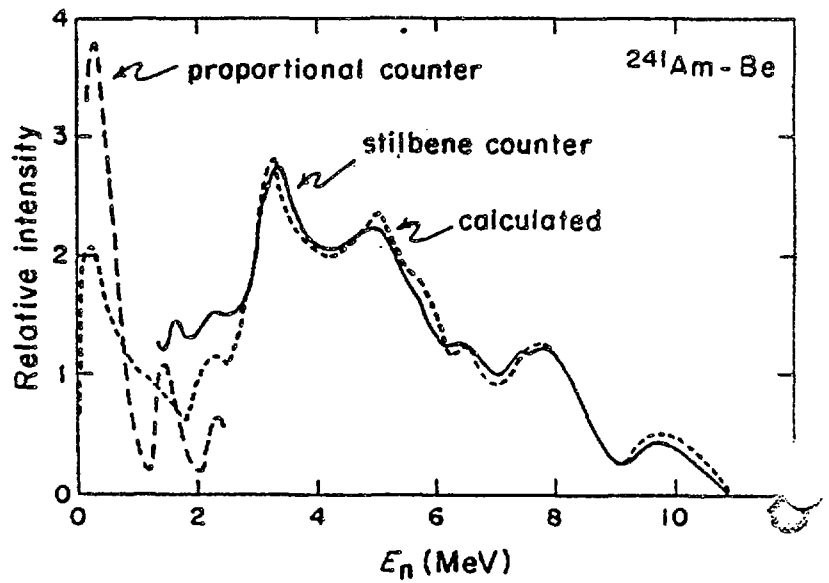


Fig. 18  
 $^{242}\text{Cm}-\text{Be}$  source spectra. Calculation of  
KUM77b compared to calculation given in  
Fig. 15 and measurement by LOR73.

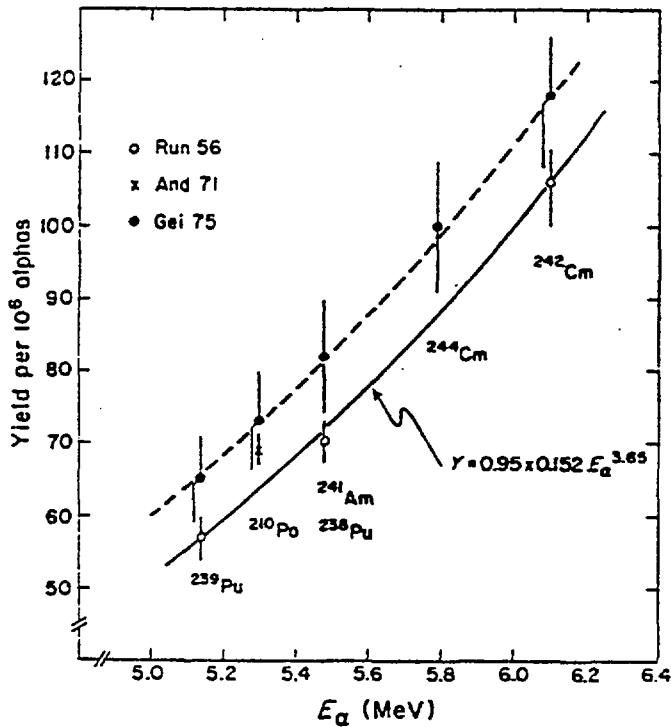


Fig. 19  
Calculated yields from table 1 compared to measurements by AND71 and RUN56.

Fig. 20  
Calculated low energy neutron component from table 1 compared to measurements, given by horizontal bars. Boxes indicate the spread of measurements.

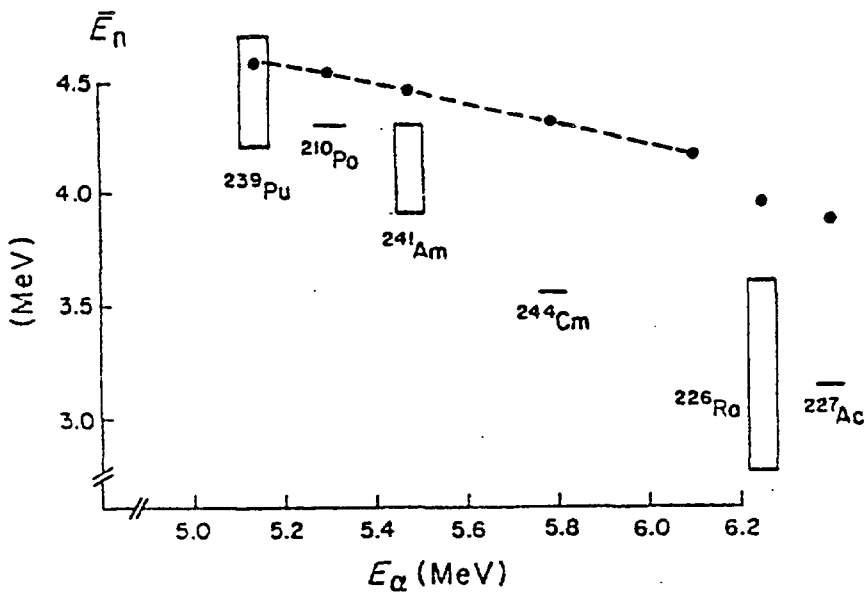
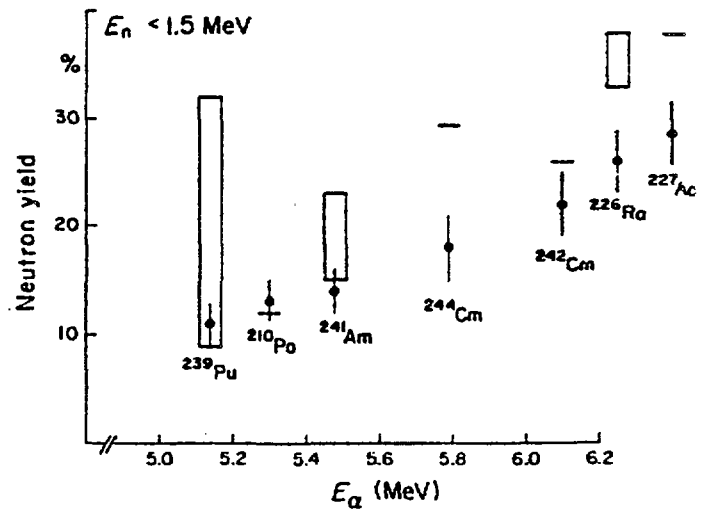


Fig. 21  
Average neutron energies. Displayed as in Fig. 20.



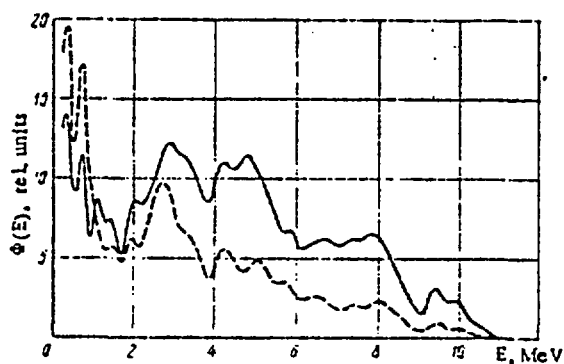


Fig. 22  
 $^{210}\text{Po}$ -Be source spectrum. The dashed curve shows the spectrum when 10 of these sources are measured as an assembly. From TYU73.

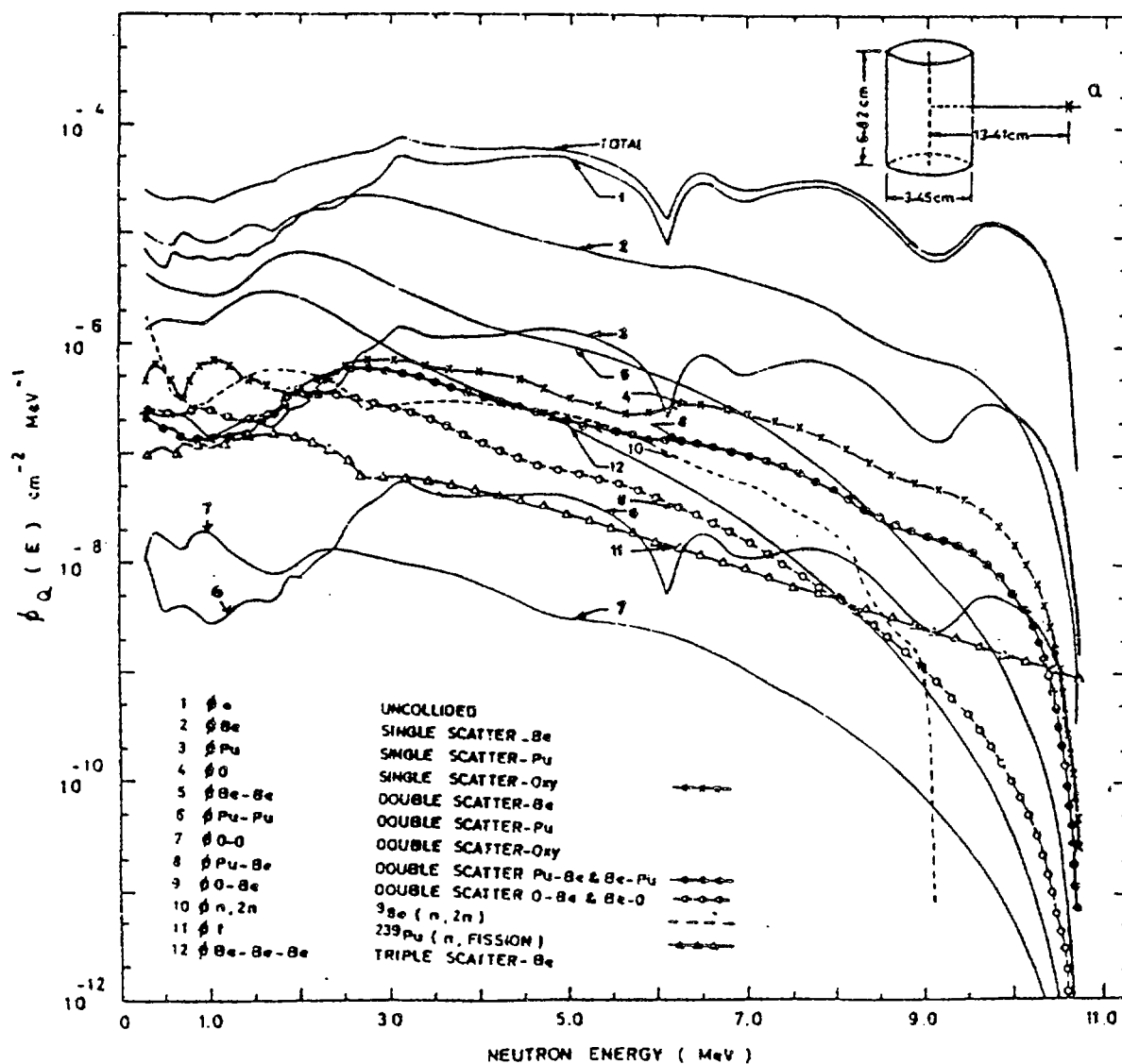


Fig. 23  
 Components of the modified spectrum from a 10 Ci  $^{239}\text{Pu}$ -Be source. From KUM77a.

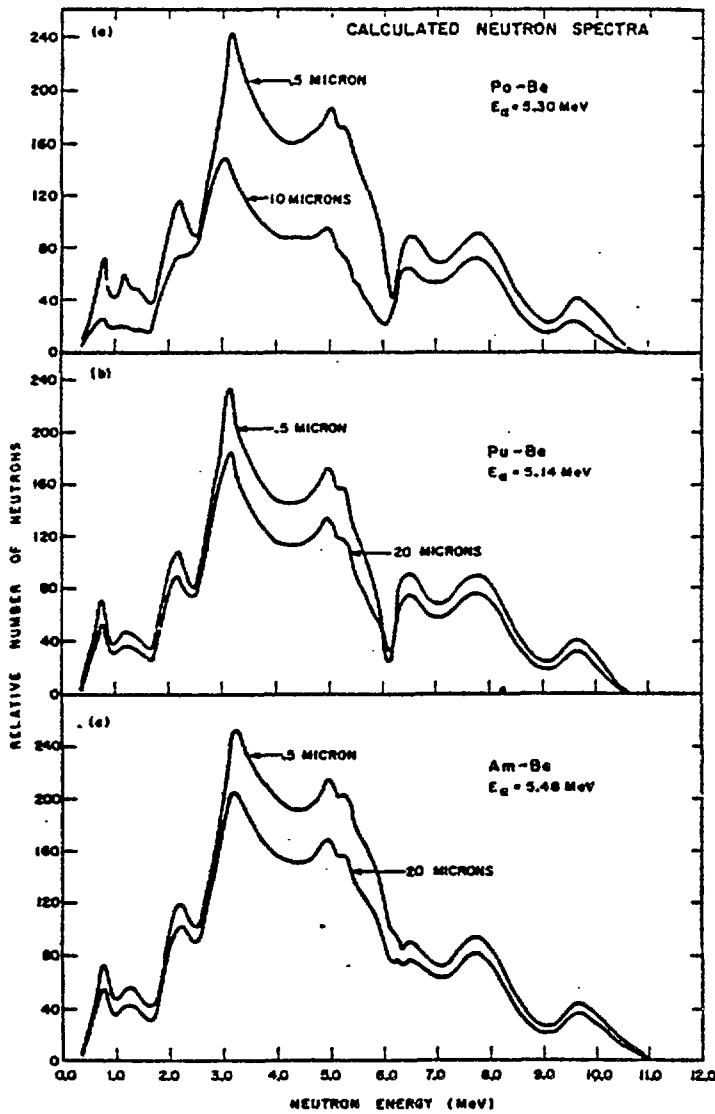


Fig. 24  
Top: spectrum modification caused by  $\alpha$ -emitting  $^{210}\text{Po}$  clusters in a beryllium matrix. The two lower spectra refer to  $\text{PuBe}_{13}$  and  $\text{AmBe}_{13}$  clusters. From VDZ68.

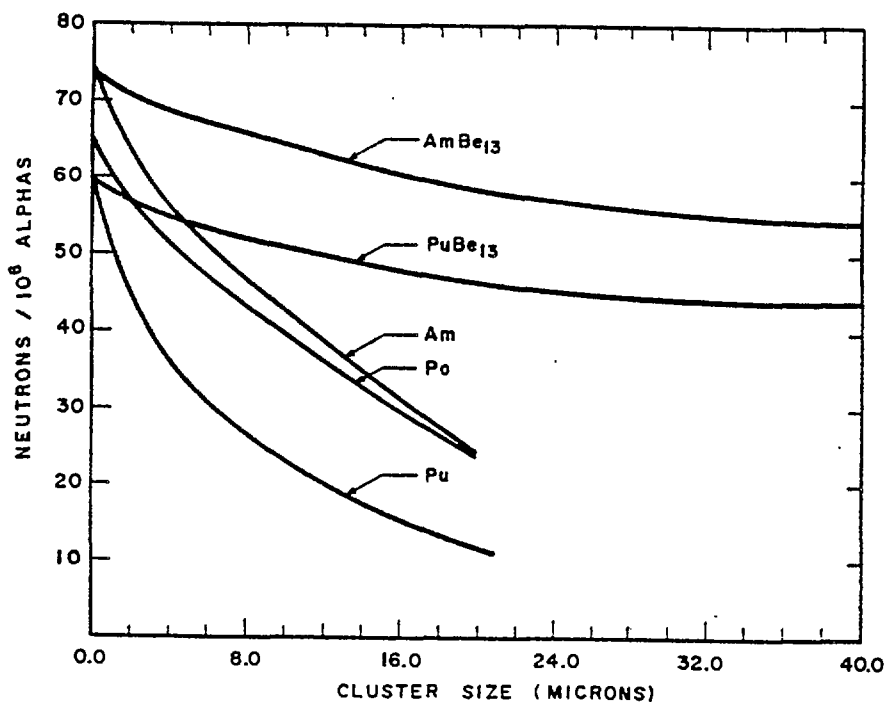


Fig. 25  
Yields for different size clusters in a beryllium matrix. From VDZ68.

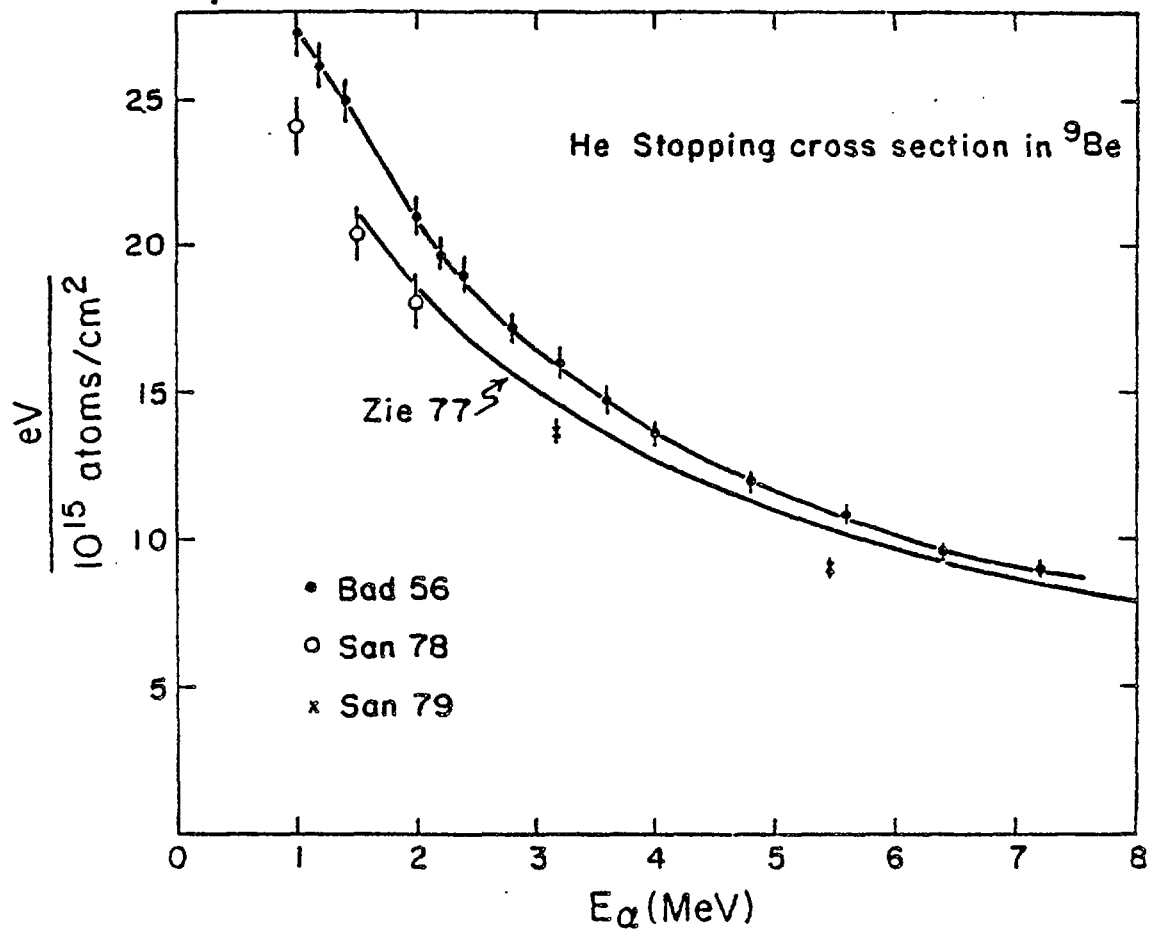


Fig. 26  
Helium stopping cross sections in Be.

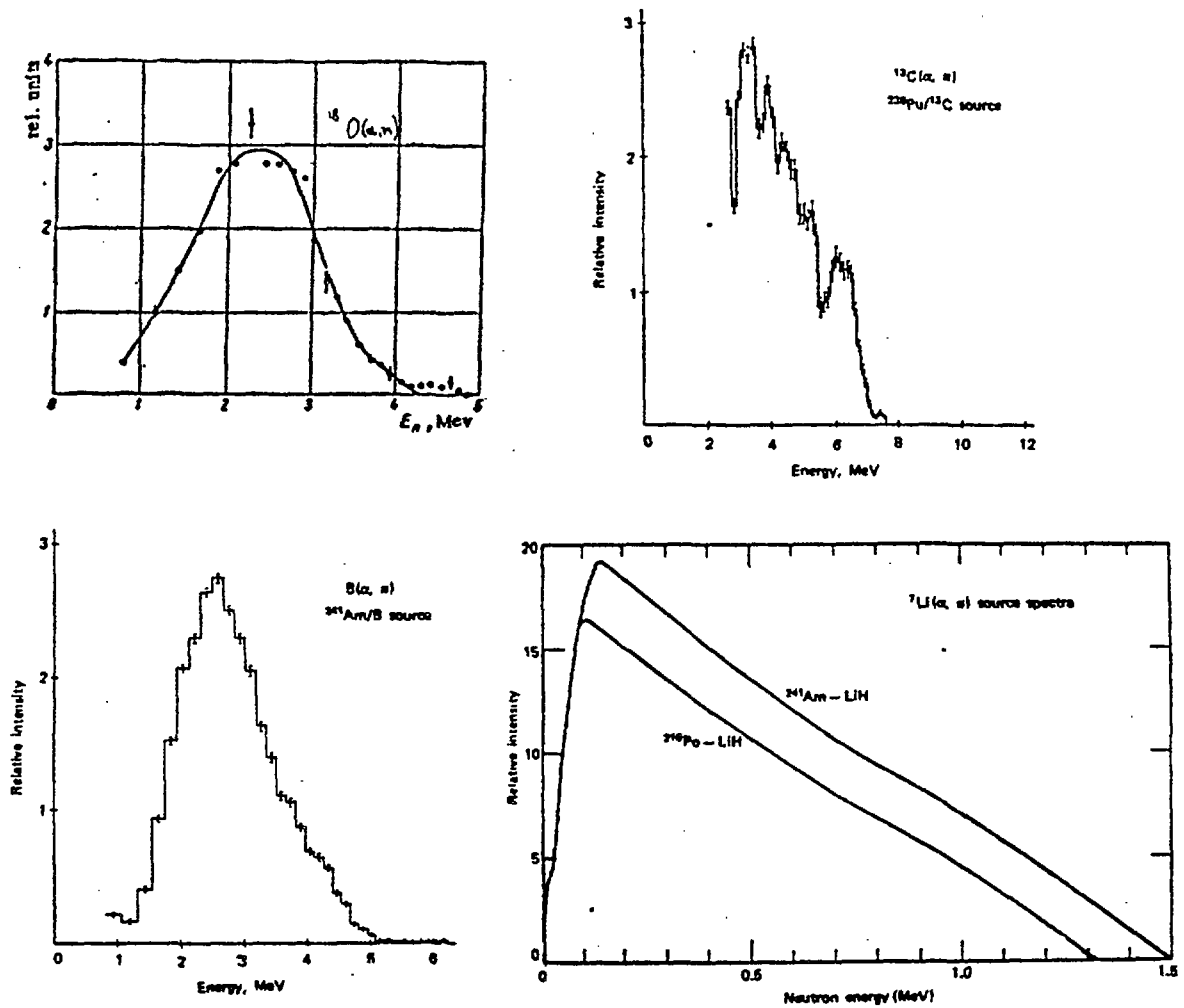


Fig. 27  
Other  $(\alpha, n)$  neutron spectra. B and  $^{13}\text{C}$ : LOR73;  $^{18}\text{O}(\text{H}_2\text{O})$ : KHA 69;  
LiH: GEI71.

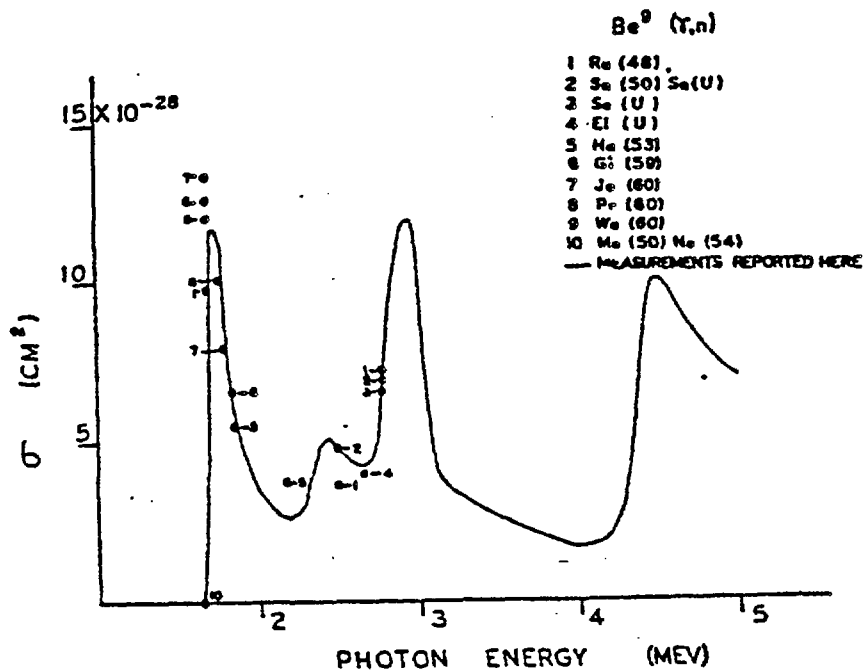


Fig. 28  
 $\text{Be}(\gamma, n)$  photoneutron cross section from data measured at  $90^\circ$  neutron emission angle (JAK61). The errors below  $E_\gamma = 3$  MeV are in the order of  $\pm 15\%$ .

Fig. 29  
Be( $\gamma$ ,n) photoneutron cross section using a  $4\pi$  neutron detector (HUG75).

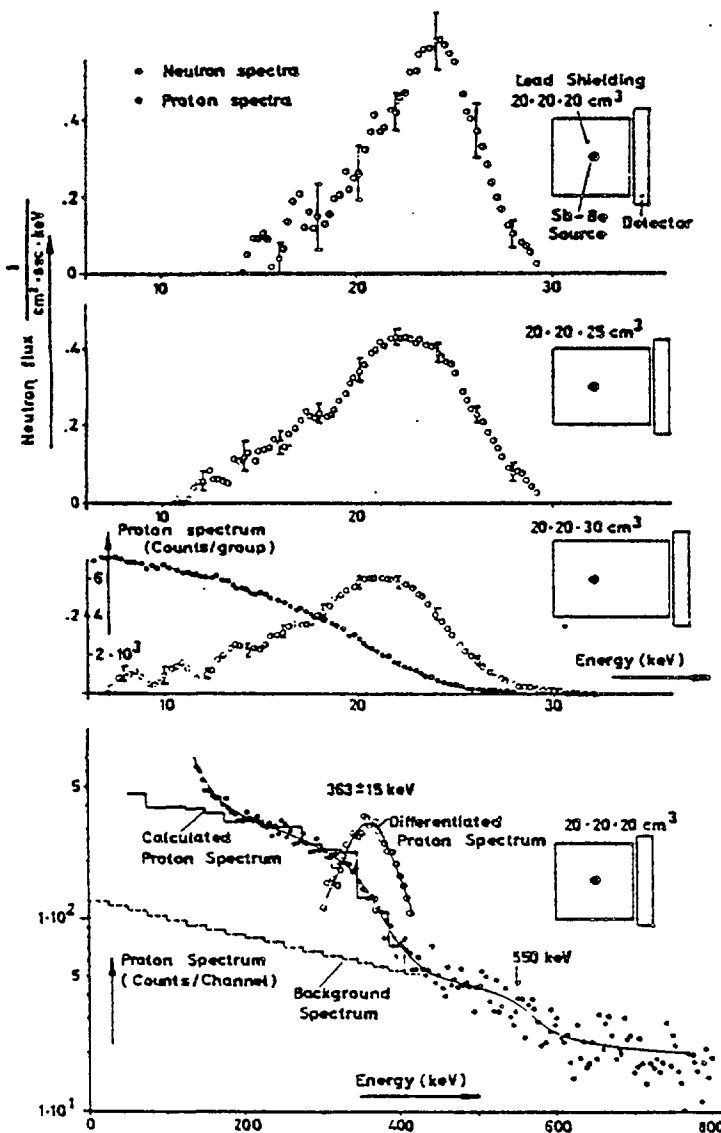
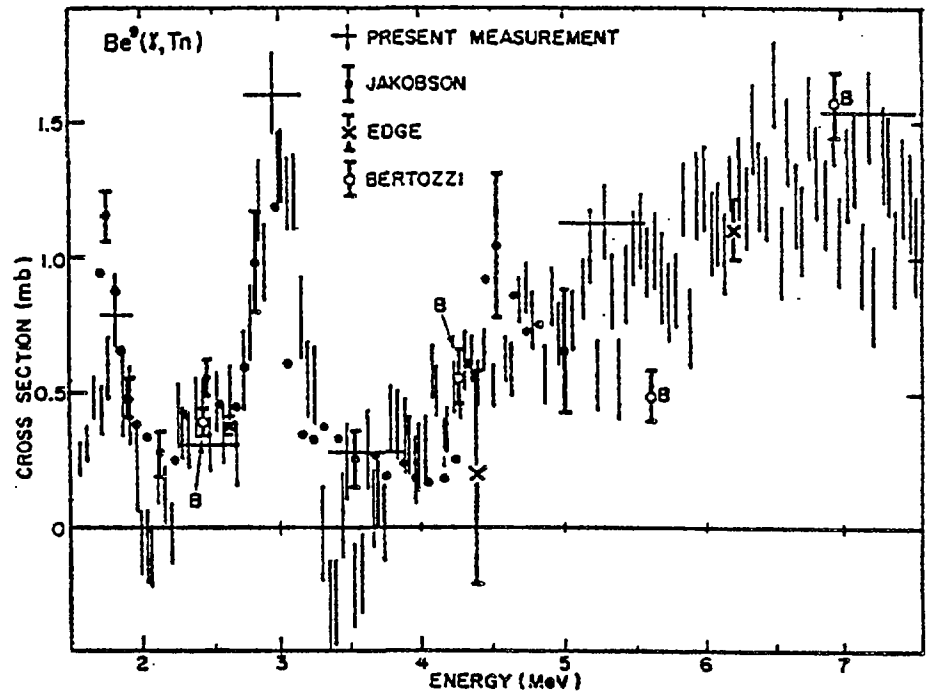


Fig. 30  
Neutron spectra from Sb-Be( $\gamma$ ,n) source in various lead shields, measured with proportional counter (LAL70).

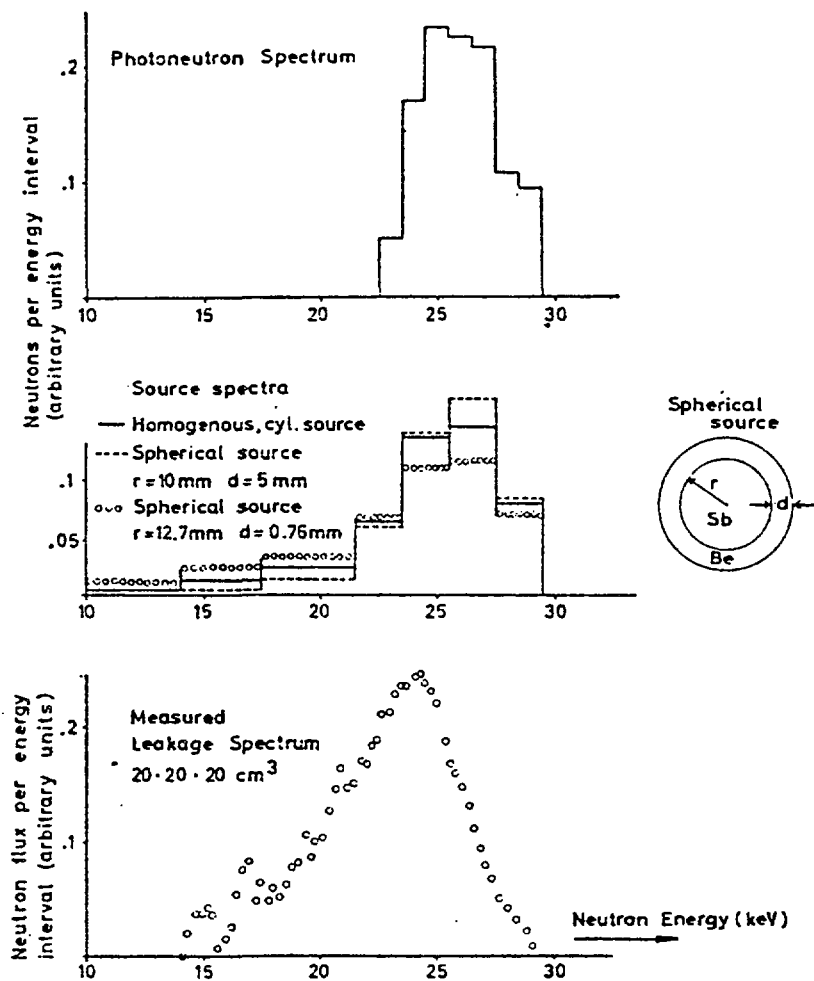


Fig. 31  
 Top: primary source spectrum derived from spectra of  
 rig. 30. Center: spectra derived from actual sources.  
 Bottom: measured spectrum for source in lead shield.



# NEUTRON ENERGY SPECTRA OF SPONTANEOUS FISSION SOURCES (Review)

M. V. Blinov

V. G. Khlopin Radium Institute, Leningrad, USSR

## Abstract

Some characteristics of energy distributions of neutrons from spontaneous fission sources are presented. The data on neutron energy spectrum of  $^{252}\text{Cf}$  are considered in detail. Main properties of neutron source on the basis of  $^{252}\text{Cf}$  are discussed.

## 1. INTRODUCTION

During the last years spontaneous fission sources became more important among the other isotope neutron sources than earlier. The intensity of neutron emission from these sources can vary within a large range and attain the values which are comparable with accelerator neutron fluxes. From practical point of view the use of these sources is stimulated by the similarity of their neutron spectrum to that from the fission events in nuclear installations. So, the various physical values necessary for the practical purposes, for example the fission cross-sections, can be determined in



neutron fluxes from spontaneous fission sources. A broad-range energy fission neutron spectrum enables by using one source to calibrate neutron spectrometers over a large energy interval. This feature is already widely used in physical experiments and engineering.

Different isotopes of heavy nuclei may be used as spontaneous fission neutron sources. Among these sources  $^{252}\text{Cf}$  is the most convenient; it has been recommended by the IAEA [1] as a standard. In this review I shall discuss the present status of investigations on energy distributions of prompt neutrons from spontaneous fission sources;  $^{252}\text{Cf}$  will be considered in detail.

## 2. SYSTEMATICS OF SPONTANEOUS FISSION NEUTRON ENERGY SPECTRA

### 2.1. Some comparable characteristics of spontaneously fissionable isotopes

Up to date spontaneous fission of nuclei from  $Z = 90$  to  $Z = 107$  has been known. The half-lives for spontaneous fission are within the range from  $10^{17}$  years to the values less than one second. Isotopes with  $Z$  more than 100 (Fm) cannot be obtained in sufficient quantities, therefore they are excluded from the further discussion. The average number of neutrons emitted per fission event increases from  $\bar{\nu} = 1,3$  for some thorium isotopes up to  $\sim 4$  for fermium. We do not consider here spontaneously fissionable isomers produced in different nuclear reactions. They decay too fast ( $T \leq 10^{-2}$  sec) to be used as neutron sources. The analysis of known properties of various spontaneously fissionable nuclei leads to the conclusion that Pu, Cm, Bk and Cf are now seen as the most convenient sources. The isotopes of Th, Pa, U and Np have low neutron yields and the known isotopes of Es and Fm have too short half-lives.

The most convenient isotopes as spectral neutron sources seem to be  $^{240}\text{Pu}$ ,  $^{242}\text{Pu}$ ,  $^{244}\text{Cm}$ ,  $^{246}\text{Cm}$ ,  $^{248}\text{Cm}$ ,  $^{252}\text{Cf}$  and

$^{254}\text{Cf}$  as regards to simple production, neutron yield, half-life and  $N_\alpha/N_f$  ratio. Some of their characteristics are presented in Table I. Plutonium isotopes have greater  $T$ , but their fission neutron yields are comparatively low. Hence, they are applied very seldom. Curium isotopes give  $10^4$  times more intensive neutron fluxes. However,  $^{244}\text{Cm}$  has a serious drawback and namely a great number of  $\alpha$ -particles emitted per fission event. The  $N_\alpha/N_f$  ratio for  $^{248}\text{Cm}$  is much better in addition to the other good characteristics.  $^{248}\text{Cm}$  is expected to be used as a long-lived source of spontaneous fission neutrons. The isotope of  $^{254}\text{Cf}$  is of interest due to its particularly great neutron yield, but its relatively low half-life ( $\sim 60$  days) would significantly limit its use. The most convenient neutron source on the basis of spontaneous fission is now  $^{252}\text{Cf}$ . Its characteristics, namely great neutron yield ( $10^9$  1/mg.s) with low weight, good  $N_\alpha/N_f$  ratio, simplicity of production, comparatively long half-life (2,6 years), meet many necessary requirements. That is why the IAEA recommended to use this spectrum as an international standard.

## 2.2. Experimental data on energy spectra

The available data on the average energy of spontaneous fission neutron spectra are presented in Fig. 1, 2 and Table II. The "hardness" of spectrum is shown to increase with increase of  $Z^2/A$  and  $\bar{\nu}$ . The spectra of plutonium and curium isotopes were measured by time-of-flight method [3, 4], using  $^3\text{He}$ -spectrometer [5] and by means of amplitude distributions of recoil protons in single-crystal spectrometer [6]. The first two methods were used for measurements within 0,5-7,0 MeV and the last-mentioned method for 1-12 MeV range. All the investigators came to conclusion that within the experimental accuracy the energy spectra could be described by Maxwellian distribution (Fig. 3). However, the measurement accuracy was not high because of low activity of preparations.

In the case of  $^{240}\text{Pu}$ ,  $^{242}\text{Pu}$  and  $^{244}\text{Cm}$ , the reactions  $(\alpha, n)$  could contribute appreciably to the spectrum of neutrons from the sources. So, in [6] the neutron yield of reaction  $(\alpha, n)$  on  $^{18}\text{O}$  of  $\text{PuO}_2$  ( $^{240}\text{Pu}$ ) at the energy 3 MeV. was comparable with the yield of spontaneous fission neutrons. Because of that the authors had to prepare another  $\text{PuBr}_4$  source. For  $^{242}\text{Pu}$  (oxide) the effect of this reaction was also found to be considerable ( $\sim 25\%$ ) [3]. However, the  $\gamma$ -quanta coincidence technique permitted to make this effect five times less. The data on energy neutron spectrum of  $^{252}\text{Cf}$  spontaneous fission will be discussed later in detail. There are no data on  $^{254}\text{Cf}$ -spectrum in the literature.

### 2.3. Mathematical representation of the fission neutron spectra

To describe the fission neutron spectra, Maxwellian distribution is generally used

$$N(E) \sim \sqrt{E} e^{-E/T}, \quad \bar{E} = \frac{3}{2}T \quad (1)$$

or sometimes Watt distribution

$$N(E) \sim e^{-E/T} \text{sh} \frac{2\sqrt{WE}}{T}, \quad \bar{E} = W + \frac{3}{2}T \quad (2)$$

where  $E$  - neutron energy,

$W$  - average kinetic energy of a fragment per one nucleon,

$T$  - "hardness" parameter which is named as temperature. Although having been used for a long time, these expressions have no strict theoretical substantiation. However they define rather well experimental distributions. Both dependencies give very similar predictions of spectrum shape over a wide energy interval and only at higher energies their discrepancy is essential (the difference at 10 MeV - 25%).

For approximate determination of  $\bar{E}$  (if there are no reliable direct measurements) one can use Terrell semiempirical relation [7] deduced from the simplified Weisskopf evaporation model:  $\bar{E} = 0,78 + 0,621\sqrt{\bar{V} + 1}$  (3)

### 3. ENERGY SPECTRUM OF $^{252}\text{Cf}$ SPONTANEOUS FISSION NEUTRONS

#### 3.1. Spectrum measurement techniques

Measurements of  $^{252}\text{Cf}$  fission neutron spectrum were made for the first time in 1955 and continue up to now. This subject has been discussed in about 30 papers. The data of these papers are presented in Table III. In recent years the number of experiments increased sharply and the quality and accuracy of spectrum measurements substantially improved. In most investigations  $^{252}\text{Cf}$  fission neutron spectrum was measured by time-of-flight method. High accuracy of measurements performed with this technique attracts many investigators. In a number of works the method of registration of recoil proton energy and of  $^3\text{He}$  (n, p) and  $^6\text{Li}$  (n,  $\alpha$ ) reaction products was used. The method of threshold detectors (activation of different foils) also was applied. Spectrum average energy was defined with moderation spheres (Bramblett counter) and manganese bath.

In the case of time-of-flight method as the most accurate one, the characteristics of neutron detectors used for measurements should be considered. The detectors can be divided into three groups according to the energy intervals where they are used. For energies above 0,5-1 MeV different organic scintillators are usually used. Detectors based on  $^6\text{Li}$  (n,  $\alpha$ ) reaction (lithium glasses,  $^6\text{LiI}(\text{Eu})$  crystals) are applied for energies below 2-3 MeV without principal restriction of low limit. Fission chamber with  $^{235}\text{U}$  layers is a detector for the whole energy interval (0-15 MeV). Its substantial drawback is low efficiency. This makes it difficult to use great flight distances and to provide a high energy resolution. It is also difficult to achieve a high statistical accuracy at spectrum edges.

The efficiency of neutron detectors based on  $^6\text{Li}$  (n,  $\alpha$ ) and  $^{235}\text{U}$  (n, f) reactions is determined according to the known standard cross-sections of these reactions. The effi-

ciency of organic scintillators is usually determined by special measurements in each work. In this case precision measurements of monochromatic neutron fluxes of different energies are necessary. It requires significant additional efforts of the experimentators, and they not always pay the due attention to this problem. However it should be noted that accuracy of efficiency measurements substantially improved after publication of the Recommendations of Meeting on fission neutron spectra in 1972 [1].

### 3.2. Spectrum measurements within the energy range from 1 to 8 MeV

This range covers 70-75% of the whole spectrum intensity. Naturally, it was studied most intensively. The authors of all papers noted a good agreement of experimental data in this energy interval with Maxwellian distribution. The values of parameter  $T$  in different papers performed by differential methods are in the range from 1,39 to 1,52 MeV, the most part of data being about 1,41-1,43 MeV. The work [23] done recently with threshold detectors showed the value of  $T$  which agrees with these data (1,41 MeV). "Age" method gives a somewhat higher value of  $T$  (1,48 MeV) [19, 23]. Note, that the comparison of results of different authors using only parameter  $T$  is not very informative as it does not provide a detailed definition of spectrum shape. The IAEA recommended to present information in the form of deviation of experimental data from Maxwellian distribution, for example, with  $T = 1,42$  MeV obtained as a result of evaluation [32]. Fig. 4 shows the results of some works in this form. In [30] experimental data did not deviate from distribution with  $T = 1,42$  MeV by more than  $\pm 2\%$  in the energy range from 1 to 6 MeV. In [16] these deviations were less than  $\pm 4\%$  (1-8 MeV). In other works substantially greater deviations were observed. It should be noted that in many even detailed measurements there were some negative features leading to consequences that have not been sufficiently analyzed. So, in [28]

fission gamma-quanta counter was used as "o"-time detector, but the influence of its characteristics on the spectrum was not studied. In [16] a very powerful fission source was used in a counter having a long light flash. As a result, the efficiency of registration was only 70% and the absence of low energy fragment discrimination was not shown. In [21] an appreciable part of fragments correlated by angle with neutron motion direction was not registered. The author of [33] noticed that in measurements by the time-of-flight method corrections for true-random coincidences sometimes were not taken into consideration. Thus, a detailed analysis of conditions of every experiment seems to be necessary to understand the causes of disagreement in results of different works.

### 3.3. Measurements in the energy region below 1 MeV

This energy range is difficult for measurements, and the difficulties increase with energy decrease. They are connected with absence of high effective, fast, insensitive to gamma-rays neutron detectors for measurements in keV-range. Since this part of spectrum contains essential part ( $\sim 25\%$ ) of the total intensity, therefore International Meetings [1, 34] recommended to pay a special attention to the necessity of precision measurements in this energy region. Fig. 5 shows experimental data for this part of spectrum. As it is seen (from the Figure) there is a great dispersion of data which indicate a significant neutron excess in comparison to Maxwellian distribution in this region (for example, at  $E = 50$  keV the excess reaches 40%). In some papers [25, 31, 35] devoted to the study of low energy part of spectrum it was shown that the spectrum shape is greatly influenced by neutron scattering on detectors, on components of experimental facility and in the environment. In [31] the measurements were supplemented by calculation of neutron scattering using Monte-Carlo method for definite experimental conditions.

The calculation was made for the case of scattering process evolution in the time scale. Experiment and calculation showed that even comparatively small scintillation detectors of neutrons and fragments noticeably distort low energy neutron fields. Taking into account the scattering effect along with the improvement of experimental conditions led the authors of [31] to the conclusion about possibility of description of neutron spectrum in the range from 1 keV to 1 MeV by one-parameter Maxwellian distribution.

Taking into consideration substantial effect of neutron scattering on spectrum shape as well as the results of recent work [36] it can be explained too high spectrum intensities ( $E < 100$  keV) (Fig. 5) by systematic errors. This also caused a significant disagreement (up to 70%) in results of two works made by one group of authors [27, 29]. In some papers [21, 28] a small neutron excess was observed (5-10%) for the range from 0,5 to 1,0 MeV. However, due to proximity of this part of spectrum to the threshold of neutron detector registration, it can not be considered as an established fact.

Thus, the spectrum shape for energy region below 1 MeV does not differ significantly from Maxwellian one.

#### 3.4. Spectrum measurements in the energy region above 8 MeV

Difficulties of studying this part of spectrum are connected with low intensity ( $\sim 2\%$  of total number of neutrons). Data of several papers are presented in Fig. 6. In the range of energies below 10 MeV the results are sufficiently close to Maxwellian distribution with  $T = 1,42$  MeV and at higher energies the data substantially diverge; besides, measurement errors become too high.

Measurements were finished in the region of 15 MeV as spectrum intensity becomes too low.

### 3.5. Irregularities in the spectrum

In  $^{252}\text{Cf}$  fission neutron spectrum within wide energy range (1 keV - 5 MeV) irregular deviations from smooth curve reaching 15% of continuous spectrum level above it ("fine structure" of spectrum) were observed in some works [37-40]. Special search for this effect in the range of 1-5 MeV led to negative result [41, 42] (the limit being  $\pm 2\%$ ). In the region of low energies the search for fine structure also failed [25, 31]. At the same time in several papers [21, 28] a structure of unknown origin was found but with significantly lower value ( $\leq 5\%$ ). It should be noted that the position of structure peaks in these papers did not agree with the data of [37-40]. In [41, 42] it was reported that the appearing of the irregularities might be due to different apparatus errors and to a number of side effects, for example, neutron scattering. The work [43] showed in direct experiment that neutron scattering in air could lead to a weak structure.

At present it may be thought that irregularities  $> 2-3\%$  peculiar to emission mechanism in neutron spectrum do not exist.

### 3.6. The influence of fission neutron emission time on the spectrum shape

It is known that most of the fission neutrons ( $\sim 90\%$ ) are evaporated from excited fragments moving with the velocities  $\sim 10^9$  cm/s. If fission fragments before neutron emission are partially or completely moderated, neutron energy in laboratory system changes markedly. Fragment moderation time in dense medium is  $10^{-14}$ - $10^{-12}$  s and depends on medium properties. In this connection it is necessary to know if there is any noticeable probability that neutron emission time exceeds  $10^{-14}$  s. Since fission fragments have a significant angular momentum ( $J \approx 8 \hbar$ ) one could expect a certain delay of emission for some part of neutrons. The authors of [37, 39, 44, 45] reported the detection of noticeable part



of neutrons ( $\sim 4\%$ ) emitted by fragments in  $10^{-9}$ - $10^{-7}$  s after fission event. Such neutrons can significantly change the spectrum in some regions. However in subsequent works [35, 46-49] this effect was not confirmed;  $^{252}\text{Cf}$  fission neutron emission time does not exceed  $10^{-14}$ - $10^{-15}$  [48, 49].

### 3.7. On the possibility of accurate spectrum shape calculation

Since neutron emission occurs from fragments of various masses, charges, angular momenta and excitation energies, to calculate an integral spectrum it is necessary to know the probability of neutron emission for each state of fragments. The theory cannot yet give corresponding accurate predictions. However the attempts to calculate  $^{252}\text{Cf}$  integral neutron spectrum are made. So, authors of [50] using statistical method of Hauser-Feshbach calculated the spectrum in the energy range 0,25-10 MeV which differs from experimental one [16] by 25% at  $E_n = 1$  MeV and by 50% at 10 MeV. The authors considered this agreement to be quite satisfactory especially because they did not use any fitting parameters. In an other paper [51] neutron spectrum was calculated in the c.m. system and rather a good agreement with experimental data was obtained [10]. Such calculations are very useful although their accuracy is yet insufficient. The neutrons of the "isotropic" component ( $\sim 10\%$ ) should be taken into account in such calculations. However, since the mechanism of their emission is not clear, the introduction of this component in calculation seems to be impossible now. In this connection it is desirable to study differential characteristics of  $^{252}\text{Cf}$  fission neutron emission (angular and energy dependences on angle, mass, charge, excitation energy of fragments) for understanding the full picture of neutron emission process.

### 3.8. Characteristics of $^{252}\text{Cf}$ fission neutron spectrum. Possibilities of data refinement

Evaluation of spectrum shape made by Grundl and Eisenhower [32] according to the results of several experimental investigations for energies from 0,25 to 8 MeV showed that in this region the deviation from Maxwellian distribution with  $T = 1,42$  MeV was not more than  $\pm 5\%$ . If along with this evaluation we use the data of recent works [30, 31] it is possible to describe the whole spectrum from 1 keV to 10 MeV by one-parameter Maxwellian distribution (1,42 MeV) with possible deviation from it  $\pm 10\%$  at the ends of this range. I think that before appearance of new reliable experimental data and new evaluations it is possible to use this representation as the first approximation. But we cannot forget that considerable deviations from such representation were observed in several papers (Fig. 4, 5, 6). All this requires great efforts to obtain new accurate data for definition of standard neutron spectrum. It is particularly important as the validity of any standard is determined by the accuracy with which it is known.

Owing to the fact that at present the method of accurate calculation of  $^{252}\text{Cf}$  fission neutron spectrum does not exist, experimental methods of its investigation should be developed.

The following measures can lead to the increase of data accuracy:

1. Precision measurements of spectrum in a wide energy interval (including low energy region) by single detector and in the same experiment to avoid the operation of "joining" the data from different detectors.

2. A particular attention must be paid to the accuracy of determination of neutron detector efficiency: it should be high enough and reliably determined (with compulsory indication of errors in their determination and methods of checking).

3. It is desirable to increase energy resolution, particularly in the range of energies above 5 MeV. It is necessary to account for the resolution in the whole energy interval to restore true shape of spectrum.

4. In measurements an account must be taken of different side effects which can substantially distort the shape of spectrum (neutron scattering, delayed gamma-quanta etc.).

5. It is advisable that in all subsequent works the authors themselves should perform a detailed analysis of all possible experimental errors both statistical and systematic ones.

6. It is desirable to make a detailed reviews of available works with periodical experimental error analysis (about one time in three years), spectrum evaluations based on the analysis of works and selection of reliable results.

7. Investigation of  $^{252}\text{Cf}$  spontaneous fission neutron emission process is to be continued; the calculation method for spectrum determination should be developed.

8. It is necessary to fulfill all the requirements to experiments and their descriptions presented in the Recommendations [1].

#### 4. THE MAIN CHARACTERISTICS AND SOME FEATURES OF NEUTRON SOURCE BASED ON $^{252}\text{Cf}$ SPONTANEOUS FISSION

a) The neutron yield  $B = 2,3 \cdot 10^9 \frac{1}{\text{mg} \cdot \text{s}}$ ; the average neutron number per fission event  $\bar{\nu} = 3,747 \pm 0,009$ ; the average energy of neutron spectrum  $\bar{E} = 2,12 \text{ MeV}$ ; half-life  $T_{1/2} = 2,64 \text{ years}$ .

b) Angle neutron distribution - isotropic.

c) Low gamma-background (2 fission gamma-quanta per one neutron).

d) The spectrum does not depend on the properties of backing material as the fragments lose their energy in dense medium for  $10^{-12}$ - $10^{-14}$  s and upper limit of neutron emission is about  $10^{-14}$  s.

e) In the case of californium source as a thin layer with registration of fission fragments, it is necessary to avoid the discrimination of the fragment part in relation to energy and angle as there exists correlation between the neutron energy and these values.

f) Using the thin layer the effect of self-dispersion of californium should be taken into account.

g) The fraction of delayed neutrons is  $\sim 0,25\%$  [52].

## 5. CONCLUSION

Spontaneously fissionable isotopes of plutonium and curium have been used for a long time as neutron sources. In the last years the sources based on  $^{252}\text{Cf}$  are widely used as most convenient according to all the characteristics.

The widespread use of spontaneous fission neutron sources requires a more exact knowledge of energy neutron distribution from these sources. This is particularly important for  $^{252}\text{Cf}$  which was recommended as a standard. Despite the successful recent investigation on the shape of  $^{252}\text{Cf}$  spontaneous fission neutron spectrum, the further efforts on substantial correction of these data are necessary.

## Acknowledgements

The author would like to thank S. S. Kovalenko and I. T. Krisyuk for fruitful discussions of the problems under consideration.

# REFERENCES

- [1] Prompt Fission Neutron Spectra (Proc. Consult. Meeting Vienna, 1971), IAEA, Vienna (1972) 169.
- [2] BAK, M.A., SHIMANSKAYA, N.S., Neutron sources (Rus.), Atomizdat, Moscow (1969); GORBACHEV, V.M. etc., Radiations Interaction with Heavy Nuclei and Nuclear Fission (Rus.), Atomizdat, Moscow (1976).
- [3] BELOV, L.M. etc., Jadernaya Physika (Rus.) 9 (1969) 727.
- [4] ZHURAVLEV, K.D. etc., Neutronnaya Physika (Rus.) (Proc. II All Union Conf., Kiev, 1973) 4, Obninsk (1974) 57.
- [5] HEROLD, F., Savannah River Laboratory Report DK-949 (1969).
- [6] ALEXANDROVA, Z.A. etc., Atomnaya Energiya (Rus.) 36 (1974) 282.
- [7] TERRELL, J., Phys. Rev. 113 (1959) 527.
- [8] HJALMAR, E.M. etc., Ark. Fys. 10 (1955) 357.
- [9] SMITH, A.B., FIELDS, P.R., ROBERTS, J.H., Phys. Rev. 108 (1957) 411.
- [10] BOWMAN, H.R., Phys. Rev. 126 (1962) 2120.
- [11] CONDE, H., DURING, G., Ark. Fys. 29 (1965) 313.
- [12] MEADOWS, J.W., Phys. Rev. 157 (1967) 1076.
- [13] GREEN, L., Nucl. Sci. Eng. 37 (1969) 232.
- [14] ZAMJATNIN, Yu.S. etc., Nucl. Data for Reactors (Proc. II Intern. Conf., Helsinki, 1970) IAEA, Vienna (1970) 183.
- [15] EKI, L. etc., Atomnaya Energiya 33 (1972) 785 (Rus.); EKI, L. etc., Prompt Fission Neutron Spectra (Proc. Consult. Meeting, Vienna, 1971) IAEA, Vienna (1972) 81.
- [16] GREEN, L., MITCHELL, J.A., STEEN, N.M., Nucl. Sci. Eng. 50 (1973) 257.
- [17] KNITTER, N.N., PAULSEN, A., LISKIEN, H., ISLAM, M.M., Atomkernenergie 22 2 (1973) 84.
- [18] WERLE, H., BLUHM, H., Prompt Fission Neutron Spectra (Proc. Consult. Meeting, Vienna, 1971) IAEA, Vienna (1972) 65.
- [19] SPIEGEL, V., Nucl. Sci. Eng. 54 (1974) 28.

- [20] BONNER, T.W., Nucl. Phys. 23 (1961) 116.
- [21] KOTELNIKOVA, G.V. etc., Report FEI-575 (1975) (Rus.); KOTELNIKOVA, G.V. etc., Nejtronnaya Physika (Proc. III All Union Conf., Kiev, 1975) 5 Obninsk (1976) 109 (Rus.).
- [22] JOHNSON, R.H. etc., Trans. Am. Nucl. Soc. 22 (1975) 727.
- [23] CSIKAI, J., DEZSÖ, Z., Ann. Nucl. En. 3 11/12 (1976) 527.
- [24] BATENKOV, O.I. etc., Nejtronnaya Physika (Proc. III All Union Conf., Kiev, 1975) 5, Moscow (1976) 114 (Rus.).
- [25] BLINOV, M.V., VITENKO, V.A., TOUSE, V.T., Neutron Standards and Applications (Proc. Intern. Symp., Gaithersburg, 1977) N 139-493 (1977) 194.
- [26] DYACHENKO, P.P. etc., Atomnaya Energiya 42 (1977) 25 (Rus.).
- [27] NEFEDOV, V.N. etc., Nejtronnaya Physika (Proc. IY All Union Conf., Kiev, 1977) 3, Moscow (1977) 205 (Rus.).
- [28] BERTIN, A., FREHAUT, J., Rapport CEA-R-4895 (1978).
- [29] STAROSTOV, B.J. etc., Report NJJAR P-22(356) Dimitrovgrad (1978) (Rus.).
- [30] BOLDEMAN, J.W. etc., Trans. Am. Nucl. Soc. 32 (1979) 733.
- [31] BLINOV, M.N. etc., Interactions of Fast Neutrons with Nuclei (Proc. IX Intern. Symp., Gaussig, GDR, 1979) ZfK, Rossendorf (1980) (to be published).
- [32] GRUNDL, J.A., EISENHAUER, C.M., Neutron Cross Sections and Technology (Proc. Conf. Washington, 1975) 1 NBS-425 (1975) 250.
- [33] CHALUPKA, A., Nucl. Sci. Eng. (1979) 339.
- [34] STEWART, L., EISENHAUER, C.M., Neutron Standards and Applications (Proc. Intern. Symp. Gaithersburg, 1977), NBS-493 (1977) 198; SMITH, A.B., 349.
- [35] BLINOV, M.V., VITENKO, V.A., KRISYUK, I.T., Report RI-30, Leningrad (1974) (Rus.); DAN 224 (1975) 802 (Rus.).
- [36] KONONOV, V.N. etc., Report KFKI 1979-72, Budapesht (1979) (Rus.).
- [37] NEFEDOV, V.N., Report NIIAR P-52, Melekess (1969) (Rus.).

- [38] PROKHOROVA, L.I. etc., Atomnaya Energiya 33 (1972) 767 (Rus.).
- [39] NEFEDOV, V.N. etc., Nejtronnaya Physika (Proc. II All Union Conf., Kiev, 1973) 4, Obninsk (1974) 155 (Rus.).
- [40] AVERCHENKOV, V.Ja. etc., Nejtronnaya Physika (Proc. II All Union Conf., Kiev, 1973) 4, Obninsk (1974) 143 (Rus.).
- [41] BATENKOV, O.I. etc., Nejtronnaya Physika (Proc. IY All Union Conf., Kiev, 1977) 3, Moscow (1977) 201 (Rus.).
- [42] SCOBIE, J., SCOTT, K.D., FEATHER, N., VASS, D.G., J. Phys. G: Nucl. Phys. 3 10 (1977) 1443.
- [43] GUENTHER, P., HAVEL, D., SJOBLUM, R., SMITH, A., Report ANL/NDM - 19 (1976).
- [44] NEFEDOV, V.N., MELNIKOV, A.K., STAROSTOV, B.I. Prompt Fission Neutron Spectra (Proc. Consult. Meeting Vienna 1971), IAEA, Vienna (1972) 89.
- [45] NEFEDOV, V.N., STAROSTOV, B.I., Nejtronnaya Physika (Proc. II All Union Conf., Kiev, 1973) 4, Obninsk (1974) 163 (Rus.).
- [46] DJACHENKO, P.P. etc., Jadernaya Physika 19 (1974) 1212 (Rus.).
- [47] PIKSAJKIN, V.M. etc., Jadernaja Physika 25 (1977) 495 (Rus.).
- [48] SKARSVAG, K., Phys. Rev. C. 16 (1977) 16.
- [49] BATENKOV, O.I. etc., Interactions of Fast Neutrons with Nuclei (Proc. Y Intern. Symp. Gaussig, GDR, 1975) ZfK-324, Rossendorf (1976) 196.
- [50] DIETRICH, F.S., BROWN, J.C., Trans. Amer. Nucl. Soc. 32 (1979) 728.
- [51] ACHMEDOV, G.M., STAVINSKY, V.S. "Vopr. At. Nauki i Techniki". Jad. Const N 4(31) (1978) 31 (Rus.).

TABLE I

Characteristics of Some Spontaneously Fissionable Isotopes [2, 38]

Element	Mass number	Half-life		$\frac{T_{sp.f}}{T_d} = \frac{N_d}{N_{sp.f}}$	Neutron yield $\frac{1}{mg \cdot s}$	Nu - bar $\bar{\nu}_p$
		$T_d$ (years)	$T_{sp.f}$ (years)			
Pu	240	$6,5 \cdot 10^3$	$1,3 \cdot 10^{11}$	$2,0 \cdot 10^7$	0,9	2,15
	242	$3,8 \cdot 10^5$	$7,2 \cdot 10^{10}$	$1,9 \cdot 10^5$	1,6	2,14
Cm	244	18,1	$1,3 \cdot 10^7$	$7,2 \cdot 10^5$	$1,1 \cdot 10^4$	2,68
	246	$4,8 \cdot 10^3$	$1,8 \cdot 10^7$	$3,8 \cdot 10^3$	$8,8 \cdot 10^3$	2,95
	248	$4,0 \cdot 10^5$	$4,2 \cdot 10^6$	10,6	$4,1 \cdot 10^4$	3,15
Cf	252	2,72	85,2	32,5	$2,3 \cdot 10^9$	3,737
	254	60	60,5 days	$3 \cdot 10^{-3}$	$1,3 \cdot 10^{12}$	3,89



TABLE II

Average Energy of Spontaneous Fission Neutron Spectra ( $\bar{E}$ )

Nuc- lide	Mass number	Year	Authors, references	Neutron energy range (MeV)	Method	Results	
						$T_{\max w}$ (MeV)	$\bar{E}$ (MeV)
Pu	240	1961	Bonner [20]	< 4	Integr. (Bramblett counter)	1,16±0,03	1,74±0,05
		1974	Alexandrova etc. [6]	2-14	Single-crystal spectrometer	1,27±0,03	1,91±0,05
	242	1969	Belov etc. [3]	0,5-6	TOF (time-of- flight)	1,21±0,06	1,82±0,09
Cm	244	1969	Belov etc. [3]	0,5-7	TOF	1,37±0,04	2,06±0,06
		1969	Herold [5]	0,5-6	<sup>3</sup> He-spectrometer	1,46±0,06	2,19±0,09
		1974	Alexandrova etc. [6]	2-14	Single-crystal spectrometer	1,33±0,03	2,00±0,05
	246	1974	Zhuravlev etc. [4]	0,4-6	TOF	1,38±0,03	2,07±0,05
		1974	Zhuravlev etc. [4]	0,4-6	TOF	1,50±0,05	2,25±0,08
	248	1974	Zhuravlev etc. [4]	0,4-6	TOF	1,43±0,04	2,15±0,06
Cf	252	1975	Grundl, Eisenhauer [32]	0,25-8	Evaluation	1,42	2,13

TABLE III

Summary of Data on Fission Neutron Spectrum of  $^{252}\text{Cf}$ 

NN	Year	Authors, references	Neutron energy range (MeV)	Method, neutron detector	Results	
					$T_{\text{maxw}}$ (MeV)	$\bar{E}$ (MeV)
1.	1955	Hjalmar etc. [8]	$> 2$	Photoemulsion	$1,40 \pm 0,09$	-
2.	1957	Smith etc. [9]	0,2-7,0	TOF, plast. scint.; photoemuls.	-	2,36
3.	1961	Bonner [20]	$< 4$	Integr (Bramblett counter)	$1,367 \pm 0,030$	-
4.	1962	Bowman etc. [10]	0,5-6,0	TOF, plast. scint.	-	$2,34 \pm 0,05$
5.	1965	Conde, During [11]	0,07-7,5	TOF, $^6\text{Li}$ -glass, plast. scint.	$1,39 \pm 0,04$	(2,09)
6.	1967	Meadows [12]	0,003-15	TOF, $^6\text{Li}$ -glass, liquid scint.	1,52	2,348
7.	1969	Green [13]	-	Integr. (Mn-bath)	1,39	(2,09)
8.	1970	Zamjatnin etc. [14]	0,005-6,0	TOF, $^6\text{Li}$ -glass, plast. scint.	$1,48 \pm 0,03$	$(2,22 \pm 0,05)$
9.	1972	Jeki etc. [15]	0,002-1,0	TOF, $^6\text{Li}$ -glass	$1,57(1,3)$	-
10.	1972	Smith, Koster [53]		Review		
11.	1976	Knitter [54]		Review		
12.	1972	Werle, Bluhm [18]	0,2-8,0	$^3\text{He}$ -spectrometer, prop. counter	$(1,42 \pm 0,015)$	$2,155 \pm 0,024$ $2,130 \pm 0,022$

TABLE III (continued)

NN	Year	Authors, references	Neutron energy range(MeV)	Method, neutron detector	Results	
					$T_{\max w}$ (MeV)	$\bar{E}$ (MeV)
13.	1973	Green etc. [16]	0,5-13	TOF, org. scint.	$1,406 \pm 0,015$	$2,105 \pm 0,014$
14.	1973	Knitter etc. [17]	0,15-15	TOF, org. scint.	$1,42 \pm 0,05$	$2,13 \pm 0,08$
15.	1974	Spiegel [19]	-	Integr. ("age")	-	$2,21 \pm 0,05$
16.	1974	Alexandrova etc. [6]	2,04-13,2	Single-crystal spectrometer	$1,42 \pm 0,03$	$(2,13 \pm 0,045)$
17.	1975	Kotelnikova etc. [21]	0,5-7,0	TOF, liquid scint.	$1,46 \pm 0,02$	$(2,19 \pm 0,03)$
18.	1975	Johnson [22]	2,6-15	Single-crystal spectrometer	$(1,42 \pm 0,02)$	$2,13 \pm 0,03$
19.	1976	Csikai, Dezsö	2,5-15	Activation detector (threshold reactions); "age"-method	$1,41 \pm 0,02$ $1,48 \pm 0,03$	$(2,12 \pm 0,03)$ $(2,22 \pm 0,05)$
20.	1976	Batenkov etc. [24]	0,02-2,0	TOF, ${}^6\text{LiI}$ -crystal	1,40	-
21.	1976	Stewart etc. [34]	-	Review		
22.	1975	Grundl etc. [32]	0,25-8,0	Evaluation	$(1,42)$	2,13
23.	1977	Blinov etc. [25]	0,01-7,0	TOF, ${}^6\text{LiI}$ -crystal, ${}^{235}\text{U}$ -chamber	$1,41 \pm 0,03$	2,12
24.	1977	Djachenko etc. [26]	< 2	Amplitud., reaction ${}^6\text{Li}(n, \alpha)\text{T}$	1,18	

TABLE III (continued)

NN	Year	Authors, references	Neutron energy range (MeV)	Method, neutron detector	Results	
					$T_{\max w}$ (MeV)	E (MeV)
25.	1977	Nefedov etc. [27]	0,01-10	TOF, metal. $^{235}\text{U}$ ; $^{235}\text{U}$ - chamber	1,28	(1,92)
26.	1978	Bertin [28]	1-10	TOF, liquid scint.	(1,51)	2,27 $\pm$ 0,02
27.	1978	Nefedov etc. [29]	0,01-10	TOF, metal. $^{235}\text{U}$ , $^{235}\text{U}$ - chamber	1,43 $\pm$ 0,02	(2,15 $\pm$ 0,03)
28.	1979	Blinov etc. [31]	0,001-1	TOF, $^6\text{LiI}$ -crystal	1,42	
29.	1979	Boldeman etc. 30	0,6-15	TOF plast. scint.	1,424 $\pm$ 0,013	2,136 $\pm$ 0,020

Note: The values of  $T_{\max w}$  and E in brackets are taken not from the reference works, but calculated according to their data.

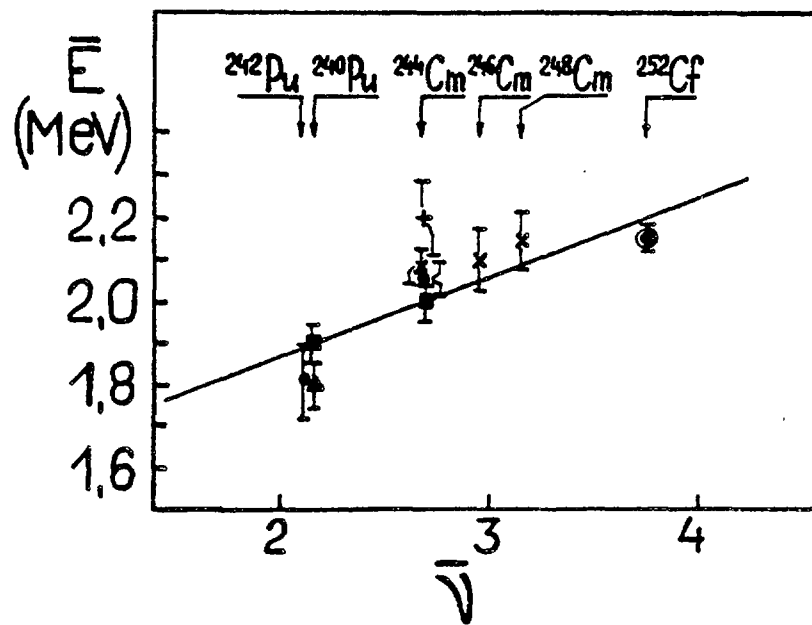


Fig. 1. The dependence of average energy of neutron spectra  $\bar{E}$  on  $\bar{\nu}$  -  $\bar{\nu}$

• - [3], x - [4], + - [5], ■ - [6], ▲ - [20], ⊙ - [32]

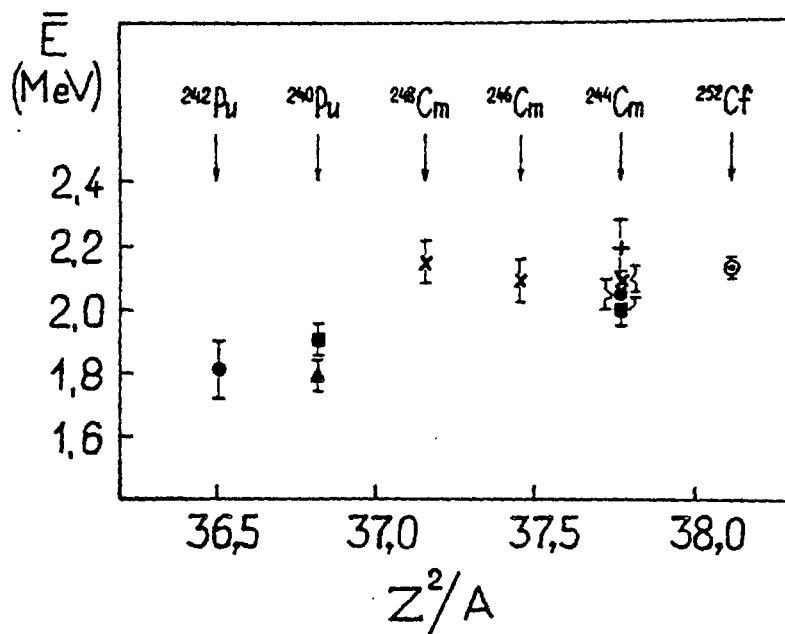


Fig. 2. The dependence of average energy of neutron spectra  $\bar{E}$  on fissionable parameter  $Z^2/A$

● - [3], × - [4], + - [4], ■ - [6], ▲ - [20], ⊗ - [32].

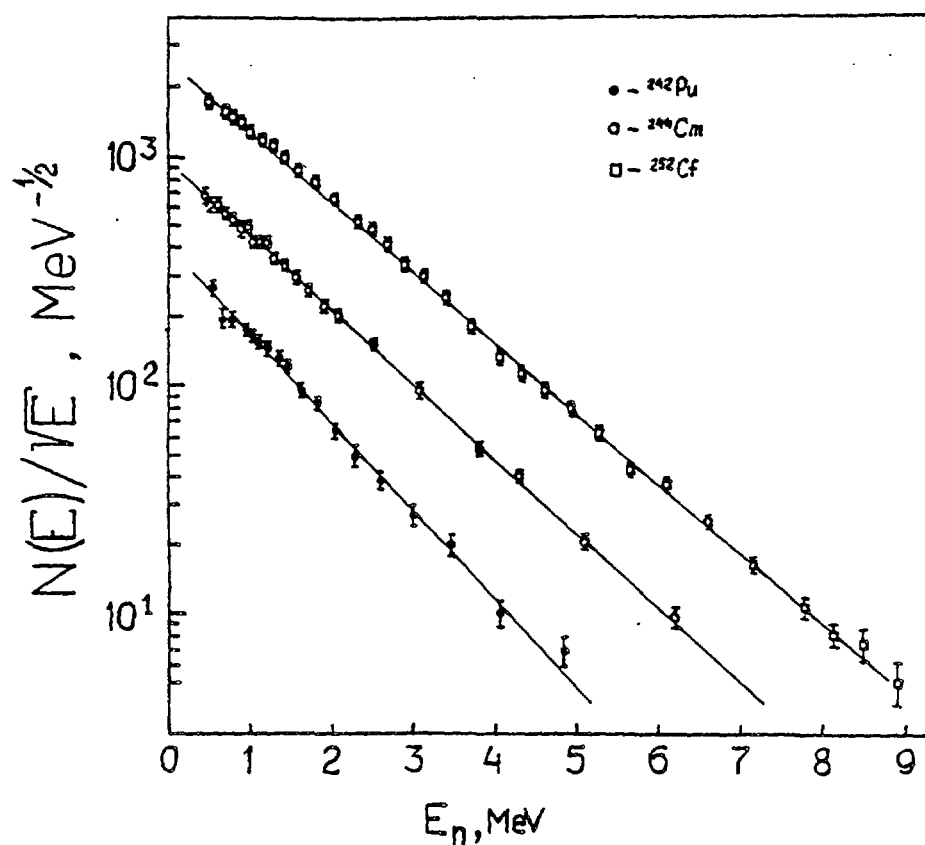


Fig. 3. Energy neutron spectra of spontaneous fission  $^{242}\text{Pu}$ ,  $^{244}\text{Cm}$ ,  $^{252}\text{Cf}$ . Straight lines - Maxwellian distributions with parameters  $T$  equal to 1,21 MeV, 1,37 MeV and 1,42 MeV.

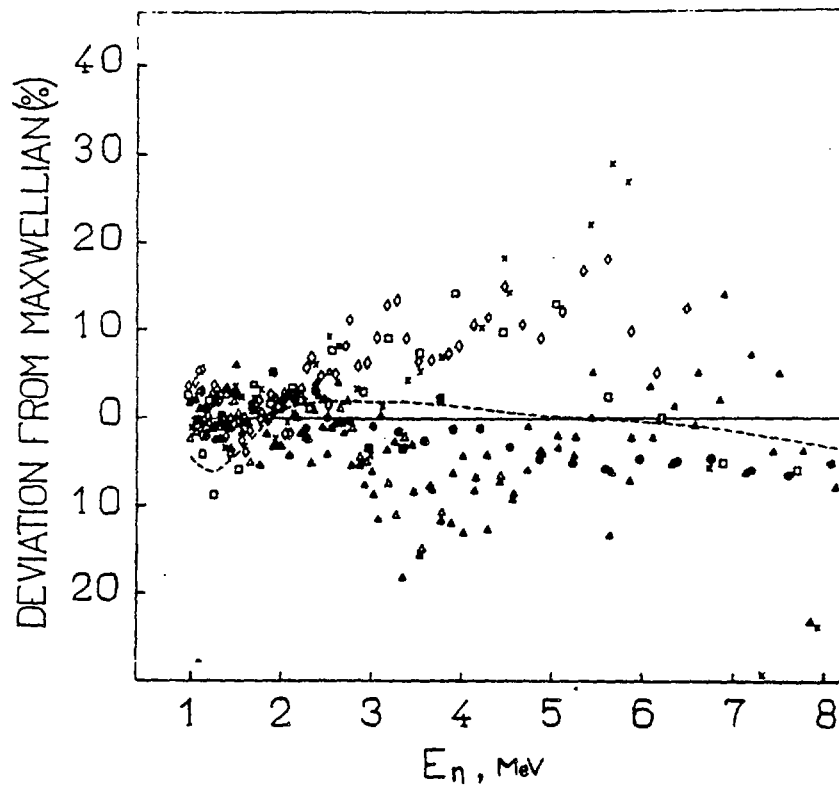


Fig. 4. The deviation of the experimental data on  $^{252}\text{Cf}$  spontaneous fission neutron spectrum from Maxwellian distribution with  $T = 1,42$  MeV. The data were normalized in the interval 1-2 MeV

● - [6], --- [16],  $\Delta$ ,  $\blacktriangle$  - [17],  $\square$ ,  $\blacksquare$  - [18],  $\diamond$  - [21], x - [29]



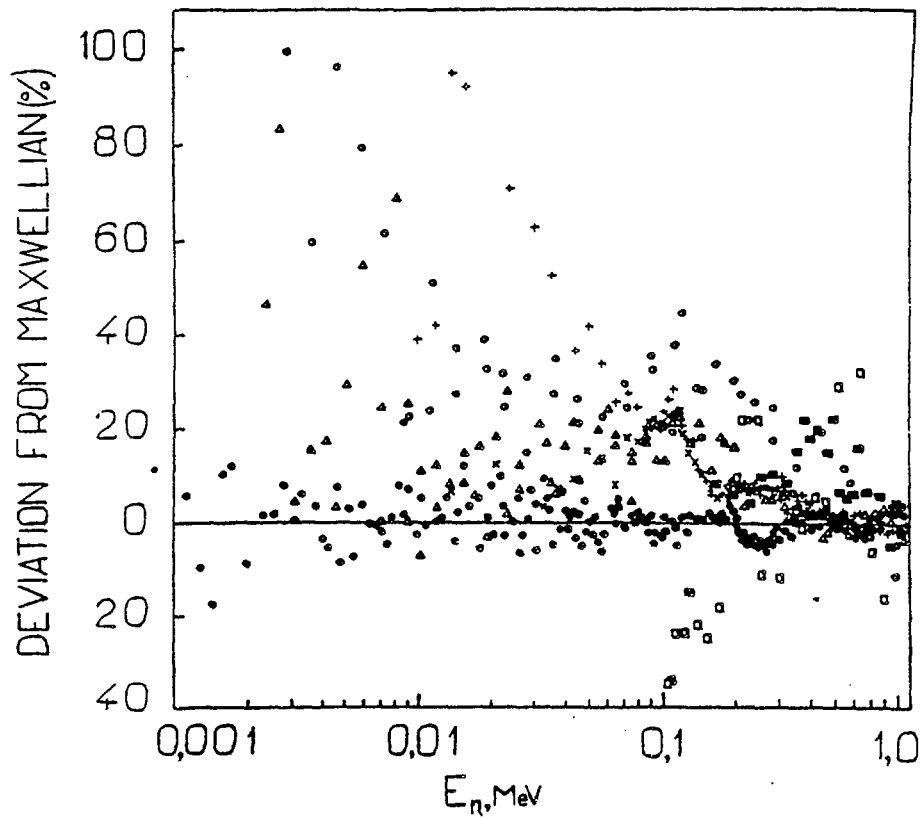


Fig. 5. The deviation of the experimental data on  $^{252}\text{Cf}$  spontaneous fission neutron spectrum from Maxwellian distribution with  $T = 1,42$  MeV. The data were normalized at 1 MeV

○ - [12], Δ - [15], □, ■ - [18], + - [27], x - [29], ● - [31]

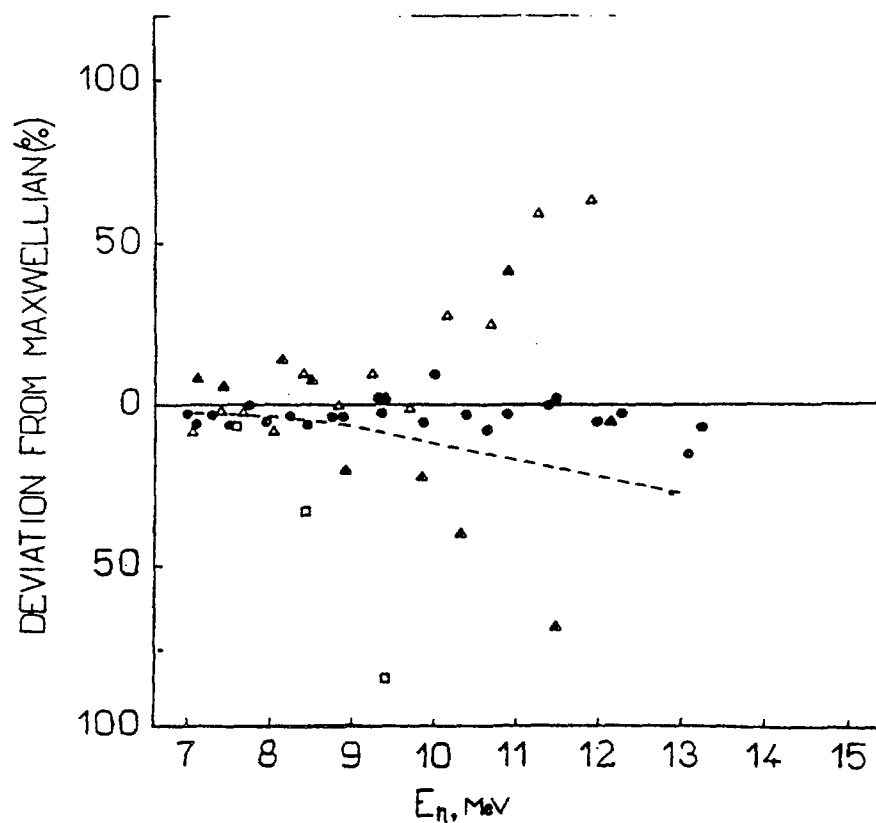


Fig. 6. The deviation of the experimental data on  $^{252}\text{Cf}$  spontaneous fission neutron spectrum from Maxwellian distribution with  $T = 1,42$  MeV. The data were normalized in the interval 1-2 MeV

● - [6],  $\Delta, \blacktriangle$  - [17],  $\square$  - [18],  $\bullet$  - [30]

# List of Figures

- Fig. 1. The dependence of average energy of neutron spectra  $\bar{E}$  on  $Nu - \bar{\nu}$ .
- - [3], x - [4], + - [5], ■ - [6], ▲ - [20],
  - ⊙ - [32].
- Fig. 2. The dependence of average energy of neutron spectra  $\bar{E}$  on fissionable parameter  $Z^2/A$ .
- - [3], x - [4], + - [5], ■ - [6], ▲ - [20],
  - ⊙ - [32].
- Fig. 3. Energy neutron spectra of spontaneous fission  $^{242}\text{Pu}$ ,  $^{244}\text{Cm}$ ,  $^{252}\text{Cf}$ . Straight lines - Maxwellian distributions with parameters  $T$  equal to 1,21 MeV, 1,37 MeV and 1,42 MeV.
- Fig. 4. The deviation of the experimental data on  $^{252}\text{Cf}$  spontaneous fission neutron spectrum from Maxwellian distribution with  $T = 1,42$  MeV. The data were normalized in the interval 1-2 MeV
- ⊙ - [6], --- [16], Δ, ▲ - [17], □, ■ - [18], ◇ - [21],
  - x - [29].
- Fig. 5. The deviation of the experimental data on  $^{252}\text{Cf}$  spontaneous fission neutron spectrum from Maxwellian distribution with  $T = 1,42$  MeV. The data were normalized at 1 MeV.
- - [12], Δ - [15], □, ■ - [18], + - [27], x - [29],
  - - [31].
- Fig. 6. The deviation of the experimental data on  $^{252}\text{Cf}$  spontaneous fission neutron spectrum from Maxwellian distribution with  $T = 1,42$  MeV. The data were normalized in the interval 1-2 MeV
- ⊙ - [6], Δ, ▲ - [17], □ - [18], ● - [30].

## Thermal and Epithermal Reactor Neutron Beams and Fields

Wolfgang G. Alberts

Physikalisch-Technische Bundesanstalt, Braunschweig,  
Fed. Rep. of Germany

### Introduction:

At present thermal neutrons seem to play a minor role in the family of neutron sources. Their radiobiological effectiveness and their destructive power, which would be significant in the fields of health physics, in radiation protection work or in material damage research, are smaller than that of faster neutrons.

It seems to me as well that the intensity of research with thermal neutrons has decreased considerably in the last decade as compared to fast neutron research, at least for these applications. I would therefore like to consider this paper rather as an introductory remark for a discussion than as a review paper as it was planned originally.

In fundamental research, e.g. in solid state and nuclear physics, there is an interest in using very slow neutrons in the meV range as probes for discovering fundamental properties of matter. There is probably some activity of this kind at almost every research reactor and for this purpose thermal or subthermal neutrons are extracted from the reactors by curved neutron guides or gained from neutron diffractometers or rotating selectors. This paper shall deal, however, with thermal neutron fields with broad spectra of preferentially Maxwellian form.

At the time of generation free neutrons are generally fast. They are slowed down in moderating media by scattering processes and lose energy until they are in "thermal equilibrium" with their ambience or vanish by absorption. Thermal neutrons are therefore produced by media with a large moderation-to-absorption ratio such as graphite or heavy water and the aim is to keep the fast and epi-thermal neutron component as small as possible at the place of interest. Thermal neutrons of this kind are responsible for

thermal fission of  $^{235}\text{U}$  and  $^{239}\text{Pu}$  and therefore essential in most of the power and research reactors in the world. It seemed necessary, therefore, to do extensive thermal neutron metrology even without reactors. In the late Sixties, for instance, an international intercomparison of the thermal neutron flux density unit was performed using mostly standard thermal neutron flux assemblies employing  $(\alpha, n)$  sources distributed in a suitable moderator. The results of this intercomparison were published in Metrologia /1/, the international journal of scientific metrology, and the participants came from the exclusive club of national laboratories. Another example: at the National Physical Laboratory in the United Kingdom a standard thermal flux assembly has been established for about a decade which comprises a graphite moderator containing two neutron sources consisting of beryllium targets bombarded by deuterons from a Van de Graaff accelerator.

Now, the subject of this paper is thermal and epithermal reactor beams and fields. I want to show you with a few examples some thermal and intermediate-energy neutron fields in and at reactors and some of their properties.

The desired properties of a thermal neutron field are strongly connected with its intended application. For some applications one needs isotropic fields with high intensity, whereas for others, one prefers monodirectional fields. From the point of view of application I would like to discuss thermal neutron fields in these two classes: cavity fields and beams.

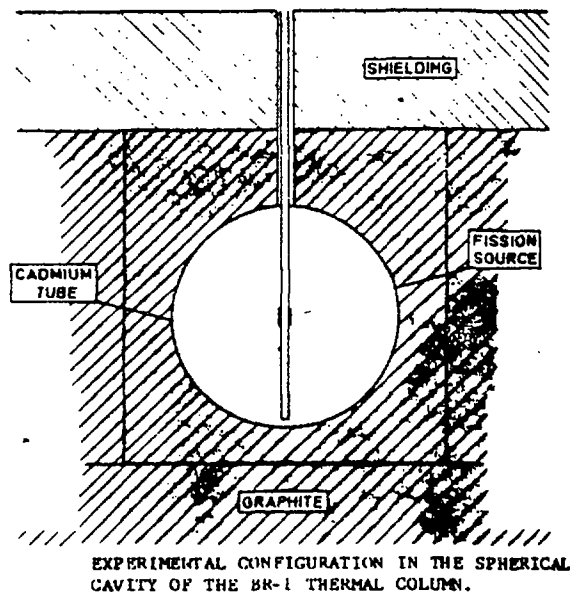
#### Cavities:

Most of the operating research reactors are equipped with a graphite thermal column. Some of these columns have a spherical cavity to provide an isotropic, well thermalized neutron field with a high neutron flux density. At present they seem to have become insignificant as thermal standard fields in comparison with their use for producing secondary neutron fields with converters. All that remains of the original field properties is the absence of fast neutrons from the reactor. Thus the characteristics of the secondary field depend exclusively on the materials within the cavity. The resulting isotropic or quasi-isotropic neutron fields are a standardized approximation of the field conditions in a reactor. Work done with such fields is well documented in IAEA publications such as from the Consultants' Meeting on Neutron Cross Sections for Reactor Dosimetry of 1976 /5/ from which the

following examples are taken <sup>\*</sup>). They all employ uranium-235 as a converter to produce an initial thermal-neutron-induced fission spectrum. Additional materials are used to give the spectrum the desired shape. The original thermal neutrons are kept away from the cavity center by shielding layers.

1. A  $^{235}\text{U}$  fission spectrum is produced in the 1 m cavity in the thermal column of the BR-1 at Mol, Belgium /2,5/.

The experimental configuration is shown below:

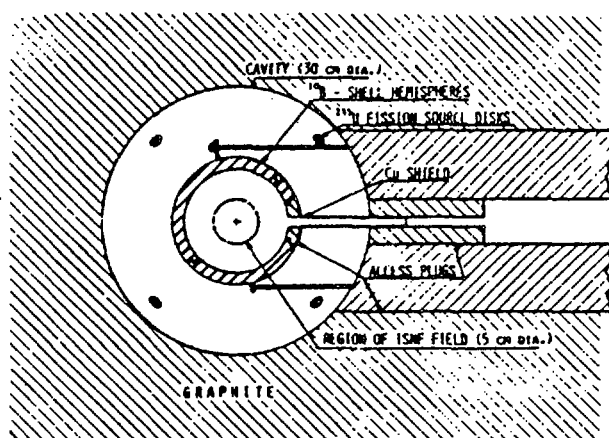


The thermal field causes thermal fission in a thin metallic 93 %-enriched uranium sheet which is wrapped around the center of a cadmium tube. In this way it produces a quasi-isotropic uranium thermal-neutron-induced fission spectrum within the center of the tube with suppression of the thermal neutrons. Problems with epithermal neutrons returned from the cavity walls are controlled by exact geometrical calculations.

2. A neutron spectrum with a strong intermediate energy component (ISNF) is generated in the 30 cm cavity in the thermal column of the 10 MW NBS reactor at Gaithersburg, USA /3,5/. A cross section of the facility is shown on the next page:

---

<sup>\*</sup>) All figures in this paper are taken from the respective references.



Intermediate-Energy Standard Neutron Field arrangement at the center of the NBS Reactor thermal column.

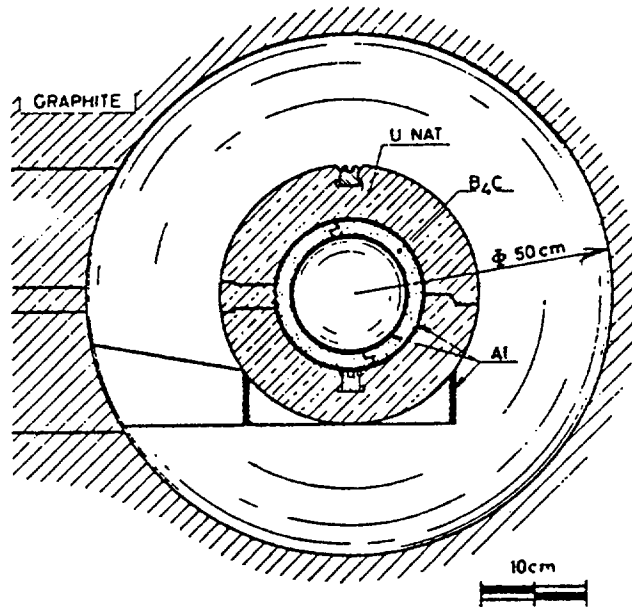
Eight 93 %-enriched uranium metal discs positioned 1 cm from the cavity wall produce fission neutrons which are partly moderated and scattered from the wall. These scattered neutrons, together with the direct component from the source disks, are transmitted through a 14 cm dia. boron-10 shell to produce the ISNF neutron field at the center of the cavity. Knowledge of the properties of the field relies on calculations which include the densities and the cross sections, all standard, of carbon, uranium and boron-10.

If the boron shell is omitted or replaced by a cadmium shell (ISNF/CV), a near- $1/E$  spectrum from 0.4 eV to 0.1 MeV is created at the center of the cavity. The total neutron flux density amounts to about  $1.6 \cdot 10^9 \text{ cm}^{-2} \text{ s}^{-1}$ .

Whereas the slowing down of fission neutrons in an infinite, non-absorbing moderator with constant scattering cross section would result in a pure  $1/E$  field above the thermalization range, in a realistic field like ISNF/CV one has to assign to measurements realistic uncertainties due to spectral shape deviations from the ideal law. Carbon cavity wall return neutron flux density spectra do not obey the  $1/E$  law but generally speaking the deviations are very well known for certain purposes, as for instance the measurement of average cross sections /4/. The calculated flux density at the center of ISNF/CV deviates from  $1/E$  by 18 % per decade over the energy range 0.4 eV to 10 keV /5/.

3. Another intermediate-energy standard neutron field called  $\Sigma\Sigma$  /5,8/ is produced in the 50 cm cavity in the thermal column of the BR-1 at Mol, Belgium.

A schematic view is shown below:



Fission neutrons, converted essentially by the first one centimeter of the outer portion of the 5 cm thick uranium shell, arrive at the center of the system degraded in energy primarily due to elastic scattering in the graphite and inelastic scattering in the uranium. The boron carbide shell preferentially absorbs the low-energy component, shaping this portion of the spectrum to make the Sigma Sigma energy distribution relevant for fast reactor application. The total neutron flux density amounts to  $7 \cdot 10^8 \text{ cm}^{-2} \text{ s}^{-1}$ ; departures between spectrometry results and calculation of the spectrum are below  $\pm 15 \%$ .

#### Beams:

The properties of thermal neutron beams differ from those of the cavity fields, which again influences the applications. Whereas the cavity neutrons form homogeneous neutron fields with various spectra at the center of the cavities and are used for the irradiation of small samples like activation foils or small fission chambers, thermal neutrons are needed as well to calibrate larger instruments which may even contain moderating material themselves, e.g. rem counters. For such calibrations cavity sources are

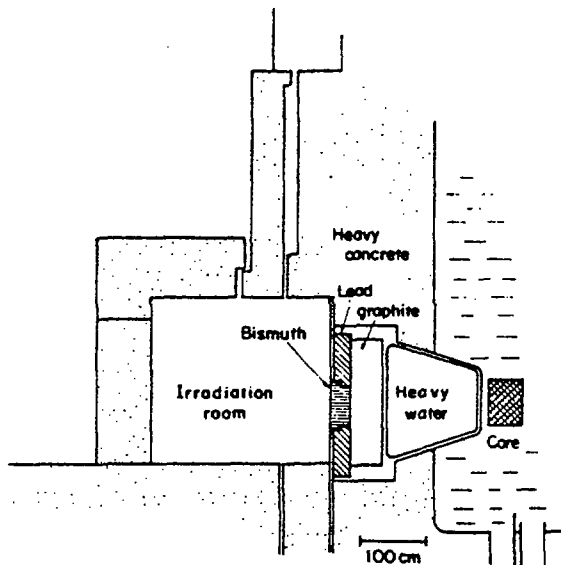


not very feasible as standards because of the strong coupling between cavity wall and instrument: the possible scattering of neutrons between detector and cavity wall causes flux density disturbances. On the other hand, the response of detectors irradiated in a thermal neutron beam, free in air, represents the quantities of the undisturbed field.

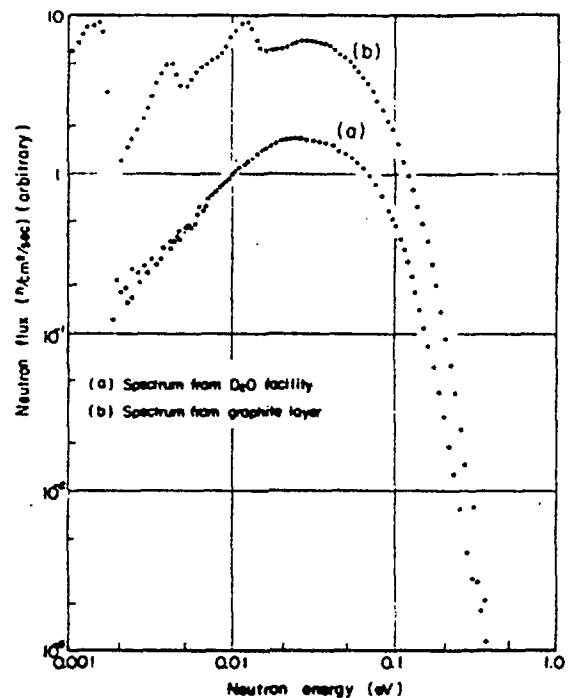
Contrary to the fields in cavities the flux density spectral characterisation, i.e. the temperature parameter of the Maxwellian distribution and deviations from the Maxwellian shape, can be achieved in beams directly by chopper time-of-flight measurements. The thermal neutron flux density is smaller by several orders of magnitude; on the other hand, the relative  $\gamma$ -ray background is usually lower than in the case of cavities.

Again a more or less arbitrary selection of three examples for thermal neutron beams:

1. The graphite reflector and column at the 10 kW, Argonaut-type Low Flux Reactor (LFR) at Petten, the Netherlands /9/. The maximum thermal neutron flux density in the central reflector region is of the order of  $10^{11} \text{ cm}^{-2} \text{ s}^{-1}$ . The total length of moderating graphite (reflector plus thermal column) is 185 cm, which produces very well-moderated thermal neutron beams without a fast (fission) neutron background (cadmium ratio for  $1/v$  absorber  $\sim 10^3$ ). At a distance of about 0.5 m from the opening in the biological shield the beam has a width (at 0.9 maximum flux density) of 23 cm with a thermal neutron flux density of  $1 \cdot 10^4 \text{ cm}^{-2} \text{ s}^{-1}$ . A central interest in these beams stems from the investigation of the neutron response of personnel neutron dosimeters.
2. Heavy water facility attached to the 5 MW Kyoto University Reactor (KUR) Japan /6/. A schematic diagram of the facility is shown on the next page together with two spectra explained below:



Kyoto University Reactor (KUR)  
Heavy Water Facility

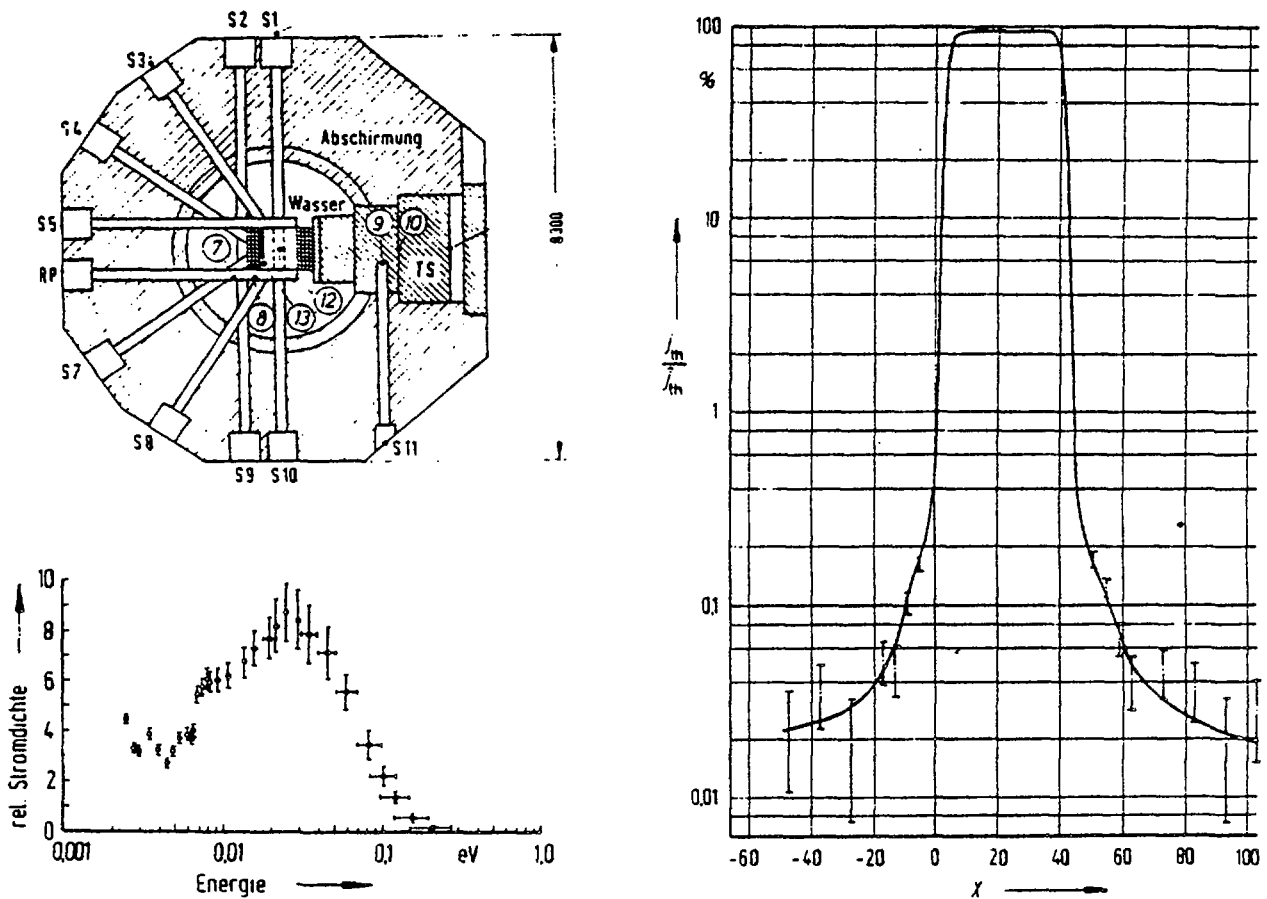


Neutron Spectra Yielded from KUR D<sub>2</sub>O Facility  
and Graphite Layer

A cone-shaped tank contains 2 tons of D<sub>2</sub>O. The layer is about 1.4 m thick and gives rise to a smooth spectrum (spectrum (a)) which is in good agreement with a Maxwellian distribution having a temperature parameter corresponding to 60 °C (slightly higher than the heavy water temperature of 40 °C). No contribution of epithermal neutrons was found; this is underlined by a cadmium ratio of  $5 \cdot 10^3$  for gold foils /6/. Spectrum (b) is taken behind an additional 48 cm graphite layer; it shows some structure at lower energies which is assumed to be due to the crystal structure of the graphite. The spectra were taken with a fast chopper measuring device. A bismuth scatterer can be applied to reduce the  $\gamma$ -ray background in the beam. A concrete-shielded 2.4 m x 2.4 m room provides comfortable irradiation conditions.

3. The thermal neutron reference beam at the 1 MW Research and Measuring Reactor (FMRB), Braunschweig, Fed. Rep. of Germany /7,10,11/.

A cross section of the reactor is shown below together with a beam profile (right) and spectrum of the beam:



The reactor has two cores weakly coupled by a  $D_2O$  tank (60 cm wide, 80 cm high) that extends over the entire fuel zone. The thermal neutron flux density at the center of the tank in the through tube is  $7 \cdot 10^{12} \text{ s}^{-1}$ . A beryllium disc scatters neutrons through a collimator system within and outside the tube S1 to produce a well-collimated beam with a diameter of 3.2 cm (0.9 maximal flux density) at the target position about 2 m from the biological shield.

The essential properties of this beam, as it was originally designed, are the sharp collimation (cf. above figure) and a well-established Westcott neutron flux density. The beam served to produce fission spectra from U and Pu converter foils in a low-scattering arrangement. Its special features, as compared to the cavity fission source mentioned above, are the directed fission neutron field and the absence of a neutron component from the beam or a cavity wall.

Now the beam is chiefly employed for calibrations of neutron monitors used for radiation protection purposes. The cadmium ratio in the beam was measured to be only 11 at the target position (20  $\mu$ m gold foil, beam geometry), which is due to the rather thin moderating D<sub>2</sub>O layer of about 25 cm between reactor core and beryllium scatterer. This is rather small as compared to the situation found at the Kyoto Reactor, for example. Therefore all irradiation experiments (activation measurements or neutron dosimeter calibrations) are invariably performed using a cadmium difference method.

The spectrum of the thermal neutrons, shown in the figure above, was measured with a chopper and can be described by a Maxwellian distribution with a temperature parameter of 63 °C in the range from 12 meV to 120 meV. The structure in the spectrum around 7 meV is due to the influence of the Bragg edge in the scattering cross section of beryllium.

Final comment:

Isotropic thermal neutron fields and beams can be produced with a spectrum rather well approximated by a Maxwellian distribution. Thermal neutron fields seem to be of minor importance as reference fields for pure metrology, perhaps with the exception of dosimeter calibration and the measurement of certain cross sections. Their actuality arises from the production of secondary fields, in cavities as well as with beams.

As for the intermediate neutron energy range, isotropic fields like ISNF cover the energy range between thermal and several keV. On the other hand, there is a gap apparent for neutron beams between the thermal range and the lowest energies achievable with filtered beams, which are discussed separately during this meeting.

Acknowledgement: The author would like to thank Mr. H. Kluge and Mr. M. Matzke for helpful discussions.

### References

- /1/ E.J. Axton, Metrologia 6 (1970), p. 25
- /2/ A. Fabry, J.A. Grundl, C. Eisenhauer, Proc. Conf. Nuclear Cross Sections and Technology, NBS Spec. Publ. 425, Washington 1975, p. 254
- /3/ C.M. Eisenhauer, J.A. Grundl, A. Fabry, Proc. Int. Specialists Symp. on Neutron Standards and Applications, NBS Spec. Publ. 493, Washington 1977, p. 329
- /4/ A. Fabry, *ibid.*, p. 290
- /5/ J. Grundl, C. Eisenhauer, Proc. Consultants' Meeting on Integral Cross-Section Measurements in Standard Neutron fields for Reactor Dosimetry, IAEA-208, Vienna 1976, Vol. I, p. 53
- /6/ K. Kanda, K. Kobayashi, T. Shibata, *ibid.* Vol. II, p. 107
- /7/ S.R. Wagner, *ibid.* Vol. II, p. 3
- /8/ A. Fabry, G. deLeeuw, S. deLeeuw, Nucl. Tech. 25 (1975), p. 349
- /9/ G. Lautenbach, private communication. The cooperation of Mr. Lautenbach from ECN Petten is gratefully acknowledged
- /10/ H. Kluge, K. Knauf, PTB-Mitt. 87 (1977), p. 38
- /11/ W.G. Alberts et al., Proc. Symp. Advances in Radiation Protection Monitoring, IAEA, Vienna 1979, p. 625

ACCELERATOR - BASED WHITE NEUTRON SOURCES

S. Cierjacks

Institut für Kernphysik  
Kernforschungszentrum Karlsruhe  
Postfach 3640, D-7500 Karlsruhe

\*

Editor's Note: This paper was not available until  
the publication.



## WHITE SOURCE USE IN A NEUTRON STANDARDS LABORATORY

C. D. Bowman, A. D. Carlson, O. A. Wasson, R. A. Schrack, J. W. Behrens,  
R. G. Johnson, and K. C. Duvall

National Bureau of Standards  
Washington, D.C. 20234 USA

### Abstract

Methods are described for accurately characterizing the neutron beam from a white source in spectral shape, absolute intensity, and source brightness distribution. Measurements can be made over more than nine decades of energy from .01 to  $2 \times 10^7$  eV from a single source. Beams with easily modified spectrum and with total intensity (integrated over energy) of  $10^6$  n/cm<sup>2</sup>-sec can be obtained. Over most of the energy range these methods can be implemented with a modest electron linac facility operating in the 10 - 12 MeV range. Such a versatile facility is perhaps within the budgetary range of even a modest laboratory.

### Introduction

The purpose of this paper is to describe measurements which characterize a pulsed white source of neutrons from an electron accelerator. While this general class of facility can take several forms,[1] attention here is directed to the electron linac based source. The typical facility accelerates pulses of electrons to the 50 to 150 MeV range which strike a tungsten target. The electron energy is converted to bremsstrahlung which then interacts with other nuclei to produce neutrons by the ( $\gamma$ ,n) reaction. The pulse width varies from a few nanoseconds to a few microseconds and thus the neutron pulse width can be varied accordingly aside from moderation effects in the target. Neutron time-of-flight



methods are then used with flight paths from 3 to 250 meters for experiments. A number of facilities of this type have been built, and over the past decade these facilities have been perhaps our most prolific source of neutron cross section data. A large effort has been expended with these facilities in improvements of neutron cross section standards. In the course of this and other types of neutron nuclear data measurement, methods have been developed for flux measurement which are now finding application in areas other than neutron standards measurements. Most of the work described here are measurements which have been developed for use at the National Bureau of Standards 100 MeV electron linac neutron source. A more general discussion of white sources is given in another paper [2] at this meeting.

#### Neutron Flux Measurement

A number of problems in neutron standards require the use of fields or beams of well-known intensity and spectral shape. For the purpose of this paper we define a neutron beam as a column of neutrons of known spectral shape and intensity all moving nearly in the same direction. A neutron "field" differs from a "beam" in that the neutron motion is not unidirectional. Detector response in a beam can be made equivalent to that in an isotropic field of known spectrum and intensity by appropriate rotation of the detector. Neutrons from spontaneous decay such as  $(\alpha, n)$ ,  $(\gamma, n)$  spontaneous fission sources and from reactor cavities generally fall into the class of fields while the accelerator sources will generally fall into the class of beams. In general, the fields are easier to use experimentally than beams. However, the parameters of the fields are usually calculated and it is difficult to confirm the calculated parameters of the field by experiment. While the implementation of the beam is more difficult, the experimental methods permit characterization of the

beam to high accuracy--presently as good as  $\pm 2\%$  in spectral shape and intensity. In addition, generally a greater degree of spectrum tailoring is possible since both the source spectrum and moderating materials can be changed with little effect on the experimental accuracy in defining shape and intensity.

At the NBS, time-of-flight methods have been developed which permit accurate beam spectral and intensity determination over almost the complete spectral range from .01 eV to 20 MeV. These presently available methods are summarized in Fig. 1. Typically, they require both the device under calibration or exposure and the neutron monitor to be located at well-separated positions on the same beam line, which may vary in length from 5 to 200 meters. This separation prevents neutron scattering between detectors, permits the location of the neutron monitor at the most appropriate position for good performance, and allows the neutron intensity on the device or sample under calibration to be changed at will. The method requires that neutron collimation be arranged so that the neutron monitor and all parts of the calibrated device see all of the neutron source. In this case inverse  $r^2$  scaling can be used to convert the measured intensity to that at the device under calibration. Two neutron producing targets are available at NBS--the tungsten target giving a fission-like spectrum and a tungsten-Be target giving a harder spectrum with a tail extending up to 30 MeV and with average energy near 8 MeV.

Beginning with the highest energy, the annular proton detector (APD) is useful in the energy range from 1 to 20 MeV. It is shown in Fig. 2. Neutrons collimated to an annular beam pass through a thin hydrogenous radiator and knock out protons which are then detected by a detector on the beam axis which is shielded from direct neutrons. This detector is located at 60 meters where

it can be operated at full linac power (4 kW) with no problem from  $\gamma$ -flash and where it has adequate timing resolution to achieve 10% energy resolution for 20 MeV neutrons. Convenient positions for measurements or calibrations are in the 4 - 10 meter range and with some compromise in beam quality at 1 meter. The flux integrated over energy at 4 meters is  $4 \times 10^6$  n/cm<sup>2</sup>-sec. This system is now being used to calibrate a proton spectrometer which will be used to measure spectra at the world's most intense accelerator-based neutron source, the Facility for Materials Irradiation and Testing (FMIT), under construction at Richland, Washington.

For measurements from 0.200 to 2 MeV the black detector [4] is positioned at 200 meters as shown in Fig. 3. This plastic scintillator detector is designed to absorb nearly all of the kinetic energy of a neutron so that the pulse height response shows a peak well separated from low amplitude noise rather than the shelf which is more commonly observed for neutrons in a thin plastic scintillator. Detector efficiency can be calculated accurately using Monte Carlo methods and at NBS has been measured absolutely using the associated particle techniques. Time-of-flight measurements are possible owing to its fast timing capabilities. The neutron spectral shape from the white source may be tailored using any source and moderator configuration from a quite soft spectrum to that of a fission spectrum. Convenient positions for irradiations are located at 60 meters, 4 meters, and with less beam quality at 1 meter.

For measurements at still lower energy, the hydrogen proportional counter (HPC)[4] can be located at 200 meters. The 5-cm diameter detector is used with a 2.5-cm diameter collimator as shown in Fig. 4. Below 40 keV no recoil protons are allowed to strike the walls so that wall effect is eliminated. At higher energies the pulses are allowed to saturate the detector. Therefore,

for this detector wall effects on efficiency determination are eliminated. Since the detector is 60 cm long, the end effect is greatly reduced. The effective length of the detector can be calibrated to  $\pm 2\%$  (1 SD) using a collimated low energy  $\gamma$ -ray source. The other limitation on accuracy is the accuracy in alignment of the collimator which introduces a  $\pm 2\%$  (1 SD) accuracy uncertainty. Backgrounds in this detector from  $\gamma$ -rays can be separated from neutrons by pulse shape discrimination. The detector has been used as low as 3 keV but can be used reliably between 8 and 800 keV and, therefore, has a wide region of overlap with the black detector. The irradiation positions on this flight path are the same as those used with the black detector.

Finally, at low energies there are the  $1/v$  detectors which have a useful range from .01 to  $10^4$  eV. The reactions  $^3\text{He}(n,p)$ ,  $^6\text{Li}(n,\alpha)$ , and  $^{10}\text{B}(n,\alpha)$  are all useful reactions of this type. The  $1/v$  detectors have been used for many years as absolute flux monitors and at NBS for flux shape measurement. Modest absolute accuracy of about 5% can be achieved by several methods with the flux monitor located 10 or 20 meters from the source and with irradiations made at 5 meters or perhaps 1 meter from the source. Czirr [6] has proposed a black detector for low energy neutrons using a combination of Li glass and other Li compounds, which should approach a 1% accuracy throughout the energy range.

All of these methods require a greater amount of experimental complexity than other methods, but the potential for more accurately simulating a flux shape encountered in some practical application and of directly measuring the absolute intensity and flux shape will be important considerations in some experiments.

### Position-Sensitive Detectors

A further addition to our neutron beam characterization capability is the NBS-ORNL development of high resolution position-sensitive detectors for eV and MeV neutrons. [7] We are now using these detectors in the pinhole geometry shown in Fig. 5 to characterize the neutron intensity distribution of eV neutrons at the surface of the target moderator. A proportional counter 5 cm long containing 3 atmospheres of  $^3\text{He}$  and 7 atmospheres of Xe has been used to detect eV neutrons with a position-resolution along the tube axis of 1 mm. This resolution is five times better than that now commercially available. The position-sensitivity is obtained by measuring the time difference between the signals from both ends of the counter. [8] A two-dimensional neutron detector of area 5 cm by 5 cm is also being tested with a resolution of 1 mm x 1 mm. The filling gas is approximately the same, but the geometry permits a much higher neutron detection efficiency. The detector also can be filled with  $^4\text{He}$  instead of  $^3\text{He}$  in which case it should be useful for imaging a source of high energy neutrons by  $^4\text{He}$  recoils.

The NBS is currently carrying out a study of the use of a pinhole camera with a two-dimensional detector containing  $^4\text{He}$ . The intent would be to image the neutron source for the FMIT facility referred to earlier for the purposes of providing feedback on beam position for accelerator operation and of providing a source term for neutron transport studies in the irradiation volume.

### Source Considerations

The typical white source for neutron work makes use of a high energy accelerator which is both large and expensive. If such an accelerator is not available at a neutron standards laboratory, it is perhaps possible to carry out experiments at a white source facility as a visiting scientist using methods described here. However, recent studies at the NBS [9] have demonstrated that

intense pulsed white sources need not necessarily be as expensive as now thought to be. These studies indicate that neutrons can be produced with as much power efficiency with pulsed 10 - 12-MeV electrons as with 100-MeV electrons. The number of neutrons produced per joule of accelerated electron energy is very nearly the same.

There are a number of advantages in using lower energy electrons. Since the energy is much lower, the accelerator length can be greatly reduced--probably down to about 3 meters. Also, since there is no high energy tail on the neutron spectrum, the concrete shielding around the source can perhaps be reduced to only 1 meter. The savings in the building to house such an accelerator are therefore large. A number of other advantages also arise from the use of low energy electrons. Since the energy is only slightly above the particle emission threshold for most materials, activation of the target and the accelerator should be quite small with a significant simplification in safety procedures. Such an accelerator probably would be a one-section accelerator with one modulator and therefore with greatly simplified operation and maintenance. The two disadvantages of the concept are that the neutron producing target would be about 30 cm long giving a relatively low source brightness, and that no neutrons would be available above about 4 MeV. Nevertheless, it appears that a very versatile pulsed white source with intensity in the  $10^{12}$ - $10^{13}$  n/sec range could be acquired and made operational within the budgetary restraints of a modest laboratory.

#### Summary:

In summary, this paper described methods for accurately characterizing the neutron beam from a white source in spectrum shape, intensity, and source

brightness distribution. More than nine decades of energy from .01 to  $2 \times 10^7$  eV can be explored. Beams with easily modified spectrum and with total intensity in the  $10^6$  n/cm<sup>2</sup>-sec range can be obtained. Over most of the energy range, these methods can be implemented with a modest electron linac facility operating in the 10 - 12 MeV range. Such a versatile facility is therefore within the budgetary range of even a modest laboratory.

### References

1. G. A. Bartholomew, "High Intensity Neutron Sources" in "Neutron Capture Gamma Ray Spectroscopy," pp. 503-519, edited by Robert E. Chrien and Walter R. Kane, Plenum Press, New York, N.Y. (1978).
2. See paper by S. Cierjacks entitled "Accelerator-Based White Sources" in these proceedings.
3. A. D. Carlson and B. H. Patrick, "Measurements of the <sup>235</sup>U Fission Cross Section in the MeV Region" in Proceedings of an International Conference on Neutron Physics and Nuclear Data, Harwell, U.K., p. 880 (1978).
4. G. P. Lamaze, M. M. Meier, and O. A. Wasson, "A Black Detector for 250-1000 keV Neutrons," Proceedings of a Conference on Neutron Cross Sections and Technology, NBS Special Publication 425 p. 73 (1975), and M. M. Meier, "Associated Particle Methods," Proceedings of a Symposium "Neutron Standards and Applications" NBS Special Publication 493, p. 221 (1977).
5. O. A. Wasson, R. A. Schrack, and G. P. Lamaze, Nucl. Sci. Eng. 68, 170 (1978).
6. J. B. Czirr, Consultant to NBS, private communication (1978).
7. J. W. Behrens, R. A. Schrack, A. D. Carlson, and C. D. Bowman, "Resonance Neutron Radiography for Nondestructive Evaluation and Assay Applications,"

References (continued)

- Proceedings of the Int. Conf. on Nuclear Cross Sections for Technology, Knoxville, TN. (1979). Proceedings to be published by NBS.
8. C. J. Borkowski and M. K. Kopp, Rev. Sci. Inst. 48, 951 (1975).
  9. C. D. Bowman, "Efficient Neutron Production Using Low Energy Electron Beams," Proceedings of the Int. Conf. on Nuclear Cross Sections for Technology, Knoxville, TN. (1979). Proceedings to be published by NBS.



### Figures

- Fig. 1. A Summary of High Accuracy Absolute Flux Measurement Methods for Use with Pulsed White Sources. These methods are discussed in detail in the text except the lithium black detector proposed by Czirr [6] which has not been constructed. Each is capable of  $\pm 2\%$  (1 SD) flux measurement accuracy in its energy range of usefulness and of  $\pm 5\%$  accuracy in energy resolution or better for practical flight path position.
- Fig. 2. The Annular Proton Detector. Neutrons collimated to an annular beam pass through the radiator and knock out protons which are detected near the beam axis. The pulse height spectrum at 10 MeV is shown in the inset. The absolute accuracy of the system requires an accurate weight and area measurement of the radiator and the accurate measurement of the radiator-detector spacing.
- Fig. 3. The Black Detector. This detector absorbs nearly all the energy of a neutron so that all neutrons of a given energy have approximately the same pulse shape. The pulse shape for this detector is shown in the inset.
- Fig. 4. The Hydrogen Proportional Counter. The hydrogen pressure in the detector is 760 Torr so that with 2.5 cm diameter collimation, there is no wall effect below 40 keV. Since the detector is 60 cm long, the end effect is reduced. The effective length of the detector can be calibrated to  $\pm 2\%$  (1 SD) using a collimated low energy  $\gamma$ -ray source. The other limitation on accuracy is the accuracy in alignment of the collimator which introduces a  $\pm 2\%$  (1 SD) accuracy limit on the system.

Figures (continued)

Fig. 5. Pinhole Camera Geometry. The source is viewed through a "pinhole" which projects an inverted image on the detector. The detector is either a one-dimensional position-sensitive detector which is moved across the image plane to produce the two-dimensional image or it could be the two-dimensional position-sensitive detector for eV and MeV neutrons now under development at the NBS.

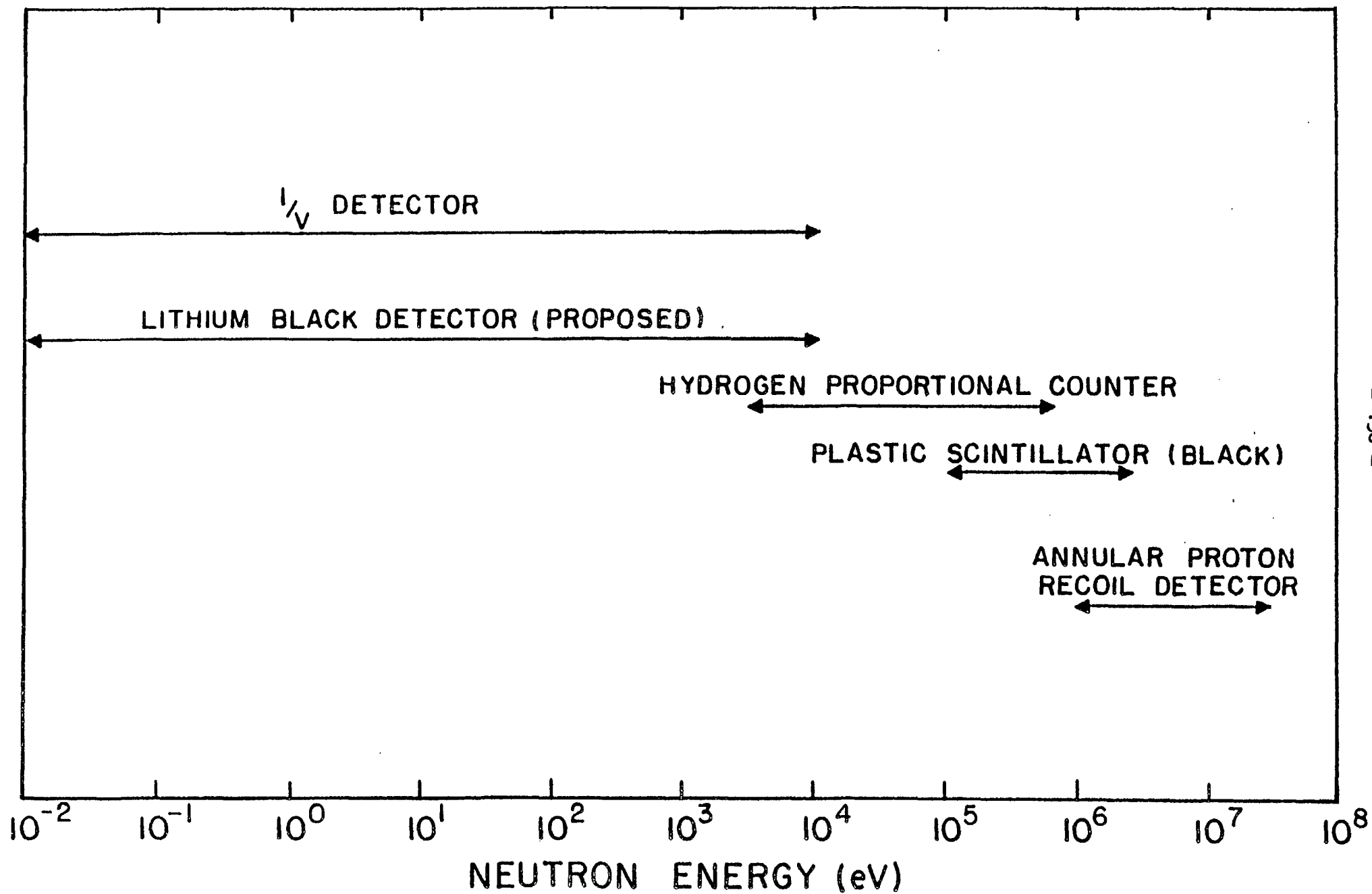


Fig. 1

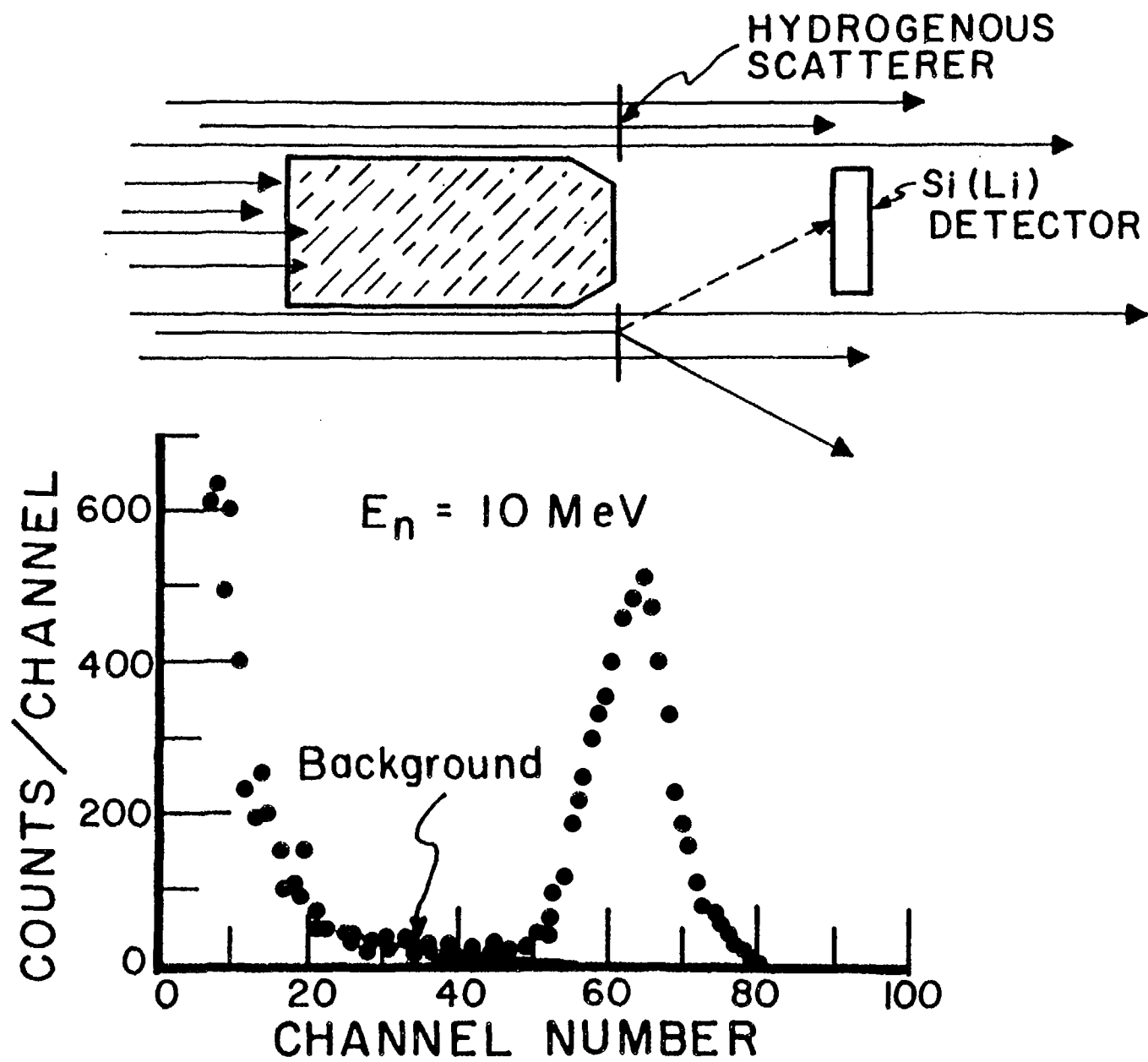


Fig. 2

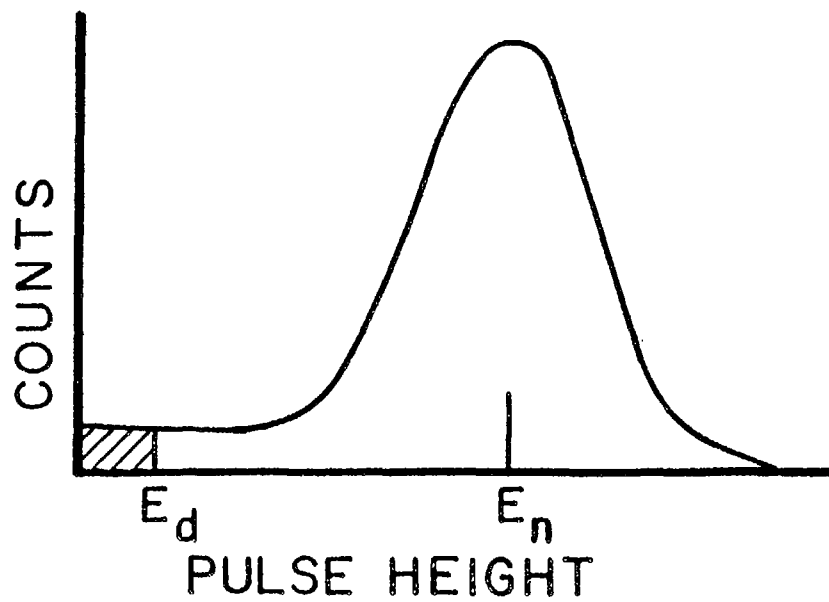
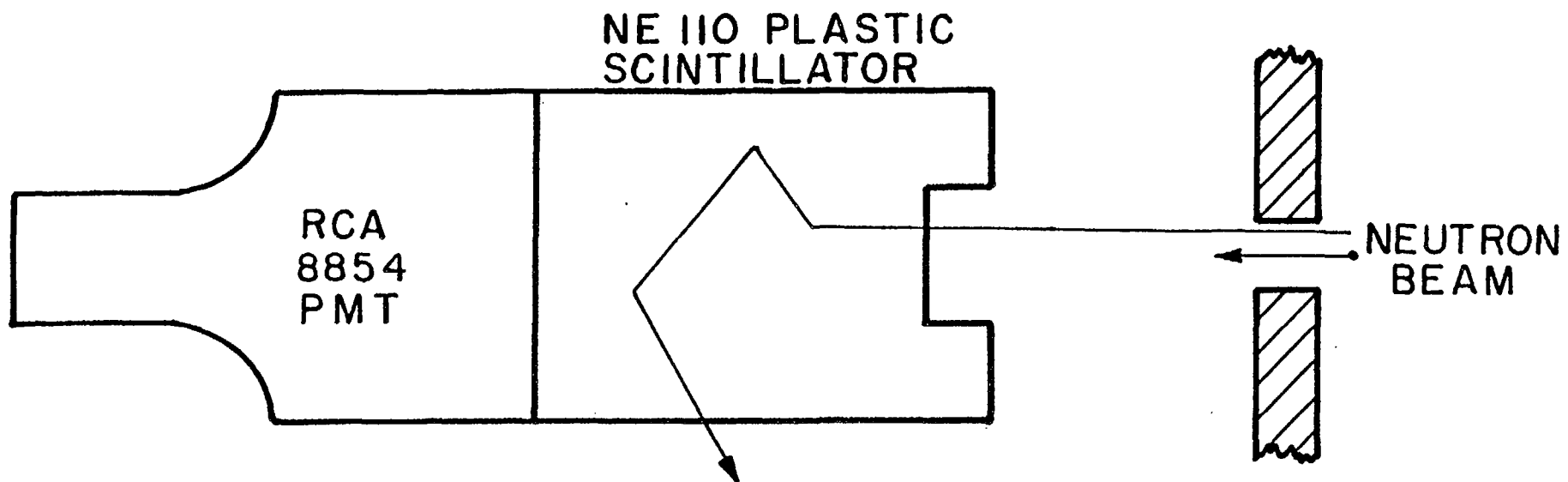


Fig. 3

## GAS COUNTER GEOMETRY

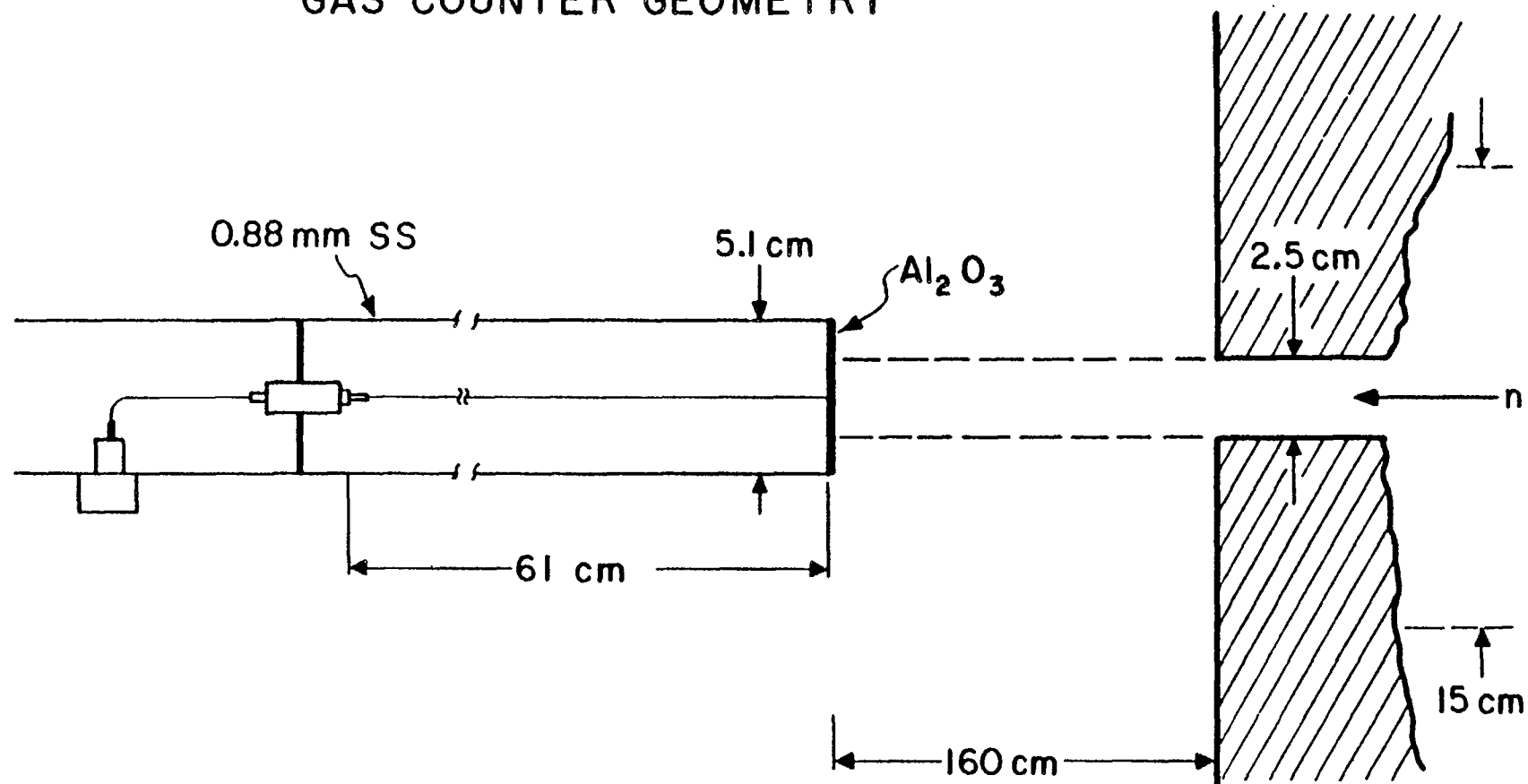


Fig. 4

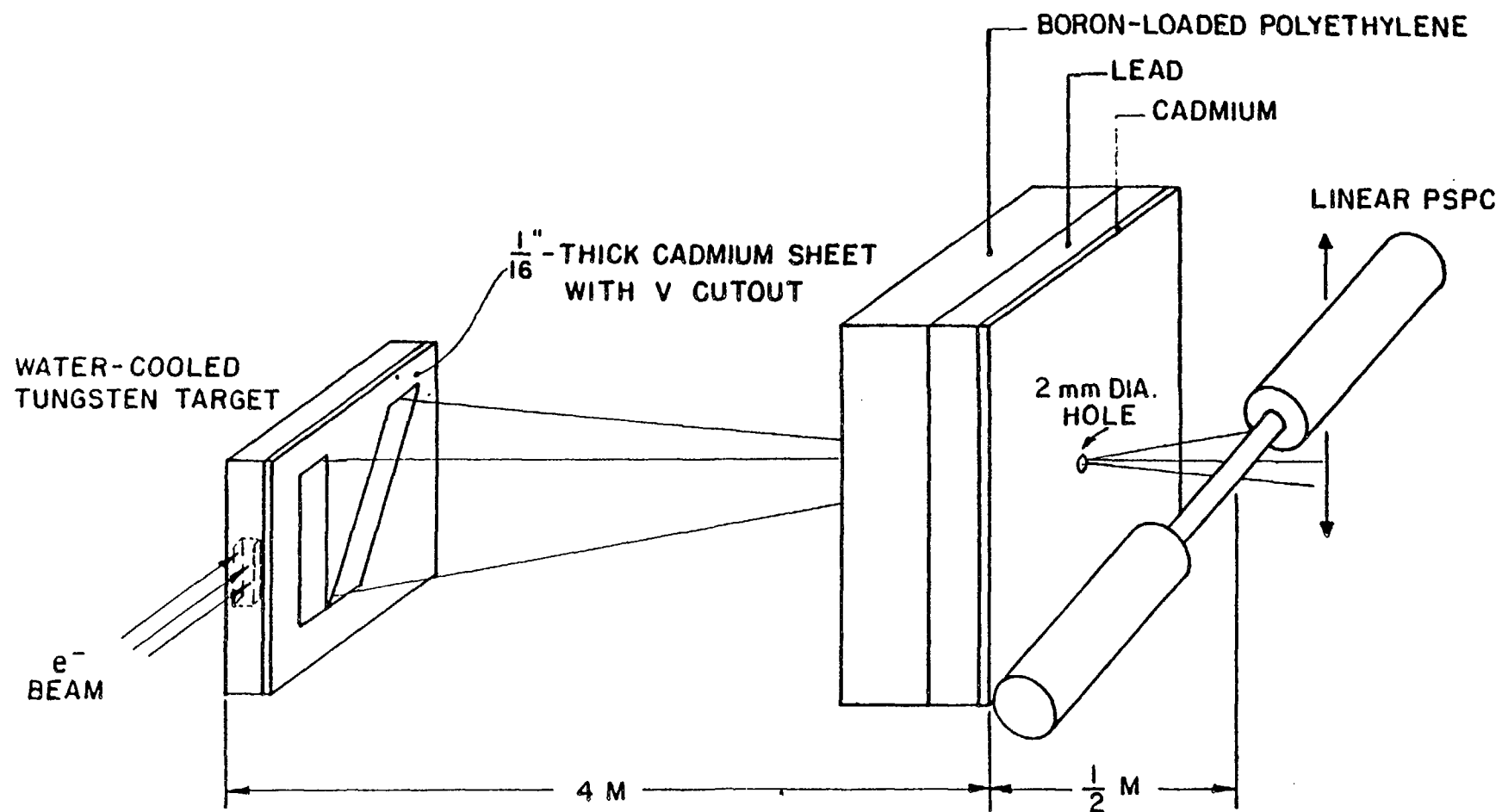


Fig. 5

Reactor - and Accelerator-Based Filtered Beams

- by -

A. J. Mill and J. R. Harvey

Berkeley Nuclear Laboratories,  
Central Electricity Generating Board,  
Berkeley, England, GL13 9PB



## CONTENTS

1. INTRODUCTION
2. MONO-ENERGETIC NEUTRONS
  - 2.1 General Techniques
  - 2.2 Neutron Filters
3. NEUTRON WINDOWS
4. NEUTRON WINDOW FILTERS
  - 4.1 General Considerations
  - 4.2 Filter Materials
5. FILTERED NEUTRON BEAM FACILITIES
  - 5.1 Reactor-Based Facilities
  - 5.2 Accelerator-Based Facilities
6. APPLICATIONS OF FILTERED BEAMS
  - 6.1 Cross-section Measurements .
  - 6.2 (n, $\gamma$ ) Spectrometry
  - 6.3 Shielding Studies
  - 6.4 Instrument Calibration and Development
  - 6.5 Biological and Medical Studies
  - 6.6 Neutron Radiography
7. CURRENT STATUS OF AND FUTURE PROSPECTS FOR FILTERED BEAMS

## REFERENCES

## TABLES

## FIGURES

## 1. INTRODUCTION

The neutrons produced in high flux nuclear reactors, and in accelerator induced fission and spallation reactions, represent the most intense sources of neutrons available for research. However, the neutrons from these sources are not mono-energetic, covering the broad range extending from  $10^{-3}$  eV up to  $10^7$  eV or so. For moderated spallation neutrons the range may be even greater. Many measurements with these sources can be made at high resolution with the time-of-flight technique using a mechanical chopper or a pulsed source. This method is extensively used for total neutron cross-section measurements. However, there are several situations where this method cannot be applied - for example when the response time of the irradiated object is comparable with or greater than practical flight times or when high intensities are required. Examples occur in health physics, radiobiology and nuclear physics. For many measurements it is also desirable to eliminate the large accompanying gamma-ray flux which may make the evaluation of the effects of neutrons or detection of neutrons and capture gamma-rays difficult. Examples of experiments where such difficulties may arise are: the evaluation of the biological effects of neutrons, the measurement of inelastic scattering cross-sections, Doppler effect measurements and the evaluation of the response of radiation doseimeters.

Thus, in order to make many quantitative measurements of the effects of neutrons and their dependence on neutron energy it is desirable to have mono-energetic neutron sources. The next section deals briefly with methods of obtaining mono-energetic neutrons and with different methods of filtration. This is followed by more detailed discussion of neutron window filters and a summary of the filtered beam facilities using this technique. The review concludes with a discussion of the main applications of filtered beams and their present and future importance.

## 2. MONO-ENERGETIC NEUTRONS

### 2.1 General Techniques

For energies from about 20 meV up to 10 eV or so, the use of Bragg scattering from single crystals has, for many years, provided a very valuable source of mono-energetic neutrons (one of the earliest reports of a crystal spectrometer was by Zinn (1947) and a recent report by Briggs and Stirling (1976) reviews the large number of such facilities available in Western Europe). The energy range capability depends upon the plane spacings in the crystal and the energy of the neutron beam can be continuously varied by changing the angle of the crystal with respect to the main beam. The resultant diffracted mono-energetic beam is essentially free of gamma-rays and is usually well collimated. It is possible to extend the energy range to below 1 meV (ultra-cold neutrons) using Doppler-shifted Bragg scattering (Dombeck, Lynn, Werner, Brun, Carpenter, Krohn and Ringo, 1979). However, for neutron energies above 10-20 eV the angle of reflection is very small and the available diffracted intensity becomes very low as the crystal reflectivity varies inversely as the neutron energy.

Neutron generating nuclear reactions produced by accelerated charged particles have for many years been used for producing neutrons at intermediate and fast energies. In this way mono-energetic neutrons down to 1 or 2 keV have been obtained, thereby establishing an overlap with the energy range conveniently accessible with fast choppers. One of the most useful reactions for producing intermediate energy neutrons is the  ${}^7\text{Li} (p,n) {}^7\text{Be}$  reaction although only above neutron energies of 120 keV are mono-energetic neutrons produced in the forward direction. Lower energy neutrons are emitted at backward angles, but the neutron yield decreases as the backward angle increases and measurements in the backward directions pose some difficulties. There are several other useful reactions producing mono-energetic intermediate energy neutrons. These include proton reactions with scandium, copper and

vanadium targets which can provide mono-energetic neutrons of energies down to 2 keV in the forward direction. Mono-energetic neutrons covering the range 0.6 to 30 MeV are supplied by the reactions of accelerated protons and deuterons on deuterium or tritium targets. For all these nuclear reactions there will be some accompanying gamma-rays from  $(p, p'\gamma)$  and  $(p, \gamma)$  reactions.

These procedures for the production of mono-energetic neutron beams have the advantage of allowing a continuous variation of the neutron energy. However, towards the limits of their energy ranges these methods yield very low intensities.

## 2.2 Neutron Filters

Neutron filtration was, in fact, one of the earliest methods of making crude energy selection from a wide spectrum neutron source such as a reactor (Hughes, 1954).

Cadmium which was one of the first materials to be used as a filter (Szilard, 1935), acts by removing thermal neutrons and leaving the epithermal and fast neutrons, thus enabling separation of thermal and fast neutron effects. A strong absorption resonance at 0.178 eV dominates the thermal region and strongly absorbs neutrons below about 0.5 eV. A measure of the effects of thermal neutrons may therefore be obtained with a cadmium filter by a difference method. Cadmium is also used to define the "cadmium ratio" of a reactor beam by measuring the response of detectors with and without a cadmium sheath. Other materials similarly used as high energy band pass filters are boron and gadolinium.

Another early type of filter was based on the fact that in a polycrystalline material no Bragg reflection occurs for neutron wavelengths that are larger than twice the largest lattice spacing. Hence such a filter has a cut-off energy above which no neutrons can pass through it. The only remaining processes which remove neutrons from the beam are incoherent

scattering and neutron capture. Materials which have been most extensively used for this type of filter include graphite, beryllium, and beryllium oxide with cut-off wavelengths respectively of 0.67 nm, 0.4 nm and 0.43 nm (these correspond to energy cut-off values of 1.8 meV, 5.1 meV and 4.0 meV respectively), hence they transmit only cold neutrons. Like cadmium filtered beams, the resulting beam is not mono-energetic but it does have an exceedingly sharp cut-off energy. The intensity of the cold neutron beam can be considerably increased by cooling the filter in liquid nitrogen (Barton, 1965) and it is possible to use a bismuth crystal to filter out the gamma radiation. Such cold neutron beams are useful for the radiography of small hydrogenous objects through large thicknesses of polycrystalline materials such as iron or lead. They are also used for primary filtering prior to the production of mono-energetic cold neutron beams by diffraction from a single crystal.

Miller and Watanabe (1971) have developed filters of rare earths which pass neutrons in selected energy bands. The filters (referred to as foil filters) consist of several thin metal plates or other materials used in combination to remove neutrons of certain energies from the beam. Rare earth elements make very good filters because of the many large resonances in their neutron cross-sections. To select a suitable combination of foils transmission versus energy plots (calculated from the cross-sections) for each filter material can be overlayed in order to give an indication of the transmission of the filter combination. Such filters have been used to increase the contrast of neutron radiographs and can be used in the energy range 0.3-15 eV.

Any material with a large resonance can be used to remove a specific energy band from a neutron beam. For instance plutonium-239, which has a strong resonance at 0.3 eV, is often used to remove the second order from the diffracted beam of a single crystal spectrometer while allowing the

first order neutrons of a lower energy to pass. Anderson's (1969) design for a resonance scattering facility utilises a thin absorption filter in order to quantify the effects of unwanted scattering by the difference method. Similarly it is possible to use a small quantity of any material with a large resonance absorption peak to deplete the spectrum of a reactor neutron beam of neutrons around the resonance energy. Such a source may be termed a "negative" neutron source and the difference in response of, say an instrument, to the two source conditions (i.e. with and without absorber) gives an estimate of the response at this energy (Mijnheer and Aten, 1973). Clearly there are potential problems with such a method: the "negative" source strength may be low and the response is derived from small differences.

Another type of filter is the neutron window filter. This type of filter has a large dip (the window) in its cross-section and if an appropriate length of this material is inserted in a beam tube of a reactor only neutrons of energy corresponding to the window energy will pass through. The filter is also very effective in stopping gamma radiation. The technique was first developed by Simpson and Miller (1968) who produced a mono-energetic neutron beam of 2 keV by inserting a length of scandium into the beam tube of a nuclear reactor. Later, filters of iron and silicon were developed to give mono-energetic beams at 24 keV and 144 keV respectively (Brugger and Simpson, 1973). Several similar filter facilities have now been developed for reactors throughout the world. More recently, filters of uranium (Royer and Brugger, 1977), giving 186 eV neutrons and of liquid oxygen (Koeppel and Brugger, 1980), giving 2.35 MeV neutrons, have been developed. In principle, mono-energetic neutron beams for a large number of different energies are possible by using other elements and enriched stable single nuclides as filters (Harvey and Mill, 1978; Mill and Harvey, 1978). Moreover this

appears to be the only method of producing high intensity mono-energetic neutron beams in the energy range from several electronvolts to several tens of kilo-electronvolts.

### 3. NEUTRON WINDOWS

One of the phenomena occurring when neutrons interact with nuclei is that of nuclear resonance. This is observed experimentally as sharp increases in the total cross-section of the target nucleus at discrete energies of the incident neutrons. Resonances can occur for elastic scattering, inelastic scattering, capture, fission and various other reactions. The total cross-sections are properly described by R-matrix formalism (Lane and Thomas, 1958), however, for many cases the simple Breit and Wigner (1936) formula gives a good description of the cross-section in the region of an isolated s-wave resonance. For such a resonance the cross-section,  $\sigma(E)$ , is given by:

$$\sigma(E) = 4\pi(R')^2 + \frac{\pi \lambda^2 g \Gamma_n \Gamma}{(E-E_0)^2 + (\Gamma/2)^2} + \frac{4\pi\lambda R' g \Gamma_n (E-E_0)}{(E-E_0)^2 + (\Gamma/2)^2}$$

where  $\Gamma$  = total width at resonance (this is related to the lifetime of the compound nucleus formed by the interaction of a neutron with a stable nucleus).

$\Gamma_n$  = neutron scattering width

$E_0$  = resonance energy

$\lambda$  = reduced neutron wavelength

$R'$  = nuclear radius for potential scattering

$g$  = a statistical weighting factor.

$$= \left| \frac{2I+1 \pm 1}{2(2I+1)} \right|$$

$I$  = spin of target nucleus

This simple Breit-Wigner formula is valid for  $R' \ll \lambda$  i.e. for  $E \lesssim 0.5$  MeV. The first term of the equation describes pure resonance scattering without the formation of a compound nucleus and the second term describes pure resonance interaction. The third term describes the interference between resonance and potential scattering. For energies less than the resonance energy the interference term is negative and there can occur an energy band where potential and resonance scattering cancel each other out to produce small cross-sections, although this can only occur in s-wave interactions. (In s-wave interactions the orbital angular momentum of the neutron relative to the target nucleus is zero.) These regions of low cross-section are known as windows. Figure 1 shows the general shape of the cross-section near an s-wave scattering resonance. For neutron energies outside the range  $R' \ll \lambda$  the interference dip will occur at higher energies with respect to the resonance energy. In fact the interference minimum in oxygen-16 occurs just above resonance.

For nuclides of odd mass number the total angular momentum of the compound nucleus can take on two possible values in s-wave scattering, however, the interference between resonance and potential scattering will occur only in the resonant spin state. Hence there will still be a contribution to the total cross-section in the window from the non-resonant spin state. Typically, for an isolated resonance the cross-section at the minimum will be about a half of the potential scattering cross-section (as  $g = \frac{1}{2}$  for both spin states). However, for nuclides with even atomic numbers and even mass numbers there is only one possible spin state (and  $g = 1$ ) and for these nuclides the cross-section can fall to very low values in the window. (In fact if there were no other decay modes the cross-section would fall to zero apart from contributions from other levels and from p-wave scattering.) The cross-section can also reach these low values in



odd mass nuclides when two resonances, of opposite spin state, occur close enough together such that their interference dips overlap. Such a deep window occurs in scandium-45 at 2 keV.

#### 4. NEUTRON WINDOW FILTERS

##### 4.1 General Considerations

The existence of cross-section windows suggests the means for making suitable neutron filters; and nuclides with even mass numbers and even atomic numbers are the most promising in this respect. However, all nuclides which have even numbers of protons and neutrons occur in mixtures of isotopes, the result being that, in the natural element, a window in one isotope is usually obscured by the potential or resonance scattering background of the other isotopes present. Nevertheless, useful filters have been constructed using elemental iron (91.7%, iron-56), silicon (92.2%, silicon-28), oxygen (99.8%, oxygen-16) and uranium (99.3%, uranium-238) as well as scandium (100%, scandium-45) - which is an odd mass number nuclide. Elemental sulphur (95.0%, sulphur-32) is also a promising filter material. In order to extend the range of filter materials and make use of the numerous windows present in even-even nuclides it is necessary to use enriched nuclides as filters. At present this approach has been adopted only for iron-56 (Liou, Chrien, Block and Singh, 1979) although a proposal to use other enriched nuclides has been made (Mill and Harvey, 1978); and there are proposals to use zinc-64 in conjunction with scandium to give 2 keV neutrons (Brugger, 1979).

One major drawback with neutron window filters is that they invariably have more than one isolated s-wave resonance, and hence there may be several windows present in addition to the main one. Transmission of neutrons through these subsidiary windows may be significant and it is generally unwise to rely simply on a single filter component to obtain a mono-energetic neutron beam. There are two techniques which can be adopted,

either singly or in combination, which are usually effective in eliminating the effect of neutrons transmitted through secondary windows. The first method is to use another (secondary) filter which has a window (or a region of relatively low cross-section) at the same energy as the main window in the primary filter while no other regions of low cross-section coincide. For example, iron and aluminium both have windows at 25 keV. Generally this method is of limited application when using elemental materials. Alternatively materials for use on secondary filters can be chosen on the basis that they have a resonance at an energy corresponding to one of the secondary windows in the main filter. In this case only a small thickness of the secondary filter is required. An example here is the use of titanium in scandium filtered beams to suppress the transmission through the secondary windows at 7 and 24 keV in scandium.

The second method is the use of resonance scattering. Here a material having a large scattering resonance peak at the energy of interest is placed in the filtered beam and will preferentially scatter these energy neutrons out of the primary beam. Other resonance peaks in the scatterer should not coincide with any of the secondary windows in the filter. In order to minimise scattering of neutrons whose energies do not coincide with the resonance energy, the scatterer should be thin. Manganese can be used as a scatterer for a scandium filtered beam. It is also possible to use the scatterer prior to filtration to preferentially scatter neutrons corresponding to the resonance peaks into the filter. This is particularly effective when the filter is placed in the through tube of a reactor.

One major advantage with neutron window filters is that the large length of material used generally reduces the gamma-ray dose-rates to very low levels.

Figure 2 shows typical layouts of filtered beam facilities at a reactor. The beam tubes in Figures 2(a) and 2(b) are radial ones directed

at the reactor core. In Figure 2(c) the beam tube is a through tangential one and a scatterer must be placed at the centre of the tube in order to scatter or reflect neutrons towards the filter. The arrangement with the external scatterer provides a much lower fluence rate at the sample position than either of the other arrangements.

There are several factors to be considered when designing a filter facility. For instance, window filters act by scattering neutrons out of the beam, and not by absorption. Therefore it is important not to locate the sample too close to the end of the filter where scattered and thermalised neutrons may be present. Other factors to be considered are the effects of collimation, neutron streaming, the design of the sheilding, and, of course, the actual thickness of the filter. For example, the bandwidth of the filtered neutron beam may be made narrower by successively reducing the filter length. However, this occurs at the expense of decreasing the intensity of the transmitted beam; although background (both gamma-rays and fast neutrons) will also be decreased, and by a much larger factor. A useful discussion of the practical aspects of filter beam design is being prepared by Block and Brugger (1980).

## 4.2 Filter Materials

### 4.2.1 Scandium

It has been known for 25 years that there is a significant dip in the total cross-section of scandium metal at  $\sim 2$  keV. This window is due to the fact that the interference dips from the 4.33 keV resonance (which has spin,  $J = 4$ ) and the 3.30 keV resonance (spin,  $J = 3$ ) are close to each other. Pattenden (1955) reported that the cross-section dropped to 0.5 barn at 1 keV; Simpson and Miller (1968) confirmed the existence of this window. Measurements, on rather purer scandium, reported in their paper suggested that the cross-section was 0.05 barn at 2 keV. It was on the basis of this very low cross-section value that scandium filters were first installed in

beam tubes at reactors in the USA. Scandium also has many windows at higher energies (Cho, Fröhner, Kazerouni, Muller and Rohr, 1970) and those at 24 keV, 40 keV and 76 keV are particularly deep. More recently, measurements with an energy resolution far superior to the earlier work have been made in order to determine the minimum cross-section more accurately (Liou, Chrien, Block and Kobayashi, 1978; Chrien, Liou, Block and Kobayashi, 1977). This was undertaken because a scandium filter installed at the High Flux Beam Reactor at Brookhaven National Laboratory produced an output substantially lower than that expected from a 0.05 barn minimum. In fact Liou et al (1978) showed the dip at 2 keV was approximately an order of magnitude higher in cross-section, at  $0.71 \pm 0.03$  barn. Their results near the minimum (which is actually at  $2.05 \pm 0.02$  keV) are shown in Figure 3.

The results of Liou et al (1978) have serious implications for the effective use of scandium as a filter for 2 keV neutrons as many of the higher energy windows have comparable cross-sections. In fact many of the scandium filtered beams have high contamination from fast neutrons, although this can be reduced by the addition of small thicknesses of titanium which is particularly effective in reducing the transmission through the windows at 7 keV and 24 keV. Most scandium filtered beam facilities have 1-2 cm of titanium as an additional filter. It is also possible to reduce the high energy background by using a resonance scatterer of manganese which has a broad scattering resonance at 2.38 keV.

As the backgrounds with scandium filtered beams can be large a difference technique is often used to measure signal and background. A difference filter of cerium and manganese, or just manganese can be effectively used to remove 2 keV neutrons from a filtered beam while reducing the background only slightly. This gives a measure of the background, while the open beam gives a measure of signal plus background.

The current cost of scandium is high and typical filters 60-110 cm long may use 1-2 kg of scandium. Thus compared to filters made of iron, silicon and aluminium, the scandium filtered beams are relatively expensive.

#### 4.2.2 Iron

The well-known interference window in iron is on the low energy side of the 27.7 keV resonance. This is an s-wave resonance in iron-56 (92% of natural iron) and it produces a deep window at  $\sim 24.5$  keV.

Some particularly accurate measurements have been made on this window by Harvey (1972) and by Liou et al (1979). Both sets of measurements used the filtered beam technique. Harvey (1972) reported the minimum in natural iron to be  $0.43 \pm 0.005$  barn at an energy of 24.5 keV. Later measurements by Kobayashi, Fujita and Ogawa (1977) gave similar results:  $0.40 \pm 0.02$  barn at  $24.3 \pm 0.1$  keV. The cross-section for natural iron as reported by Harvey (1972) is shown in Figure 4. The contributions of iron-54 and iron-57 to this window were also estimated by Harvey (1972) and shown to account for essentially all of the observed cross-section. This also applied to the other deep minima at 82.0 keV, 128.7 keV, 137.5 keV and 168.1 keV. The measurements of Liou et al (1979) on iron-56 indicate a minimum cross-section of  $7.5 \pm 4.2$  mbarn at 24.4 keV. Their results are shown in Figure 5. As the minimum cross-section in iron-56 is considerably smaller than the minimum cross-section in natural iron, a filter of iron-56 would result in a much more intense beam of 24 keV neutrons than a natural iron filter. For example, a 70 cm long filter of iron-56 would result in a transmission of  $\sim 75\%$  at the minimum whereas through natural iron the transmission is 9%. Thus an iron-56 filter could be used in very thick configurations to reduce unwanted fast neutrons and gamma-rays. However, successful natural iron filters have been assembled at several reactors with very low contributions from fast neutrons and gamma-rays.

Aluminium, which has a shallow window at  $\sim 25$  keV, has been used as an additional filter material with all iron filtered beams. Also the addition of small amounts of sulphur (5-8 cm) are desirable for the suppression of high energy neutrons. Titanium, which has a broad resonance area centred at 17.5 keV, may be used as resonance scatterer in conjunction with iron filtered beams. Titanium can also be used as a difference filter for the determination of signal and background.

Being relatively inexpensive, iron/aluminium combinations have been widely used to produce very pure 25 keV neutron beams. Typically 25-70 cm of iron and 20-40 cm of aluminium have been used in the construction of iron/aluminium filter facilities.

#### 4.2.3 Aluminium

Aluminium has a broad s-wave resonance at 34.7 keV resulting in an interference dip at 25 keV. Aluminium which is a single isotopic element, has an odd atomic number and the cross-section in the broad minimum falls to 0.54 barn while the average cross-section elsewhere is about 2 barn. There is another window at 400 keV. Although aluminium has never been used as a filter in its own right, it makes an excellent secondary filter for iron and is effective in reducing transmission through the high energy windows in iron. The cross-section of aluminium near 25 keV is shown in Figure 6 (Garber and Kinsey, 1976).

#### 4.2.4 Silicon

Silicon (92.2%, silicon-28) has a strong s-wave resonance at 188 keV which produces a very broad window at 147 keV. A smaller window at 54.5 keV is the result of the 55.6 keV resonance. There are no windows above 147 keV. The data at these minima from Garber and Kinsey (1976) suggest a value of 0.42 barn for a 144 keV minimum, while at 54.4 keV no window is shown. Kobayashi et al (1977) report values of  $0.093 \pm 0.004$  barn

at the  $147 \pm 1$  keV minimum and  $0.14 \pm 0.04$  at the  $54.5 \pm 0.3$  keV minimum. Their results are shown in Figure 7.

As there are no windows above 147 keV the transmission of fast neutrons is not a problem. However, as silicon is a crystalline material, it also allows low energy neutrons below the Bragg cut-off at 2 meV to be transmitted. These low energy neutrons can be easily removed by the addition of boron-10. Another problem (even with 100-200 cm of silicon) is the gamma-ray transmission, and it is usually necessary to use some lead ( $\sim 10$  cm) to reduce this to an acceptable level. Some titanium is also necessary to suppress neutrons transmitted through the window at 54.5 keV. However, this window may be utilised to produce mono-energetic neutrons at 55 keV, when it is necessary to add some sulphur to suppress the neutrons at 147 keV. Difference filters of sulphur (for 147 keV) or titanium (for 54.5 keV) may be used to evaluate signal and background.

#### 4.2.5 Uranium

Uranium-238, which comprises 99.3% of natural uranium, has a neutron window at 186 eV due to the strong s-wave resonance at 189.7 eV. However, there are several other windows present at higher energies, up to 6 keV or so, and many of these are as deep as the 186 eV window. To reduce the background from these windows small amounts of materials having large resonances which overlap these background windows are needed. Beam purity may still be low and a more successful technique for extracting a relatively pure beam of 186 eV neutrons may be to use a resonance scatterer. For example, neodymium-143 has a strong s-wave resonance at 186.6 eV which matches the window in uranium very well. Similarly it may be possible to extract mono-energetic neutrons of several other energies by identifying suitable scatterers to match other windows in uranium. Germanium-73, for example could be used to extract a beam of 100 eV neutrons (Harvey, 1979).

As many of the windows and resonances in this energy region are narrow, ideal matching may be difficult for more than a few cases. However, it would seem feasible to use a single filter of uranium, combined with several different resonance scatterers to provide a range of mono-energetic neutron beams between 100 eV and 6 keV. The transmission of neutrons through a 18.4 cm uranium filter is shown in Figure 8 (Harvey, 1979).

#### 4.2.6 Oxygen

Oxygen, 99.8% of which is oxygen-16, has a large window in its cross-section at 2.35 MeV, due to a s-wave resonance at 2.35 MeV. The cross-section falls to 0.13 barn in the window (Mughabghab and Garber, 1973); also there are several other regions of low cross-section between 5 and 8 MeV. The only practicable form for the filter is liquid oxygen which does present some problems in handling. Additional filtering materials are needed to reduce high energy neutron and gamma-ray contamination. The cross-section of oxygen near 2.35 MeV is shown in Figure 9 (Garber and Kinsey, 1976).

#### 4.2.7 Other Materials

As well as the six elements described above there are a few other elements which have windows in their cross-section and which are suitable for use as neutron filters. Sulphur, for example, has a broad minimum near 70 keV where the cross-section falls to 0.1 barn. Another possibility is neon, where the cross-section falls to 0.2 barn at 400 keV. Nitrogen has windows at 0.97 MeV and 4.8 MeV, however the cross-sections here fall only to 0.9 barn.

The range of filter materials can be considerably extended by utilising enriched nuclides. Mill and Harvey (1978) have identified several suitable such filters: neutron beams of 60 eV, 160 eV, 400 eV, 2 keV, 4 keV and 13 keV may be obtained by using filters of erbium-170, tungsten-184,



zinc-68, zinc-64, nickel-60 and nickel-58 respectively. The windows in these nuclides were identified by theoretical means (Mill, 1979) and, so far, measurements on thick samples of enriched nuclides have confirmed the existence of windows in nickel-60, nickel-58 and zinc-64 (Harvey, 1979). Figure 10 shows the cross-section of nickel-58 near the minimum at 13 keV.

## 5. FILTERED NEUTRON BEAM FACILITIES

### 5.1 Reactor-Based Facilities

This Section covers some of the properties of reactor-based filtered beams. To date, only a few reactors have, or have had, a filtered beam facility; these are listed in Table 1. Specific details of these filtered beams are to be found in Tables 2, 3, 4, 5 and 6 which deal respectively with scandium, iron/aluminium, silicon, uranium and oxygen filtered beams.

The first neutron window filters were used on the Materials Testing Reactor (MTR) (Simpson, Smith and Rogers, 1971); however, this reactor was closed down in 1970 and the filters were transferred to the National Bureau of Standards Reactor (NBSR) as part of the neutron standards programme (Hoy and Schwartz, 1976). Many of the filter facilities have been designed for the ease of insertion and interchange of filters. At the High Flux Beam Reactor (HFBR) this is achieved by using a 4-position collimator located external to the biological shield. Similarly the iron filtered beams at the High Flux Reactor (HFR) and the R2 Research Reactor are installed in rotary collimators. The Missouri University Research Reactor (MURR) has a specially designed filter tube system and several different filter systems are in use. The filter facility at the HFR is rather unique in that the neutron beam is focussed by a series of neutron mirrors. The mirror system acts as a collimator with 90 nickel plates (each 200 cm x 20 cm x 0.1 cm) focussing the neutrons on a horizontal plane 5 m from the reactor core.

All the reactors are light or heavy water moderated apart from the First Atomic Power Reactor (APS-1) which is moderated by graphite. The reactor APSARA and the Forschung - und Messreaktor (FMRB) are swimming pool reactors while the other water moderated reactors are of the high flux type.

The most widely utilised filter combination is that of iron/aluminium/sulphur. This is presumably due to the low cost of this filter combined with the relative ease of obtaining a pure 25 keV neutron beam with a high flux reactor. The MURR 25 keV beam is particularly pure (Tsang and Brugger, 1976) although the iron beams at the FMRB (Alberts, 1978) and at the APS-1 (Kuzin, Belov, Dvukhshestnov, Furmanov and Shchadin, 1973) have relatively high fast neutron components. In order to estimate the output at 25 keV and to use these later two beams experimentally it was necessary to employ the difference technique using a difference filter of titanium. The fast neutron components in the difference (or signal) beam were typically 10-20 times lower than in the open beams.

Initially the iron filter at the NBSR was placed in a radial beam tube and used in conjunction with a titanium scatterer located between the fuel elements (McGarry and Schroder, 1975). Later, a through tube with a graphite scatterer was used, although this does not seem to be especially advantageous (Schwartz, 1977).

The combinations of iron, aluminium and sulphur in the 25 keV beams were usually optimised by varying the thickness of the filter components and measuring the transmitted neutron spectra with recoil proton detectors. At the reactor APSARA an absorption method was also used for optimisation (Kondaiah, Anand and Bhattacharya, 1973). The iron filter from the APSARA has now been transferred to the 40 MW high flux reactor CIRUS (Kondaiah, 1979).

Several scandium beams have also been developed despite some difficulties with high energy neutron contamination. Titanium has usually been used as a secondary filter. In general the filter components have not been optimised to the same degree as for the other filter materials. The problem with the fast neutron background arose because the cross-section of scandium was originally thought to be 0.05 barn at 2 keV while, in fact, it is actually 0.7 barn. Hence large thicknesses of scandium are unlikely to provide pure 2 keV neutron beams with high outputs. The scandium beam at the MTR (Simpson et al., 1971) had a 40% contribution from fast neutrons due to neutrons transmitted through the high energy windows in scandium and a difference filter of cerium and manganese was used for measuring the signal spectrum. However, by using a resonance scatterer of manganese located at the centre of a through tube it is possible to reduce this background. At the NBSR, where this method was adopted using the scandium transferred from the MTR, the fast background is reduced to 3% (Schroder, Schwartz and McGarry, 1975). The scandium beam at the FMRB also uses a manganese scatterer. Here, however, the fast background for the difference beam is 15% (Alberts and Knauf, 1977; Alberts, Cosack, Kluge, Lesiecki, Wagner and Zill, 1979) and no values are reported for the open beam. A similar value for fast neutron contamination in the 2 keV difference beam from the Obninsk reactor is reported by Kuzin et al (1973); this beam, however, does not utilise a manganese scatter.

Greenwood and Chrien (1976) at the HFBR undertook a study to determine whether materials other than titanium could be used to reduce the fast neutron background. They tried magnesium, aluminium, sulphur, titanium, vanadium, chromium, iron, cobalt and nickel, and concluded that scandium, cobalt and titanium should provide the purest 2 keV beam. However, the fast neutron component was still high (9%) with this combination.

Brugger (1979) is planning to install a scandium filter on the MURR. It is planned to add a mixture of titanium, cobalt, iron-54, nickel-60 and zinc-64 to reduce the fast neutron background.

Silicon filters have been developed at the MTR, the NBSR, the MURR and at the Obninsk reactor. The main problem at the MTR was the large gamma-ray component in the beam (Simpson et al., 1971). Although this could be reduced with the addition of lead the beam intensity at 144 keV was also reduced considerably. Tsang and Brugger (1976) assembled a much longer filter compared to that at the MTR and reduced the gamma-ray background significantly. The silicon filter at the NBSR is at the other end of the through tube from the iron filter and hence views the same graphite scatterer. This also greatly reduces the gamma-ray background, but at the expense of some intensity. As there are no windows at energies above 144 keV, there are no problems with fast neutrons. However, there is a small window at 55 keV and silicon, being polycrystalline, transmits neutrons below the Bragg cut-off at 2 meV. These lower energy components can be removed by the addition of titanium and boron-10. The Russian group (Kuzin et al., 1973) used a sulphur filter to measure the difference spectrum in their silicon beam. They probably found the need for this method as their silicon filter is only 51 cm compared to the 100-200 cm used by others. They also used a silicon filter (combined with some sulphur to remove neutrons at 144 keV) to extract a beam of 55 keV neutrons.

In addition to iron and silicon filters, uranium and liquid oxygen filters have been developed at the MURR to give filtered beams at 186 eV and 2.35 MeV respectively. Uranium has several other windows between 100 eV and 3 keV and many of these are as deep as the one at 186 eV. Consequently the beam purity with 43 cm of uranium was only 46% and it was necessary to add small amounts of selenium, germanium and manganese.

For measuring spectra, the detector was surrounded by interchangeable polyethylene spheres. However, the presence of the background windows and the poor energy resolution of the spheres made a difference technique necessary. Tungsten was used for this purpose (Royer and Brugger, 1977).

For safety reasons (radiation converts oxygen to ozone which presents an explosion hazard) it was necessary to place the liquid oxygen filter just outside the end of the filter tube and other shielding material - uranium and bismuth - was placed in the filter tube to reduce the background. The beam purity with 1.8 m of liquid oxygen is good although greater output would be obtainable if the filter were placed inside the biological shield (Koeppe and Brugger, 1980).

Some sample spectra for transmitted beams of scandium, iron, silicon and oxygen are shown in Figures 11-17.

## 5.2 Accelerator-Based Facilities

Accelerator-based filtered beams have been used exclusively in time-of-flight systems for precise evaluation of cross-sections. Because of the general set-up involved in these systems, accelerator-based filtered beams cannot be generally regarded as permanent or semi-permanent facilities as are the reactor-filtered beams.

The filtered neutron beam has several advantages over white sources. In particular the filter strongly absorbs background off-energy neutrons and gamma-rays and also allows the measurement of this background during the experiment. Most filters produce several energy bands of filtered beams separated by their time of flight, and this enables experiments to be carried out simultaneously at several energies corresponding to the minima in the filter materials. As the transmission of neutrons whose energies correspond to the minima is high, the intensity of these neutrons is comparable to that obtained without the filter. With time-of-flight systems it is not necessary to add additional filter material to suppress

unwanted neutrons. Also large thicknesses of filter are not required as the attenuation of neutrons either side of the minima is generally high.

Most of the reported filtered beams have been from pulsed electron linear accelerators using a photoneutron target and a polyethylene moderator. Filters of iron have been used at the Oak Ridge Electron Linear Accelerator (ORELA) (Harvey, 1972), at the Kyoto University Linear Accelerator Laboratory (KUR) (Block, Fujita, Kobayashi and Oosaki, 1975) and at the Gaerttner Linear Accelerator Laboratory, Rensselaer Polytechnic Institute (RPI) (Liou et al., 1979). Silicon has been used at the KUR (Kobayashi et al., 1977) and scandium at the RPI (Liou et al., 1978). At the KUR (Block et al., 1975; Fujita, Kobayashi, Oosaki and Block, 1976; Yamamura Doi, Miyagawa, Fujita, Kobayashi and Block, 1978) part of the iron filter was placed immediately in front of the collimator system, thus scattering most of the unwanted neutrons and gamma-rays out of the flight path before they could enter the collimating system. Additional iron was placed further along the flight path to complete the filtering of the neutron beam. The technique was also used for the silicon filter (Kobayashi et al., 1977).

Some details of accelerator-based filtered beams are shown in Table 7 and Figure 18 shows the spectrum through an iron filter placed in the KUR neutron beam.

## 6. APPLICATIONS OF FILTERED BEAM

### 6.1 Cross-section Measurements

Filtered beams, both in experimental reactors and also in pulsed time-of-flight experimental systems, have found increasing applications in recent years for the measurement of cross-sections. It might seem, at first sight, that filtered beams would have few advantages compared with broad spectrum neutron sources combined with highly accurate time-of-flight systems since filtered beams are available at relatively few energies.

However, difficulties do arise in white source measurements due to scattered neutrons which interfere with the neutrons of interest. Thus the white source techniques are ideal for measuring the relative magnitude of cross-sections at different energies but can give difficulties when absolute values of cross-section are required with high precision. The filtered beams are ideal for benchmark measurements of high accuracy to which, in principle, other measurements can be related.

Filtered beams are also useful for precision measurements of the cross-section at the minima in the cross-section of the material of the filter itself, since contaminating radiation is kept to a minimum. Such minimum values are of great importance in shielding calculations since the precision with which the flux at depth in a shield can be estimated depends crucially on the value of the cross-section at the minima (Goldstein, Lidofsky, Oblow, Preeg, Soran and Weisbin, 1971). A material to which such considerations obviously apply is iron and measurements with filtered beams, using time-of-flight techniques have been reported (Harvey, 1972; Liou et al., 1979).

Accurate cross-section measurements of fissile and fertile materials are similarly of importance for reactor design and a silicon filtered beam has been used to measure the differential cross-section of uranium-238 at 144 keV (Tsang and Brugger, 1978) and an iron filtered beam to measure the cross-section of thorium at 24 keV (Kobayashi, Fujita, Oosaki and Block, 1978).

Measurements of the fission cross-sections of uranium-235 and plutonium 239 have been made at 2, 24, 55 and 144 keV (Zhuravlev, Kroshkin and Karin, 1977).

The effect of Doppler broadening on the uranium-238 and uranium-238 oxide cross-sections at 24 and 144 keV have been measured for the temperature range 38 K - 1100 K (Tsang and Brugger, 1980a). Similar measurements have been made of the tin cross-section at 24 keV (Tsang and Brugger, 1980b).

Accurate measurements of the (n,p) scattering cross-section have been used to confirm theoretical studies of nucleon-nucleon interactions (Fujita et al., 1976) and measurements of the total neutron cross-sections of beryllium, carbon and oxygen at 24 keV have been compared with the predictions of nuclear theory and used as bench-marks for conventionally measured cross-sections (Block et al., 1975).

Extensive measurements of neutron capture cross-sections at 24 keV have been made on the Indian iron filtered beam, some cross-section values differing widely from measurements made elsewhere (Anand, Jhingan, Bhattacharya and Kondaiah, 1979). A notable example is the capture cross-section for cerium-142,  $19 \pm 4$  mbarn which contrasts with values reported by other authors of  $425 \pm 43$  mbarn and  $525 \pm 50$  mbarn. Similar measurements of neutron capture cross-sections of a range of nuclides at 24 keV have been reported by Yamamuro and coworkers (Yamamuro, et al., 1978).

These and similar measurements are reviewed comprehensively by Block and Brugger (1980), as are the (n, $\gamma$ ) spectrometry data discussed in the next section.

## 6.2 (n, $\gamma$ ) Spectrometry

Filtered beam facilities lend themselves to a study of (n, $\gamma$ ) reactions because of the high fluxes and energy spreads in the beams. For low-Z nuclei, which have widely spaced resonances, the capture gamma-ray lines often arise from discrete resonances whereas for higher-Z targets, the capture gamma-ray spectrum is a composite resulting from many resonances. Average resonance capture is discussed in detail by Greenwood and coworkers (Greenwood, Harlan, Helmer and Reich, 1969) who show that such spectra give information on the multipolarities of the primary gamma-ray transitions and the possible range of spin values of the final states populated by the primary transitions.



Filtered beams have also been used to give information on the  $(n, \gamma)$  spectra of nuclides which are very difficult to study with thermal neutrons because neighbouring or impurity nuclides have very large thermal neutron cross-sections giving rise to serious contamination problems. An example is the gamma-rays produced by 2 keV neutron absorption of gadolinium-156 (Greenwood and Chrien, 1976).

Early studies of this type were discussed by Brugger and Simpson (1973) and Gamalii, Zemtsev, Ivanov, Nesterov and Kham'yanov (1972) and in more recently by Stecher-Rasmussen and Ratynski (1979).

### 6.3 Shielding Studies

Many of the filtered beams are ideally suited for bench-mark measurements to check shielding calculations. The time-scale of moderation and absorption processes in a thick shield precludes the use of time-of-flight techniques and since 2 keV neutrons are at the limit of energies obtainable by alternative systems, a scandium beam would yield valuable information if used with integrating detection systems. The iron and oxygen filtered beams give neutrons of energies at which shield penetration can be a maximum since, of course, these materials are incorporated in shields.

### 6.4 Instrument Calibration and Development

The development of many neutron sensitive instruments has long been bedevilled by the fact that appropriate neutron sources are not available throughout much of the intermediate energy region. The use of time-of-flight techniques is often difficult or impossible because of either the requirement to modify the detector in the instrument or the fact that the response time of the instrument is comparable with, or greater than, the flight times involved. This latter consideration is particularly relevant to all instruments which are based on large moderating assemblies. Examples are

the widely used Andersson-Braun type of instrument used for environmental surveys for radiological protection purposes, the "long counter" instruments, often used as primary neutron flux transfer standards and spectrometry systems based a range of moderating spheres.

Many instruments are well calibrated at energies down to 25 keV or so with conventional mono-energetic neutron sources. Generally, the response of instruments over the six decades of energy between 0.025 eV and 25 keV is either ignored or estimated by interpolation. The wide range of instruments to which these comments apply has been well summarised by Anderson (1969).

A knowledge of the response of health physics instruments in this energy region is important for three reasons. Firstly, many surveys have shown that a significant proportion of neutron dose in many different working environments around reactors and other neutron producing installations is due to neutrons with energies less than 30-100 keV. These surveys, which are summarised by Harvey and Beynon (1972), are of course subject to the very uncertainties which stem from the lack of adequate instrument calibration facilities in the intermediate energy region. Secondly, a widely used type of personal dosimeter, the albedo dosimeter, which utilises devices which are sensitive to neutrons reflected from the wearer's body is sensitive principally below 10 keV (Harvey, Hudd and Townsend, 1969; 1973). Not only is the response of such dosimeters therefore poorly verified throughout the energy region in which they are sensitive but readings are often modified on the basis of instrumental surveys of the environments in which the personnel are exposed (Harvey et al., 1973; Hankins, 1976). Inadequacies in understanding of the characteristics of the survey instruments are therefore reflected in the overall accuracy of the personal dosimetry system. The third reason for the importance of this energy region in the context of health physics instrumentation stems from the fact that the dose equivalent-fluence relationship changes abruptly at 10 keV. The response

function of a typical detector based on neutron moderation on the other hand is likely to change smoothly with neutron energy in this region. It follows that such instruments which purport to measure dose-equivalent rate are most likely to be in error at energies around 10 keV.

Work in this area has been performed principally at two centres; NBS Washington DC and Physikalisch-Technische Bundesanstalt (PTB) Braunschweig. The NBS beams have been used for calibrating health physics monitoring instruments and "albedo" personal neutron dosimeters (Hankins, 1977). Characteristics of the beams and application to such measurements have been discussed by Hoy and Schwartz (1976) and Hoy (1976). The average dose equivalent rates in the beams are;  $140 \text{ mrem h}^{-1}$  ( $1.4 \text{ mSv h}^{-1}$ ) at 2 keV,  $150 \text{ mrem h}^{-1}$  ( $1.5 \text{ mSv h}^{-1}$ ) at 25 keV and  $3.2 \text{ rem h}^{-1}$  ( $32 \text{ mSv h}^{-1}$ ) at 144 keV. The beam diameters at 2.25 m from the reactor are 4.25 cm (2 keV), 6 cm (25 keV) and 4.5 cm (144 keV). Instruments with dimensions larger than the beam diameters are exposed on a movable platform which performs a raster movement, so that all parts of the instrument are exposed. This factor can be advantageous, since it allows an exploration of the variation of sensitivity with position on an instrument. The concomitant disadvantage is that for overall sensitivity measurements the instrument response has to be integrated over one or more raster cycles and the effects of relatively low background fluxes of neutrons are more noticeable. An instrument of the size of an Andersson-Braun remmeter for example (approximately 22 cm x 22 cm) is effectively exposed to a dose rate 2.9% of that in the beam, i.e.  $4.1 \text{ mrem h}^{-1}$  at 2 keV, which is comparable to background neutron dose rate in the vicinity of the reactor. This implies a need for care in the application of the beam but does not, of course, preclude accurate calibration.

The PTB beams have been used for similar pioneering measurements in Europe. The PTB made the beams available to scientific groups in Europe for an intercomparison of instrument calibrations (Alberts et al., 1979)

at intermediate and other energies. The reactor at PTB has a lower intermediate energy flux than other reactors used for filter beam experiments (of order  $6 \times 10^{10} \text{ cm}^{-2} \text{ s}^{-1}$  as compared with  $4 \times 10^{12} \text{ cm}^{-2} \text{ s}^{-1}$  at the NBS for example). In consequence a somewhat shorter filter length is used (71 cm of scandium as opposed to 110 cm at the NBS) and the proportion of unwanted neutrons and gamma radiation is correspondingly greater. The measurements have therefore been made with a "difference" technique in which instruments are exposed to the filtered beams, both with and without foils to absorb the wanted neutron energies. The foils consist of 5 mm of titanium for the 24 keV beam and 25 mm of manganese powder for the 2 keV beam. This gives rise to somewhat larger uncertainties than would apply to irradiations in beams without a difference technique. The use of the beams has been a significant step forward in extending the range of neutron energies available for the calibration of neutron sensitive instruments in Europe.

Such measurements (Alberts, 1978) have confirmed theoretical predictions (Tessler and Glickstein, 1975) and measurements with a moderated antimony-beryllium source (Harvey, Lavender and Thompson, 1976; Harrison, Harvey and Boot, 1978) which suggest that a number of commonly used instruments are oversensitive to neutrons in the energy band 100 eV - 10 keV by factors which can be as large as four.

Included in the instruments calibrated at the PTB have been spectrometry systems based on a range of moderating spheres. Although attempts have been made to calibrate spherical moderator systems with time-of-flight methods (Wetzel, Kneske, Taut, Algnikov, Komozkov, Nazarov and Klapper, 1969; Basson, 1962) interpretation of the results is difficult. This follows from the fact that the mean lifetime of the neutrons in the moderator is often greater than the required "live-time" of the instrument.

Because of the difficulty in deriving reliable response functions experimentally a number of attempts have been made to calculate the detection efficiencies by Monte Carlo computer codes. Nachtigal and Burger (1972) summarising these data conclude that there exists "a remarkable uncertainty as to the true response curves". The same authors emphasise the experimental measurement of the response functions should be undertaken and that filtered beams would be particularly appropriate..

Proton recoil spectrometry systems can also be calibrated with the filtered beams. The routine calibration of the proportional counter is frequently based on either alpha particles from an internal source or protons from the  $^3\text{He}(n,p)^3\text{H}$  reaction in added helium-3 gas. This later reaction has a Q value of 765 keV. Overall calibration and system linearities are checked by reference to presently available mono-energetic sources at energies above 10 keV or so and an extension to lower energies is valuable. Rogers (1970a, b) and Powell and Rogers (1970) have described the use of scandium and iron filtered beams for the calibration of a proton recoil spectrometer, and the related study of the way in which W values change with neutron energy for proportional counters filled with hydrogen and methane gases.

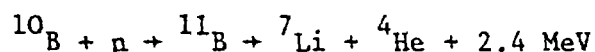
#### 6.5 Biological and Medical Studies

It is possible to use filtered intermediate energy neutron beams to produce significant fluxes of thermal neutrons inside the human body. The advantage of using intermediate energy neutrons is that they produce much lower thermal neutron fluxes at the surface of the body for a given flux at depth than do thermal beams and also do not give a significant knock-on proton dose in the thermalisation process as do fast neutrons. The variation of thermal neutron flux with depth for incident 2 keV neutrons is shown in Figure 19 where it is compared with the flux profiles resulting

from incident thermal neutrons and neutrons from a heavy water moderated californium-252 source which has been proposed for experiments of this type (Murray, Deutsch, Zamenhof, Pettigrew, Rydin and Brownell, 1975).

Two applications have been proposed to take advantage of this thermal neutron flux profile:- boron neutron capture therapy (BNCT) and "in vivo" measurement of the cadmium content of organs.

Neutron capture therapy involves the selective up-take by a tumour of a nuclide having a high neutron capture cross-section followed by irradiation with neutrons. Nuclides which may be used include boron-10, lithium-6 or uranium-235; of which boron-10 is most often considered. The reaction of slow neutrons with boron-10 produces fission fragments of very short range and high linear energy transfer.



The alpha particle and the lithium-7 nucleus have a range of less than 11  $\mu\text{m}$  and hence irradiate only a single cell and its immediate neighbours.

There is a permeability difference between brain tumour and normal tissue and several studies have shown that many compounds whose entrance into normal brain tissue is restricted are not impeded in penetrating brain tumours. Thus BNCT was first attempted on brain tumours, especially Glioblastoma multiforme, a rapidly growing neoplasm giving an average survival time of less than a year when treated with conventional radiotherapy. The initial trials (e.g. Astbury, Ojemann, Nielsen and Sweet, 1972) were disappointing for two reasons. Firstly, it was found that the circulating blood retained a high concentration of boron-10, approximately three to four times that in the tumour. This gave rise to a large intracapillary dose in the normal parts of the brain. A second problem was that the dose to the surface of the brain was high due to the rapid fall-off of flux with depth for thermal neutrons.

Recently new boron-loaded compounds have been developed which bind to tumorous tissues so that neutron irradiation can be delayed until these compounds have cleared from the systemic blood (Hatanaka and Sweet, 1975). In addition a large dose of adrenocorticosteroids can be given to prevent radiation damage to normal cerebral blood vessels. The possible use of these new techniques has revived interest in BNCT. However, the problem of a high surface dose which still exists could, in principle, be solved with filtered neutron beams at intermediate energies. Mill and Harvey (1978) calculate that a scandium filtered beam from a typical high flux reactor would deliver a dose rate to the tumour equivalent to a gamma dose rate of  $260 \text{ rad h}^{-1}$ . This would be adequate for experimental radiotherapy.

The second application which makes use of the thermal neutron flux profile produced by intermediate energy neutrons is the study of the cadmium content of human organs. Cadmium is not only hazardous to workers in cadmium-related industries but also to the general public because of its persistence in the environment and the consequent slow build-up with time. Ryde (1980) has shown that intermediate energy neutron beams constitute an effective method of monitoring cadmium levels, particularly in kidney and liver which can contain a significant proportion of the cadmium content of the whole body. The method is based on the reaction  $^{143}\text{Cd} (n, \gamma) ^{144}\text{Cd}$  which has a cross-section of 20,000 barn at thermal energies and gives rise to gamma radiation of 558 keV which can readily be detected outside the body with for example a Ge(Li) spectrometry system. Ryde, using a simple humanoid phantom has shown that it is possible to detect 4 mg of cadmium in the kidneys with a precision of  $\pm 3 \text{ mg}$  for an exposure in an iron filtered beam of one minute giving a dose of 32 mrad to local tissues.

Direct irradiation of biological specimens with intermediate energy beams could give useful information about the mechanisms of the interaction of ionising radiation with cellular systems. Neutrons, although themselves

non-ionising, produce densely ionising short range particles within irradiated tissue. The dimensions of the tracks of these particles may be comparable to the dimensions of important cellular components and can give valuable insights into the mechanisms of radiation injury. However, almost all studies to date have been with neutrons of energy greater than 100 keV (Hall, Novak, Kellerer, Rossi, Marino, Goodman, 1975). An important exception is the work of Bergman (1974) who worked with neutrons having a mean energy of 8 keV. The paucity of data is due to the difficulty of producing suitable sources of these neutrons rather than a lack of interest in intermediate energy neutrons.

There are two reasons why studies using intermediate energy neutrons are important. Firstly, the ranges of protons produced by these neutrons are less than cellular dimensions and may therefore be used to gain information concerning the size and separation of radiosensitive elements in cells. Secondly protons in this energy range lose a significant proportion of their energy by non-ionising direct recoil interactions with hydrogen nuclei. The proportion of energy lost by such collisions is 9% at 2 keV (ICRU, 1970). The possible implications of such interactions are uncertain and the only relevant experiments which can be performed at the present time involve the use of charged particles incident directly onto very thin enzyme samples (Sutcliffe and Watt, 1974; Jung and Zimmer, 1966).

Mill and Harvey (1978) have shown that an average high flux reactor could give filtered beam dose rates of  $5 \text{ rad h}^{-1}$  at 2 keV and  $7 \text{ rad h}^{-1}$  at 24 keV. The dose rates quoted here are kerma in small tissue elements which is the parameter appropriate to biological experiments of this type. The biological samples would have to be small in order to minimise thermalisation and the dose rates quoted are adequate for carefully chosen biological experiments. As far as we are aware no such experiments have yet been attempted using filtered beams.



## 6.6 Neutron Radiography

There are a number of reports of the use of filtered beams for radiography. The most obvious application is the use of an iron filtered beam for radiographing materials encased in a thick iron container because the container will in general not attenuate the neutron flux significantly. The principle difficulty is in finding a detection system which is particularly sensitive to intermediate energy neutrons. For this reason a tomographic technique is attractive since the detector can then be a thermal neutron detector inside a moderator. In such applications the detector can be located behind a collimator and the object rastered in the beam. This approach has been used to radiograph voids in 83 mm of polyurethane sandwiched between 130 mm of steel (Tsang, Alger and Brugger, 1978), the arrangement being used to simulate an explosive device. Another application is the tomography of copper pins in graphite inside a stainless steel pipe having a wall thickness of 32 mm. This test was designed to simulate fast breeder reactor fuel in sodium inside a stainless steel pipe (Brugger, 1979). Miller and McNeece (1969) were able to detect a small plastic tube behind 50 cm of steel.

An early theoretical analysis was made of the possible use of an iron filtered beam for human radiography (Bryant and Bull, 1974). Although good contrasts could be achieved the dose from high energy contamination was too high for the technique to be tried. The technique is attractive although overall transmission through the body would be low.

## 7. CURRENT STATUS OF AND FUTURE PROSPECTS FOR FILTERED BEAMS

Over the last decade there has been a steady increase in number of reactors with installed filters, in the energy of beams available and in the number of applications of filtered beams. It is most probable that this trend will continue.

There is, for example, considerable scope for increasing the range of energies. At low energies filters of high atomic mass are used. The one which has currently been realised is the 186 eV beam from a uranium filter. As can be seen from Figure 8, other useful windows exist in uranium throughout the energy range 20 eV - 2.5 keV. It will be possible to utilise a number of these with the aid of scattering foils which have peaks at appropriate energies.

The highest energy window of significance in uranium (2.5 keV) ties in very well with the lowest energy window in medium atomic mass materials, that at 2 keV in scandium.

Several well-utilised windows in medium atomic mass materials cover the range 2 keV - 144 keV. It should be possible to use low and medium atomic mass materials to give beams at energies between 144 keV and 2.3 MeV the energy of the oxygen beam. Iron, for example, has useful windows in the energy range 244-376 keV, scandium has windows at 190 keV and 345 keV. It might be possible to utilise the 420 keV window in neon, if practical problems do not preclude the use of liquid neon.

It seems most likely therefore that beams will be produced with energies throughout the range 20 eV - 2 MeV with a set of filters and scattering foils of common and relatively inexpensive materials. The range of energies could be further extended by the use of single nuclide filters. Considerable masses of separated nuclides are available as by-products of the separation of low abundance nuclides at the Oak Ridge National Laboratory, USA. If these were purchased, the charges offset over a ten year period would not be excessive (Mill and Harvey, 1978). Alternatively they could be hired for periods of a year or so at relatively small cost. Separated iron-56 has been used at the HFBR (Liou et al., 1979) and there are plans to use zinc-64, iron-54 and nickel-60 in conjunction with a scandium filter (Brugger, 1979).

In summary there are currently some six energies which have been practically realised. This could be extended to possibly as many as 20 energies throughout the energy range 30 eV - 2.3 MeV.

If the various filters and scattering foils were easily interchangeable as for example in a revolving filter assembly, then any given energy could be established rapidly by appropriate juxta position of filter and scattering foil. Such a facility would be very useful for certain applications where neutron beams are required within a wide energy range, such as in the development and calibration of neutron sensitive instruments. At present it is expensive and time consuming to have access to a range of neutron energies. Energies from a few keV to 14 MeV can be derived from a number of charged particle reactions with a Van de Graaff accelerator, but to cover the full range involves time consuming procedures such as measuring threshold energies for each target. Energies below a few keV are not available from charged particle reactions.

There are currently three reactors with filtered beams in the United States, three in Europe, two in Russia and one in India. The need for filtered neutron beams has been demonstrated recently by the response to a questionnaire widely distributed in Europe (Harvey, 1980). The response indicated that some 25 laboratories would use a range of filtered beams, the requirements ranging from less than one day per year to several months per year. The distribution of the required utilisation times by scientific discipline is illustrated in Figure 20. The aggregated requirement would be for more than 500 days per year, roughly twice the time that could be provided by a single beam tube. These considerations would seem to indicate the need for a centralised facility in Europe. This should be based on a high flux reactor since this gives scope for higher fluxes and hence more applications, and greater beam purities. It would seem to be

an ideal area for an international agency to play a coordinating role. Seven high flux reactors in Europe would be particularly appropriate from a scientific point of view (Mill and Harvey, 1978): BR-2, Mol, Belgium; Pluto/Dido, Harwell, England; DR-3, Riso, Denmark; Dido-Julich, Julich, Federal Republic of Germany; HFR, Petten, Holland; High Flux Reactor, Grenoble, France and the R-2, Studsvik, Sweden. It is also possible to utilise neutrons produced by high energy charged particle accelerators, many of which are being converted to neutron generation (Dore, 1978; Southworth, 1976). Rough calculations suggest that the time-averaged intermediate fluence in the moderator block of such a device would be one or two orders of magnitude less than in the core of a high flux reactor. This disadvantage would be offset by the fact that filters could probably be placed closer to the source than with a high flux reactor since less biological shielding would be needed. Also a pulsed source would allow very good beam spectrometry by time-of-flight methods.

In summary, the filtered beam facilities which are available at a few reactor establishments have been shown to be useful in a wide range of scientific disciplines. There is considerable scope for extending the energies available and many scientific groups have indicated a need for a range of filtered neutron beams. It is possible that if the potential range of energies and simplicity of operation can be realised, filter beams could replace accelerators in applications where fixed energy beams are required over a wide energy range.

#### ACKNOWLEDGEMENT

We are indebted to those who sent us information relating to the status and applications of their filtered beams.

This paper is published with the permission of the Central Electricity Generating Board.

## REFERENCES

- Alberts, W. G., 1978. Calibration of neutron monitors for radiation protection at 24.5 keV and 2 keV. *Nuclear Instruments and Methods*, 155, 307.
- Alberts, W. G., Cosack, M., Kluge, H., Lesiecki, H., Wagner, S. and Zill, H. W., 1978. European workshop on neutron dosimetry for radiation protection. Report PTB-ND-17. Physikalisch-Technische Bundesanstalt, Braunschweig, W. Germany.
- Alberts, W. G. and Knauf, K., 1978. The 2 keV and 24.5 keV filtered neutron beam facility at the PTB Reactor, Braunschweig. In: *Proceedings of the third symposium on neutron dosimetry in biology and medicine* (Munich, 23-27 May, 1977) EUR 5848 DE/EN/FR. Commission of the European Communities, Luxembourg.
- Anand, R. P., Jhingan, M. L., Bhattacharya, D. and Kondaiah, E., 1979. 25 keV - neutron capture cross-sections, *Il Nuovo Cimento*, 50A, 247.
- Anderson, L. L., 1969. Mono-energetic neutrons of intermediate energy; a calibration facility design. *Health Physics*, 16, 359.
- Astbury, A. K., Ojemann, R. G., Nielsen, S. L. and Sweet, W. H., 1972. Neuropathologic study of fourteen cases of malignant brain tumours treated by neutron capture therapy using boron-10. *Journal of Neuropathology and Experimental Neurology*, 31, 278.
- Barton, J. P., 1965. Radiographic examination through steel using cold neutrons. *British Journal of Applied Physics*, 16, 1833.
- Basson, J. K., 1962. A detector for intermediate energy neutrons. Report AERE-R3864, United Kingdom Atomic Energy Authority. Her Majesty's Stationary Office, London.
- Bergman, R., 1974. Intermediate neutron-induced slow recoil particles applied in radiobiology. In: *Proceedings of a symposium on the effects of neutron irradiation upon cell function*. (Munich, 22-26 October, 1973) STI/PUB/352. International Atomic Energy Agency, Vienna.
- Block, R. C., and Brugger, R., 1980. Filtered beams. Chapter V of "Neutron Physics and Nuclear Data in Science and Technology". To be published.
- Block, C., Fujita, Y., Kobayashi, K. and Oosaki, T., 1975. Precision neutron total cross-section measurements near 24 keV. *Journal of Nuclear Science and Technology*, 12, 1.
- Breit, G. and Wigner, E. P., 1936. Capture of slow neutrons. *Physics Review*, 49, 519.
- Briggs, G. A. and Stirling, W. G., 1976. Neutron diffraction facilities at Western European medium flux reactors. Report, Institut Max von Laue-Paul Langevin, Grenoble, France.

- Broder, D. L., Gamalii, A. F., Zemtsev, B. V., Nesterov, B. V. and Kham'yanov, L. P., 1971. Measurement of  $\gamma$ -ray spectra from capture of intermediate energy neutrons. *Yadernaya Fizika*, 13, 3.
- Brugger, R. M., 1979. Private communication.
- Brugger, R. M. and Simpson, O. D., 1973. Resonance window filters of neutrons for research and development. In: Proceedings of a symposium on irradiation facilities for research reactors. (Teheran, November 6-10, 1972) STI/PUB/316. International Atomic Energy Agency, Vienna.
- Bryant, K. R. and Bull, S. R., 1974. Resonance energy neutron beams from reactors for radiobiology studies. In: Symposium on the effects of neutron irradiation on cell function. (Munich, October 22-26, 1973) STI/PUB/351. International Atomic Energy Agency, Vienna.
- Cho, M., Fröhner, F. H., Kazerouni, M., Muller, K. N and Rohr, G., 1970. Total cross-sections of  $^{45}\text{Sc}$ ,  $^{47}\text{Ti}$ ,  $^{49}\text{Ti}$ ,  $^{53}\text{Cr}$ , and  $^{61}\text{Ni}$  in the keV-region. In: Proceedings of the second international conference on nuclear data for reactors (Helsinki, June 15-19, 1970) STI/PUB/259. International Atomic Energy Agency, Vienna.
- Chrien, R. E., Liou, H. I., Block, R. C. and Kobayashi, K., 1977. Neutron resonances in  $^{45}\text{Sc}$  and their relation to thermal scattering parameters. *Physics Letters*, 71B, 311.
- Dombeck, T. W., Lynn, J. W., Werner, S. A., Brun, T., Carpenter, J., Krohn, V. and Ringo, R., 1979. Production of ultra-cold neutrons using Doppler-shifted Bragg scattering and an intense pulsed neutron spallation source. *Nuclear Instruments and Methods*, 165, 139.
- Dore, J., 1978. Pulsed neutrons at the Rutherford. *New Scientist*, 78, 160.
- Fujita, Y., Kobayashi, K., Oosaki, T. and Block, R. C., 1976. Measurement of the neutron-proton total cross-section using 24 keV iron filtered neutrons. *Nuclear Physics*, A258, 1.
- Gamalii, A. F., Zemtsev, B. V., Ivanov, V. B., Nesterov, B. V. and Kham'yanov, L. P., 1972. Gamma radiation in intermediate neutron radioactive capture. *Yadernaya Fizika*, 15, 3.
- Garber, D. I. and Kinsey, R. R., 1976. Neutron cross-sections volume II, curves. Brookhaven National Laboratory Report 325, third edition. United States Energy Research and Development Administration, Springfield.
- Goldstein, H., Lidofsky, L. T. Oblow, E., Preeg, W. E., Soran, P. and Weisbin, C. R., 1971. The role of cross-section minima in the deep penetration of fast neutrons. In: Proceedings of the third conference on Neutron Cross-sections and Technology (Knoxville, March 15-17, 1971) CONF-71031. United States Atomic Energy Commission, Springfield.
- Greenwood, R. C. and Chrien, R. E., 1976. Filtered reactor beams for fast neutron capture gamma-ray experiments. *Nuclear Instruments and Methods*, 138, 125.

- Greenwood, R. C., Harlan, R. A., Helmer, R. G. and Reich, C. W., 1969. Neutron capture gamma-ray measurements with a reactor produced 2 keV beam. In: Proceedings of a symposium on neutron capture gamma-ray spectroscopy (Studsvik, 11-15 August, 1969) STI/PUB/235. International Atomic Energy Agency, Vienna.
- Hall, E. J., Novak, J. K., Kellerer, A. M., Rossi, H. H., Marino, S. and Goodman, L. J., 1975. RBE as a function of neutron energy I. Experimental observations. Radiation Research, 64, 245.
- Hankins, D. E., 1976. Evaluation of the fast neutron dose equivalent using the thermal neutron response of LiF TL material. Health Physics, 31, 170.
- Hankins, D. E., 1977. Energy dependence measurements of remmeters and albedo neutron dosimeters at neutron energies of thermal and between 2 keV and 5.67 MeV. In: Proceedings of the IVth International Congress of the International Radiation Protection Association (Paris, 24-30 April, 1977). International Radiation Protection Association, Fontenay-aux-Roses, France.
- Harrison, K. G., Harvey, J. R. and Boot, S. J., 1978. The calibration of neutron instruments and dosimeters at intermediate energies. Nuclear Instruments and Methods, 148, 511.
- Harvey, J. A., 1972. keV neutron total cross-section measurements at ORELA. In: Proceedings of ANS Topical Meeting on New Developments in Reactor Physics and Shielding Calculations. (Kiamesha Lake, 12-15 September, 1972) CONF-720901. United States Atomic Energy Commission, Springfield.
- Harvey, J. R., 1979. The status of current measurements of neutron "windows" in single isotopes being undertaken at the Oak Ridge National Laboratory, USA. Report RD/B/N4657. Central Electricity Generating Board, Berkeley, England.
- Harvey, J. R., 1980. Analysis of replies to a questionnaire on the potential utilisation of a proposed intermediate-energy neutron facility. Report RD/B/N4726. Central Electricity Generating Board, Berkeley, England.
- Harvey, J. R. and Beynon, S., 1972. A neglected energy range. In: Proceedings of the first symposium on neutron dosimetry in biology and medicine (Munich, 15-19 May, 1972) EUR 4896 d-f-e. Commission of the European Communities, Luxembourg.
- Harvey, J. R., Hudd, W. H. R. and Townsend, S., 1969. A personal dosimeter which measures dose from thermal and intermediate energy neutrons and from gamma and beta radiation, Report RD/B/N1547. Central Electricity Generating Board, Berkeley, England.
- Harvey, J. R., Hudd, W. H. R. and Townsend, S., 1973. Personal dosimeter for measuring the dose from thermal and intermediate - energy neutrons and from gamma and beta radiation. In: Proceedings of a symposium on neutron monitoring for radiation protection purposes. (Vienna, 11-15 December, 1972) STI/PUB/318. International Atomic Energy Agency, Vienna.
- Harvey, J. R., Lavender, A. and Thompson, I. M. G., 1976. The calibration of a number of neutron sensitive instruments with a novel source emitting neutrons around 0.5 keV. Health Physics, 31, 363.

- Harvey, J. R. and Mill, A. J., 1978. A proposed intermediate energy neutron facility and possible applications. In: Proceedings of the third symposium on neutron dosimetry in biology and medicine (Munich, 23-27 May, 1977) EUR5848 DE-EN-FR. Commission of the European Communities, Luxembourg.
- Hatanaka, H. and Sweet, W. H., 1975. Slow-neutron capture therapy for malignant tumours. Its history and recent development. In: Proceedings of a symposium on biomedical dosimetry (Vienna, 10-14 March, 1975) STI/PUB/401. International Atomic Energy Agency, Vienna.
- Hoy, J. E., 1976. Using the NBS neutron calibration facility. In: Proceedings of the Annual ERDA Health Protection Meeting. (Denver, 7 February, 1976). United States Research and Development Administration, Springfield.
- Hoy, J. E. and Schwartz, R. B., 1976. User's Manual. Standard neutron fields at NBS. United States Department of Commerce, Washington DC.
- Hughes, D. J., 1954. Neutron optics. Interscience Publishers Incorporated, New York and London.
- ICRU, 1970. Linear energy transfer. Report 16. International Commission on Radiation Units and Measurements, Washington DC.
- Jung, H. and Zimmer, K. G., 1966. Some chemical and biological effects of elastic nuclear collisions. Current Topics in Radiation Research, 2, 69.
- Kobayashi, K., Fujita, Y. and Ogawa, Y., 1977. Measurements of neutron total cross-section minima in natural iron and silicon. Annals of Nuclear Energy, 4, 449.
- Kobayashi, K., Fujita, Y., Oosaki, T. and Block, R. C., 1978. Neutron total cross-section measurement of thorium near 24 keV with an iron filtered neutron beam. Nuclear Science and Engineering, 65, 347.
- Koepe, R. A. and Brugger, R. M., 1980. Improvement of an oxygen filtered neutron beam of 2.35 MeV. Nuclear Instruments and Methods, (in press).
- Kondaiah, E., Anand, R. P. and Bhattacharya, D., 1973. 25 keV neutron beam facility at the reactor "Apsara". Nuclear Instruments and Methods, 111, 337.
- Kondaiah, E., 1979. Personal communication.
- Kuzin, E. N., Belov, S. P., Dvukhshestnov, J. G., Furmanov, V. M. and Shchadin, N. N., 1973. Spectra of filtered neutron beams from the Obninsk reactor. Atomnaya Energiya, 35, 391.
- Lane, A. M. and Thomas, R. G., 1958. R-Matrix theory of nuclear reactions. Reviews of Modern Physics, 30, 257.
- Liou, H. I., Chrien, R. E., Block, R. C. and Kobayashi, K., 1978. The total neutron cross-section of scandium from 0.005 to 22 keV. Nuclear Science and Engineering, 67, 326.



- Liou, H. I., Chrien, R. E., Block, R. C. and Singh, U. N., 1979. The transmission of neutrons through iron-56 at 24.37 keV. Nuclear Science and Engineering, 70, 150.
- McGarry, E. D. and Schroder, I. G., 1975. A 25 keV neutron facility at NBS. In: Proceedings of a conference on neutron cross-sections and technology (Washington DC, 3-7 March, 1975). National Bureau of Standards Special Publication 425. United States Department of Commerce, Washington DC.
- Mijnheer, B. J. and Aten, A. H. W., 1973. A negative neutron source in the eV region. In: Proceedings of a symposium on neutron monitoring for radiation protection purposes (Vienna, 11-15 December, 1972). International Atomic Energy Agency, Vienna.
- Mill, A. J. and Harvey, J. R., 1978. Intermediate energy neutron production; a survey of existing techniques, a proposed source and its application. Report RD/B/N4324, (and Report EUR 6107EN). Central Electricity Generating Board, Berkeley, England.
- Mill, A. J., 1979. A computer code for calculating neutron cross-sections from resonance parameter data. Report RD/B/N4632. Central Electricity Generating Board, Berkeley, England.
- Miller, L. G. and McNeece, J. P., 1969. Demonstration of the need for a high flux neutron beam in neutron radiography development. Transactions of the American Nuclear Society, 12, 468.
- Miller, L. G. and Watanabe, T., 1971. Enhancing contrast of neutron radiographs by energy tailoring of beams. In: Proceedings of the sixth international conference on non-destructive testing (Hanover, 1-5 June, 1970).
- Mughabghab, S. F. and Garber, D. I., 1973. Neutron cross-sections Volume I resonance parameters. Brookhaven National Laboratory report 325, third edition. United States Energy Research and Development Administration, Springfield.
- Murray, B. W., Deutsch, O. L., Zamenhof, R. G., Pettigrew, R. I., Rydin, R. A. and Brownell, G. L., 1975. New approaches to the dosimetry of boron neutron capture therapy at MIT-MGH. In: Proceedings of a symposium on biomedical dosimetry. (Vienna, 10-14 March, 1975) STI/PUB/401. International Atomic Energy Agency, Vienna.
- Nachtigall, D. and Burger, G., 1972. Dose equivalent determinations in neutron fields by means of moderator techniques. In: Topics in Radiation Dosimetry, supplement to Radiation Dosimetry; editor P. H. Attix. Academic Press, New York and London.
- Pattenden, N., 1955. The slow neutron cross-section of scandium. Proceedings of the Physical Society, A68, 104.
- Powell, J. E. and Rogers, J. W., 1970. Fast neutron spectrum measurements in the MTR scandium and iron filtered beams. Nuclear Instruments and Methods, 87, 29.

- Rogers, J. W., 1970a. Proton-recoil calibration studies in the MTR neutron beams with hydrogen and methane detectors. Report IN-1317, United States Atomic Energy Commission, Springfield.
- Rogers, J. W., 1970b. A method for calibrating a proton-recoil spectrometer. Nuclear Instruments and Methods, 80, 313.
- Royer, R. B. and Brugger, R. M., 1977. Development of a  $^{238}\text{U}$  filtered beam of 186 eV neutrons. Nuclear Instruments and Methods, 145, 245.
- Ryde, N., 1980. Personal communication.
- Schroder, I. G., Schwartz, R. B. and McGarry, E. D., 1975. The 2 keV filtered beam facility at the NBS reactor. In: Proceedings of a conference on neutron cross-sections and technology (Washington DC, 3-7 March, 1975). National Bureau of Standards special Publication 425. United States Department of Commerce, Washington DC.
- Schwartz, R. B., 1977. Calibration and use of filtered beams. In: Proceedings of the international specialists symposium on neutron standards and applications (Gaithersburg, 28-31 March, 1977). National Bureau of Standards special Publication 493. United States Department of Commerce, Washington DC.
- Stecher-Rasmussen, F. and Ratynski, W., 1979. Gamma-rays from capture of filtered reactor neutrons. Report ECN-79-034. Stichting Energieonderzoek Centrum Nederland, Petten, Netherlands.
- Simpson, O. D. and Miller, L. G., 1968. A technique to measure neutron cross-sections in the low keV energy region. Nuclear Instruments and Methods, 61, 245.
- Simpson, O. D., Smith, J. R. and Rogers, J. W., 1971. Filtered-beam techniques. In: Proceedings of a symposium on neutron standards and flux normalisation (Argonne, 21-23 October, 1970) CONF-701002. United States Atomic Energy Commission, Springfield.
- Southworth, B., 1976. Neutron source at Rutherford. CERN Courier, 16, 170.
- Sutcliffe, J. F. and Watt, D. E., 1974. Inactivation cross-sections for ribonuclease irradiated by H, He and N beams at energies less than 10 keV. In: Proceedings of the fourth symposium on Microdosimetry (Verbania Pallanza, 24-28 September, 1973) EUR 5122 d-e-f. Commission of the European Communities, Luxembourg.
- Szilard, L., 1935. Absorption of residual neutrons, Nature, 136, 950.
- Tessler, G. and Glickstein, S. S., 1975. Monte Carlo calculation of the response of the portable neutron monitor, Snoopy. Health Physics, 28, 197.
- Tsang, F. Y., Alger, D. M. and Brugger, R. M., 1978. Neutron gauging to detect voids in polyurethane. Nuclear technology, 37, 73.
- Tsang, F. Y. and Brugger, R. M., 1976. A versatile neutron beam filter facility with silicon and iron filters. Nuclear Instruments and Methods, 134, 441.

- Tsang, F. Y., Brugger, R. M., 1978. The differential neutron scattering cross-sections of Uranium 238 at 144 keV. Nuclear Science and Engineering, 65, 70.
- Tsang, F. Y. and Brugger, R. M., 1980a. Doppler effect measurements of Uranium 238. Nuclear Science and Engineering. (to be published).
- Tsang, F. Y. and Brugger, R. M., 1980b. Doppler effect measurements of tin by the filtered neutron beam technique. Nuclear Science and Engineering. (to be published).
- Wetzel, L., Kneske, G., Taut, G., Alejnikov, V. E., Komozkov, M. M., Nazarov, B. M. and Klapper, F., 1969. Experimental investigation of the sensitivity of a LiF (Eu) scintillation counter with spherical polythene moderators. In: Proceedings of a symposium on Radiation Protection Problems with accelerators and charged particles (Dubna, 4-11 July, 1968) STI/PUB/189. International Atomic Energy Agency, Vienna.
- Yamamuro, N., Doi, T., Miyagawa, T., Fujita, Y., Kobayashi, K. and Block, R. C., 1978. Measurement of neutron capture cross-sections with Fe-filtered beams. Journal Nuclear Science and Technology, 637.
- Zhuravlev, K. D., Kroshkin, N. I. and Karin, L. V., 1977. Uranium 235 and Plutonium 239 cross-sections for fission by 2, 24, 55 and 144 keV neutrons. Atomnaya Energiya, 42, 56.
- Zinn, W. H., 1947. Diffraction of neutrons by a single crystal. Physical Review, 71, 52.

TABLE I  
Reactor-Filtered Beam Facilities

REACTOR AND LOCATION	REACTOR TYPE, ENRICHMENT, MODERATOR	POWER MW	MAXIMUM THERMAL NEUTRON FLUENCE RATE/cm <sup>2</sup> -s	FILTERED BEAMS	METHODS USED FOR EVALUATING NEUTRON INTENSITIES AND SPECTRA	MAIN APPLICATIONS	ADDITIONAL COMMENTS
Materials Testing Reactor, Idaho Falls, USA	Tank, 93%, light water	40	$5 \times 10^{14}$	scandium iron silicon	Proton recoil spectrometry at 24 keV and 144 keV. Time-of-flight spectrometry at 2 keV 24 keV	standard cross-section measurements radiography shielding studies Doppler effect studies biological irradiations	Reactor closed down in 1970 and filters transferred to the NBSR
National Bureau of Standards Reactor, Gaithersburg, USA	Tank, 90%, heavy water	10	$1 \times 10^{14}$	scandium iron silicon	Proton recoil spectrometry at 25 keV and 144 keV. Boron-10 trifluoride counter at 2 keV and 25 keV	personal dosimetry cross-section measurements spectrometer calibrations shielding studies	Filtered beams provide neutron standards at NBS Filter installed in through-tubes with manganese and graphite reflectors
Missouri University Research Reactor, Columbia, USA	Pool, 93%, light water	10	$7 \times 10^{13}$	iron silicon oxygen uranium	Proton recoil spectrometry	radiography and tomography Doppler broadening measurements	Facility built into 'F' beamport providing easy interchange of filters. Scandium filter in preparation
High Flux Beam Reactor, Upton, USA	Tank, 90%, heavy water	40	$7 \times 10^{14}$	scandium iron iron-56	Proton recoil spectrometry Boron-10 trifluoride counter	cross-section measurements neutron capture gamma-ray experiments	Filters inserted in a 4-position rotary collimator in H18 beam channel. Epithermal neutron flux in H1 beam tube is $3 \times 10^{13}$ cm <sup>-2</sup> s <sup>-1</sup> per unit lethargy
APSARA, Trombay India	Pool, 46%, light water	1	$2 \times 10^{13}$	iron	Proton recoil spectrometry and activation of indium foil	neutron capture gamma-ray experiments	Filters transferred to 40 MW CIRUS reactor
R2 Research Reactor, Studsvik, Sweden	Tank, 90%, light water	50	$3 \times 10^{14}$	iron	Proton recoil spectrometry	medical and biological studies	Filter installed in a rotary collimator
High Flux Reactor, Petten, Holland	Tank, 90%, light water	30	$1 \times 10^{14}$	iron	Intensity measurements by gold foil activation	neutron capture gamma-ray experiments	Filter installed in rotary collimator in the "large facility". Scandium filter proposed
First Atomic Power Station, Obninsk, USSR	Pressurised water, 6%, graphite	30	$8 \times 10^{13}$	scandium iron silicon	Proton recoil spectrometry	neutron capture gamma-ray experiments neutron cross-section measurements	
Forschungs-und Messreaktor, Braunschweig, Germany	Pool, 90%, light water	1	$1 \times 10^{13}$	scandium iron	Proton recoil spectrometry	health physics instrument calibrations	Scandium filter installed in a through-tube with manganese reflector
SM-2 Reactor, Dimitrovgrad, USSR	Tank, 90%, light water	75	$3 \times 10^{15}$	iron		neutron capture gamma-ray experiments	No details of neutron intensity or spectrum

TABLE 2  
Scandium Filtered Beams

REFERENCE	REACTOR	BEAM TUBE	BEAM TUBE DIAMETER/cm	DIAMETER OF BEAM /cm	QUOTED ENERGY /keV	LENGTH OF FILTER/cm		OTHER MATERIALS	NEUTRON INTENSITY /s <sup>-1</sup>	NEUTRON FLUX AT 2 keV /cm <sup>-2</sup> s <sup>-1</sup>	HIGH ENERGY NEUTRON CONTAMINATION	GAMMA-RAY DOSE-RATE /mR h <sup>-1</sup>	ADDITIONAL COMMENTS
						SCANDIUM	TITANIUM						
Simpson et al (1971)	NTR	HB-1; horizontal beam tube directed at core	15	2.5	210.7	107	1.4	-	$1 \times 10^7$	$5 \times 10^6$	0.4	<1	Cadmium ratio in beam tube < 4. Difference filter of 2.5 cm manganese and 1.6 cm of cerium used to evaluate background.
Kuzin et al (1973)	APS-1	horizontal channel entering core	5	2	210.7	71	1.5	0.2 cm boron-10		$5 \times 10^5$	0.15*	"practically none"	Measurements at 12 MW. *Values refer to difference beams, using a difference filter of 0.6 cm manganese.
Schwartz (1977)	NBSR	through-tube passing within 10 cm of core	11.4	1.75	2	110	1	manganese-aluminum scatterer	$6.5 \times 10^5$	$3 \times 10^5$	0.01	8	90 cm <sup>2</sup> , 3 mm thick manganese - aluminum scatterer located 2.38 m from scandium. Uncertainty on intensity measurements ± 5%. Beam diameter at 2.75 m is 4.25 cm and flux is $1.9 \times 10^5$ cm <sup>-2</sup> s <sup>-1</sup> .
Greenwood and Chrien (1976)	HFR	HB; tangential thimble tube	8.9	2.7 (square)	210.9	63 63	0 1.9	- 3	$1.1 \times 10^7$	$6.5 \times 10^6$ $2 \times 10^6$	0.10 0.09	340	Thermal neutron flux = $100$ cm <sup>-2</sup> s <sup>-1</sup> . Several additional filter materials investigated. Calculated and measured fluxes agreed within 20%.
Alberts and Knaut (1978)	FHRB	S5; horizontal tangential beam tube	14.8	13.5	2	71	1.5	manganese scatterer	$2.5 \times 10^5$ *	$1.6 \times 10^5$	2.21/0.15*	28/8*	10% uncertainty in flux estimated. *Values refer to difference beams, using a difference filter of 2.5 cm of manganese. 0.6 cm thick manganese scatterer located close to reactor core.

TABLE 3  
Iron-Aluminium Filtered Beams

REFERENCE	REACTOR	BEAM TUBE	BEAM TUBE DIAMETER/cm	DIAMETER OF BEAM /cm	QUOTED ENERGY /keV	LENGTH OF FILTER/cm			OTHER MATERIALS	NEUTRON INTENSITY /s <sup>-1</sup>	NEUTRON FLUX AT 24 keV /cm <sup>-2</sup> s <sup>-1</sup>	HIGH ENERGY NEUTRON CONTAMINATION	GAMMA-RAY DOSE-RATE /mR h <sup>-1</sup>	ADDITIONAL COMMENTS
						IRON	ALUMINIUM	SULPHUR						
Simpson et al (1971)	HFR	DB-2; inclined beam directed at core	5	10.2	24.5 ± 1.8	68	21	5.9	-	4 × 10 <sup>7</sup>	6 × 10 <sup>5</sup>	0.02	< 20	Beam diameter variable from 0.6 to 10.2 cm.
Broder et al (1971)	SM-2			2	25 ± 2.5	18	16	10	-			< 0.25		
Kuzin et al (1973)	APS-1	Horizontal beam tube entering core region	5	2	24.5 ± 10	30 30 30 21	0 7 15 15	0 2.8 2.8 2.8	- boron-10 boron-10 boron-10	*	2 × 10 <sup>4</sup> 1.5/1.2 × 10 <sup>4</sup> 1.0/0.8 × 10 <sup>4</sup> 2.0/1.6 × 10 <sup>4</sup>	0.82 0.43/0.09* 0.26/0.03* 0.34/0.06*		Measurements taken at 12 MW. *Difference beam measurements with 0.25 cm titanium as difference filter. Detectors located 5 m from core boundary.
Kondalah et al (1973)	APSARA	2; horizontal beam to be directed at core	13.6	5.6	25 ± 5	38	23	7.6	-	4.7 × 10 <sup>5</sup>	1.5 × 10 <sup>4</sup>	0.02	25	Boron, sulphur and aluminium absorbers used in absorption method for optimisation. Measurements taken at 400 kW.
McGarry and Schroder (1975)	NBSR	Vertical thimble entering core region		1	25 ± 2.5	30	35	0	boron-10 titanium scatterer		5 × 10 <sup>5</sup>	0.01	< 2	Titanium scatterer located at reactor end of beam tube; not in the best geometry.
Schwartz (1977)	NBSR	through-tube	10	2.5	24 ± 2	25	36	0	graphite scatterer		2 × 10 <sup>5</sup>			Intensity measurements taken with two types of detector agreed within 7%. Beam diameter at 225 cm is 6 cm and flux is 3.6 × 10 <sup>4</sup> cm <sup>-2</sup> s <sup>-1</sup>
Kyle (1980)	R2	H4; horizontal beam tube directed at core	15	3	24.5	25	39	7	-	5.7 × 10 <sup>6</sup>	10 <sup>6</sup>	0.035	< 120	Thermal flux = 600 cm <sup>-2</sup> s <sup>-1</sup>
Tsang and Brugger (1976)	HMRR	F; horizontal beam tube directed at core	10	3.8	24 ± 1.8 24 ± 1.6 24 ± 1.6	51 58 58	20 20 20	5.1 5.1 5.1	- - 5.1 cm lead	1.4 × 10 <sup>7</sup> 5.3 × 10 <sup>6</sup> 1.8 × 10 <sup>6</sup>	1.2 × 10 <sup>6</sup> 4.6 × 10 <sup>5</sup> 1.6 × 10 <sup>5</sup>	0.15 0.06 < 0.01	44 15 9	Measurements reported for many filter combinations. Detector located 50 cm from end of filter. Thermal flux = 20-850 cm <sup>-2</sup> s <sup>-1</sup> .
Greenwood and Chrien (1976)	HFRB	H1B; tangential thimble tube	8.9	2.7 (square)	24 ± 2.0	23	36	6.4	0.15 cm cadmium	9.3 × 10 <sup>6</sup>	1.3 × 10 <sup>6</sup>	0.02	40	Thermal flux = 50 cm <sup>-2</sup> s <sup>-1</sup> Calculated and measured fluxes agreed within 2%. Have also installed an iron-56 filter consisting of 11 cm of iron-56 and 78 cm of aluminium, producing a neutron intensity of 3.7 × 10 <sup>7</sup> s <sup>-1</sup> and a gamma-ray dose-rate < 1 mR h <sup>-1</sup> .
Alberts and Knauf (1978)	HMRB	S4; horizontal beam tube directed at "north" core	14.8	8.5	24.5	35	23	7.5	-	1.3 × 10 <sup>5</sup> *	3.2/2.1 × 10 <sup>3</sup>	0.08/0.01*	6/1*	20% uncertainty on flux measurements. Plateau width of beam = 4.5 cm. *Difference beam measurements using 0.5 cm of titanium.
Stecker-Kasamussen and Katynski (1979)	HFR	Large facility; horizontal radial beam tube	60	0.6 x2	24	30	21	6	-	10 <sup>6</sup>	10 <sup>5</sup>		"not high"	System nickel mirrors focusses neutron beam 5 m from reactor core. Filter positioned at end of focussing module.

TABLE 4  
Silicon Filtered Beams

REFERENCE	REACTOR	BEAM TUBE	BEAM TUBE DIAMETER/cm	DIAMETER OF BEAM/cm	QUOTED ENERGY /keV	LENGTH OF SILICON /cm	OTHER MATERIALS	NEUTRON INTENSITY /s <sup>-1</sup>	NEUTRON FLUX AT QUOTED ENERGY/cm <sup>-2</sup> s <sup>-1</sup>	NEUTRON CONTAMINATION	GAMMA-RAY DOSE-RATE /mR h <sup>-1</sup>	ADDITIONAL COMMENTS
Simpson et al (1971)	HTR	DB-2; inclined beam tube directed at core	5	10.2	144±30	102	10 cm lead 0.32 cm boron-10	10 <sup>9</sup>	10 <sup>7</sup>		500	Silicon filter inserted in iron collimator. No fast neutron contamination.
Kuzin et al (1977)	APS-1	horizontal beam tube entering core region	5	2	144±15	51	1.7 cm titanium 0.2 cm boron-10		8.0/4.0*10 <sup>4</sup>	0.12/0.04*		*Values refer to difference beams. Difference filters were 2.8 cm sulphur (for 144 keV) and 1.7 cm of titanium (for 55 keV). Measurements at 12 MW. Detectors located 5 m from core boundary.
					55±5	38	17 cm sulphur 0.2 cm boron-10		10 <sup>4</sup> *	0.25*		
Schwartz (1979)	NBSR	through-tube	10	2.5	143	136	2 cm titanium graphite scatter		4.5x10 <sup>5</sup>	0.015	40	Silicon filter opposite end of through-tube as iron filter. At 2.25 m, beam diameter is 4.5 cm and flux is 1.4x10 <sup>5</sup> cm <sup>-2</sup> s <sup>-1</sup> .
Tsang and Brugger (1976)	MURR	F; horizontal tube directed at core	10	3.8	144±25	211	-	1.1x10 <sup>7</sup>	9.3x10 <sup>5</sup>	≤ 0.01	1200	Measurements repeated for many filter combinations. The neutron contamination is essentially all from thermal neutrons. Detector located 50 cm from end of filter.
					144±22	211	10.2 cm lead	3.7x10 <sup>5</sup>	1.3x10 <sup>4</sup>	> 0.36	180	
					144±22	211	10 cm lead	2.5x10 <sup>5</sup>	2.2x10 <sup>4</sup>	0.16	15	
					144±28	211	0.2 cm cadmium	2.8x10 <sup>7</sup>	2.5x10 <sup>6</sup>	0.01	1500	
						153	-					

TABLE 5

The Uranium Filtered Beam at the MURR (Royer and Brugger, 1977)

BEAM TUBE	BEAM TUBE DIAMETER/cm	DIAMETER OF BEAM/cm	QUOTED ENERGY /eV	LENGTH OF FILTER/cm				NEUTRON INTENSITY /s <sup>-1</sup>	NEUTRON FLUX AT 186 eV /cm <sup>-2</sup> s <sup>-1</sup>	HIGH ENERGY NEUTRON CONTAMINATION	GAMMA-RAY DOSE-RATE /mR h <sup>-1</sup>	THERMAL NEUTRON FLUX/cm <sup>-2</sup> s <sup>-1</sup>	ADDITIONAL COMMENTS
				URANIUM	SELENIUM	MANGANESE	GERMANIUM						
F; horizontal beam tube directed at core	10	2.7	186±1.9	21.6	-	-	-	1.8x10 <sup>7</sup>	3.1x10 <sup>6</sup>	0.80	38	850	Beam purity determined using 0.25 cm tungsten difference filter.
			186±1.5	43.2	-	-	-	4.1x10 <sup>6</sup>	7.2x10 <sup>5</sup>	0.54	7.5	180	
			186±1.5	43.2	0.23	0.90	0.32	1.9x10 <sup>6</sup>	3.3x10 <sup>5</sup>	0.32	7.5	130	

TABLE 6

The Oxygen Filtered Beam at the MURR (Koeppe and Brugger, 1980)

BEAM TUBE	BEAM TUBE DIAMETER /cm	DIAMETER OF BEAM /cm	QUOTED ENERGY /MeV	LENGTH OF FILTER/cm			NEUTRON INTENSITY /s <sup>-1</sup>	NEUTRON FLUX AT 2.35 MeV /cm <sup>-2</sup> s <sup>-1</sup>	NEUTRON CONTAMINATION	GAMMA-RAY DOSE-RATE /mR h <sup>-1</sup>	THERMAL NEUTRON FLUX /cm <sup>-2</sup> s <sup>-1</sup>	ADDITIONAL COMMENTS
				LIQUID OXYGEN	URANIUM	BISMUTH						
F; horizontal beam tube directed at core	10		2.35±0.1	91.5	-	-	5.9x10 <sup>6</sup>	1.1x10 <sup>6</sup>	0.15	> 10000	< 150	Filters placed just outside end of beam tube.
				183	-	-	2.1x10 <sup>6</sup>	3.6x10 <sup>5</sup>	0.02	< 1000	< 100	
				183	-	8	4.9x10 <sup>5</sup>	8.5x10 <sup>4</sup>	0.02	< 25	< 100	
				183	4	-	4.9x10 <sup>5</sup>	8.5x10 <sup>4</sup>	0.02	< 25	< 100	



TABLE 7  
Accelerator-Based Filtered Beams

REFERENCE	ACCELERATOR	FILTER	FLIGHT PATH	ADDITIONAL COMMENTS
Harvey (1972)	ORELA 140 MeV electrons	10 cm and 24 cm of iron	80 m and 200 m	Filters placed 8 metres from photoneutron target.
Liou et al (1978)	RPI 70 MeV electrons	10 cm of scandium	28 m	
Liou et al (1979)	RPI	20 cm of iron	28 m	
Block et al (1975)	KUR 46 MeV electrons	30 cm of iron	22 m	20 cm of filter placed at 1 m and further 10 cm of filter placed at 12 m.
Yamamuro et al (1978)	KUR	15 cm of iron	12 m	5 cm of filter placed at 2.5 m and further 10 cm of filter placed at 7 m.
Kobayashi et al (1977)	KUR	57 cm of silicon	22 m	

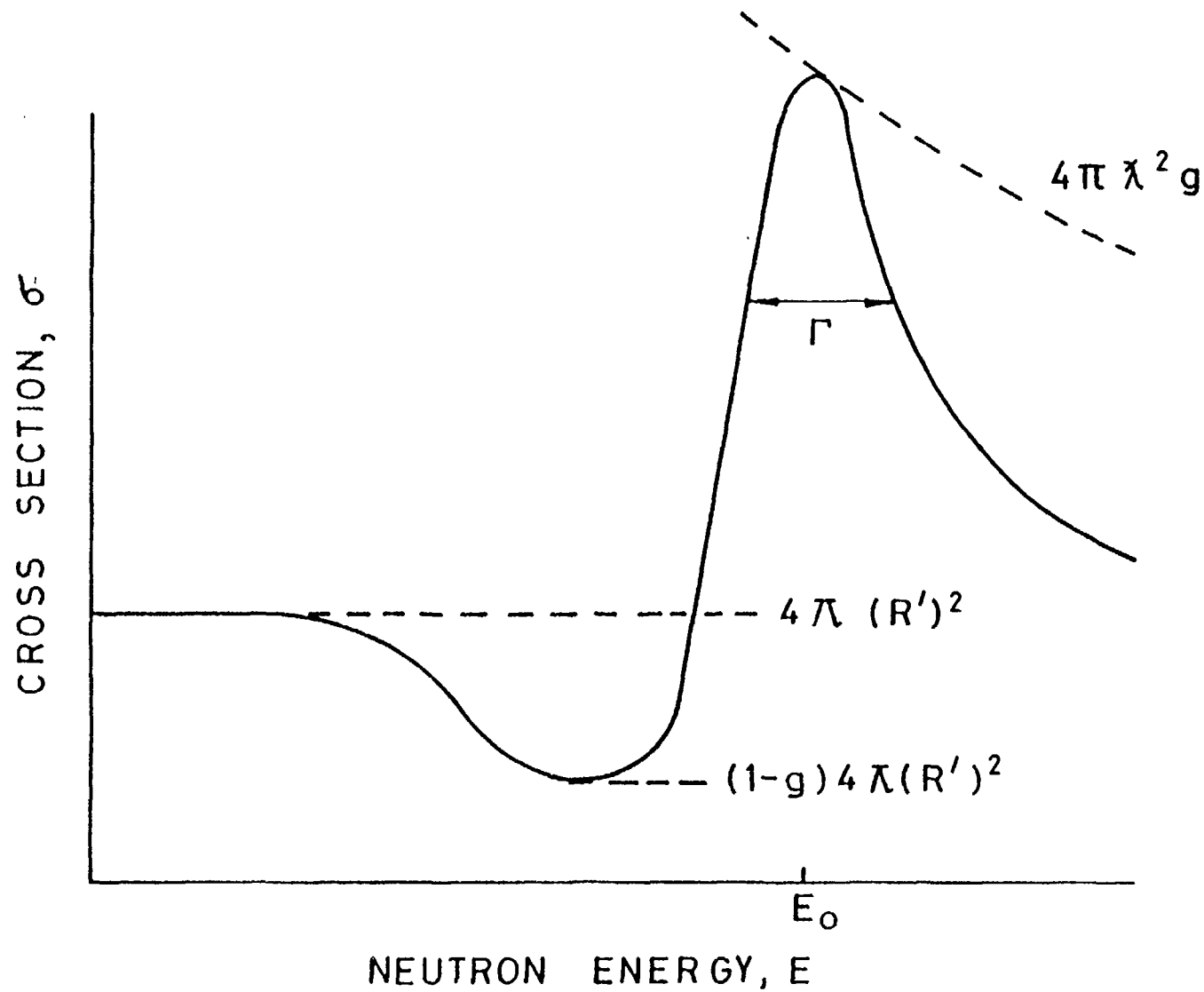


FIGURE 1. CROSS SECTION FOR S-WAVE NEUTRONS NEAR AN ELASTIC SCATTERING RESONANCE.

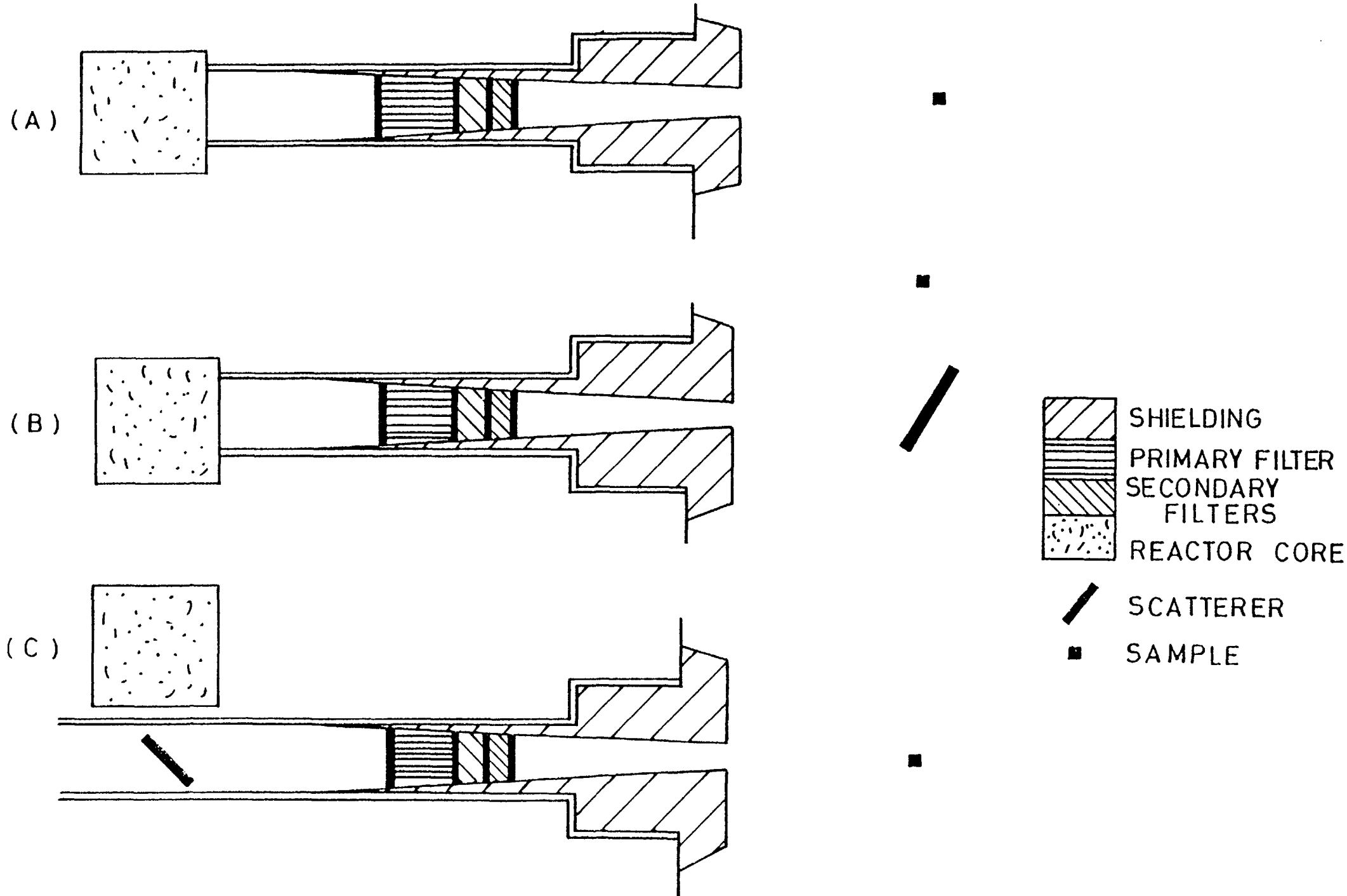


FIGURE.2. TYPICAL LAYOUTS FOR FILTERED BEAM FACILITIES.

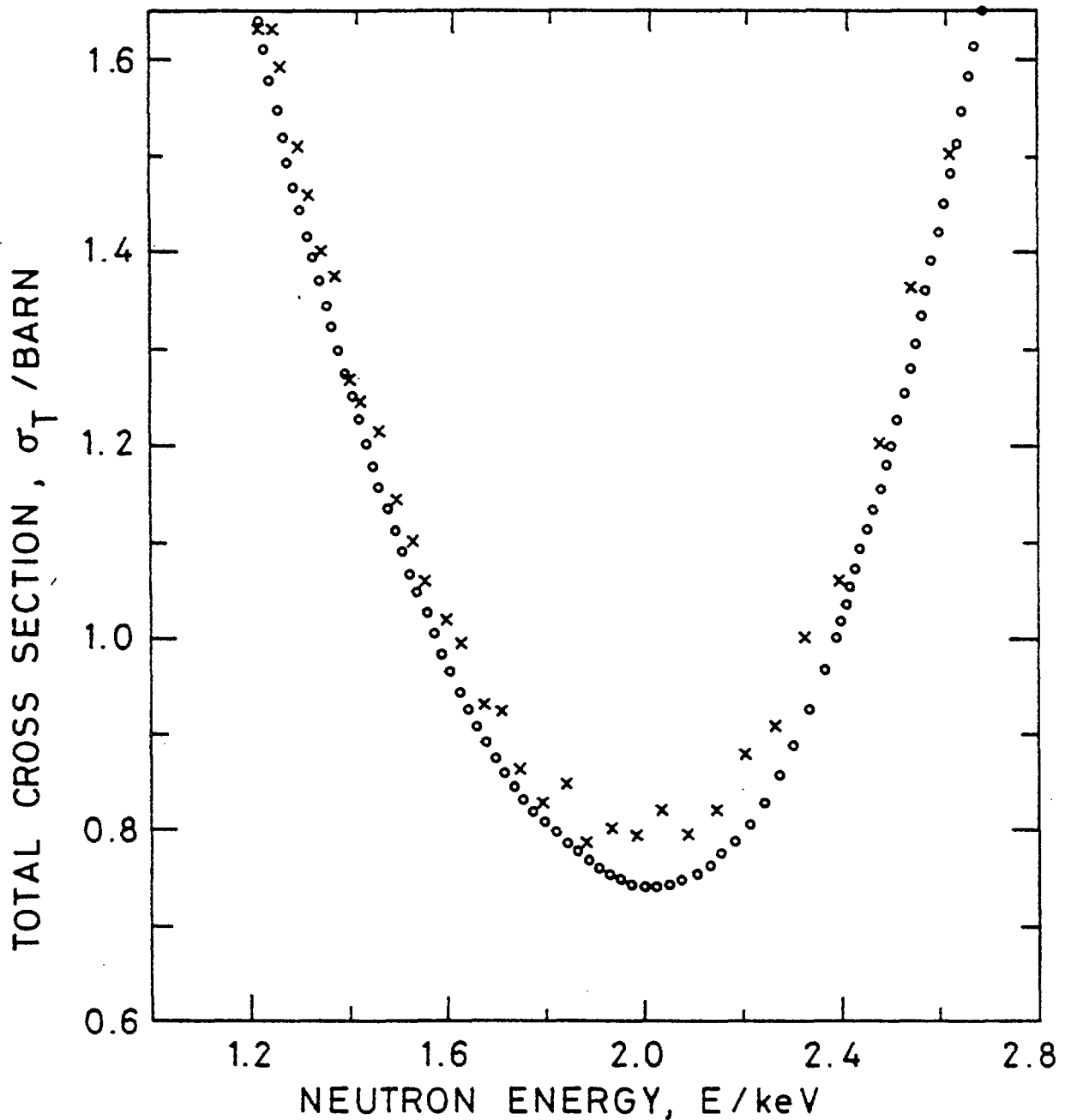


FIGURE 3. SCANDIUM TOTAL CROSS-SECTION  
NEAR THE 2keV MINIMUM FOR TWO  
INDEPENDENT MEASUREMENTS MADE  
AT THE HFBR ( x ) AND AT THE RPI ( o )  
( AFTER LIOU ET AL, 1978 )

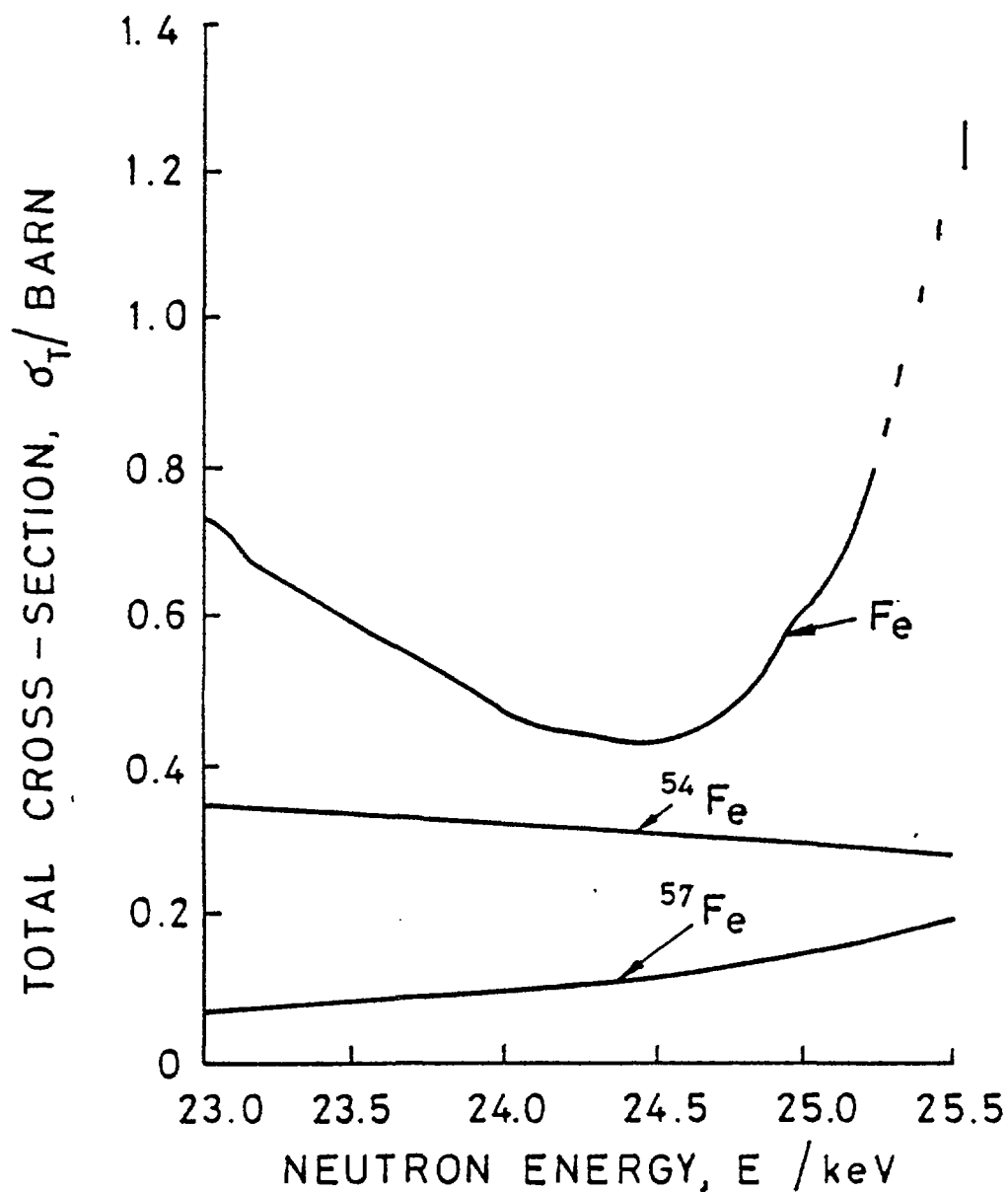


FIGURE 4. THE TOTAL CROSS-SECTION OF IRON AT THE 24.5 keV WINDOW SHOWING THE CONTRIBUTION OF THE IRON-54 AND IRON-57 ISOTOPES (AFTER HARVEY 1972).

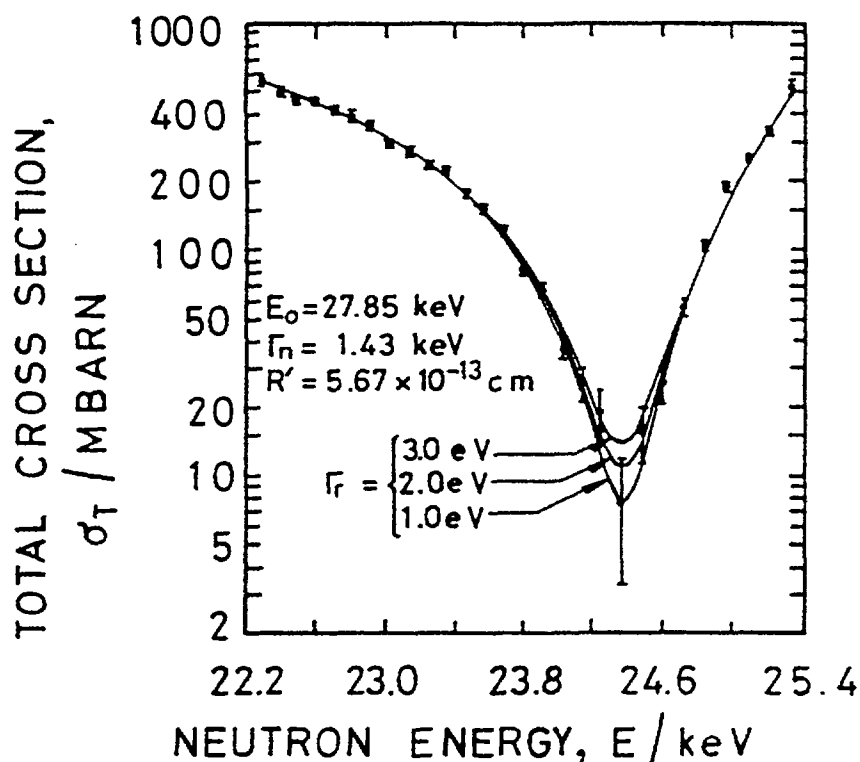


FIGURE.5. THE TOTAL CROSS SECTION OF IRON-56 NEAR THE 24.37 keV MINIMUM. THE CURVES SHOW THE BEST FITS FOR THREE DIFFERENT RADIATION WIDTHS (AFTER LIOU ET AL, 1979).

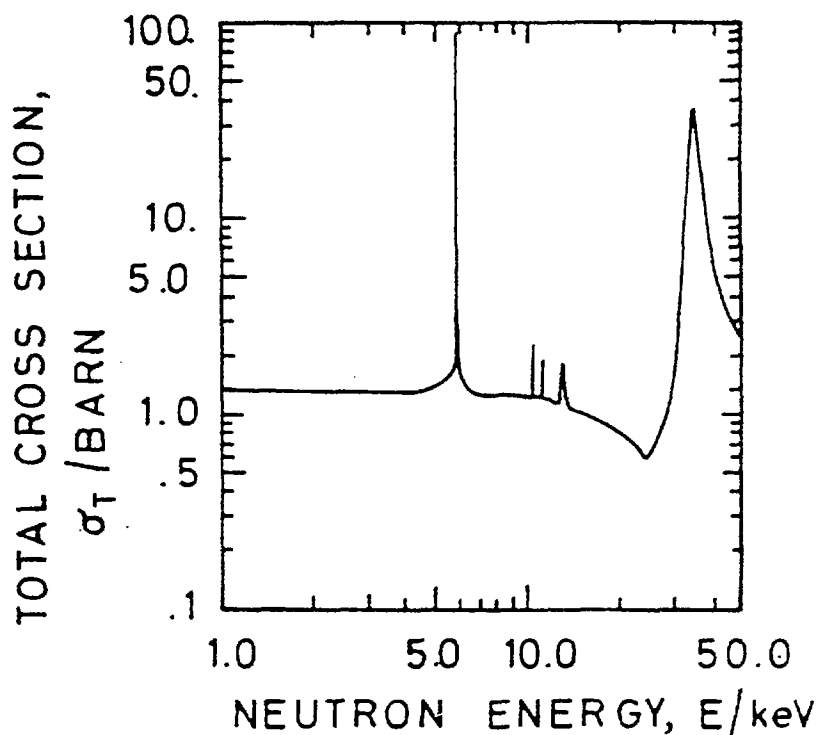


FIGURE.6. THE TOTAL CROSS-SECTION OF ALUMINIUM (AFTER GARBER AND KINSEY, 1976.)

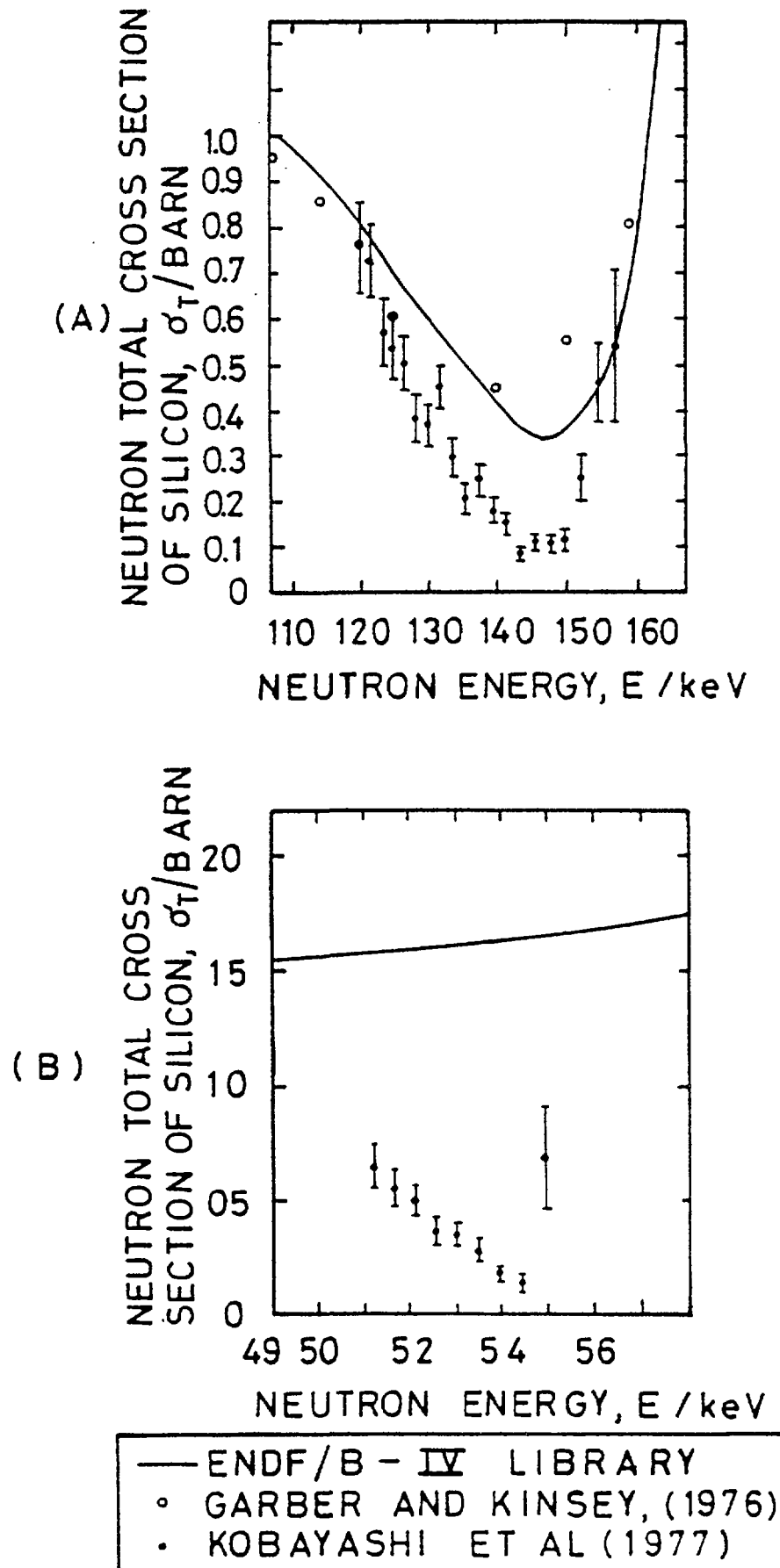


FIGURE .7. THE TOTAL CROSS - SECTION OF SILCON  
 NEAR THE MINIMA AT 147 keV AND  
 54.5 keV ( AFTER KOBAYASHI ET AL,  
 1977. )

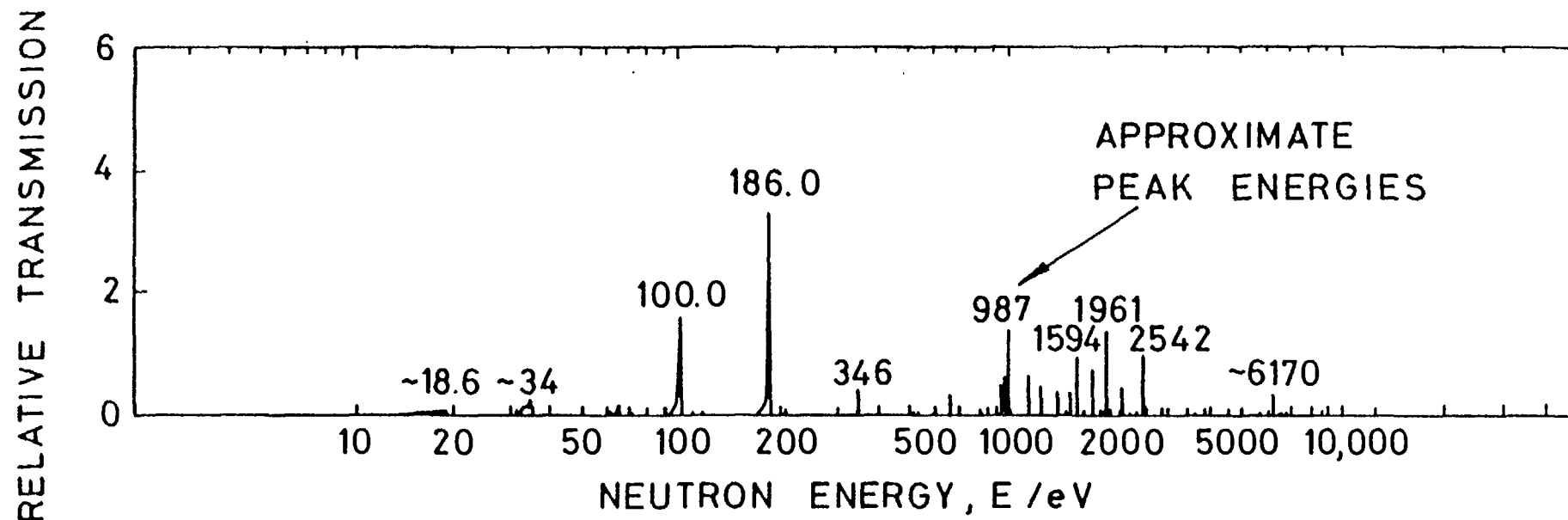


FIGURE.8. THE TRANSMISSION OF NEUTRONS THROUGH URANIUM



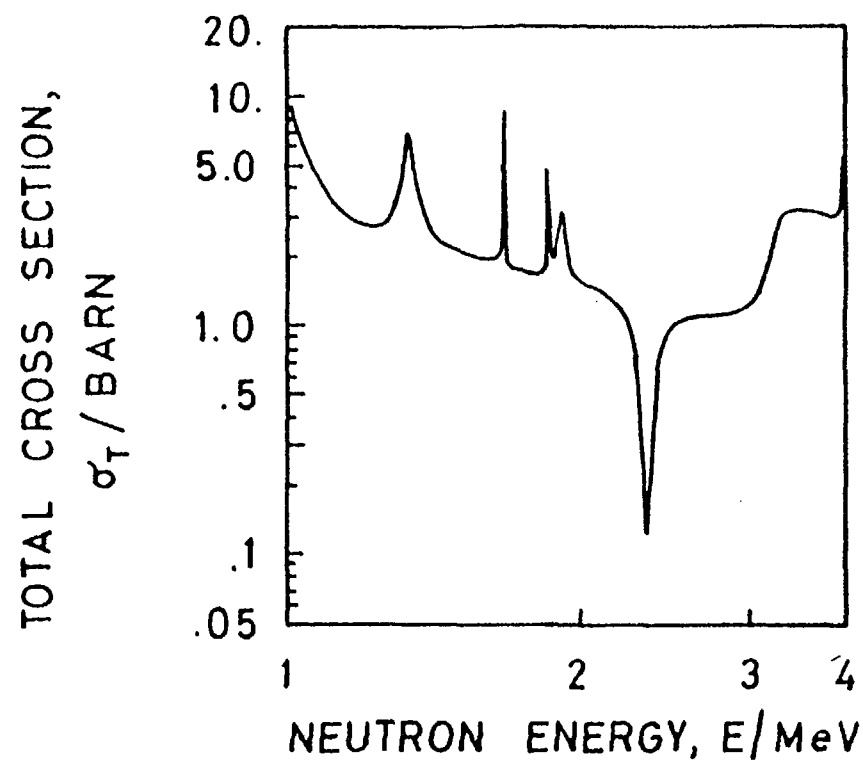


FIGURE.9. THE TOTAL CROSS-SECTION OF OXYGEN  
( AFTER GARBER AND KINSEY, 1976 )

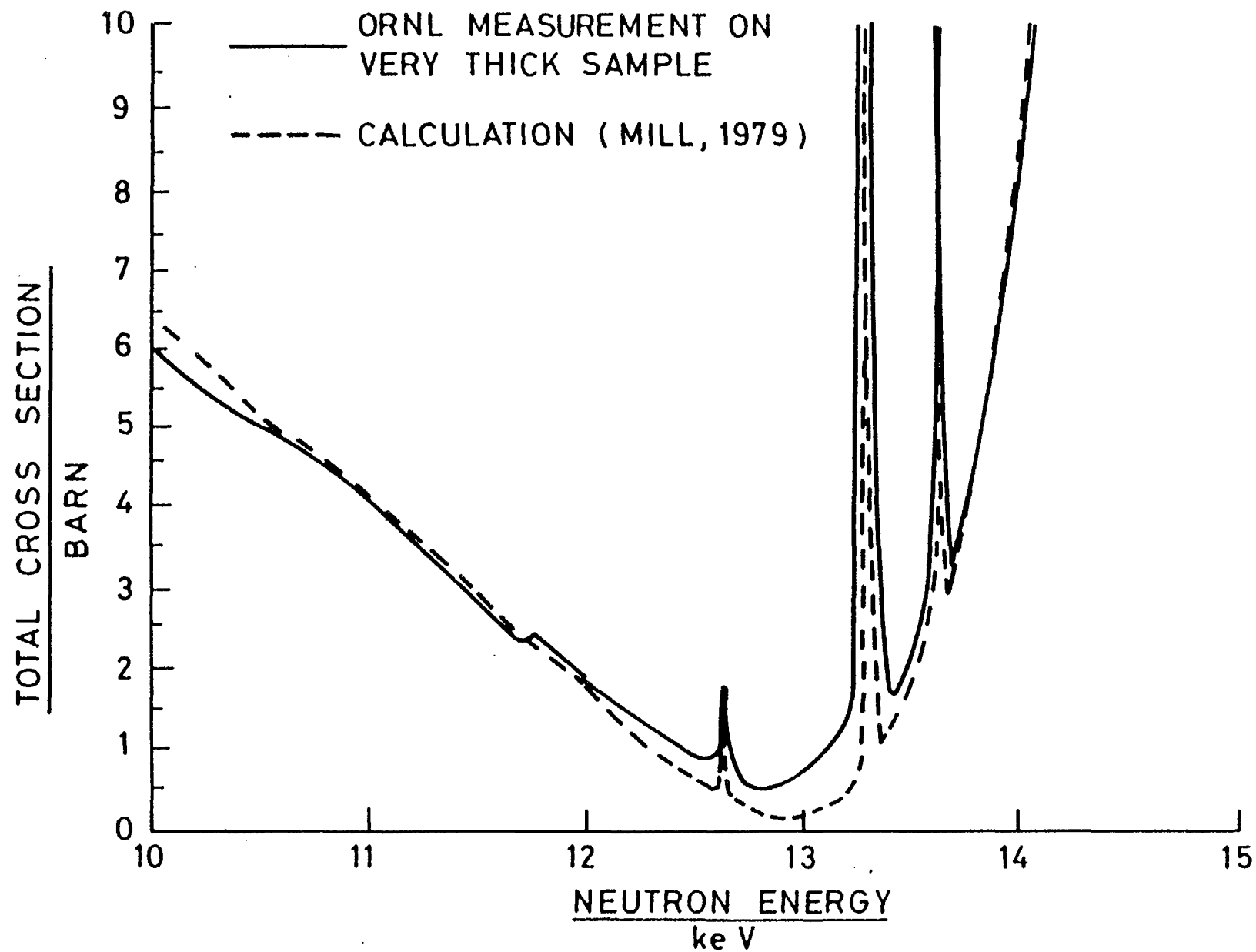


FIGURE 10. THE CROSS-SECTION OF NICKEL-58 IN THE REGION  
OF THE 12 keV WINDOW

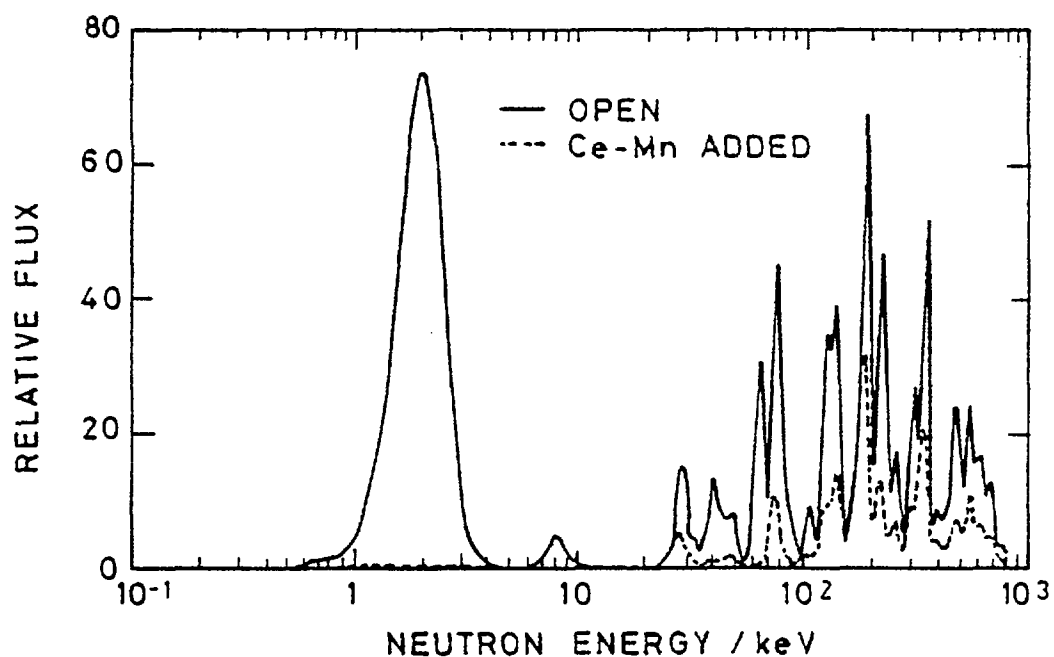


FIGURE 11. TRANSMISSION OF NEUTRONS THROUGH THE MTR SCANDIUM FILTER. ( BRUGGER & SIMPSON , 1973 )

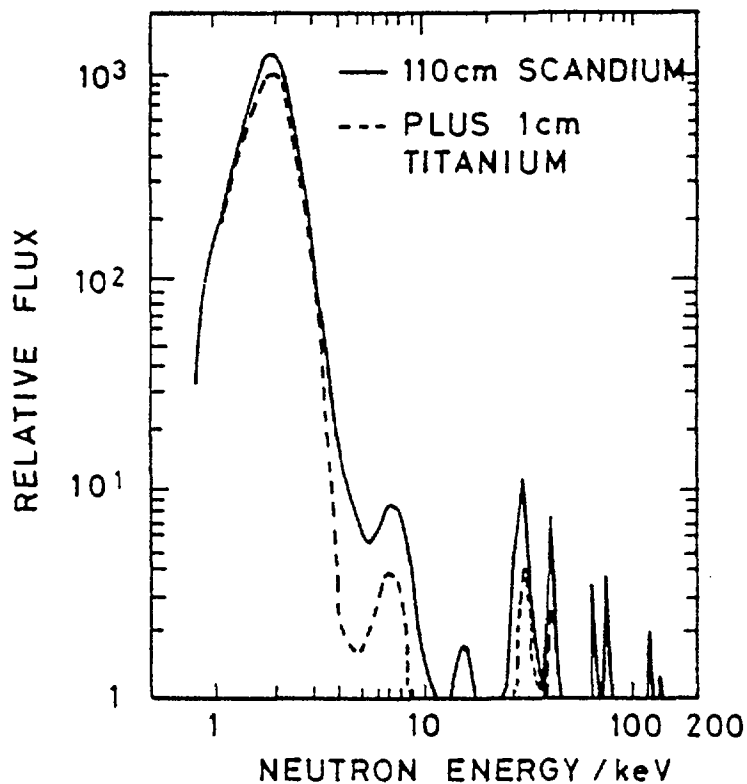


FIGURE 12. THE NEUTRON SPECTRUM THROUGH THE NBS SCANDIUM FILTER ( SCHWARTZ, 1977 )

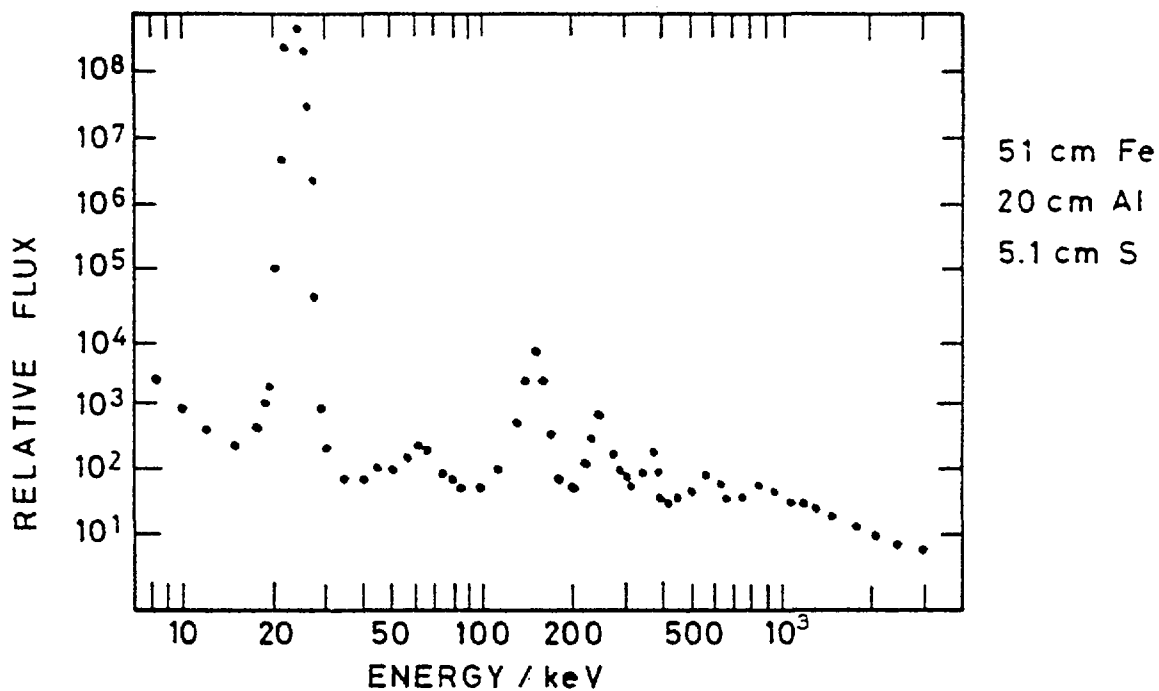


FIGURE 13. NEUTRON SPECTRUM THROUGH THE IRON FILTERED BEAM AT THE MURR ( TSANG & BRUGGER, 1976 )

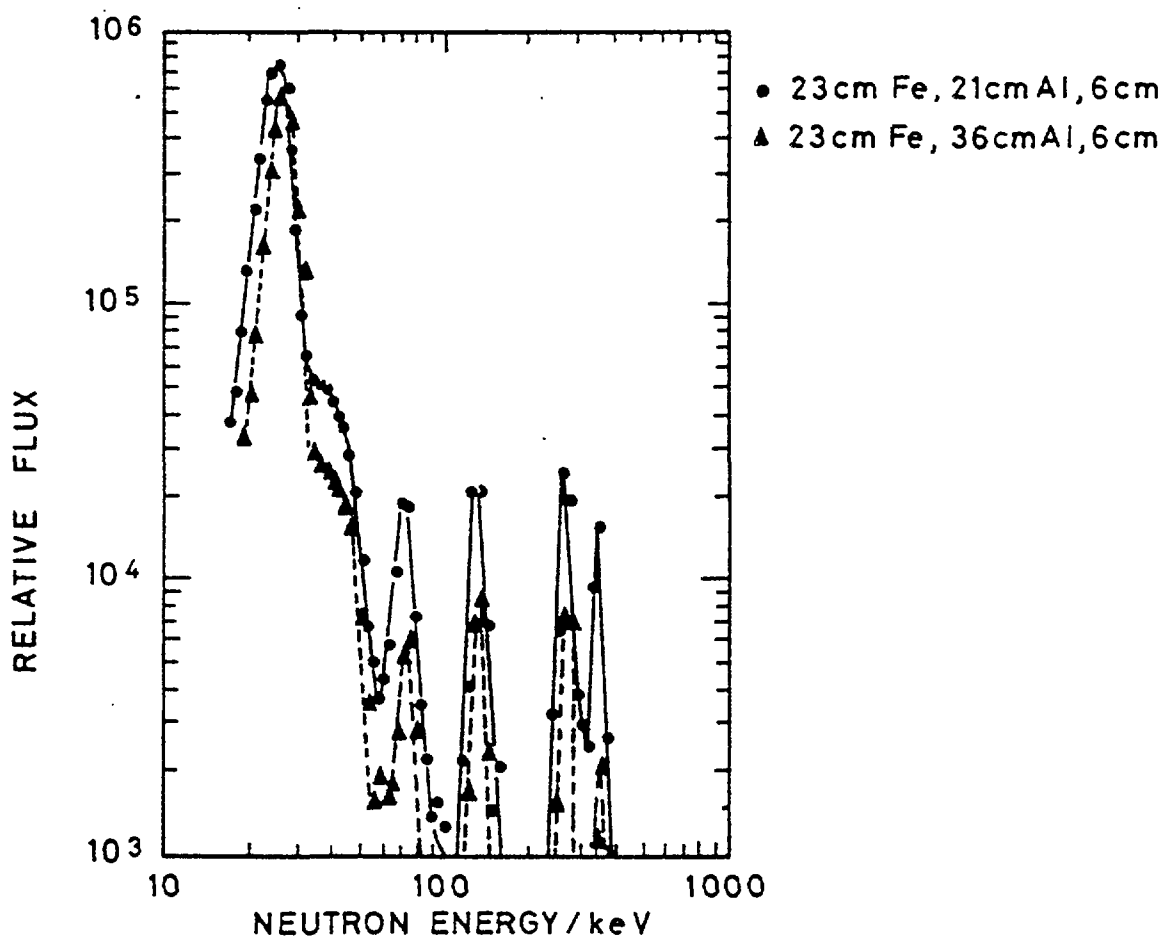


FIGURE 14. NEUTRON SPECTRUM THROUGH THE IRON FILTERED BEAM AT THE HFBR ( GREENWOOD & CHRIEN, 1976 )

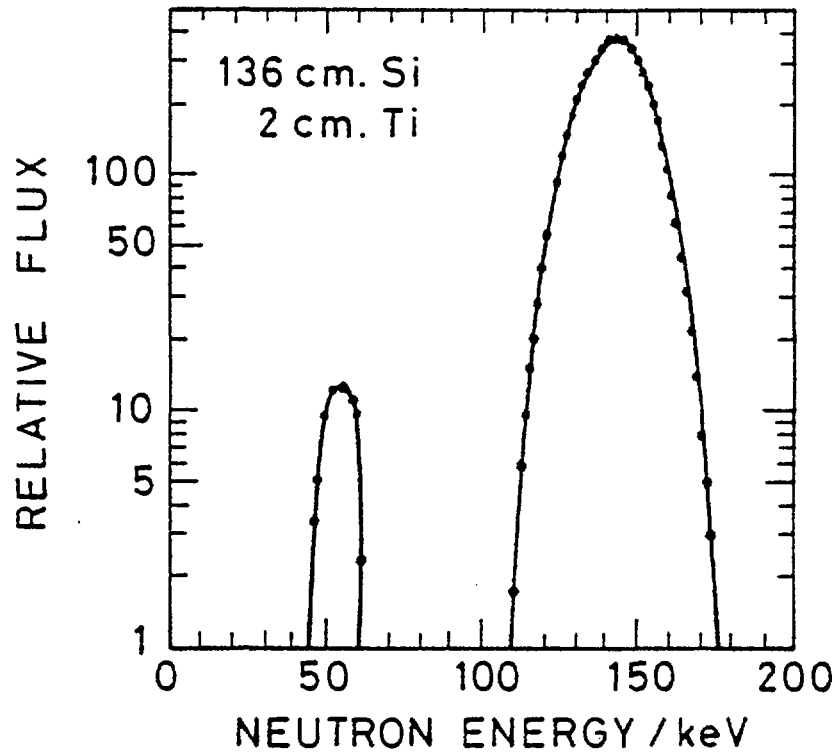


FIGURE 15. NEUTRON SPECTRUM THROUGH THE SILICON FILTER AT THE NBSR(SCHWARTZ, 1977)

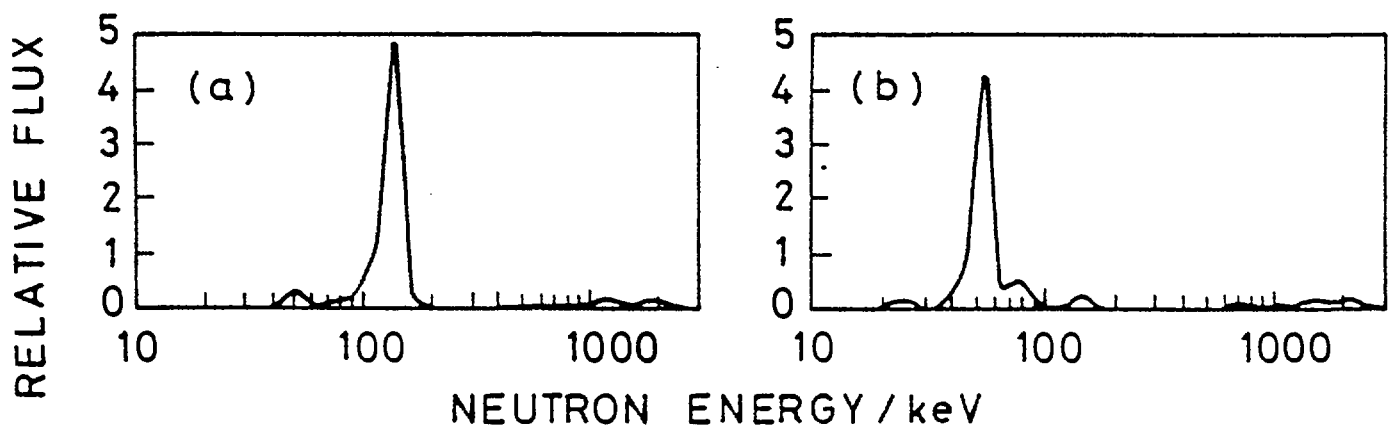


FIGURE 16. NEUTRON SPECTRUM THROUGH THE SILICON FILTERS AT THE APS-1 (KUZIN ET AL, 1973)  
(a) 51 cm Si, 1.7 cm Ti.  
(b) 38 cm Si, 17 cm S.

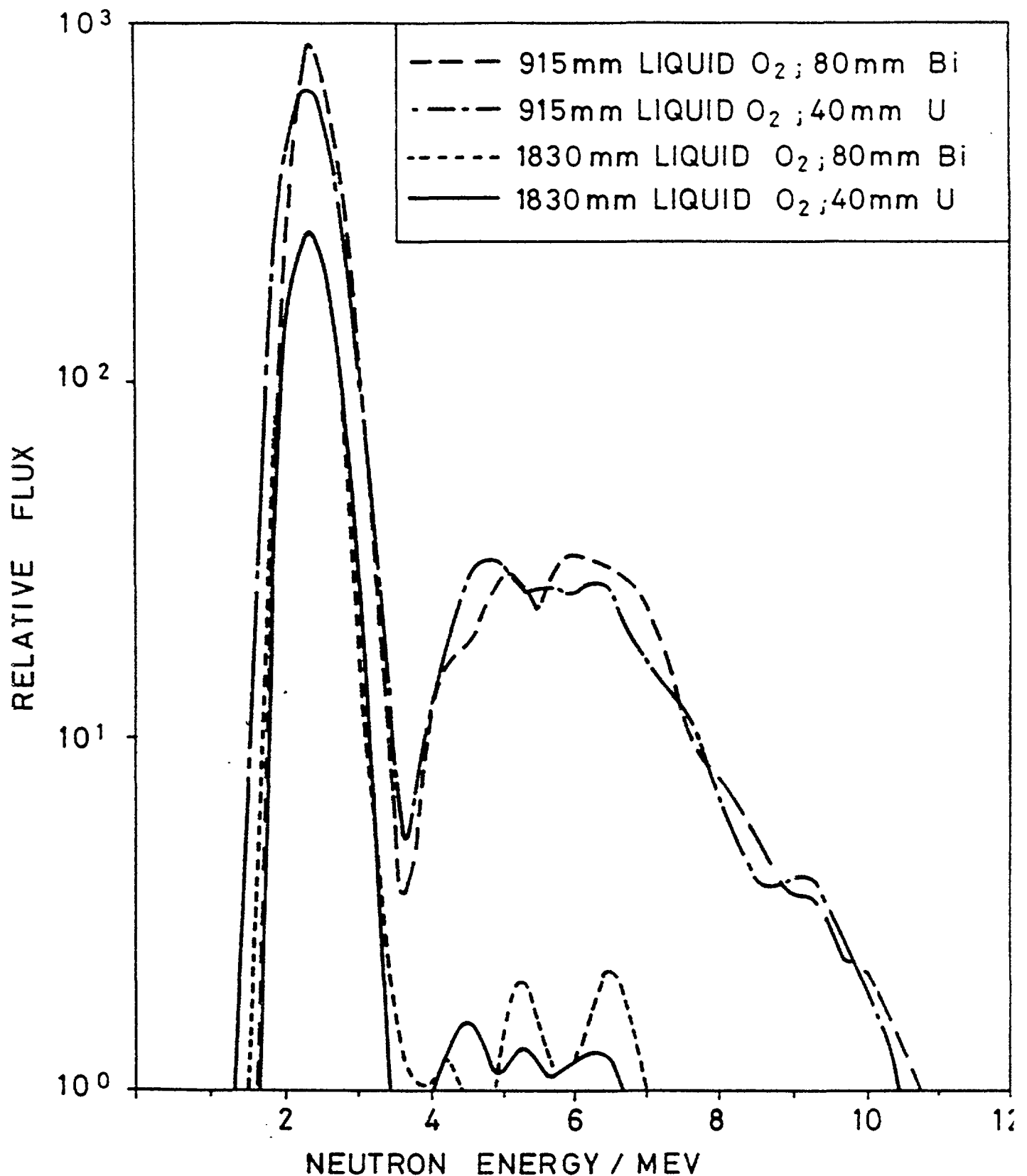


FIGURE 17. THE NEUTRON SPECTRUM THROUGH THE OXYGEN FILTERED BEAM AT THE MURR. ( KOEPPE & BRUGGER, 1980 )

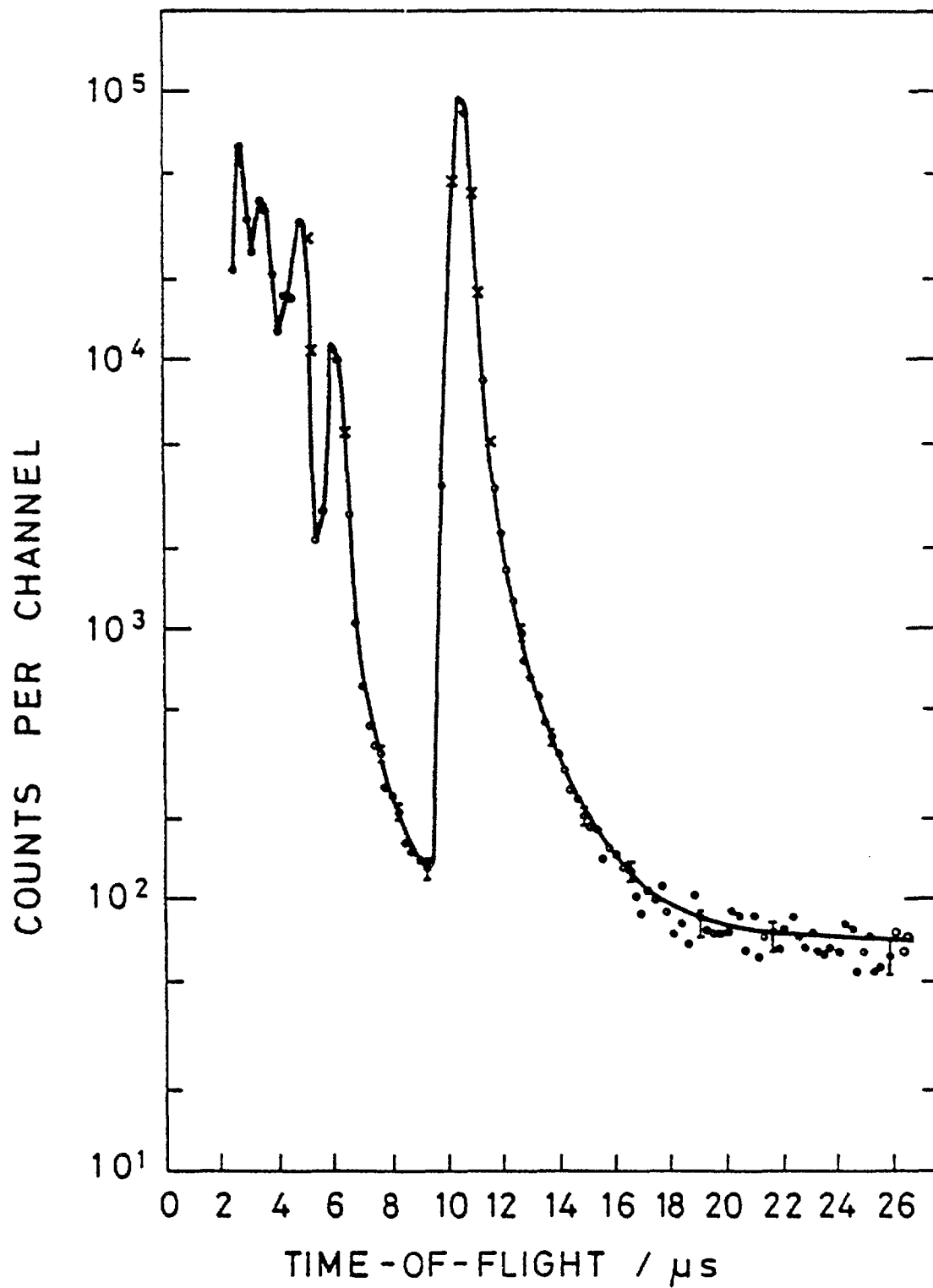


FIGURE 18. THE COUNTING SPECTRUM FOR  
THE IRON FILTERED BEAM AT THE  
KUR (BLOCK ET AL, 1975 )

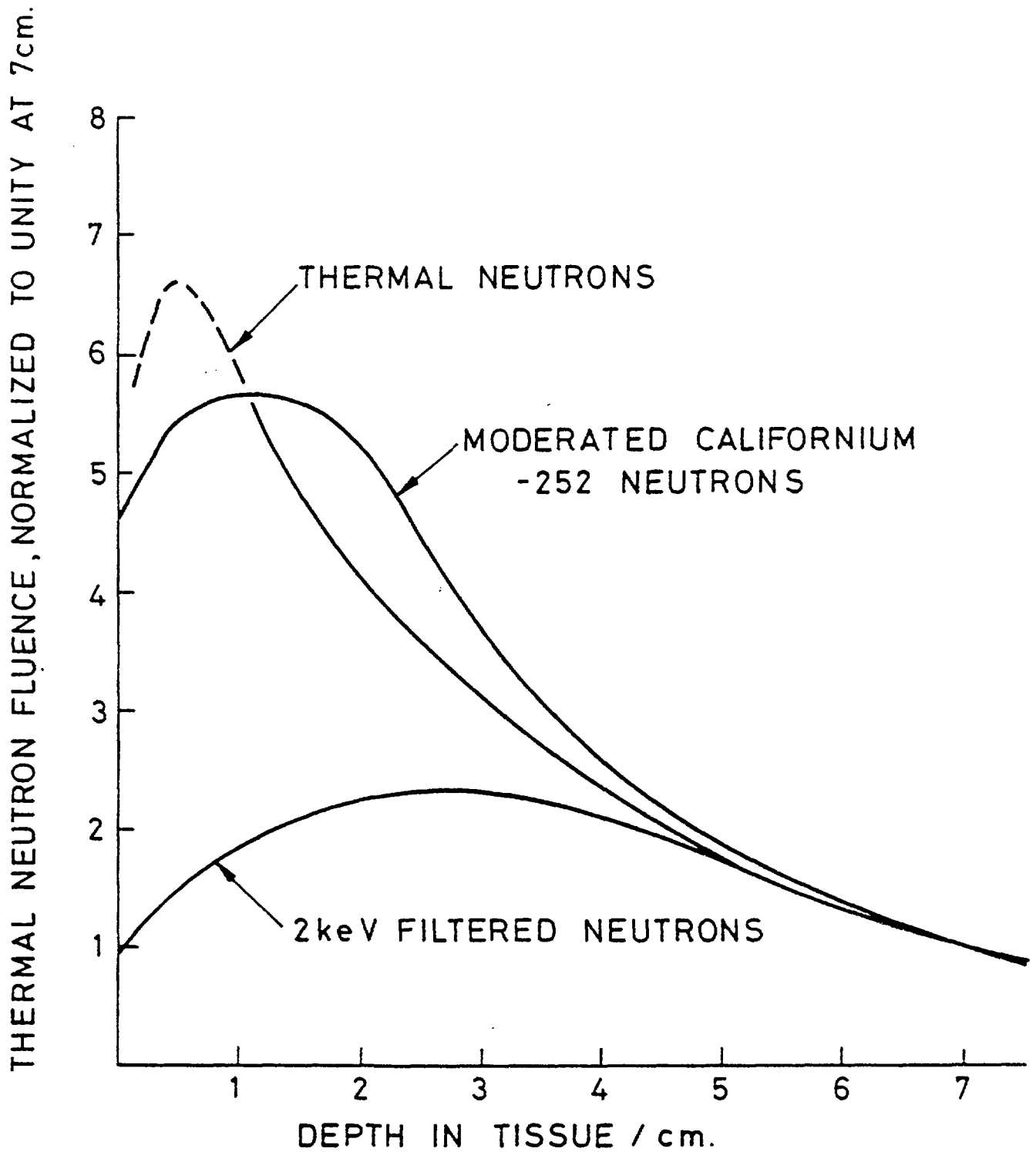


FIGURE 19. FLUENCE VERSUS DEPTH FOR VARIOUS NEUTRON SOURCES



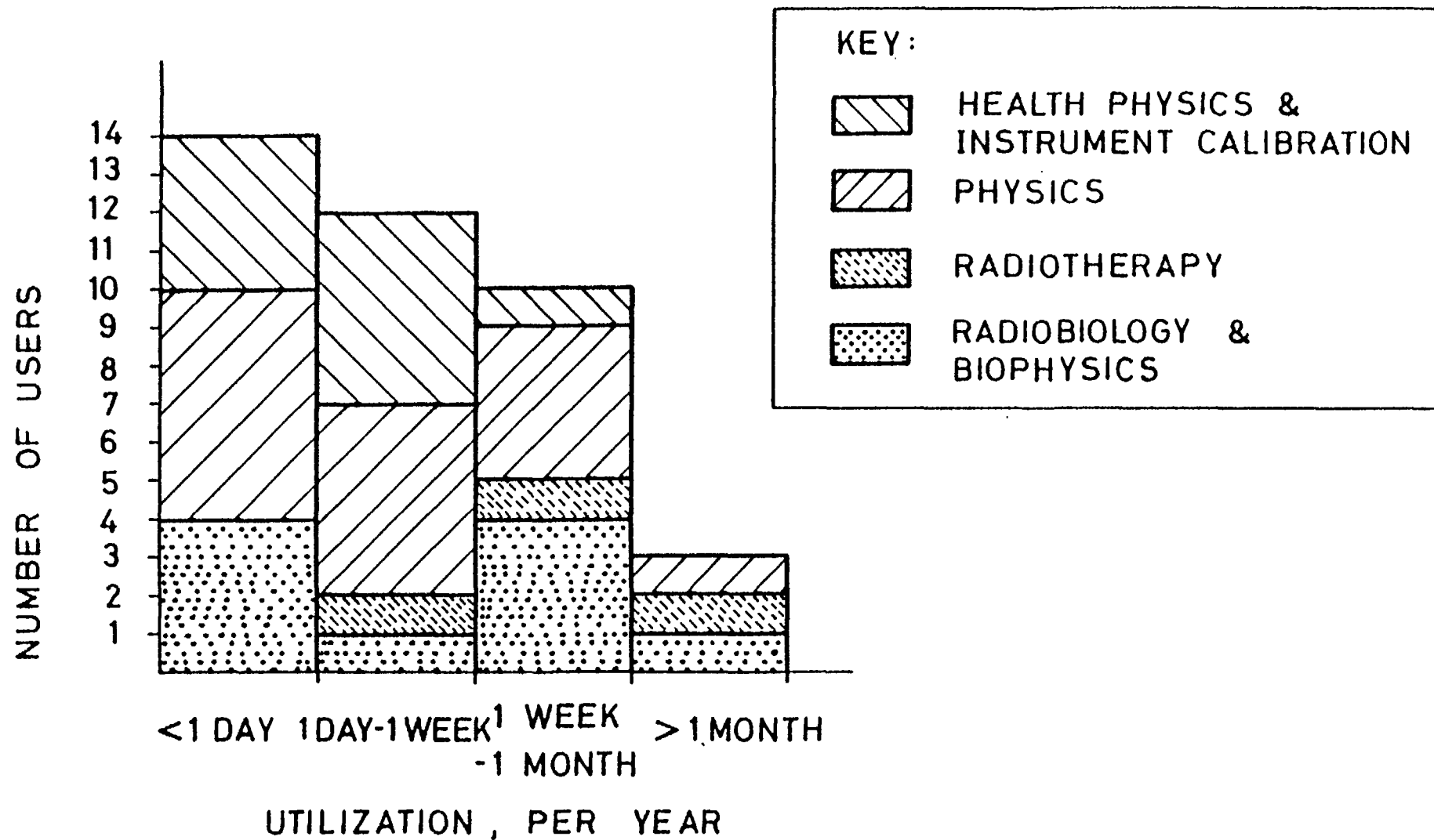


FIGURE. 20. POTENTIAL UTILIZATION OF A PROPOSED FILTERED BEAM FACILITY IN EUROPE.

Production of Fast Monoenergetic Neutrons by Charged Particle Reactions among the Hydrogen Isotopes. Source properties, experimental techniques and limitations of the data.

M. Drosig

University of Vienna, Institut für Experimentalphysik,  
A-1090 Wien, AUSTRIA and  
Los Alamos Scientific Laboratory, Los Alamos, N.M.87545, USA

#### Abstract

All five reactions  $^2\text{H}(\text{d},\text{n})^3\text{He}$ ,  $^1\text{H}(\text{t},\text{n})^3\text{He}$ ,  $^3\text{H}(\bar{\text{p}},\text{n})^3\text{He}$ ,  $^3\text{H}(\text{d},\text{n})^4\text{He}$  and  $^2\text{H}(\text{t},\text{n})^4\text{He}$  are discussed with special emphasis on recent developments and on the higher neutron energy range up to 40 MeV. It is discussed how inclusion of recent data will change previous evaluations of the p-T system at lower energies. Breakup data of all reactions are collected. Experimental techniques and uncertainties of neutron source property measurements are discussed and recommendations for future work are given.

#### I. Introduction.

Neutron producing reactions among the hydrogen isotopes are not only of interest for fusion applications but also as sources of monoenergetic neutrons. Properties of these neutron sources are important for many applications, e.g. neutron dosimetry, calibration of neutron detector efficiencies or simply as source of neutrons. Previous evaluations were limited to 10 MeV <sup>1)</sup> and 20 MeV <sup>2)</sup> respectively. During the last years it became apparent that radiation damage experiments and medical therapy require cross sections for neutron energies up to about 40 MeV <sup>3)</sup> and consequently neutron sources in this energy range as well.

Because some applications require "clean" monoenergetic sources neutron background accompanying neutron sources is very important. Therefore the abundance of background neutrons is an important source property, especially at higher energies.

The present work extends the previous evaluation <sup>2)</sup> to higher neutron energies. In addition, the impact of several recent papers 4-6) on the low energy evaluation <sup>1)</sup> is shown. Special emphasis is laid on the measurement methods and background neutrons.

## II. Measurement Methods

Monoenergetic neutron production by the hydrogen isotopes and the associated particle method for neutron flux determinations are closely connected. Although this method has been known for about 30 years <sup>7)</sup> and has been reviewed only recently <sup>8)</sup> the close connection with monoenergetic neutron production makes it mandatory to deal with it here. Furthermore I want to include one more method which seems to have been overlooked among the associated particle methods.

The associated particle methods are based on the fact that for each neutron produced in a monoenergetic neutron source reaction there will be a charged partner with uniquely determined kinematic properties. Because charged particles can be detected with 100% efficiency and neutrons generally not, neutron fluxes can be measured absolutely by counting the associated charged particles.

A straight application of this method is the so called time uncorrelated associated particle method. In this method the associated charged particles are collimated and counted in a detector. From this yield the neutron flux for the corresponding neutron angle is calculated. Accurate measurements of the effective solid angles for both the neutron detector and the charged particle collimator are vital. In addition the angles of both detectors are critical.

In the time correlated method individual reaction partners are identified by their correlation in time. Therefore this method depends on good timing characteristics of both detectors. The associated neutron cone determined by the solid angle of the charged particle detector must be smaller than the neutron detector. Thus solid angles need not be known. Only the correct angular alignment of the neutron detector remains vital, making sure that all of the neutron cone goes through the sensitive volume of the detector. (Uniformity of the detector is essential!) In addition, this method allows discrimination against background, because neutron background events will not have a time correlated associated charged particle of the right kind, energy and angle.

Thus monoenergetic neutron beams can be produced electronically. There are two major drawbacks of the time correlated method: The counting rate and hence the neutron flux is limited by chance coincidences and the neutron detector cannot be used with its full aperture but only spotwise. Therefore additional uncertainties will occur when the efficiency of all of the detector must be determined. Nevertheless this method proved successful in calibrating a neutron detector between 2 and 25 MeV within  $\pm 2\%$  <sup>9)</sup>.

One other major drawback of any associated charged particle method is that it cannot be applied to neutron production at  $0^\circ$ . Neutron production at  $0^\circ$  is, however, very desirable: usually the differential production cross section is forward peaked, has at  $0^\circ$  only a small dependence on angle and the neutrons are unquestionably unpolarized; besides the neutron energy is highest at  $0^\circ$ .

Our concern here is not so much the absolute measurement of neutron fluxes and calibration of neutron detectors - although they have some bearing on our subject as well - but the status of neutron source properties. And to my knowledge there are no published measurements on differential neutron production cross sections using the time correlated or uncorrelated method.

However a different type of associated particle method has been applied for neutron production measurements for some time <sup>2)</sup>. This method uses very accurate charged particle cross sections <sup>10)</sup> of the reactions in question as cross section standard to calibrate the experimental set-up. These differential cross sections fulfill both requirements of a standard for a high quality cross section ratio measurement

- 1) They are very accurate (uncertainties of less than 1%)
- 2) They are practical standards and can be applied very easily

Because cross sections of the target itself are used as a standard there is no difference in geometry and sample mass. In such a type of experiment most absolute experimental errors drop out because only changes in the experimental conditions must be recorded rather than their absolute values. (Therefore these measurements are also called "quasiabsolute").

Table 1 compiles uncertainties of absolute measurements of differential neutron production cross sections using gaseous targets. Differences in uncertainties for absolute and quasi-absolute measurements and estimates of error limits are given. This shows that the quasiabsolute method has smaller uncertainties.

Having a versatile accelerator available, cross section standards of different source reactions can be combined <sup>2)</sup> for the calibration of the experimental set-up by using the identical target with different bombarding particles, e.g.  ${}^2\text{H}(\text{d},\text{n}){}^3\text{He}$  -  ${}^2\text{H}(\text{t},\text{n}){}^4\text{He}$  and  ${}^3\text{H}(\text{p},\text{n}){}^3\text{He}$  -  ${}^3\text{H}(\text{d},\text{n}){}^4\text{He}$ .

Because the center-of-mass cross sections for  $\text{d}-{}^3\text{H}$  and  $\text{t}-{}^2\text{H}$  are identical (at the corresponding energies), all 3 reactions can be combined <sup>2)</sup> and measured with the same scale uncertainty.

Owing to the wide neutron energy range the accuracy of the final result depends strongly on the quality of the efficiency curve.

Here, again, the exchange of bombarding and target nuclei is of great benefit. Fig. 1 demonstrates this for the 10 MeV  $\text{d}-{}^3\text{H}$  distribution. The complementary distribution is  $\text{t}-{}^2\text{H}$  at  $E_t = 14.975$  MeV.

To each center-of-mass cross section belongs a pair of neutron energies from the two distributions. The efficiency ratio at these energies is given by the (center-of-mass) yield ratio. Recently <sup>11)</sup>, complementary distributions of  $\text{p}-{}^3\text{H}$  and  $\text{t}-{}^1\text{H}$  were used to obtain the low energy part of a low bias efficiency curve. Fig. 2 shows the resulting curve. The interesting feature of the low bias curve is the structure due to inelastic carbon interactions for energies as low as 5.3 MeV. Indications of this structure can be found in the literature <sup>12,13)</sup> although it seems

that no attention was paid to it until now. Reported structure in the higher energy part of neutron spectra of  $^{252}\text{Cf}$  could probably be due to this kind of efficiency structure. Table 2 gives some idea of present consistency of evaluated differential cross section data of the  $^2\text{H}(\text{d},\text{n})^3\text{He}$  reaction. This table compares redundant efficiency measurements using 5 and 6 MeV differential cross section predictions <sup>2)</sup> as reference. Note that there is no scale adjustment ! These measurements prove the consistency of the 5 and 6 MeV data to about  $\pm 1\%$ . This high precision was made possible by accurate charged particle reference cross sections in connection with the quasiabsolute measuring technique. The latter includes the experimental determination of the energy dependence of the neutron detection efficiency under the actual experimental conditions. This takes care of parasitic effects like small angle scattering in the collimator bore (at least to a first order), of geometric effects and of the attenuation in the air. At the same time Table 2 shows how the quasiabsolute method can be used most powerfully. Provided that data can be measured reproducibly at all, differential cross sections of the same reaction at various energies can be checked for inconsistency the following way: yield ratios at angles with the same neutron energy must equal the corresponding cross section ratios. In such a measurement the neutron detector efficiency does not enter.

### III. Quality of data.

What accuracy of the neutron production cross section should we aim at?

Adequacy in data must always be addressed in terms of specific applications. Since the overall accuracy of the result is important uncertainties in the cross section need not be much less than those of all other contributions. Therefore all pertinent properties of a neutron source must be appraised with the specific application in mind. Obviously the highest accuracies will be needed for data to be used as secondary standards either for calibration or for efficiency determination purposes. But also in these cases other source properties will be important. Which properties of a practical monoenergetic neutron source must be considered?

- 1) intensity
- 2) energy resolution (and time resolution in case of time-of-flight measurements)
- 3) energy definition
- 4) energy and intensity anisotropy
- 5) cleanness (contamination with unwanted neutrons)
- 6) practicability

These characteristics are a mixture of physical properties and technical possibilities. (The following discussion is restricted to gaseous targets and neutron emission at  $0^\circ$ .)

#### III. A. Neutron Source Intensity

The intensity depends on the cross section, the target thickness, and the beam current (and therefore on the heat sink capability of the target). Therefore intensity comparisons are

often made for equal energy loss in the target<sup>14)</sup>. This procedure is good enough for sketching a rough picture. It assumes that the current capability of the accelerator is independent of the type (and energy) of the charged particles and that the limitations in the target constructions depend on the energy loss in the target. Neither is usually the case. Fig.3. provides lab cross sections for the neutron production by all five reactions for neutron energies up to 40 MeV. From this graph can be seen that - except for the resonance above 14 MeV in the d-T reactions - the t-H reaction provides the highest cross sections for neutron production between 1 and 40 MeV. At 5.3 MeV the cross section is bigger by a factor of 15 than those of the competing reactions. This high cross sections together with the other favourable properties discussed below makes the t-H reaction a very attractive source. Unfortunately only few installations can provide triton beams.

### III.B. Energy and Time Resolution

The energy resolution depends on the energy loss in the target (i.e. on the target thickness), on the straggling in the entrance foil, on the energy spread and energy variations of the incoming charged particles and on the neutron energy anisotropy within the relevant outgoing neutron cone.

The time resolution in time-of-flight experiments is not only limited by the energy resolution, but also by the transit time of the charged particles through the target (target length and velocity of the charged particles) and the time spread of the incoming charged particles. The timing uncertainties in the detector and its associated electronics are, however, independent of the source reaction. The experimental time resolution in TOF set-ups is a combination of the intrinsic energy and intrinsic time resolution. Therefore this total resolution must be considered when investigating the suitability of a neutron source. In a particular application it was shown<sup>15)</sup> that even at an energy as low as 8 MeV the p-T reaction can compete with the d-D reaction when the total resolution is considered.

### III.C. Energy Definition

For gaseous targets the determination of the mean neutron energy is no real problem if the accelerator energy is well calibrated and all energy degrading and smearing effects are taken into account. In favourable cases a final uncertainty of less than 5 keV may be reached. Due to the finite energy spread the effective mean neutron energy will be different if the neutron cross section under investigation is nonlinear as is the case in threshold reactions.

For solid targets the determination of the mean interaction energy is not so simple<sup>16)</sup>.

There are several cases among the neutron production cross sections where the energy uncertainty limits the final accuracy.

This happens not only at the slopes of the resonances of the p-T and d-T reaction but also with the d-D reaction: The 17.5-deg laboratory excitation function of  ${}^2\text{H}(\text{d}, {}^3\text{He})\text{n}$  changes near 6 MeV by as much as 27% per MeV <sup>2)</sup>

### III.D. Anisotropy

In general, there is both an angular dependence of the neutron energy and of the neutron flux. First we will consider disadvantages of these anisotropies.

If the neutron flux was not measured for the solid angle actually in use, the angular dependence of the neutron production cross section must be considered in the correction. The anisotropy of the neutron energy increases the energy (and time) spread of the neutrons reaching the sample (and/or the detector) and lowers the mean energy.

On the other hand one can take advantage of the anisotropy. The biggest anisotropy occurs when the mass of the accelerated particle is bigger than that of the target nucleus as is the case for the  ${}^1\text{H}(\text{t}, \text{n}){}^3\text{He}$  reaction <sup>17)</sup>. In this case the neutrons are emitted into a cone around  $0^\circ$  with a semiangle  $\theta$  of approximately

$$\theta = \arcsin \left( 1 - E_{\text{thr}}/E_t \right)^{1/2}$$

Where  $E_{\text{thr}}$  is the threshold energy of the reaction and  $E_t$  the triton energy in the lab system. The advantage of such a behaviour is tremendous: no shadow bar is needed to shield the source for scattering at back angles.

For the other reactions forward peaking of the flux and of the neutron energy is less pronounced but often sufficient to reduce the background. First, the room background is proportional to the total neutron production cross section whereas the signal is proportional to the differential cross section at the angle chosen (usually  $0^\circ$ ). Second, if the usable neutrons have the highest energy, background from the other neutrons can be shielded more easily. This was realized, e.g. at the elastic neutron scattering from  ${}^3\text{He}$  <sup>18)</sup>. In this case 14.4 MeV neutrons were produced by the p-T reaction rather than the usual d-T reaction. For the p-T reaction the flux drops by more than a factor of four and the energy by more than a factor of two when moving from  $0$  to  $90$  degree.

The production of 14 MeV neutrons by the d-T reaction is the worst choice with regard to anisotropy: both the flux and energy anisotropy are small.

### III. E. Neutron background

At high enough charged particle energies the monoenergetic neutron spectrum will be contaminated by secondary neutrons from competing neutron reactions in the target and by background neutrons from the target (and beamline) structure. Whereas the

first contribution is a property of the source reaction and therefore unavoidable, the other one is design-dependent.

In principle the structure background can be corrected for by a background run with an empty target. However, this does not always work out properly for two reasons:

- 1) Due to changes in beam steering this background may change in time.
- 2) The charged particle beam will not undergo an energy degradation in the empty target therefore the background will be higher. For protons a dummy filling of hydrogen can correct for that. Better practice, however, is to keep this background small from the beginning.

For proton beams materials with high (p,n) thresholds are available for the entrance foils and the beamstop (e.g.  $^{58}\text{Ni}$ ,  $^{12}\text{C}$ ,  $^{28}\text{Si}$ ,  $^{19,20}\text{O}$ ). At 14.9 MeV incident proton energy background from a  $^{28}\text{Si}$  beam stop is more than a factor of 100 less than that from a gold beam stop <sup>20)</sup>.

In Fig.4 zero degree neutron spectra of (p,n) reactions in carbon,  $^{28}\text{Si}$  and  $^{58}\text{Ni}$  for 14.9 MeV incoming protons are given.

The unavoidable background cannot be completely subtracted by a background run with an empty target. Nevertheless, some success was reported for the d-D reaction <sup>21)</sup> by taking advantage of a similarity in the deuteron break-up in helium and deuterium.

In cases where the energy gap between the primary and secondary neutrons does not help and no alternative source is available, calculated corrections of the unavoidable background must be applied <sup>22)</sup>. For this end the energy spectra of the breakup neutrons must be known very well. Therefore good knowledge of double differential cross sections  $d^2\sigma/d\Omega dE$  became important during recent years. Table 3 summarizes such measurements for the d-D reaction.

Up to 17.5 MeV neutron energy there are no break-up neutrons from the  $^1\text{H}(t,n)^3\text{He}$  reaction. Together with its high cross section, nearly an ideal source. It has been used for measurements of the continua in neutron emission reactions in light elements (e.g. Ref.24). For the t-H reaction only the structure background (from the triton breakup in the entrance foil and the beam stop) must be corrected. This was done by subtracting a background run without gas. The energy difference of the tritons hitting the beam stop was approximately compensated for by reducing the total background yield by a few percent as determined by a side experiment using scattering from hydrogen <sup>25)</sup>. Background conditions for production of neutrons of 10 and 11 MeV by the t-H reaction can be found in Ref.20. Fig. 5 and 6 are taken from



that work. Fig.5 shows that the unavoidable background from the d-D reaction is more than a factor of ten bigger than that of the p-T reaction when producing monoenergetic 14 MeV neutrons of the same intensity. Fig.6 compares experimental signal-to-background ratios when producing 10 MeV neutrons by the  $^1\text{H}(t,n)^3\text{He}$ ,  $^3\text{H}(p,n)^3\text{He}$  and  $^2\text{H}(d,n)^3\text{He}$  reactions under varying experimental conditions. With regard to total background the p-T reaction with a  $^{28}\text{Si}$  beamstop is best, as was shown up to neutron energies of 14 MeV<sup>20)</sup>.

This fact and other advantages like better time resolution and negligible self target build up makes the p-T reaction better suited for many experiments above 10 MeV than the d-D reaction. This was demonstrated years ago by accurate elastic scattering measurements of neutrons on  $^3\text{He}$  at 12, 13.6 and 14.4 MeV <sup>18)</sup> showing that the upper limit for the use of the p-T reaction is not 11 MeV as some authors (e.g. Ref.26) believe. In addition smaller unavoidable background results in smaller systematic errors in experiments that are background sensitive. Here, too, p-T is better than d-D even if the statistical precision is inferior.

### III. F. Practicability

The final decision on what source reaction to use is determined by the practicability, i.e. by the availability of a specific charged particle with the necessary energy and the corresponding target. In some laboratories, like the Los Alamos Scientific Laboratory, this point is unimportant because bunched p,d and t beams up to 17 MeV are available and gaseous tritium targets <sup>27)</sup> have been routinely used for a very long time.

In some cases, however, one has the impression that mainly the practicability is considered when choosing a neutron source thus making the routinely used source reaction the best source for all applications.

Usually gas targets will give the better performance<sup>28)</sup>:

- smaller energy spread at a given intensity due to higher purity
- amount of target material can easily be adjusted
- change of target thickness in time can easily be recorded
- structural background can be minimized by choosing optimum beam stop and window materials.

However, the increased target length has at least two disadvantages:

- 1) The time spread is bigger
- 2) The source is extended rather than pointwise thus complicating the geometry.

### IV. Status of Cross Sections:

#### IV. A. $^3\text{H}(p,n)^3\text{He}$ and $^1\text{H}(t,n)^3\text{He}$ Reactions

Table 4 summarizes measurements included in this evaluation but not in the previous ones<sup>1,2)</sup>. With support of the high energy data <sup>29-31)</sup> the zero degree excitation function was extended to 50 MeV. Matching the slope of the data below 20 MeV<sup>2)</sup> and that of the higher energy data <sup>29)</sup> gives the recommended data of Fig.7.

Fig.8 shows a new analysis of the zero degree excitation function near the resonance <sup>6)</sup>. This work was triggered by complete angular distributions at 2.5 and 4.0 MeV using the  $^1\text{H}(t,n)^3\text{He}$  reaction for the back angle data. These were the first distributions measured over all the angular range. They give a backward peaking that is stronger by 17% than the previous (extrapolated) data. Inclusion of these new data in the general analysis gave the following differences <sup>6)</sup> to the best previous evaluation <sup>1)</sup>: Below 2 MeV and above 5.5 MeV the two solutions coincide. In between (at the resonance) the new solution is up to 10% lower. A scale error of 4% was deduced combining the internal error contributions. Fig.9 shows the energy dependence of the total cross section. Between 3 and 8 MeV the lower curve coincides with the previous evaluation <sup>1)</sup>. Below 3 MeV the new curve is typically 4% lower. (Shifting the new curve by about 50 keV to lower energies would give even better agreement). The  $^3\text{H}(p,n)^3\text{He}$  reaction contributes as inverse reaction to the total n- $^3\text{He}$  cross section. However, at 2 and 3.5 MeV neutron energy the sum of partial cross sections did not add up to the total <sup>32)</sup>. New measurements of the total cross sections are about 5% higher <sup>33)</sup> so that this discrepancy was settled. However, now elastic n- $^3\text{He}$  scattering data at 6 MeV and 7.9 MeV, from two different authors <sup>18,34)</sup>, or the total  $^3\text{H}(p,n)^3\text{He}$  at the corresponding energies of 7.02 and 8.92 MeV appear to be discrepant by more than two error bars. Or is it due to the total n- $^3\text{He}$  cross section?

In Fig.10 the zero degree breakup cross sections are extended to 50 MeV by means of (incomplete) high energy data <sup>29,35)</sup>. Table 4 also cites another reference on Russian work on p-T breakup <sup>36)</sup>.

Fig.11 shows the reduced Legendre coefficients for energies up to 30 MeV. The high energy analysis depends on the  $0^\circ$  data shown in Fig.7 and on charged particle data up to 32.8 MeV <sup>37)</sup>.

#### IV. B. $^2\text{H}(d,n)^3\text{He}$ Reaction

Table 5 summarizes references that were not included in previous evaluations <sup>1,2)</sup>. The extension of the zero degree excitation function of Fig.12 beyond 28 MeV is based on (extrapolated) information of incomplete angular distributions at higher energies <sup>38-41)</sup>. The only actual measurements <sup>42,43)</sup> lie within the energy range of the previous evaluation <sup>2)</sup>. It is very pleasing that the predicted energy dependence up to 28 MeV which is in strong disagreement with data by Dietrich et al. <sup>44)</sup> was verified very recently by Ref.43.

New relative distributions at very low energies <sup>4,5)</sup> will change the recommended Legendre coefficients between 0.1 and 0.4 MeV. As can be seen from Fig.13, the anisotropy at 0.2 MeV is probably 4% bigger than obtained from the previous evaluation <sup>1)</sup>. A similar difference (in the opposite direction) was noted previously <sup>2)</sup> at 6 MeV.

Fig.14 was taken from Ref.2. New breakup data points between

5.3 and 7.2 MeV <sup>26)</sup> were added. They practically coincide with the curve. From the scatter about the curve it can be concluded that the uncertainties of these data points are too big to add significant information. The insert in this fig. shows total breakup cross sections at higher energies <sup>23,45)</sup>. This allows to estimate how the zero-degree excitation function will behave beyond 20 MeV where no data are available. The importance of the d-D breakup spectra <sup>22)</sup> is emphasised by Table 3. It compiles published information on breakup neutron spectra and angular distributions at the various energies.

Fig. 14 shows the total  $^2\text{H}(d,n)^3\text{He}$  cross section in reduced form up to 100 MeV. No new data became available to support or to disprove this parametrization <sup>46)</sup>.

Fig. 15 shows the reduced Legendre coefficients for the differential cross sections of the d-D reaction for deuteron energies up to 25 MeV.

#### IV. C. $^3\text{H}(d,n)^4\text{He}$ and $^2\text{H}(t,n)^4\text{He}$ Reactions.

Since the last evaluation <sup>2)</sup> no new data were reported. Table 6 compiles breakup measurements for the d-T reaction <sup>47-51)</sup>. Fig. 17 shows the zero degree excitation function in reduced form. This allows an easy extrapolation for a few more MeVs. This curve was solely derived from experimental data of Ref.2. As was shown in Fig.13 of Ref.2 it is in very good agreement with all data up to 19 MeV.

Fig. 18 shows the reduced Legendre coefficients of the  $^3\text{H}(d,n)^4\text{He}$  differential cross sections up to 19 MeV.

### V. Discussion and Recommendations

The adequacy of the neutron production cross sections can only be discussed in connection with specific applications.

#### V. A. General Physics

The cross sections discussed in this paper belong to reactions in the mass 4 and 5 system which have for some time, been subject to R-matrix analyses <sup>52)</sup>. In spite of some success the amount of input data is too sparse or not enough consistent to allow reliable predictions especially at higher energies. The problem is twofold

- 1) Not enough data
- 2) Data with too big systematic errors.

From the present evaluation the need of high quality data (total error less than 3%) at the following energies and angles is evident:

- 1)  $^3\text{H}(p,n)^3\text{He}$ 
  - a) Absolute zero-degree values of the maximum at 3.1 MeV and of the minimum near 8 MeV.
  - b) 180-degree excitation function (by means of the t-H reaction) between 2 and 5 MeV proton energy. Even relative data would be beneficial.

- c) One complete angular distribution as high in energy as possible (limited by the energy requirements for the triton beam)
  - d) Total cross sections at 7 and 8.9 MeV would help to clarify the total cross section discrepancy in the  $n$ - $^3\text{He}$  system (see Sect. IV.A.)
  - e) Angular distributions of the (inverse)  $^3\text{He}(n,p)^3\text{H}$  reaction could provide very valuable back angle data at any energy.
- 2)  $^2\text{H}(d,n)^3\text{He}$ : Some improvement of the previous evaluation <sup>1)</sup> in the low energy range (around 0.2 MeV) seems necessary due to new data <sup>4,5)</sup>. New neutron data at higher energies will suffer from the huge background and do not seem worthwhile. Due to the strong anisotropy at higher energies special attention must be paid to an accurate angle determination
- 3)  $^3\text{H}(d,n)^4\text{He}$ : Absolute zero degree data between <sup>5</sup> and 7 MeV are necessary to verify the evaluated data there <sup>2)</sup>. Below 1 MeV the total cross section is not well determined (5 - 10%).

#### V. B. Secondary Standard

Many desirable properties (high intensity, ease of use, wide neutron energy range) predestinate these neutron source reactions as cross section standards. They are especially useful for (relative) detector calibrations. However, the primary accurate charged particle cross sections are neither convenient with regard to machine energy (not accessible for small accelerators) nor easy to reproduce (strong angle dependence, high neutron background). Therefore the establishment of secondary standards is suggested. The properties of such secondary standards should be as follows:

- 1) Particle energy low enough to serve as many users as possible
- 2) Straightforward application (no severe energy or angle dependence of the data).
- 3) Wide energy range covered within one distribution
- 4) Neutron energy overlap when switching from one source to another

One obvious choice would be the angular distribution of  $^3\text{H}(p,n)^3\text{He}$  at the cross section maximum (3.1 MeV). For the d-D reaction the 5 MeV distribution seems to be a good candidate. The consistency of such a set of secondary standards could easily be checked by quasiabsolute measurements. A consistency of about 1% should be aimed at.

Then there is a need for accurate charged particle data with associated neutron energies bigger than 29 MeV (up to 40 MeV). This would allow to calibrate neutron detectors experimentally at the higher energies. In this case 2 to 3% charged particle data would be sufficient.

#### V. C. Monoenergetic Source:

Many applications (e.g. fast fission and other threshold reactions, measurements of neutron continua) require monoenergetic sources to avoid systematic errors.

The second neutron group of the t-H reaction is very low in intensity and energy and therefore often negligible. However, the source is not very practical and the background from the target structure is usually not negligible and must be subtracted.

The unavoidable background from p-T sources is small. In addition, the structure background can be kept small by use of materials with a high (p,n) threshold. Although the use of gaseous tritium is not as practical as that of deuterium, the p-T reaction is a good choice even for the highest energies. Up to now only little information on the p-T breakup is available. Therefore additional double differential cross sections (mainly at  $0^\circ$ ) of the p-T breakup are needed.

The amount of data on the d-D breakup below 13 MeV is abundant. However these data should be evaluated so that experimenters who have to use the d-D reaction and have to perform an experiment with monoenergetic neutrons above the breakup threshold can make the best correction possible.

#### V. D. General Use

The cross sections for neutron production at zero degree by the five reactions considered here are known to better than 10% over most of the energy range up to neutron energies of 40 MeV (maybe, excepting d-D beyond 30 MeV). This accuracy seems to be sufficient, especially for tritium targets where it takes some pain to determine the exact amount of tritium with an uncertainty of less than 5%.

Acknowledgment: I am indebted to all my friends at Los Alamos Scientific Laboratory for making my visits there efficient and pleasant. Special thanks are due to R.F.Taschek for making my first stay there possible. Besides I want to thank Prof.Weinzierl for supporting this project and Mrs.Ch.Schneider for invaluable help with the manuscript.

REFERENCES :

- 1) H. Liskien and A. Paulsen, Nucl.Data Tables, 11,569 (1973)
- 2) M.Drosg, Nucl.Sci.Eng.67, 190 (1978)
- 3) Symposium on Neutron Cross Sections from 10 to 40 MeV,edited by M.R.Bhat and S.Pearlstein, BNL-NCS 50 681, July 1977.
- 4) G. Pospiech, H. Genz, E.H. Marlinghaus, A. Richter and G. Schrieder, Nucl.Phys. A 239, 125 (1975)
- 5) N. Ying. B.B.Cox, B.K. Barnes and A.W. Barrows, Jr. Nucl.Phys. A 206, 481 (1973)
- 6) M. Drosg, The  $^3\text{H}(\bar{p},n)^3\text{He}$  Differential Cross Sections Below 5 MeV and the  $n\text{-}^3\text{He}$  Cross Sections, Report LA-8215-MS of Los Alamos Scientific Lab. (1980)
- 7) H.H. Barschall, L. Rosen, R.F. Taschek and J.H. Williams, Rev.Mod.Phys. 24, 1 (1952)
- 8) M.M.Meier, Associated Particle Methods, pp 221 of Neutron Standards and Applications, NBS Spec.Publ. 493 (1977)
- 9) J.L. Fowler, C.A. Uttley, J.A. Cookson, M. Hussian, M.T. Swinhoe and R.B. Schwartz, Bull.Am.Phys.Soc.24(4), 651 (1979)
- 10) N. Jarmie and J.H. Jett, Phys.Rev. C16, 15 (1977); also, N. Jarmie, Private Communications (~~1971~~, 1976)
- 11) M. Drosg, D.M. Drake and P. Lisowski, The Contribution of Carbon Interactions to the Neutron Counting Efficiency of Organic Scintillators, Report LA-7987-MS of Los Alamos Scientific Laboratory (1980)
- 12) H.H. Knitter, A. Paulsen, H. Liskien and M.M. Islam, Atomkernenergie 22, 84 (1973)
- 13) S.T. Thornton and J.R. Smith, Nucl.Instr.Methods 96, 551 (1971)
- 14) G. Haouat and M. Cance, this Meeting
- 15) G. Haouat, S. Seguin, J.P. Lochard, J. Sigand, J. Lachkar, Production de neutrons monocinetiques-Utilisation des cibles gazeuses de Deuterium et de Tritium, pg.21 of report CEA-N-1798 (1975)
- 16) V.E. Lewis and E.J. Axton, Nucl.Instr.Methods 159, 401 (1979)
- 17) W. Deuchars, J.L. Perkin and R. Batchelor, Nucl.Instr. Methods 23, 305 (1963)
- 18) M. Drosg, D.K. McDaniels, J.C. Hopkins, J.D. Seagrave, R.H. Sherman, and E.C. Kerr, Phys.Rev., C9, 179 (1974)
- 19) G. Haouat, S. Seguin, Realisation d'une cible gazeuse Tritium pour la production de neutrons avec un accelerateur Van de Graaff tandem, Report CEA-N-1739 (1974)
- 20) M. Drosg, G.F. Auchampaugh, and F. Gurule, Neutron Back-ground Spectra and Signal-to-Background Ratio for Neutron Production between 10 and 14 MeV by the Reactions  $^3\text{H}(p,n)^3\text{He}$ ,  $^1\text{H}(t,n)^3\text{He}$ , and  $^2\text{H}(d,n)^3\text{He}$ , Report LA-6459-MS, Los Alamos Scientific Laboratory (1976)

- 21) P. Grabmayr, J. Rapaport, S.M.Grimes, R.W. Finlay and V. Kulkarni, Bull.Am.Phys.Soc. 24(7), 878 (1979)
- 22) D.L.Smith and J.W. Meadows, Method of Neutron Activation Cross Section Measurement for  $E_n = 5.5 - 10$  MeV using the  $D(d,n)He-3$  Reaction as a Neutron Source, Report ANL/NDM-9, Argonne Natl.Lab. (1974)
- 23) J.E.A. Lys and L. Lyons, Nucl.Phys. 74, 261 (1965)
- 24) D.M. Drake, G.F. Auchampaugh, E.D. Arthur, C.E. Ragan, and P.G. Young, Nucl.Sci.Eng. 63, 401 (1977)
- 25) M. Drosch, to be published
- 26) J.W. Meadows and D.L. Smith, this Meeting
- 27) J.T. Martin and R.K. Smith, Neutron Production Gas Targets, Report LA-6237-MS, Los Alamos Scientific Laboratory (1976)
- 28) S. Mittag, W. Pilz, D. Schmidt, D. Seeliger, and T.Streil, Kernenergie 22, 237 (1979)
- 29) C.J.Batty, B.E. Bonner, A.I.Kilvington, C.Tschalär and L.E. Williams, Nucl. Instr.Methods 68, 273 (1969)
- 30) H.Langevin-Joliot, Ph. Narboni, J.P. Didelez, G. Duhamel, L. Marcus and M. Roy-Stephan, Nucl.Phys. A 158, 309 (1970)
- 31) R. Darves-Blanc, N.Van Sen, J. Arvieux, A. Fiore, J.C. Gondrand and G. Perrin, Lettere al Nuovo Cim.4, 16 (1972)
- 32) M. Drosch, Interaction of Fast Neutrons with  $^4He$ ,  $^3He$ , and  $^1He$ : Additional and Improved Data, Report LA-7269-MS, Los Alamos Scientific Laboratory, (1978)
- 33) H.O. Klages, Private Communication (1979)
- 34) J.D. Seagrave, L. Cranberg, and J.E. Simmons, Phys.Rev.119, 1981 (1960)
- 35) L.E. Williams, C.J. Batty, B.E. Bonner, C. Tschalär, H.C. Denöhr, and A.S. Clough, Phys.Rev.Lett.23, 1181 (1969)
- 36) E.A. Kuz'min, N.I. Sidorov, A.R. Faiziev, L.V. Chul'kov, and G.B. Yan'kov, Neutron Yield in Proton-Tritium Interaction, 2nd All-Union Conference on Neutron Physics, Obninsk, INIS-mf-1698, pp 315 (1974)
- 37) R.G. Allas, L.A. Beach, R.O. Bondelid, E.M. Diener, E.L. Petersen, J.M. Lambert, P.A. Treado, and I. Slaus, Phys. Rev. C9, 787 (1974)
- 38) W.T.H. Van Oers and K.W. Brockman, Jr., Nucl.Phys. 48, 625 (1963)
- 39) M. Roy, D. Bachelier, M. Bernas, J.L. Boyard, I. Brissaud, C. Dêtraz, P. Radvanyi, and M. Sowinski, Phys.Lett. 29B, 95 (1969)
- 40) H. Brückmann, E.L. Haase, W. Kluge and L.Schänzler, Z. Physik 230, 383 (1970)
- 41) R.W. Fegley, Differential Cross Sections for  $D(d,d)D$  Elastic Scattering and the  $D(d,^3He)n$ ,  $D(d,t)p$  Reactions between 12.5 and 40.0 MeV, Thesis, Univ.California, Davis (1970)

- 42) M. Chemarin, L. Feuvrais, M. Gouanère, M.-C. Lemaire, and J.L. Vidal, J.Phys. 30, 29 (1969)
- 43) B. Gomez-Moreno, W. Hardt, K. Kochskämper, W. Rosenstock and W. von Witsch, Nucl.Phys. A 330, 269 (1979)
- 44) F.S. Dietrich, E.G. Adelberger, and W.E. Meyerhof, Nucl. Phys. A 184, 449 (1972)
- 45) P.M. Hegland, and R.E. Brown, Bull.Am.Phys.Soc.18, 1381 (1973); also, R.E. Brown, Private Communication (1975)
- 46) M.Drosg, Nucl.Sci.Eng. 65, 553 (1978)
- 47) R.L. Henkel, J.E. Perry, Jr., and R.K. Smith, Phys.Rev.99, 1050 (1955)
- 48) G.F. Bogdanov, N.A. Vlasov, S.P. Kalinin, B.V. Rybakov, and V.A. Sidorov, Sov.Physics-JETP 3, 793 (1956)
- 49) N.A. Vlasov, G.F. Bogdanov, S.P. Kalinin, B.V. Rybakov, and V.A. Sidorov, "Investigations of Reactions of 18-MeV Deuterons with Light Nuclei by the Time-of-Flight Method", Int.Conf. Neutron Interactions with the Nucleus, TID-7547, W.W. Havens, Jr., Ed., Columbia University (1957)
- 50) H.W. Lefevre, R.R. Borchers and C.H. Poppe, Phys.Rev.128, 1328 (1962)
- 51) C.H. Poppe, C.H. Holbrow, and R.R. Borchers, Phys.Rev.129, 733 (1963)
- 52) G.M. Hale, Bull.Am.Phys.Soc. 24 (7), 881 (1979)



Uncertainties of Absolute Differential Cross Section Measurements.  
Comparison of absolute and quasiabsolute method

Source of error	absolute	quasiabsolute	
Accelerator connected			
energy calibration	same		
energy spread	same		
divergence of C.P.beam	same		
stability of beam steering	same		
charge collection	same		
beam pick-off (TOF)	same		
Geometry			
zero-degree offset	same		
reaction angle	same		
absolute value of solid angle	yes 1%		no
finite solid angle	same		
Target (gaseous)			
thickness (purity)	yes 1% <sup>a)</sup>		no
loss of target material		same <sup>b)</sup>	
beam heating	abs. <sup>b)</sup>		rel. <sup>b)</sup>
energy spread		same	
BG from secondary n's		same	
BG from target structure		same	
attenuation in target and structure	abs.		rel.
Electronics and Detector			
Statistical error		same	
Charge measurement	abs. >0.1%		rel. <0.1%
Dead Time	abs. 0.1%		rel. <0.1%
Multiple event probability (TOF)		same	
Detector efficiency	abs. >2%		rel. <1.3%
Cross Section Reference			
Accuracy	no	yes	<0.4%
Adjustment error	no	yes	<0.7%
Combination of given error estimates	>2,5%		<1,6%

<sup>a)</sup> for  $T_2$ -target the error will be appreciably bigger because the purity of  $T_2$  gas during the experiment will not be known with this accuracy.

<sup>b)</sup> negligible in low current experiments

T A B L E 2

Redundant Efficiency Measurements Used to Check for  
Inconsistencies in the 5 and 6 MeV d-D Cross Sections  
(Typical error of each yield  $\pm 1.1\%$ )

$E_n$	5 MeV		6 MeV		Difference %
	$\theta_{\text{Lab}}$	Y/ $\sigma$	Y/ $\sigma$	$\theta_{\text{Lab}}$	
8.24	$0.4^\circ$	4896	4750	$30.3^\circ$	-3.1
7.00	$38.0^\circ$	4985	5047	$48.2^\circ$	+1.2
6.69	$42.9^\circ$	5105	5186	$52.2^\circ$	+1.5
5.95	$54.3^\circ$	5798	5684	$61.7^\circ$	-2.0

T A B L E 3

Measurements of d-D breakup

$E_d$ (MeV)	At zero degreee		Angular distributions		Total cross section
	cross sections	spectra	cross sections	spectra	
5.3	CR56 <sup>a)</sup>	ME80			
5.8	CR56	ME80			
6.2	CR56				
6.3		CR56, ME80	CR56		
6.7		ME80			
6.8	CR56	DR76			
7.2	CR56	ME80			
7.3	CR56				
7.9	DR78	LE62, DR76			
8.8	WI61A				
8.9	DR78	AN58, LE62, DR76			
9.8	WI61A		LE62		
10.0	DR78	DR76			
10.9	WI61A	LE62			
11.0	DR78	DR76			
11.3				PO72	
11.8				AN58	
12.0		DI72 <sup>b)</sup>			
12.9	WI61A				
14.0		DI72 <sup>b)</sup>			
16.0		DI72 <sup>b)</sup>			
16.6				WE73	
17.0	DR78				
17.5					HE77
18.0	VL57	DI72 <sup>b)</sup>			
18.6				WE73	
18.8	RY61				
19.0		DI72 <sup>b)</sup>			
22.3					LY74 <sup>c)</sup>
31.3					LY74
42.8					LY74
49.6					LY74
51.5					BR70
58.1					LY74

a) Symbols see Table 5 and previous evaluations (Ref.1 and 2)

b) relative spectra only

c) Ref.23

T A B L E 4

$^3\text{H}(p,n)^3\text{He}$  Differential Cross-Section Measurements  
which are neither included in Liskien's Evaluation<sup>1)</sup>  
nor shown in Table I of Ref.2 (Symbols in accordance  
with LI73, i.e. Ref. 1)

Symbol	Author(s)	Reference	Method	Angular Range (Center-of-Mass degrees)	Proton Energy (Lab) (MeV)
Absolute Data					
BA69	Batty et al.	29	n, TOF	0	30, 50
LA70	Langevin-Joliot et al.	30	$^3\text{He}$	83.4...178	156
DA72	Darves-Blanc et al.	31	$^3\text{He}$	74...165	56.7
Relative Data					
DR80	Drosg	6	n, TOF	0...180	2.5, 4
Break up Data				(Lab. degrees)	
BA69	Batty et al.	29	n, TOF Spectra	0	30, 50
WI69	Williams et al.	35	n, TOF Spectra	2, 20	30.2
KU74	Kuz'min et al.	36	n, TOF Spectra	0	11.2, 14.2, 15.3
DR76	Drosg et al.	20	n, TOF Spectra	0	10.8...14.8

T A B L E 5

$^2\text{H}(d,n)^3\text{He}$  Differential Cross-Section Measurements which are neither included in Liskien's Evaluation<sup>1)</sup> nor shown in Table VI of Ref.2  
(Symbols in accordance with LI73, i.e. Ref.1)

Symbol	Author(s)	Reference	Method	Angular Range (Center-of-Mass degrees)	Deuteron Energy (Lab) (MeV)
Absolute Data					
VA63	Van Oers et al.	38	$^3\text{He}$	11.5...89.4	25.3
CH69	Chemarin et al.	42	n, TOF calc.	0	27.5
RO69	Roy et al.	39	$^3\text{He}$	7...91	83
BR70	Brückmann et al.	40	$^3\text{He}$	20...60	51.5
FE70	Fegley	41	$^3\text{He}$	13...102	12.5...40.2
GO79	Gomez et al.	43	n, C.T.	0	13.6, 24.3
Relative Distributions					
CH69	Chemarin et al.	42	n, TOF	0...68	27.5
YI73	Ying et al.	5	$^3\text{He}$	30...170	0.3...0.7
PO75	Pospiech et al.	4	$^3\text{He}$	20...80	0.07...0.14
Breakup Data (Lab. degrees)					
DI72	Dietrich et al.	44	E spectra no scale	0	12...19
SM74 } ME80 }	Smith and Meadows	22	E spectra	0	5.3...7.2
		26		0...30	6.7, 7.2
DR76	Drosg et al.	20	E spectra	0	6.8...11.0
DR78	Drosg	2	no spectrum	0	17

T A B L E 6

Measurements of  $d-^3\text{H}$  Breakup Cross Sections  
(Symbols are in accordance with LI73, i.e. Ref.1)

Symbol	Author(s)	Reference	Method	Angular Range (Lab.degrees)	Deuteron Energy (Lab) (MeV)
HE55	Henkel et al.	47	n,C.T. no spectra	0	3.7...6.1
BO56	Bogdanov et al.	48	n,TOF spectrum only	0	14.4
VL57	Vlasov et al.	49	n,TOF spectra	0 0...45	19 18
LE62	Lefevre et al.	50	n,TOF spectra	0	6.7...8.9
PO63	Poppe et al.	51	n,TOF spectra	0 0...70	6.3...11.9 4.8...10.9

# Figure Captions

- Fig.1. Differential center-of-mass cross section for the  $^3\text{H}(\text{d},\text{n})^4\text{He}$  reaction at  $E_d = 10$  MeV. The correlation between the neutron energies of d-T and t-D is shown.
- Fig.2. Efficiency curves of a NE213 neutron detector with biases at 0.3 and 2.0 MeV equivalent proton energy (Ref.11)
- Fig.3. Laboratory cross sections for neutron production at zero degree. The bar at each curve indicates the threshold for secondary neutron production.
- Fig.4. Comparison of the neutron output of beamstop materials at 14.9 MeV incident proton energy.  
a) carbon                      b)  $^{58}\text{Ni}$                       c)  $^{28}\text{Si}$
- Fig.5. Production of 14 MeV neutrons by the p-T reaction (a) and the d-D reaction (b).
- Fig.6. Signal-to-background (S/N) ratio for 10 MeV primary neutrons in dependence of target thickness  
a) p-T using a  $^{28}\text{Si}$  beam stop  
b) p-T using a  $^{58}\text{Ni}$  beam stop  
c) p-T using a gold beam stop  
d) d-D using a gold beam stop  
e) t-H using a gold beam stop  
The S/N ratio due to unavoidable background coincides with the upper frame line for p-T and with the arrow for d-D.
- Fig.7. Reduced zero-degree differential cross sections for the  $^3\text{H}(\text{p},\text{n})^3\text{He}$  reaction. (DR78 is Ref.2, BA69 is Ref.29).
- Fig.8. Low energy part of the zero degree excitation function (DR78 is Ref.2, the other symbols are from Ref.1)
- Fig.9. Total cross section for  $^3\text{H}(\text{p},\text{n})^3\text{He}$ . (Symbols see Ref.1, DR78 is Ref.2).
- Fig.10. Zero-degree breakup cross sections for the p-T reaction. (For the symbols see Table 4 and Ref.2)
- Fig.11. Reduced Legendre coefficients of the differential cross sections of the reaction  $^3\text{H}(\text{p},\text{n})^3\text{He}$  (Symbols see LI73, i.e. Ref.1).
- Fig.12. Zero-degree excitation function of  $^2\text{H}(\text{d},\text{n})^3\text{He}$
- Fig.13. Anisotropy ( $\sigma(90^\circ)/\sigma(0^\circ)$ ) of the differential cross sections of  $^2\text{H}(\text{d},\text{n})^3\text{He}$ . (Symbols see Table 5).
- Fig.14. Neutron production at zero degree by d-D breakup. The insert shows the total cross section for this reaction. (Symbols see Table 3)
- Fig.15. Total  $^2\text{H}(\text{d},\text{n})^3\text{He}$  cross section in reduced form (from Ref.46)
- Fig.16. Reduced Legendre coefficients of the differential cross sections of the  $^2\text{H}(\text{d},\text{n})^3\text{He}$  reaction (LI73 is Ref.1).
- Fig.17. Reduced zero degree excitation function for the  $^3\text{H}(\text{d},\text{n})^4\text{He}$  reaction. Experimental data from Ref.2.
- Fig.18. Reduced Legendre coefficients of the  $^3\text{H}(\text{d},\text{n})^4\text{He}$  differential cross sections. (Dashed curves below 5 MeV are from Ref.1).

Fig. 1

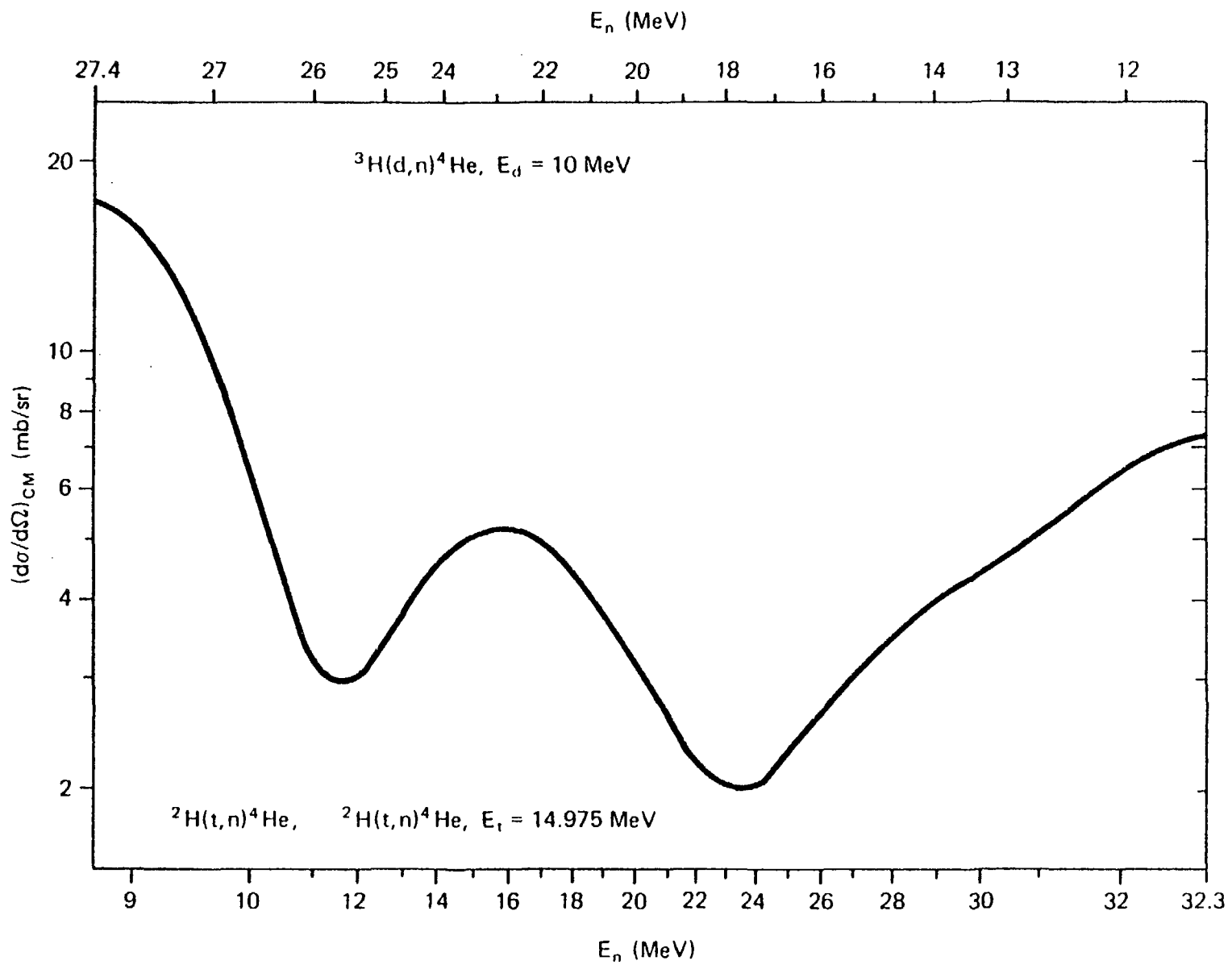




Fig. 2

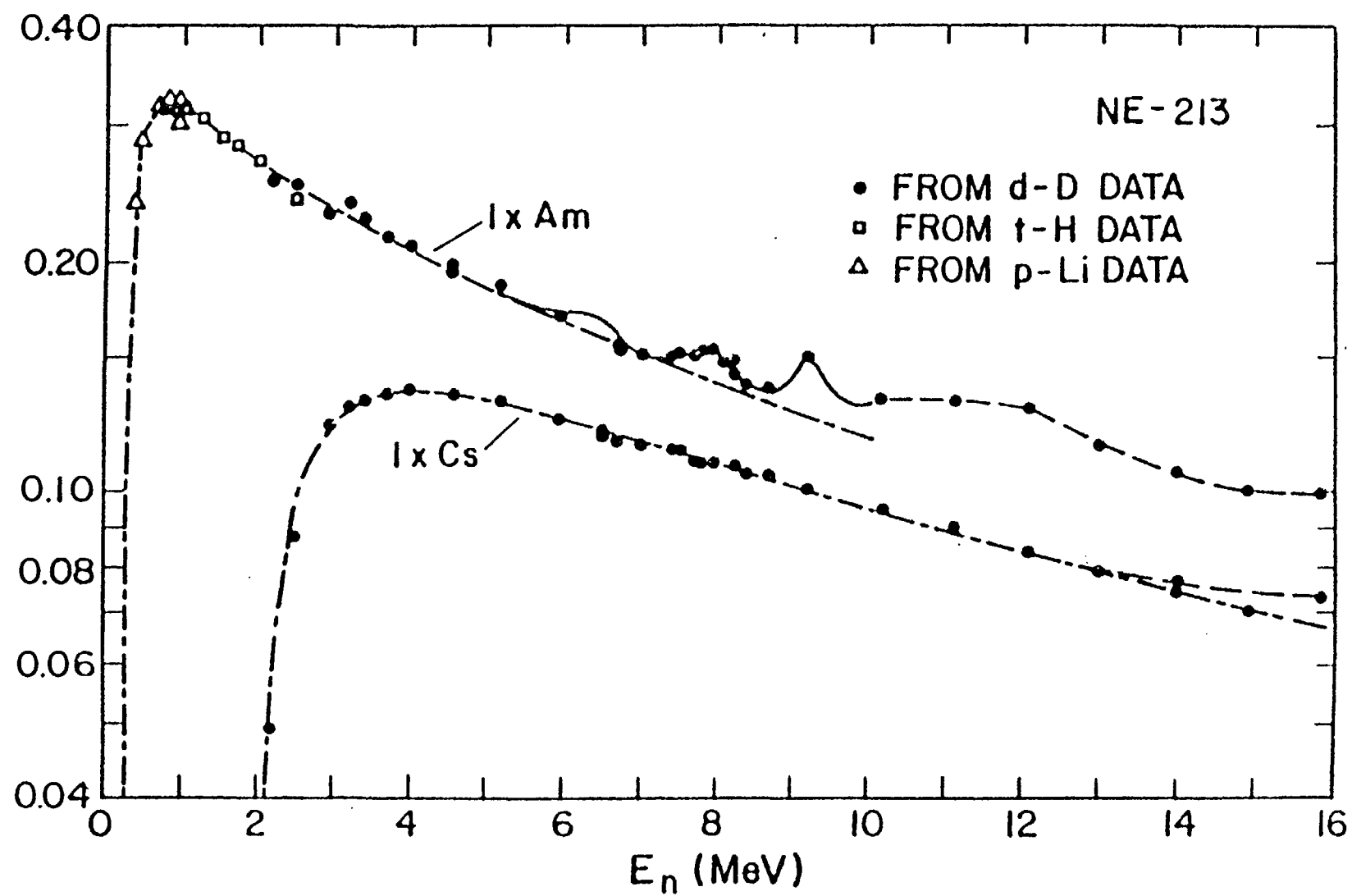
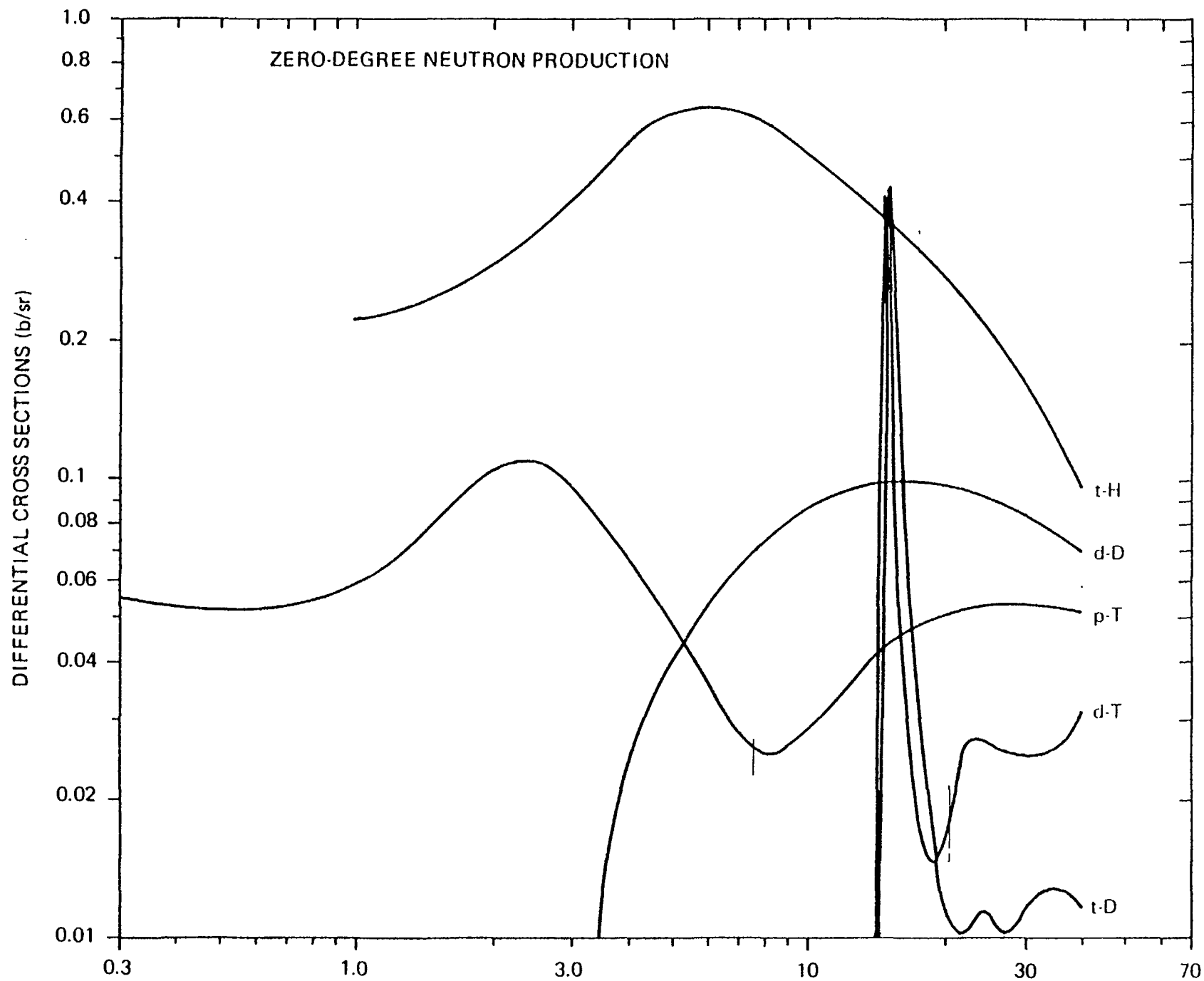


Fig. 3



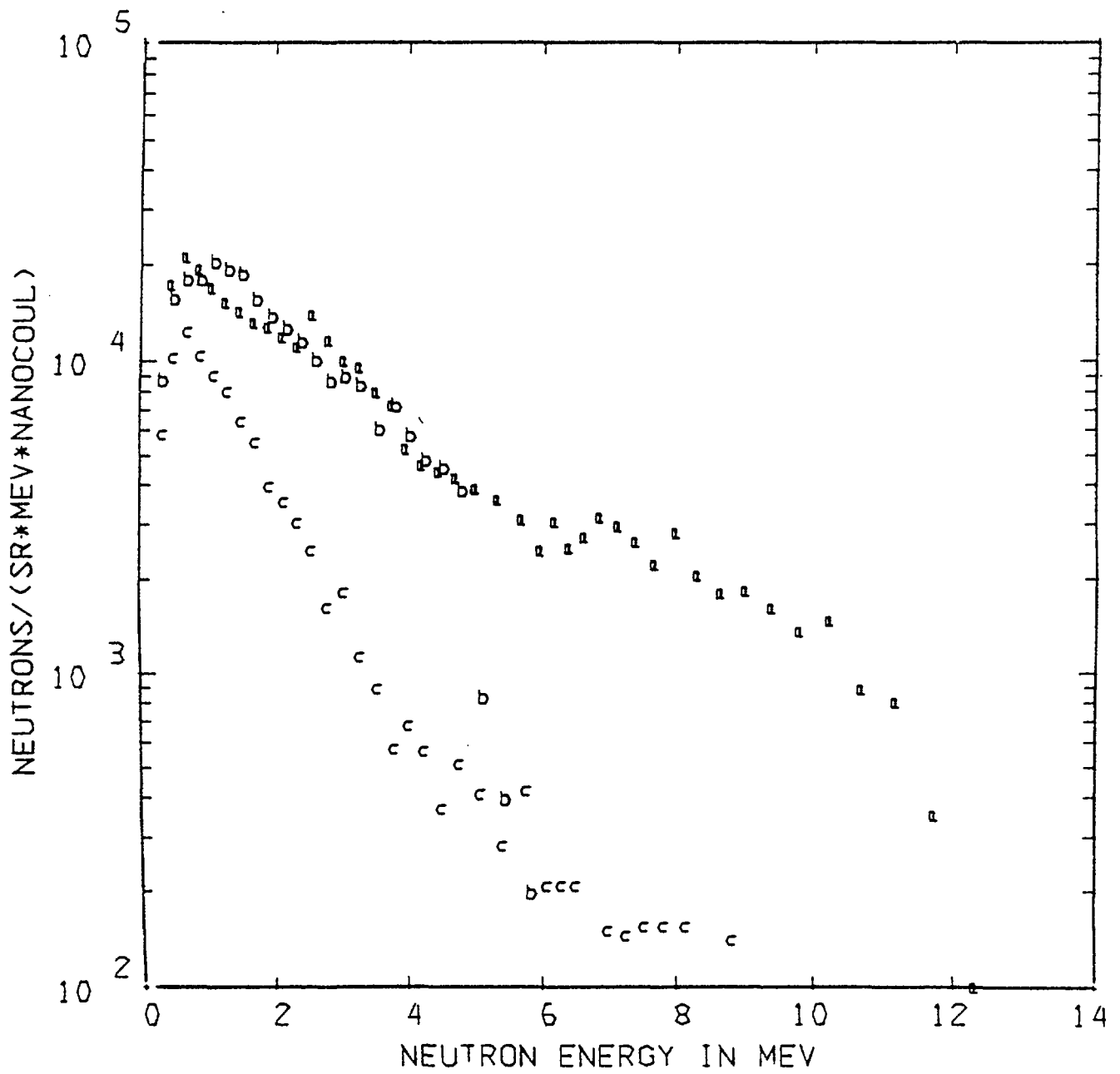


Fig. 4

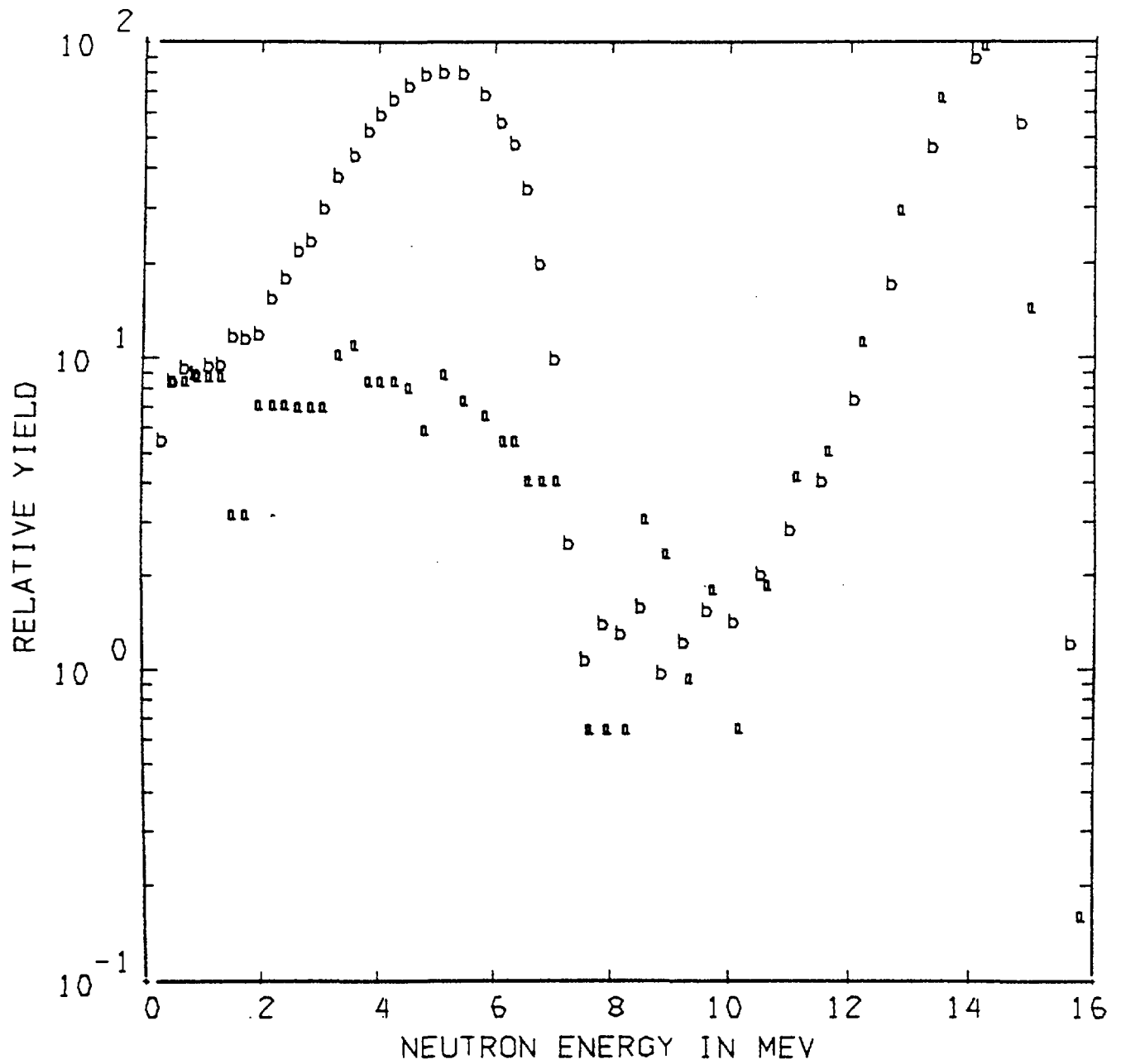
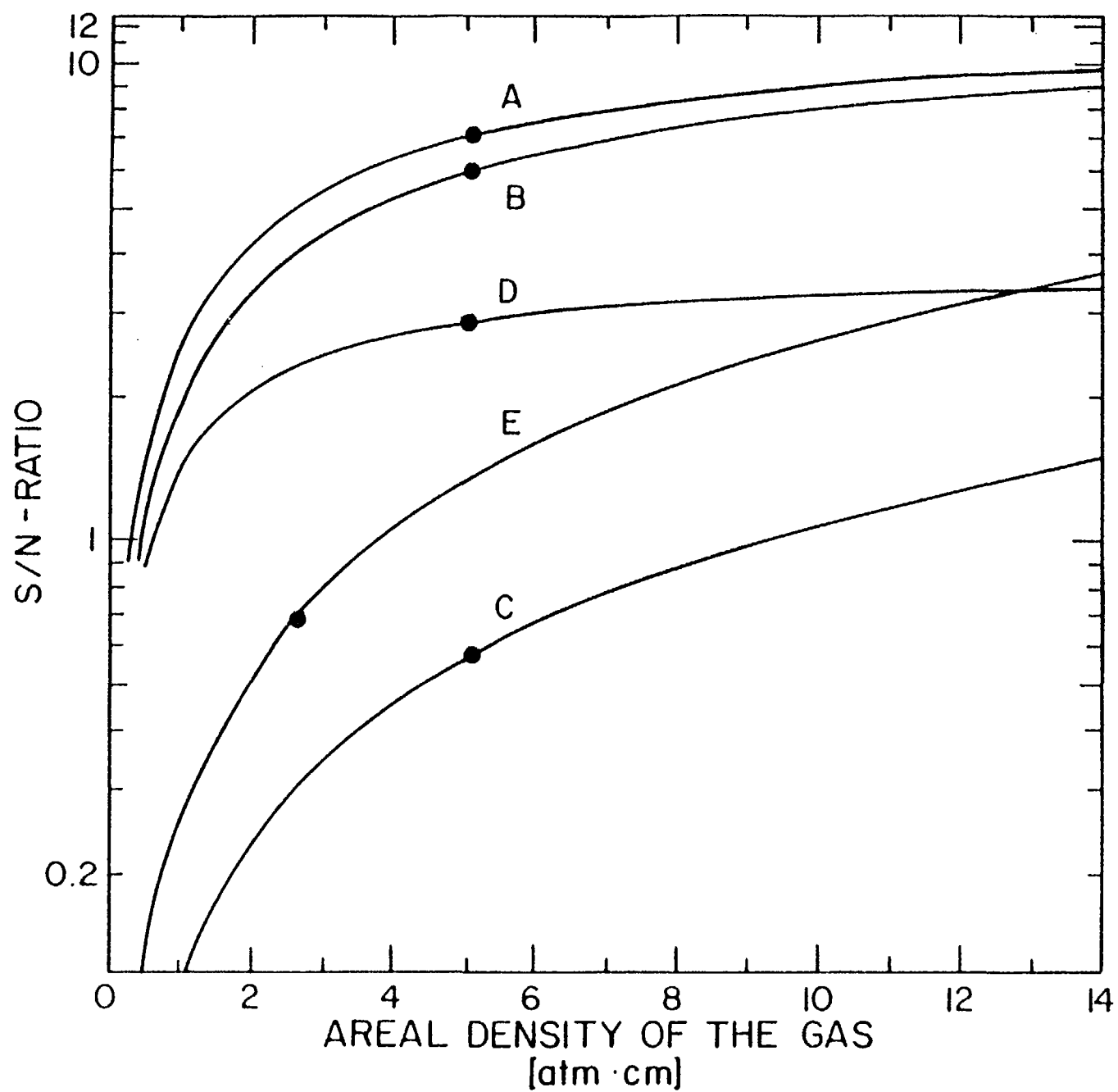


Fig. 5

Fig. 6



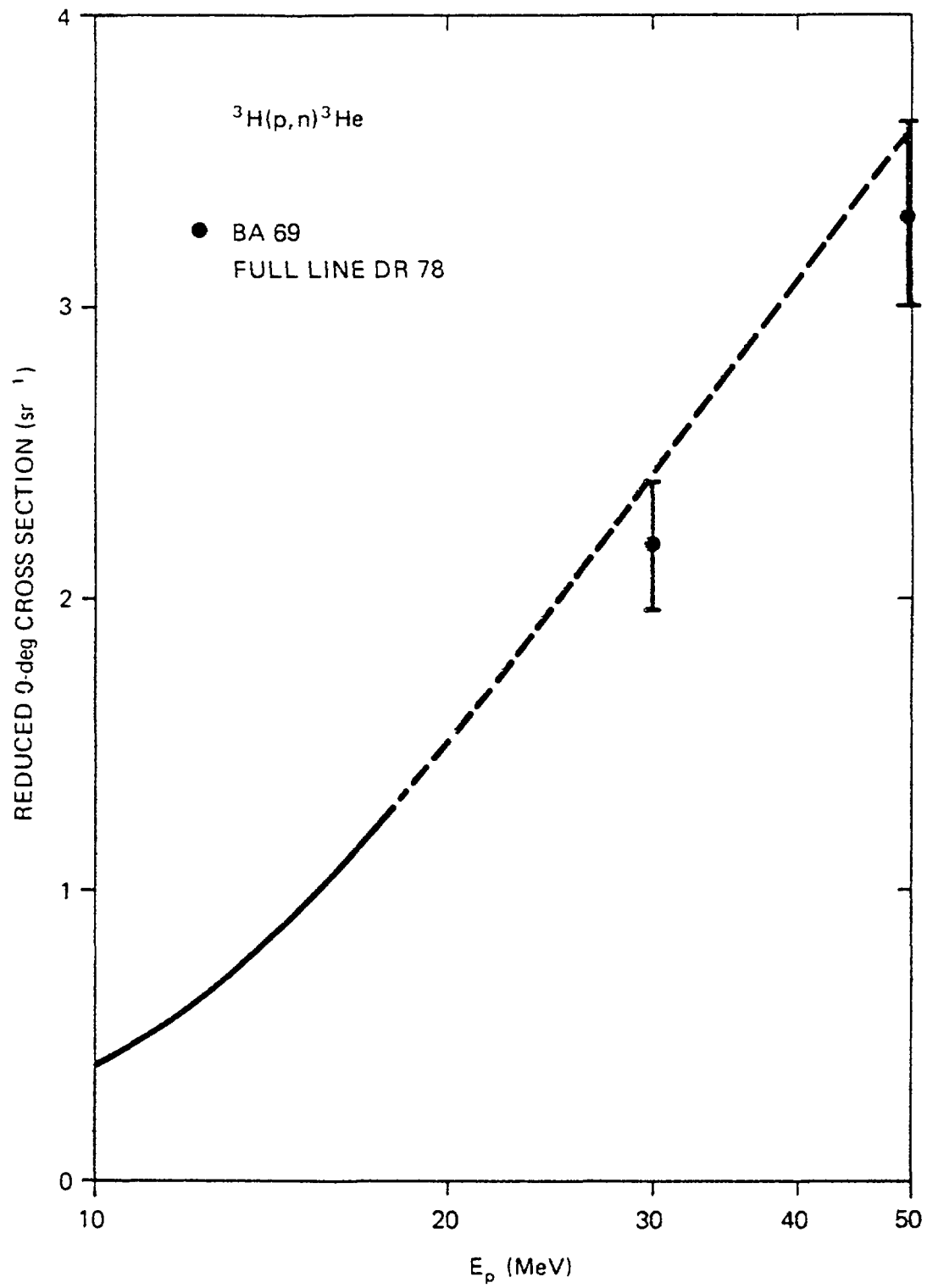


Fig. 7

Fig. 8

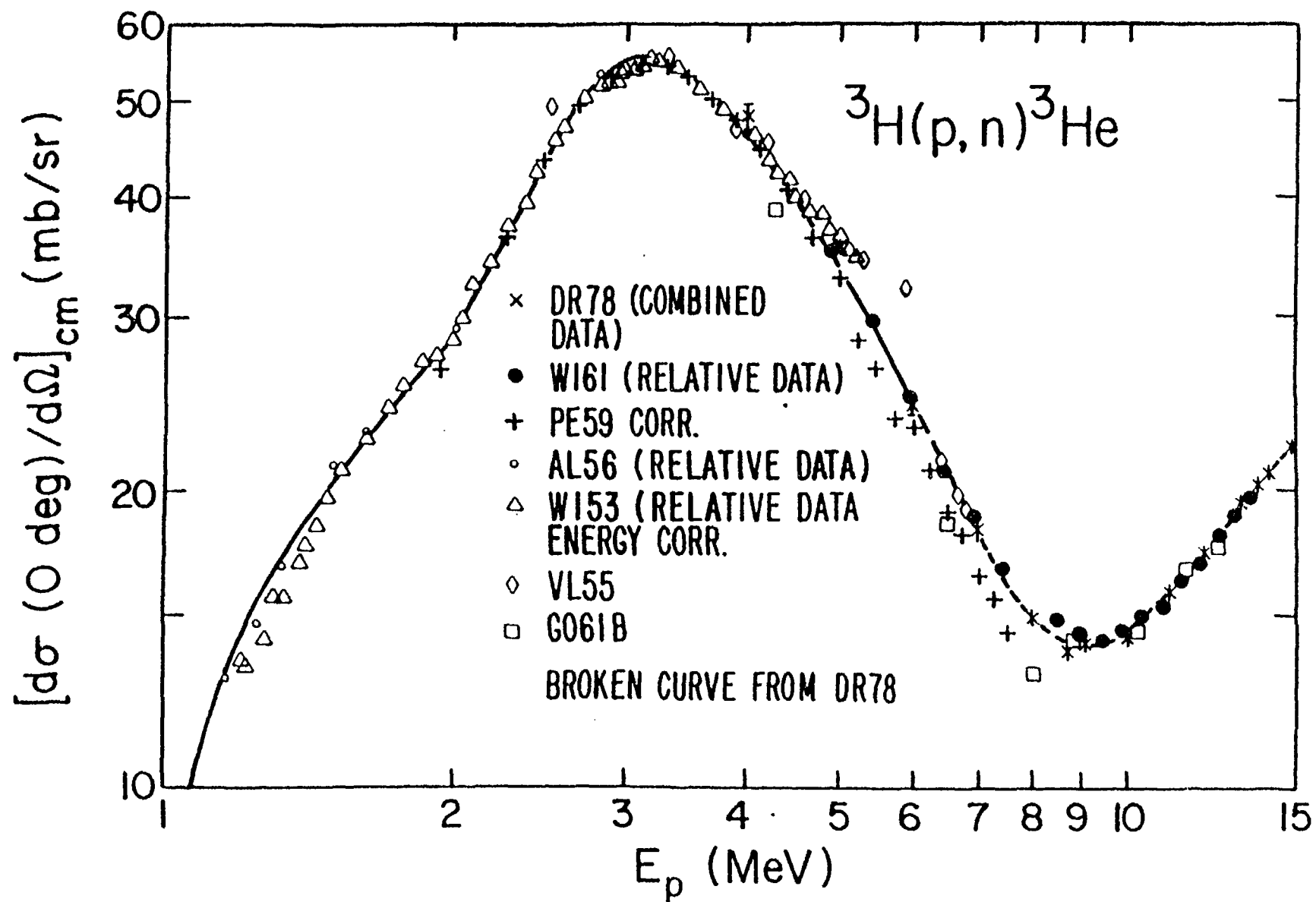


Fig. 9

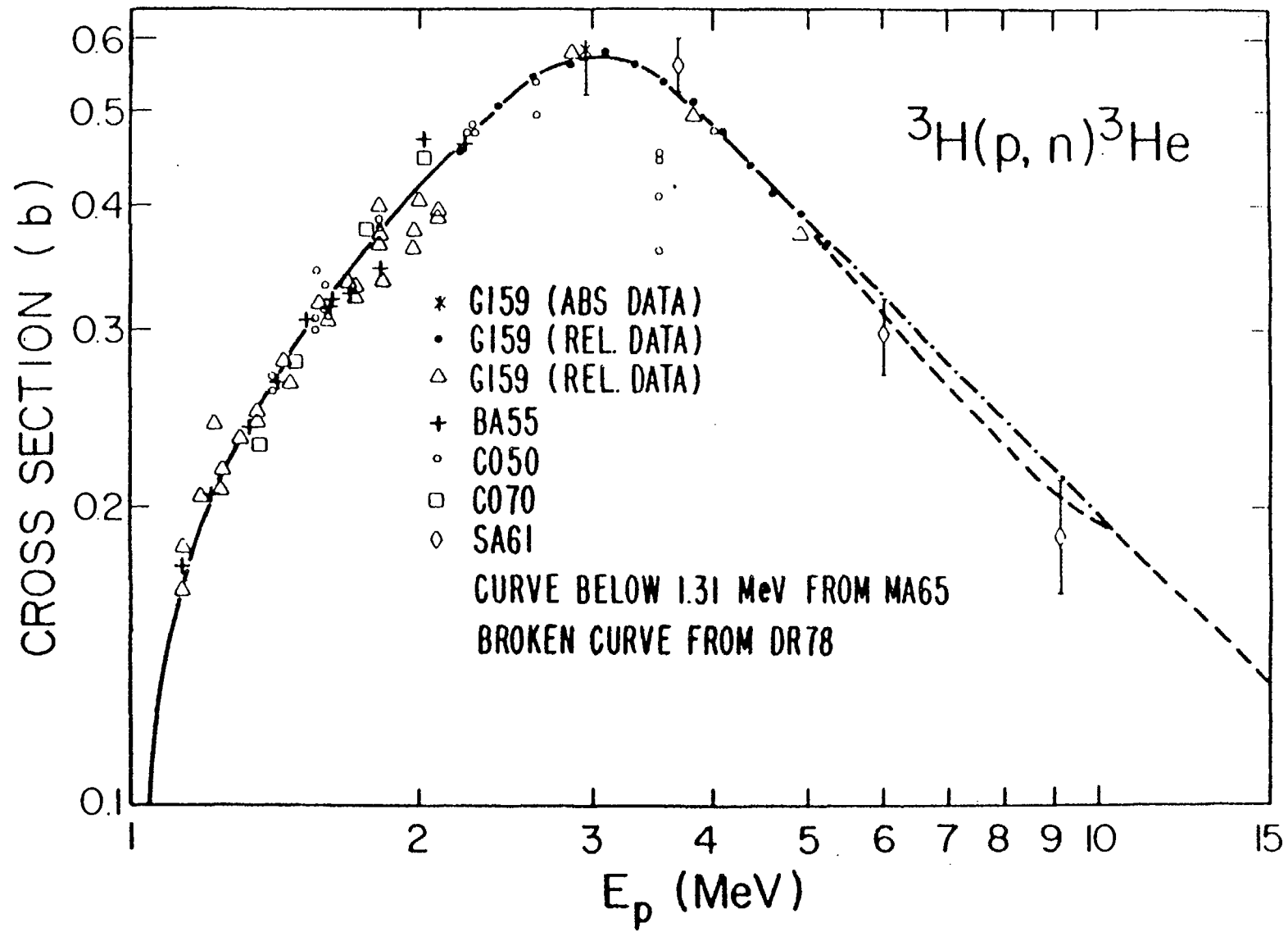
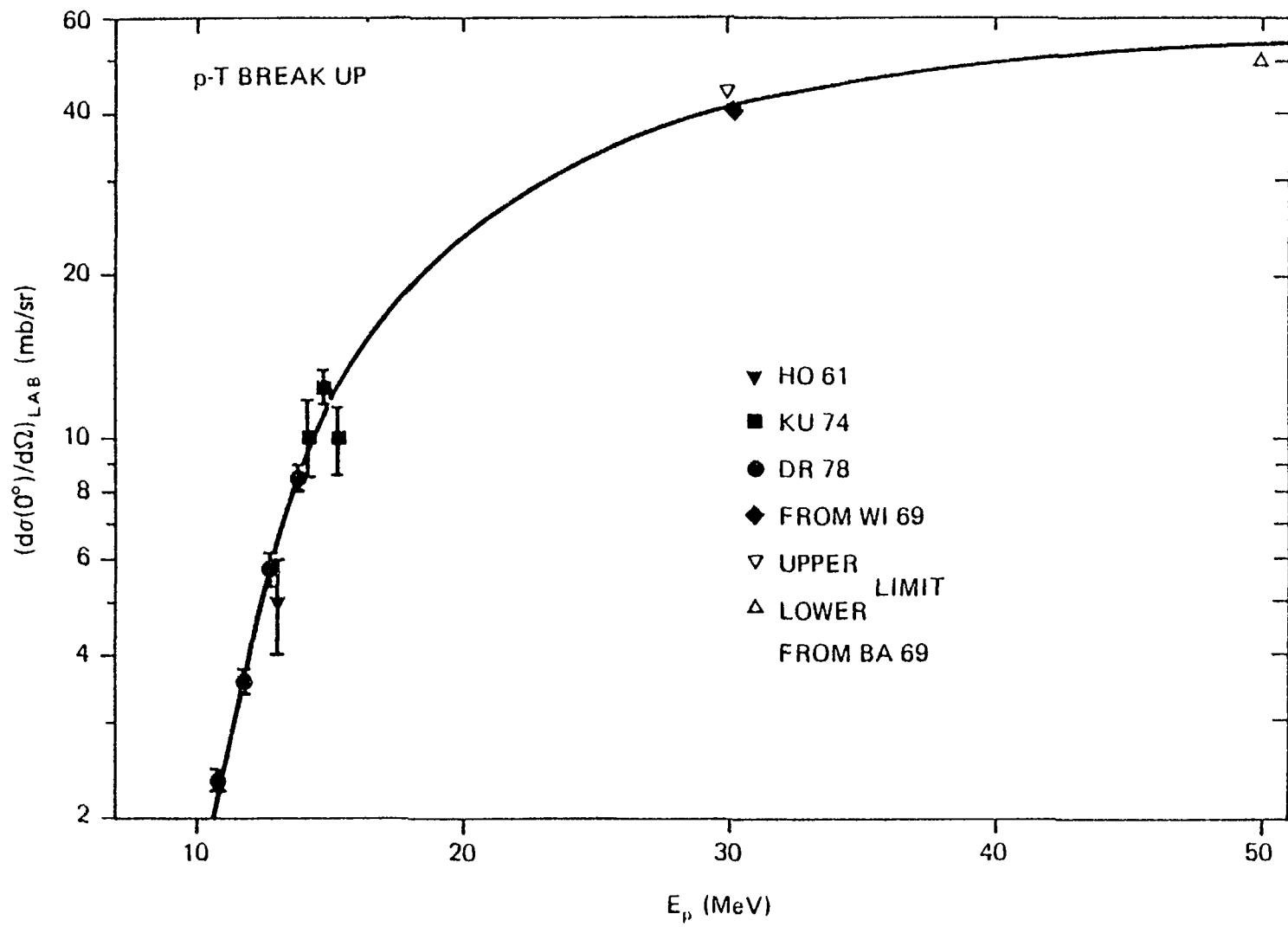




Fig. 10



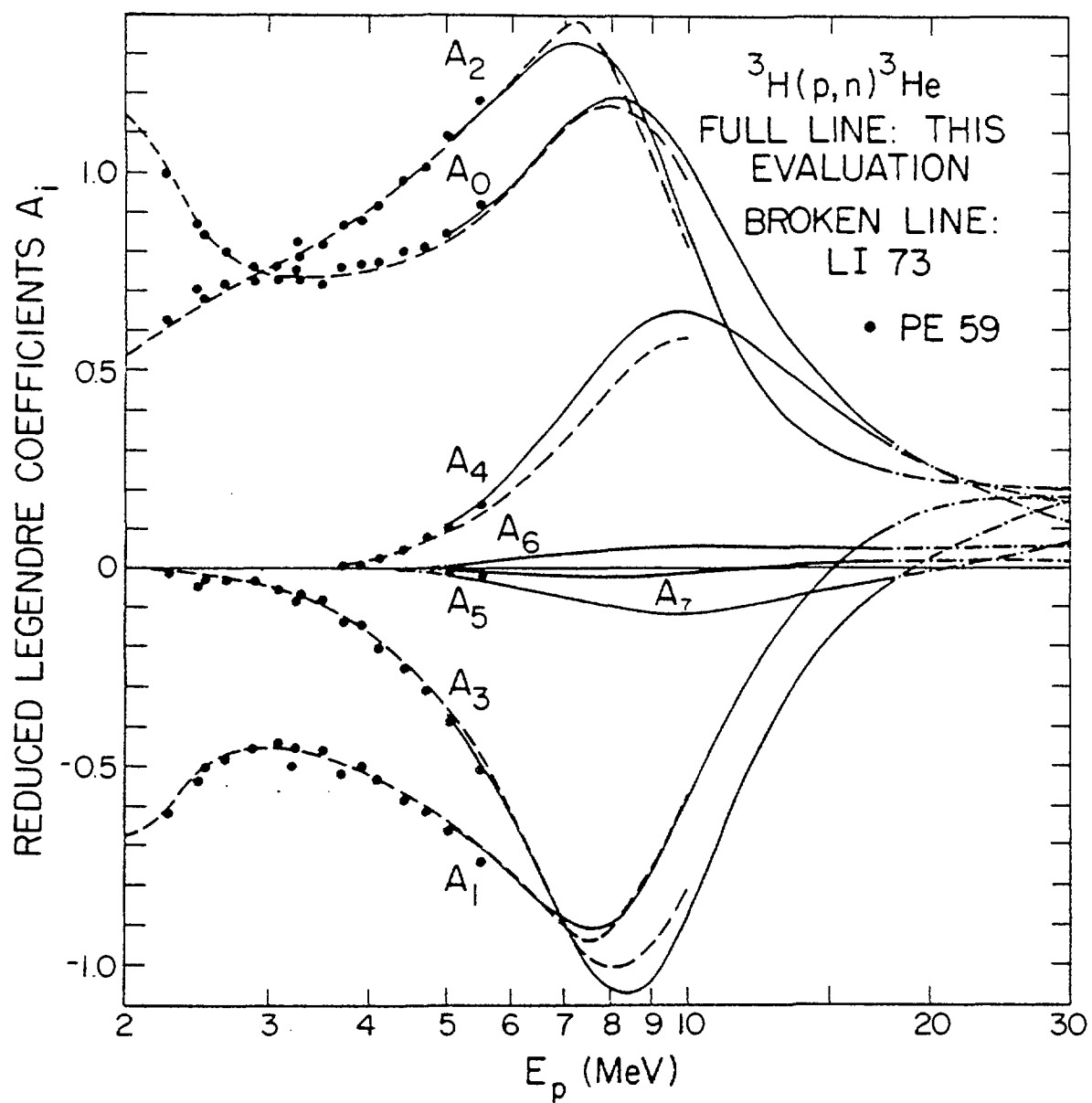


Fig. 11

Fig. 12

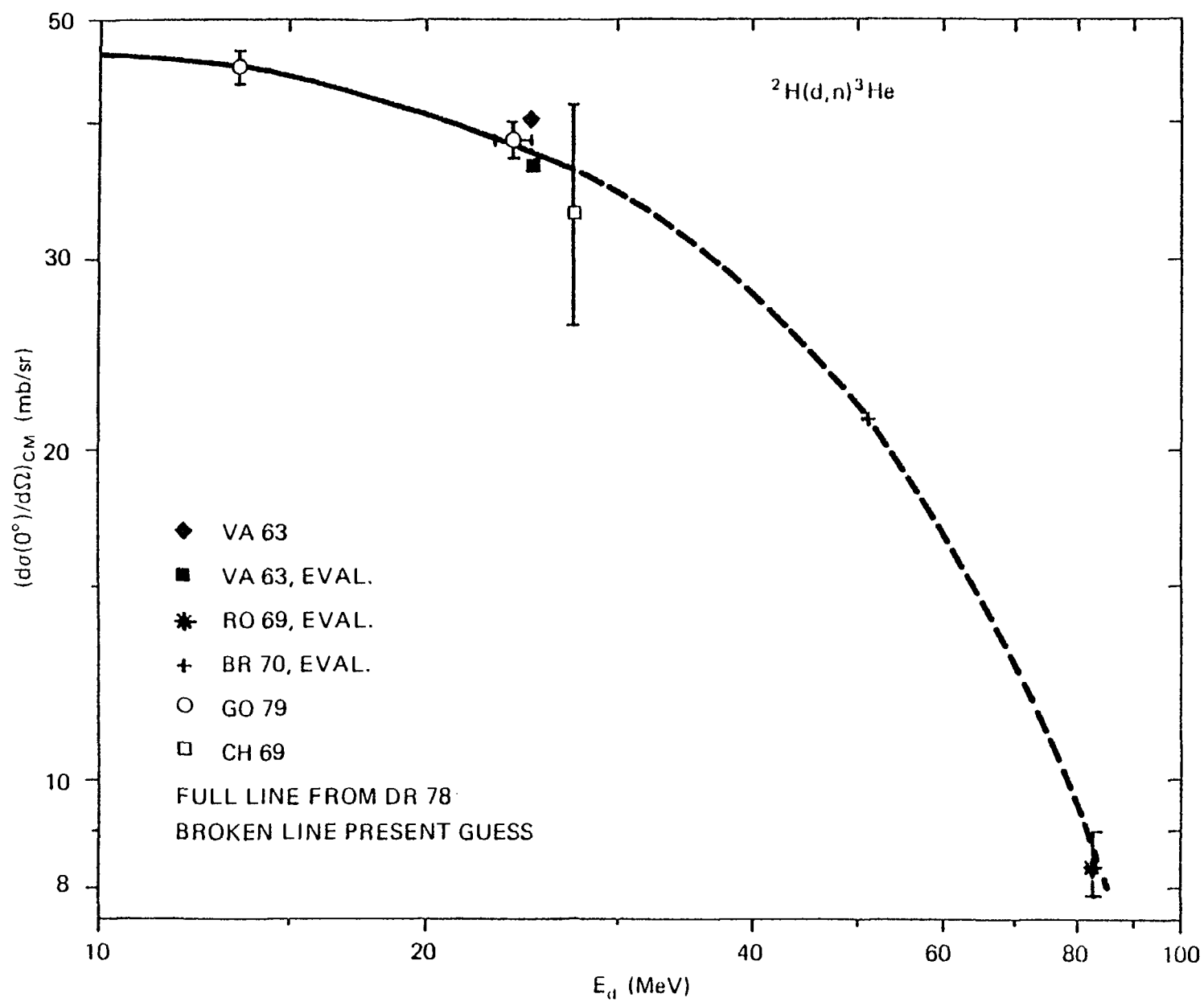
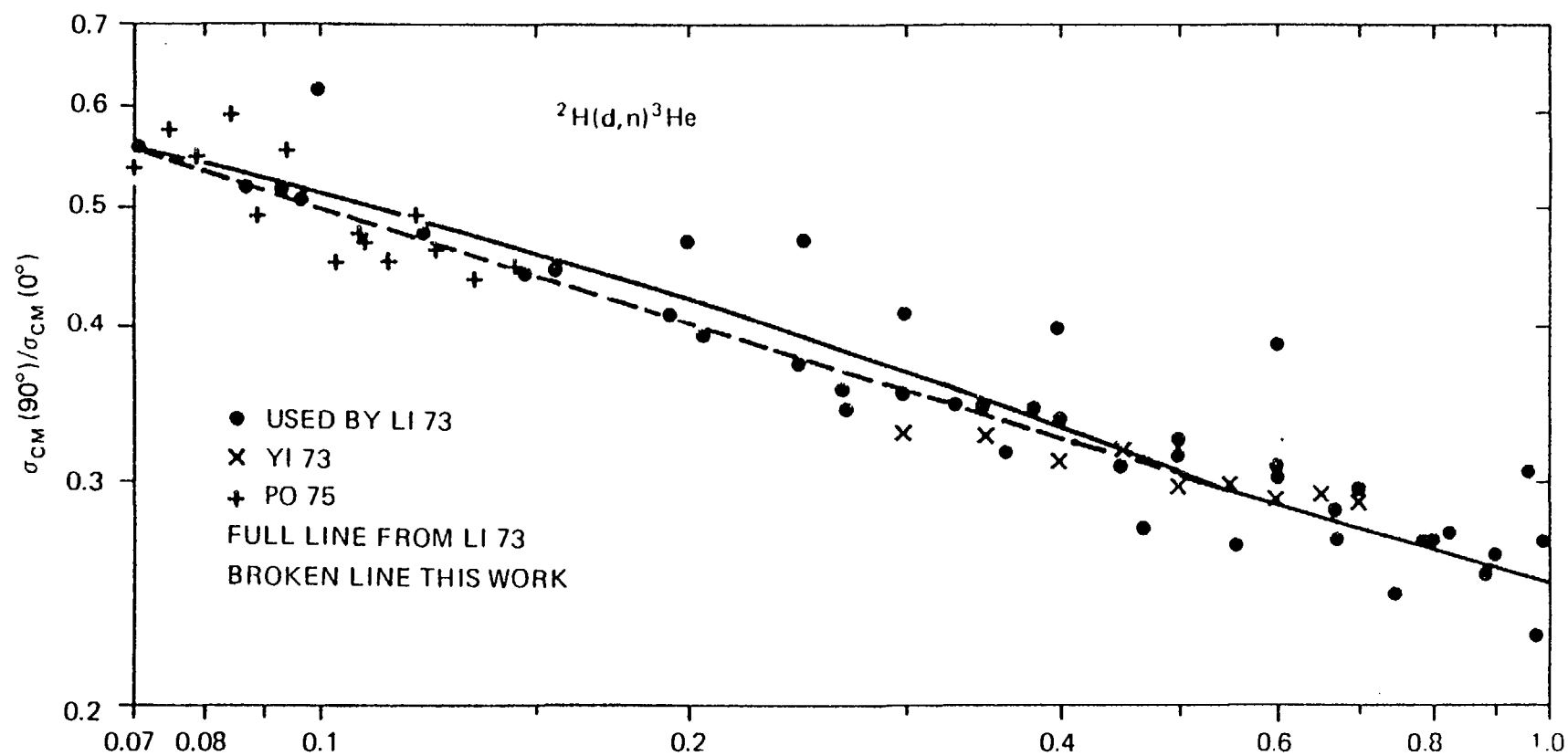


Fig. 13



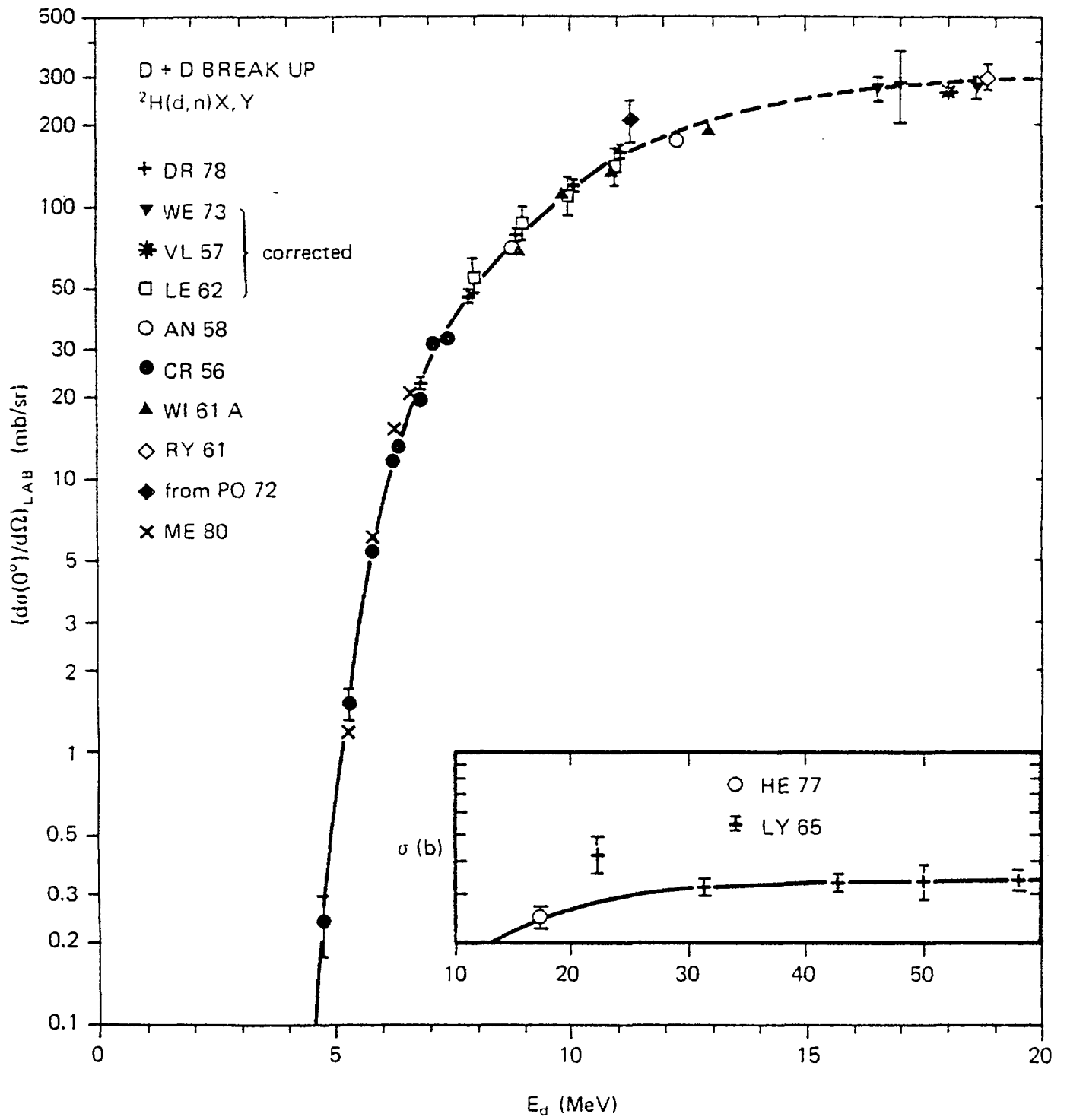
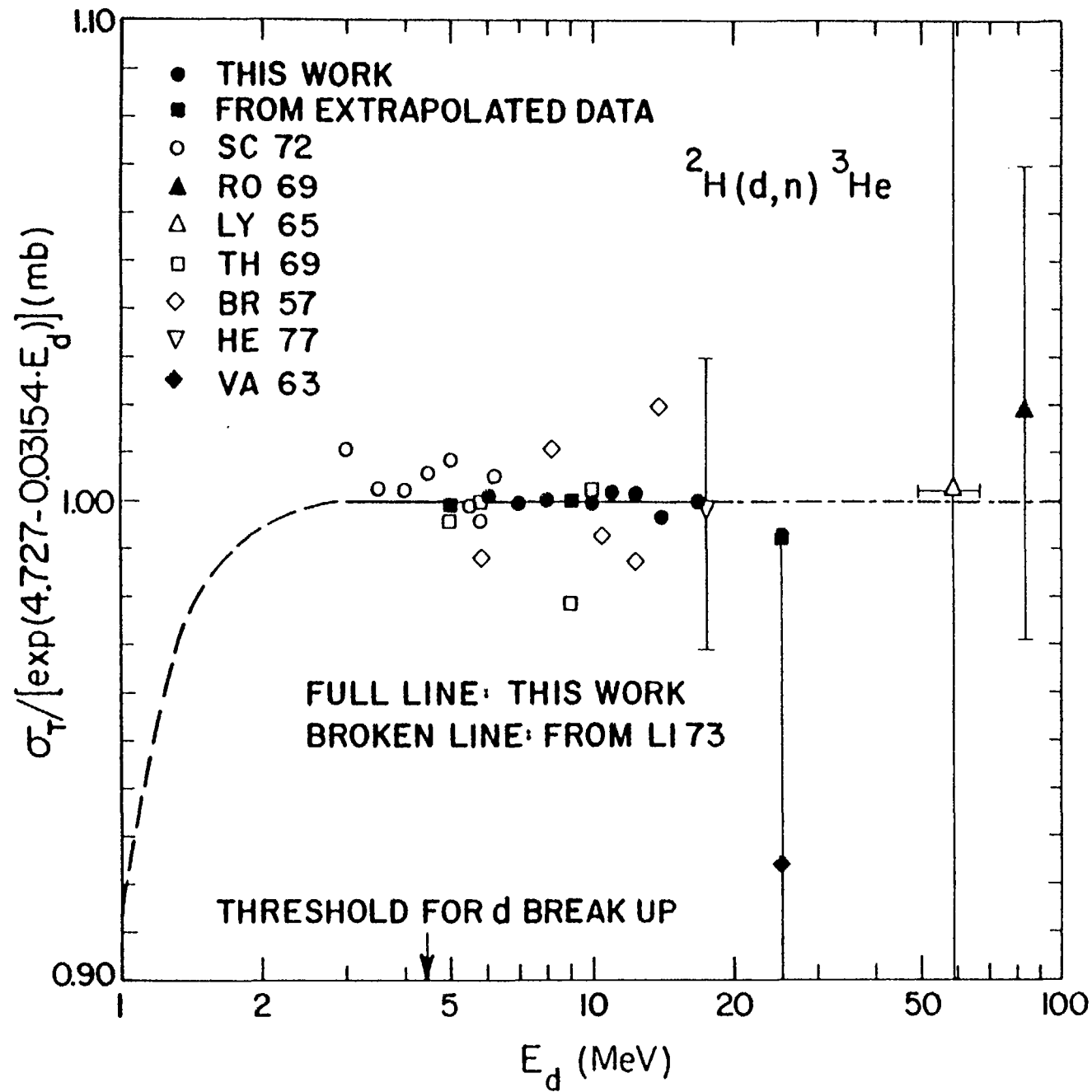


Fig. 14

Fig. 15



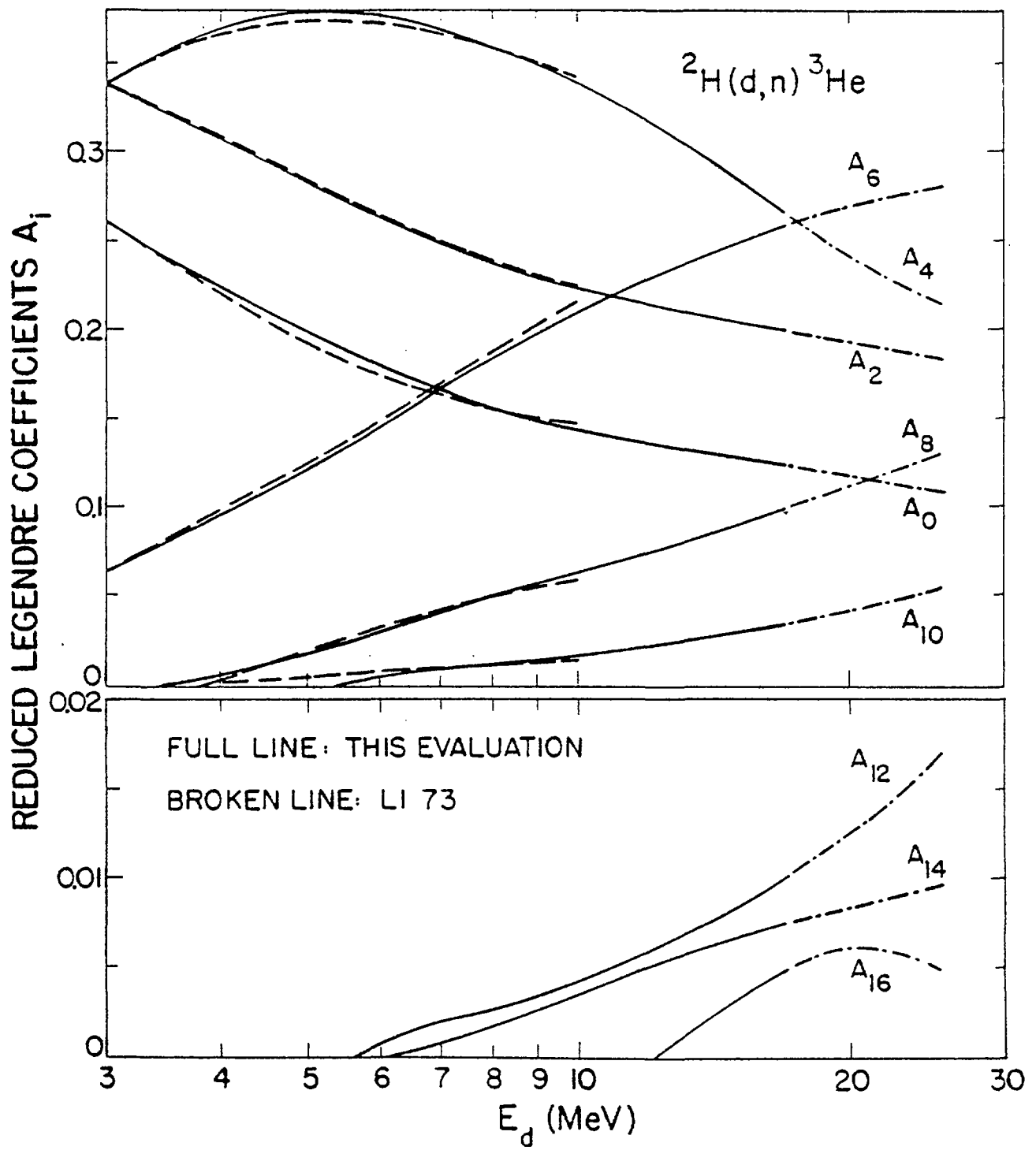


Fig. 16

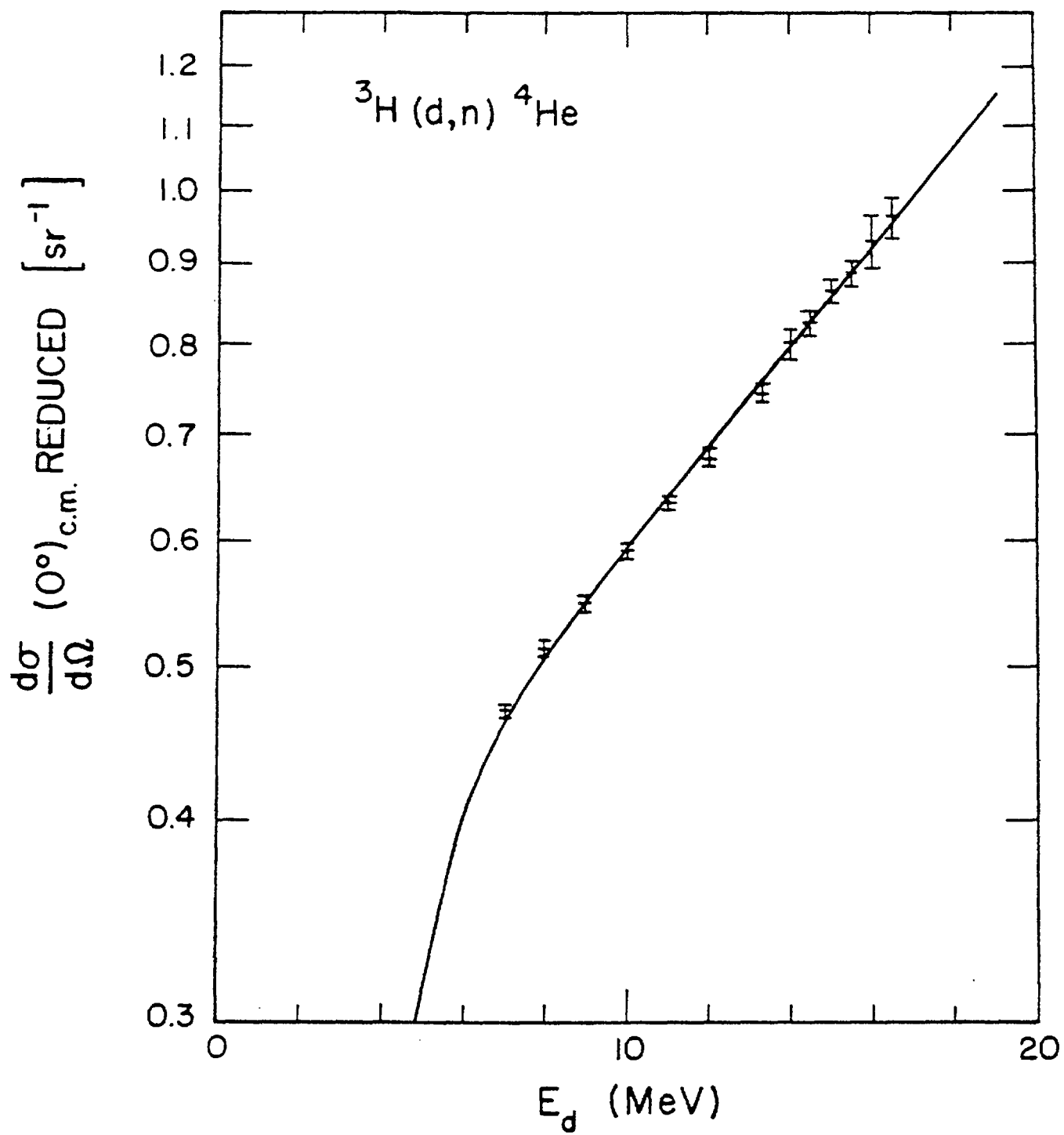


Fig. 17



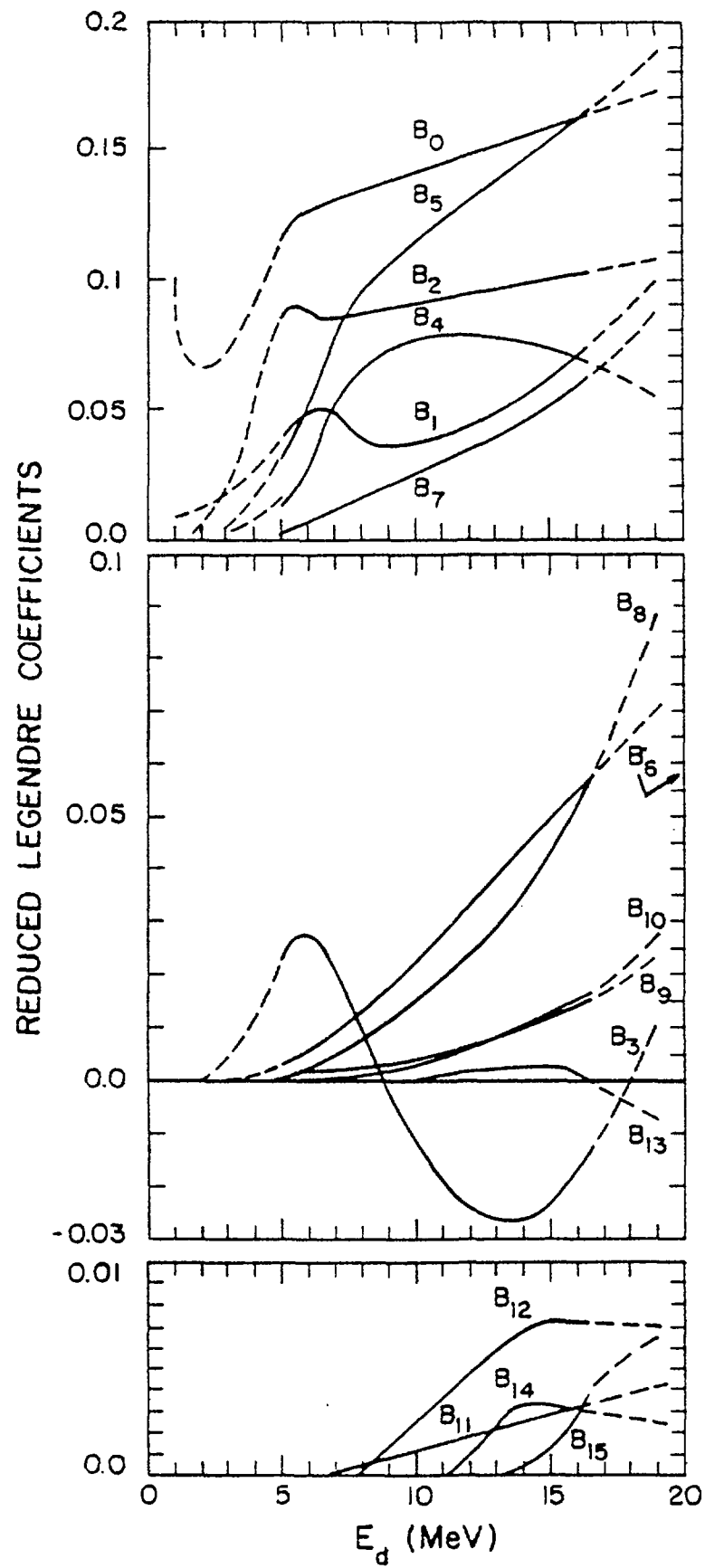


Fig. 18

Properties of Monoenergetic Neutron Sources from  
Proton Reactions with Nuclei other than Tritons.

M.Drosch

University of Vienna,  
Institut für Experimentalphysik, A-1090 Wien, AUSTRIA  
and  
Los Alamos Scientific Laboratory, Los Alamos, N.M.87545, USA

Abstract

The neutron source properties of  ${}^7\text{Li}(p,n){}^7\text{Be}$ ,  ${}^{45}\text{Sc}(p,n){}^{45}\text{Ti}$ ,  ${}^{51}\text{V}(p,n){}^{51}\text{Cr}$  and  ${}^9\text{Be}(p,n){}^9\text{B}$  are reviewed. The impact of new data on the last evaluation of the p-Li source is discussed. Special emphasis is laid on the production of neutrons below 100 keV (p-Sc and p-V) and of neutrons up to 40 MeV by the other reactions. The status is presented and recommendations for future work are given.

I. Introduction

Monoenergetic neutrons in the MeV range are usually produced by charged particle reactions among the hydrogen isotopes. This was discussed in the accompanying paper <sup>1)</sup>. However, for neutrons below 0.65 MeV the  ${}^7\text{Li}(p,n){}^7\text{Be}$  reaction has better properties than the competing  ${}^3\text{H}(p,n){}^3\text{He}$  reaction. At even lower energies also the p- ${}^7\text{Li}$  reaction fails. The minimum energy that can be produced at  $0^\circ$  is 120 keV. The production at other angles is usually much stronger contaminated by background neutrons. Therefore reactions like p-V and p-Sc with lower neutron energy limits of a few keV in the zero

degree direction can be useful despite their low cross sections.

The upper limit of monoenergetic neutron production by the hydrogen isotopes is 23 MeV (by the t-D reaction). Therefore background neutrons are unavoidable beyond that energy. At higher energies background from (p,n) reactions will obviously be smaller than that from (d,n) or (t,n) reactions where the charged particle beam itself produces background neutrons. Therefore only (p,n) reactions are considered for quasimonoenergetic neutron source reactions beyond 20 MeV. Aside from the p-T reaction <sup>1)</sup> the p-Li and the p-Be reaction are often considered, whereas for very high energy purposes the <sup>2</sup>H(p,n)2p reaction is often used.

## II. The <sup>7</sup>Li(p,n)<sup>7</sup>Be reaction

### II. A. Neutron Production below 10 MeV.

The p-<sup>7</sup>Li reaction was evaluated not too long ago<sup>2)</sup> up to 7 MeV proton energy. Neutrons from the breakup reaction <sup>7</sup>Li(p,n<sup>3</sup>He)<sup>4</sup>He with a threshold at 3.69 MeV usually limit the application of the p-<sup>7</sup>Li reaction to proton energies below 6 MeV. However, the p-Li source is truly monoenergetic only between 1.92 and 2.37 MeV proton energy, corresponding to 0.12 to 0.65 MeV neutron energy at zero degree. At 2.37 MeV is the threshold for the population of the first excited state in <sup>7</sup>Be (0.43 MeV excitation energy) so that above that energy two neutron groups with an energy separation of less than 0.5 MeV occur. At higher energies this separation is usually less than the instrumental resolution. (Reaction data are summarized in Ref.3). Table 1 summarizes measurements of the p-Li reaction which are needed to update <sup>4-7)</sup> Liskien's evaluation <sup>2)</sup> or to extend its energy range <sup>8-17)</sup>.

Fig.1 shows the integrated cross section of the p-Li reaction. New data <sup>6)</sup> deviate up to 7% near 1.9 MeV and about 3% near 3 MeV.

Fig.2 gives the zero degree excitation function. The information obtained from the three new data sets<sup>4,6,7)</sup> does not warrant any changes.

Fig.3 shows the ratio of the cross section for neutron production at zero degree through the first excited state and the ground state. It seems that in the evaluation the EL72 data<sup>18)</sup> had too much weight<sup>19)</sup>. An increase of about 5% in the 4-5 MeV range seems necessary<sup>19)</sup>. The new data<sup>4,7)</sup> in Fig.4 do not change the recommended Legendre coefficients for the angular distributions of the ground state neutrons although the coefficients near 5 MeV seem to depend too strongly on EL72<sup>18)</sup>.

Fig.5 gives the recommended Legendre coefficients for the angular distributions of neutrons from the first excited state. Due to lack of consistent data they are obviously not in a good shape. Inclusion of the new data measured with the associated gamma ray technique will improve the situation. (E.g., at 3.4 MeV the maximum disagreement in the shape of the recommended and the measured angular distribution is 10% at 77°).

Like in the p-T case one could consider to exchange target and incoming nucleus, i.e. one could consider to use the  $^1\text{H}(^7\text{Li},n)^7\text{Be}$  reaction. Between 13.1 MeV and 16.5 MeV lithium energy only neutrons from the ground state are produced with neutron energies at zero degree between 1.4 and 3.8 MeV. The cross section is extremely high (0.6b/sr for 3 MeV neutrons, however the second neutron group at 0° is neither negligible in energy nor in intensity (0.69 MeV, 75 mb/sr)).

## II. B. Neutron Production at Higher Neutron Energies

Between 6 and at least 23 MeV there is little interest in the p-Li reaction as "monoenergetic" neutron source, as both the cross section and the signal-to-background ratio are meagre. Near 30 MeV the cross section is still a factor of two less than that for the p-T reaction. However, the target is more convenient to handle so that p-Li will be the choice

for many experiments. In some cases the source energy resolution will limit its application. Due to the unresolved neutrons from the excited state it is restricted to about 0.5 MeV.

Fig.6 gives the zero degree excitation function at higher energies. From the data it can be concluded that the cross section between 30 and 50 MeV is known to better than 5%. From the point at 800 MeV <sup>20)</sup> it can be seen that the cross section continues to rise with increasing energy.

### III. Monoenergetic Neutrons below 120 KeV.

Below neutron energies of 120 keV the attractiveness of the  $p-^7\text{Li}$  reaction decreases with energy because these neutrons cannot be produced at  $0^\circ$  but only at bigger angles. Because of the anisotropy of both the intensity and the neutron energy, background from inscattered neutrons becomes more and more severe. Therefore alternative reactions must be considered to achieve clean monoenergetic conditions.

By increasing the mass of the target nucleus the lower limit for the neutron energy at zero degree can be reduced. However with heavier nuclei low lying levels become more likely. So neutron groups with lower energy will occur for energies above the corresponding threshold. Therefore only narrow energy bands for monoenergetic neutron production can be expected from these nuclei.

#### III. A. The $^{51}\text{V}(p,n)^{51}\text{Cr}$ Reaction

This reaction and some of its properties have already been reviewed in 1960<sup>21)</sup>. The threshold for the (p,n) reaction is 1.565 MeV, additional neutron groups appear at 2.335 MeV, 2.358 MeV, 2.76 MeV etc. The lower energy limit for monoenergetic neutron production at  $0^\circ$  is 2.36 keV, the upper limit 780 keV. The admixture of 0.25%  $^{50}\text{V}$  in natural vanadium does not introduce measureable background (less than 0.2%<sup>22,23)</sup>).

The differential cross section in the energy range of interest is 1 mb/sr and less, i.e. about two orders of magnitude less than corresponding backward cross sections of the  $p-^7\text{Li}$  reaction. The advantage of this source, aside from its cleanness, is the practicability of the target. It can easily be produced, is cheap, has good electrical and thermal conductivity and its stability allows high beam currents.

Because of the very small energy change between forward and backward angles the intensity can be increased in those cases which allow  $4\pi$  geometry. The source is not only isotropic with regard to neutron energies but also with regard to the intensity<sup>24)</sup>. Therefore approximate differential cross sections can be obtained from the total quite easily. However, the cross section shows many narrow resonances as shown in Fig. 7<sup>22)</sup>. They make the effective cross section at a given energy dependent on the target thickness. Therefore accurate differential cross sections with good energy resolution are of little practical value. Angular distribution measurements are reported up to  $E_p = 4$  MeV<sup>22-24)</sup>. Total cross section measurements<sup>23-30)</sup> are not very consistent. Part of the discrepancy stems from different target thicknesses and therefore resolutions, part is due to the difference in the methods: neutron detection versus associated activity method<sup>31)</sup>. By measuring the 320 keV gamma ray intensity accompanying the decay of  $^{51}\text{Cr}$  (half life 27.7 days) the amount of produced  $^{51}\text{Cr}$  and therefore the associated neutron flux can be calculated.

### III. B. The $^{45}\text{Sc}(p,n)^{45}\text{Ti}$ Reaction:

With a (p,n) threshold of 2.908 MeV this reaction is not accessible for small accelerators. Neutrons from the first excited state will be produced beyond 2.946 MeV. Therefore monoenergetic neutrons between 5.5 and 53 keV can be produced by this reaction. The disadvantage of such a small energy range compared to the p-V source is compensated for by a bigger cross section. E.g. it is about 2mb/sr for 20 keV neutrons which compares with 15 mb/sr for backangle neutron production by  $p\text{-}^7\text{Li}$ . However, the neutron spectrum is much cleaner and the gamma background smaller<sup>32)</sup>. Like in the case of the p-V reaction, the energy anisotropy is negligible. Another disadvantage compared with the p-V reaction is the short half life of 3.1 hours of the  $\beta^+$  decaying daughter nucleus. Application of the associated activity method<sup>31)</sup> for the determination of the neutron flux does not allow long irradiation times. However, a kind of associated  $\gamma$ -ray technique<sup>33)</sup> can be applied, using a

calibrated  $\gamma$ -ray detector as monitor. Even total cross section data in the energy range of interest are sparse <sup>34)</sup>. The use of the p-Sc reaction for calibrating radiation protection detectors is discussed in Ref. 35.

#### IV. Monoenergetic Neutron Production above 20 MeV

Up to 23 MeV truly monoenergetic neutrons can be produced by the t-D reaction. However, the differential cross section is rather low (about 10 mb/sr <sup>1)</sup>). In addition, the background from the target structure hit by the tritons will usually be high. At energies above 23 MeV there is no neutron source that is intrinsically monoenergetic. However, several source reactions with unfavourable signal-to-background ratio around 10 MeV become relatively cleaner with increased energy. The most important (p,n) reactions for production of neutrons at higher energies are those with D, T, <sup>7</sup>Li and <sup>9</sup>Be. Spectra for 30 and 50 MeV are given in Fig. 8 <sup>12)</sup>. The p-T reaction was discussed in the accompanying paper <sup>1)</sup> the p-<sup>7</sup>Li in chapter II. At energies around 40 MeV the <sup>2</sup>H(p,n)2p reaction, which is widely used as neutron source at very high energies, has lower cross sections and worse energy resolution than its competitors <sup>12-14)</sup>. Therefore we confine our discussion here to the <sup>9</sup>Be(p,n)<sup>9</sup>B reaction.

##### IV. A. The <sup>9</sup>Be(p,n)<sup>9</sup>B reaction

The threshold energy for the (p,n<sub>0</sub>) reaction is 2.06 MeV. However, neutron production sets in already at 1.85 MeV by the (p,p'n) reaction with a very low cross section. The threshold for the next neutron group is 4.76 MeV. As can be seen from Fig. 8 the intensity of this neutron group with a 2.43 MeV lower energy is not negligible. Angular distributions and differential cross sections at lower energies have been measured with typical errors of about 10% <sup>36-40)</sup>. These are, however, of little importance for neutron production. At 15 MeV the signal-to-background ratio is about 1/4 <sup>11)</sup>. It improves to something like 1/2 at 50 MeV.

Differential cross sections for the zero degree neutron production <sup>11-14, 36, 37, 41)</sup> are shown in Fig. 9.



## V. Conclusions and Recommendations

### V. A. ${}^7\text{Li}(p,n){}^7\text{Be}$ :

The new data for energies up to 7 MeV which were not included into Liskien's evaluation <sup>2)</sup> suggest only minor changes, although the EL72 data <sup>18)</sup> might have too much weight in the analysis <sup>19)</sup>. However, some changes regarding the cross sections of the excited state will be necessary.

From using this reaction for low energy efficiency measurements <sup>42)</sup> it appears that the  ${}^7\text{Li}(p,n){}^7\text{Be}$  cross section predictions are not as consistent as needed for a careful (relative) efficiency calibration. Therefore a consistency check with the quasiabsolute method as detailed in the accompanying paper <sup>1)</sup> at several neutron energies for as many proton energies as possible would be very valuable.

Above 25 MeV only zero degree neutron production cross sections are important. Between 30 and 50 MeV the present accuracy level of 5% seems to be adequate for most applications.

### V. B. Low Energy Sources

Judging from the few publications in this field, these sources are not in common use yet. The strong structure complicates the use of differential cross sections for flux determinations (together with current integration and determination of the target thickness). An application oriented program to measure yields for several target thicknesses over the monoenergetic energy range is needed.

### V. C. Higher Energy Sources

Cross sections for the zero degree neutron production by p-Li between 30 and 50 MeV appear to be accurate to 5% which

seems to be sufficient. The p-T cross sections, as evaluated in Ref.1 are at the upper edge of the 10% error bars of actual measurements. Verifying data will be needed to give confidence in these predictions at a 5% level. The state of the  ${}^9\text{Be}(p,n){}^9\text{B}$  data is not very good. The scatter of the points allows only to determine the cross sections between 30 and 50 MeV within  $\pm 10\%$  to  $\pm 15\%$ . There is obviously more work needed.

Up to now the  ${}^1\text{H}(t,n){}^3\text{He}$  source was not considered for producing neutrons of higher energy, although its cross section is appreciable higher than even those of the p-T reaction (see Ref.1). It remains to be seen whether the background from the structure is really so high that this source cannot compete.

Acknowledgements: Figures 1 through 5 were made available through C.A.Uttley together with valuable comments of H.Liskien. This great help is duly appreciated.

R e f e r e n c e s

- 1) M.Drosg, this Meeting
- 2) H.Liskien and A.Paulsen, Nucl.Data Tables 15, 57 (1975)
- 3) J.W.Meadows and D.L.Smith, this Meeting
- 4) C.H.Poppe, J.D.Anderson, J.C.Davis, S.M.Grimes, and C.Wang, Phys.Rev.C14, 438 (1976)
- 5) J.D.Brandenberger, F.D.Smyder, J.D.Dawson, T.W.Burrows, and F.D.McDaniel, Nucl.Instr.Methods 138, 321 (1976) and J.D.Brandenberger, Associated Gamma Ray Technique for Neutron Fluence Measurements, pp227, Neutron Standards and Applications, NBS Spec.Publ.493 (1977)
- 6) K.K.Sekharan, H.Laumer, B.D.Kern and F.Gabbard Nucl.Instr.Methods 133, 253 (1976)
- 7) C.A.Burke, M.T.Lunnon and H.W. Lefevre, Phys.Rev.C10, 1299 (1974)
- 8) S.D.Schery, L.E.Young, R.R.Doering, S.M.Austin, R.K.Bhowmik, Nucl.Instr.Methods 147, 399 (1977)
- 9) R.R. Borchers and C.H.Poppe, Phys.Rev.129, 2679 (1963)
- 10) C.Whitehead, Rev.Mod., Phys.39, 538 (1967)
- 11) M.W.McNaughton, N.S.P.King, F.P.Brady, J.L.Romero and T.S.Subramanian, Nucl.Instr.Methods 130, 555 (1975)
- 12) C.J.Batty, B.E.Bonner, A.I.Kilvington, C.Tschalär and L.E.Williams, Nucl.Instr.Methods 68, 273 (1969)
- 13) M.Bosman, P.Leleux, P.Lipnik, P.Macq, J.P.Meulders, R.Petit, C.Pirart and G.Valenduc, Nucl.Instr.Meth.148, 363 (1978)

- 14) J.L.Romero, F.P.Brady and J.A.Jungerman, Nucl.Instr.Methods 134  
537 (1976) revision of J.Å.Jungerman, F.P.Brady, W.J.Knox,  
T.Montgomery, M.R.McGie, J.L.Romero and Y.Ishizaki,  
Nucl.Instr.Meth.94, 421 (1974)
- 15) J.D.Anderson, C.Wong, and V.A.Madsen, Phys.Rev.Lett.24,  
1074 (1970)
- 16) P.J.Locard, S.M.Austin, and W.Benenson, Phys.Rev.Lett.19,  
1141 (1967)
- 17) J.W.Wachter, R.T.Santaro, T.A.Love, and W.Zobel,  
Nucl.Instr.Methods 113, 185 (1973)
- 18) S.A.Elbakr, I.J.Van Heerden, W.J.McDonald, and G.C.Neilson,  
Nucl.Instr.Methods 105, 519 (1972)
- 19) H.Liskien, private communication, transmitted through  
C.A.Uttley, 1980
- 20) P.J.Riley, C.W.Bjork, C.R.Newsom, M.L.Evans, G.Glass,  
J.C.Hiebert, M.Jain, R.A.Kenefick, L.C.Northcliffe,  
B.E.Bonner, J.E.Simmons, N.Stein, Phys.Lett.68B, 217 (1977)
- 21) J.B.Marion, in Fast Neutron Physics (eds.J.B.Marion and  
J.L.Fowler; Interscience, New York, 1960) part 1, ch.1.D.
- 22) J.H.Gibbons, R.L.Macklin and H.W.Schmitt, Phys.Rev.100,  
167 (1955)
- 23) K.K.Harris, H.A.Grench, R.G.Johnson and F.J.Vaughn,  
Nucl.Instr.Methods 33, 257 (1965)
- 24) G.Deconninck, J.Royen, Nucl.Instr.Methods 75, 266 (1969)
- 25) M.K.Mehta, S.Kailas, K.K.Sekharan, Pramana 9, 419 (1977)
- 26) J.Wing, J.R.Huizenga, Phys.Rev.128, 280 (1962)

- 27) C.H.Johnson, A.Galonsky, C.N.Inskeep, Cross Sections for (p,n) Reactions in Intermediate-Weight Nuclei, Report ORNL-2910, p25 (1960)
- 28) J.H.Gibbons and R.L.Macklin, Nucl.Instr.Methods 37, 330 (1965)
- 29) C.H.Johnson, A.Galonsky and J.P.Ulrich, Phys.Rev.109, 1243 (1958)
- 30) R.Michel, G.Brinkmann, H.Weigel, W.Herr Nucl.Phys.A322, 40 (1979)
- 31) K.K.Sekharan, Associated Activity Method, pp234 of Neutron Standards and Applications, NBS Spec.Publ.493 (1977)
- 32) D.W.O.Rogers, Nucl.Instr.Methods 142, 475 (1977)
- 33) J.D.Brandenberger, Associated Gamma-Ray Technique for Neutron Fluence Measurements, pp227 of Neutron Standards and Applications, NBS Spec.Publ.493, (1977)
- 34) G.F.Dell, W.D.Ploughe and H.J.Hausman, Nucl.Phys.64 513 (1965)
- 35) M.Cosack, S.Guldbakke and H.Klein, this Meeting
- 36) R.C.Byrd, K.Murphy, P.Guss, C.Floyd, R.L.Walter, Cross Section Measurements for  $^9\text{Be}(p,n)^9\text{B}$ ,  $^{15}\text{N}(p,n)^{15}\text{O}$  and  $^{13}\text{C}(p,n)^{13}\text{N}$  TUNL annual report, OR-1667-17 (1978)
- 37) B.D.Walker, C.Wong, J.D.Anderson, and J.W.McClure Phys.Rev.137B, 1504 (1965)
- 38) J.B.Marion and J.S.Levin, Phys.Rev.115, 144 (1959)
- 39) R.D.Albert, S.D.Bloom, and N.K.Glendenning Phys.Rev.122, 862 (1961)

- 40) C.A.Kelsey, G.P.Lietz, S.F.Trevino, and S.E.Darden,  
Phys.Rev.129, 759 (1963)
- 41) G.D.Goodman, The (p,n) reaction at intermediate energy.  
CONF-790126--2 (1979)
- 42) M.Drosg, D.M.Drake and P.W.Lisowski, The contribution  
of Carbon Interactions to the Neutron Counting Efficiency  
of Organic Scintillators, Report LA-7987MS, Los Alamos  
Scientific Laboratory, 1980.

T A B L E 1

Measurements of  $^7\text{Li}(p,n)$  Cross Sections Not Included in Ref.2  
(Symbols in accordance with Ref.2).

Symbol	Author(s)	Reference	Exc.State	Angular range (Center-of-Mass degrees)	Proton Energy (Lab) (MeV)
--------	-----------	-----------	-----------	-------------------------------------------	---------------------------------

Absolute Data

SC77	Schery et al.	8	also	0...160	24.8...45
PO76	Poppe et al.	4	also	3.5 <sup>0</sup> ...160	15.1...26
				3.5 <sup>0</sup>	4 ...12
				3.5 <sup>0</sup>	15.1...26
BR77	Brandenberger	5	only	0...155	3.1...4.9
SE76	Sekharan et al.	6	both	total	1.9...4.2
WH67	Whitehead	10	both	0	94
MC75	McNaughton et al.	11	both	0	14.3...29.6
BA69	Batty et al.	12	both	0	30,50
BO78	Bosman et al.	13	both	0,20	50
RO76	Romero et al.	14	both	0	29.4...50.6
AN70	Anderson et al.	15	both	5...140	9.8,19.6
LO67	Locard et al.	16	only	total	2.3...52
WA73	Wachter et al.	17	both	0	41,64

Relative Distributions

BO63	Borchers and Poppe	9	also	0	3.2....13
				yes	4....9
BU74	Burke et al.	7	no	0...170	2.1...3.8

F i g u r e   c a p t i o n s

- Fig.1. Integrated cross sections of the  ${}^7\text{Li}(p,n){}^7\text{Be}$  reaction. The curves are the recommended values of Ref.2. (SE76 is Ref.6)
- Fig.2. Zero degree center-of-mass neutron production cross section by the  ${}^7\text{Li}(p,n){}^7\text{Be}$  reaction. The curve is recommended by Ref.2. (For symbols see Table 1)
- Fig.3. Ratio of  $0^\circ$  center-of-mass cross sections for the reactions  ${}^7\text{Li}(p,n){}^7\text{Be}^*$  and  ${}^7\text{Li}(p,n){}^7\text{Be}$ . The curve is from Ref.2 (PO76 is Ref.4)
- Fig.4. Legendre coefficients for the reaction  ${}^7\text{Li}(p,n){}^7\text{Be}$ . Curves are the recommended values of Ref.2. (For symbols see Table 1)
- Fig.5. Legendre coefficients for the reaction  ${}^7\text{Li}(p,n){}^7\text{Be}^*$ . Curves are recommended values of Ref.2. (For symbols see Table 1)
- Fig.6. Zero degree neutron production cross sections for the  ${}^7\text{Li}(p,n){}^7\text{Be}$  ( $0+0.43$  MeV) reaction in the laboratory system (RI 77 is Ref.20, other symbols see Table 1)
- Fig.7. Forward yield of the  ${}^{51}\text{V}(p,n)\text{Cr}^{51}$  reaction. (From Ref.22)
- Fig.8. Zero degree neutron spectra from the p-D, p-T, p- ${}^7\text{Li}$  and p- ${}^9\text{Be}$  reactions at 30 and 50 MeV (from Ref.12). The energy scale gives the distance from the mono-energetic peak.
- Fig.9. Zero degree neutron production cross sections for the  ${}^9\text{Be}(p,n){}^9\text{B}$  reaction in the laboratory system. (BY 78 is Ref. 36, WA 65 is Ref. 17, GO 79 is Ref. 41, other symbols see Table 1)



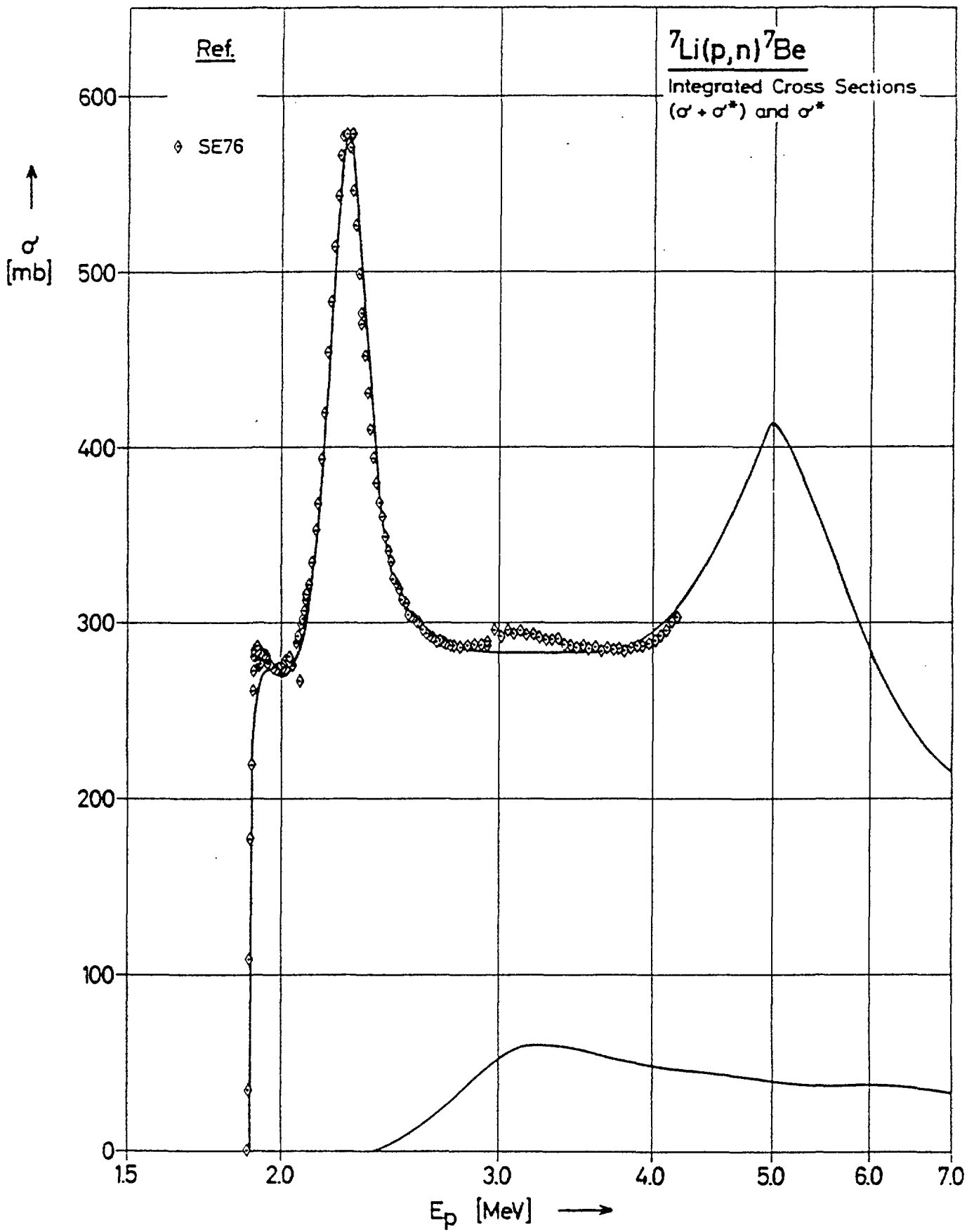


Fig. 1

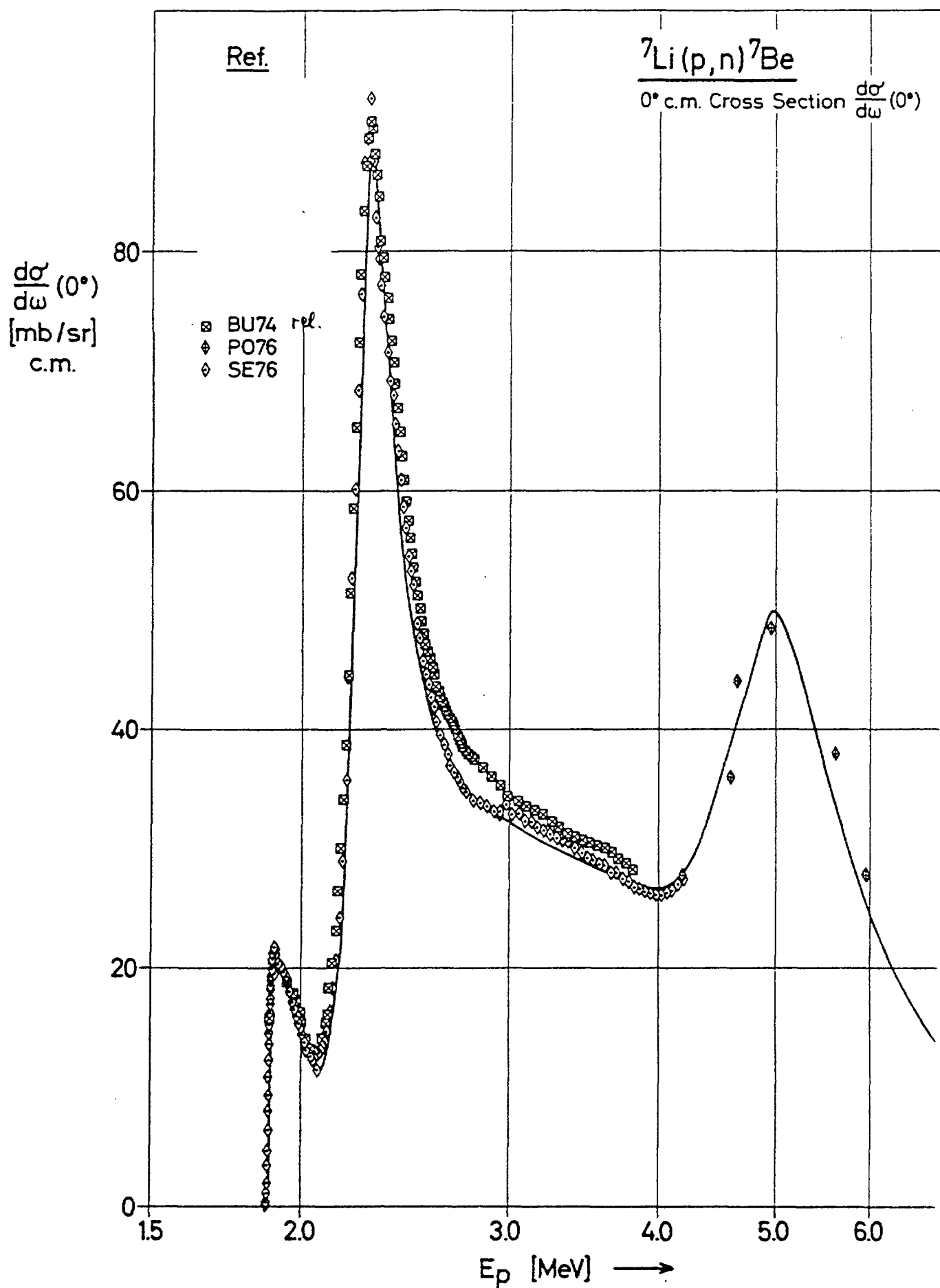


Fig. 2

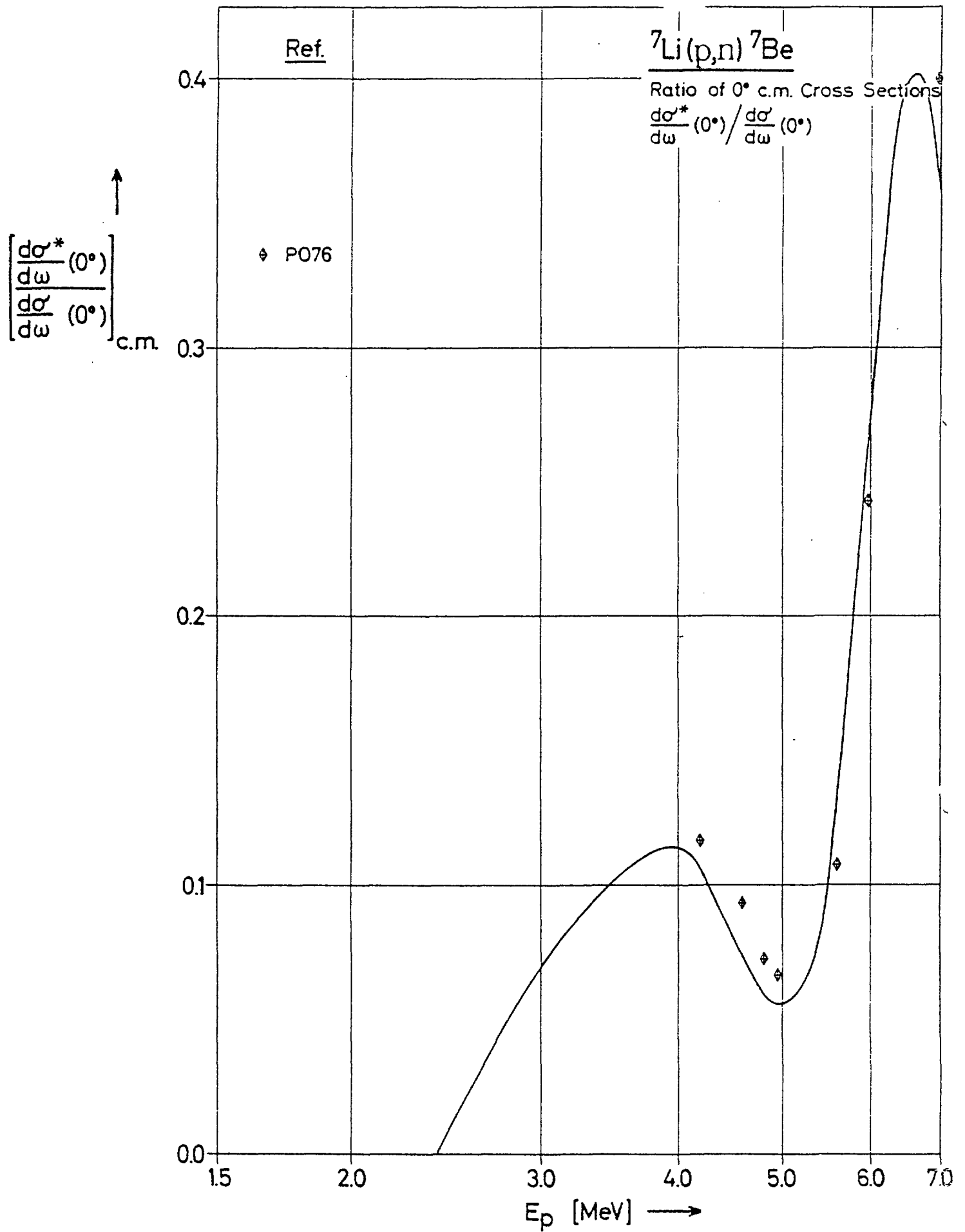


Fig. 3

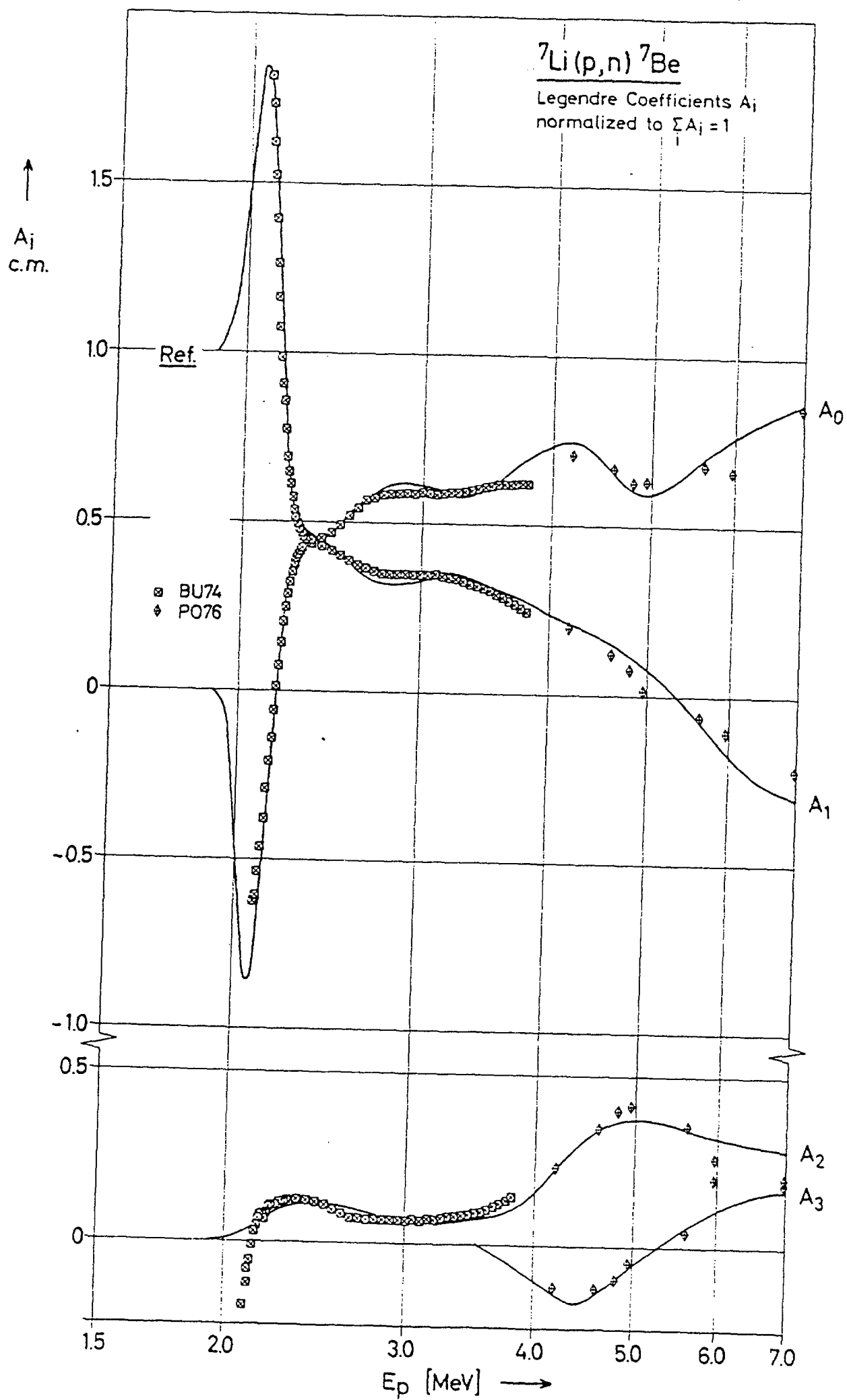


Fig. 4

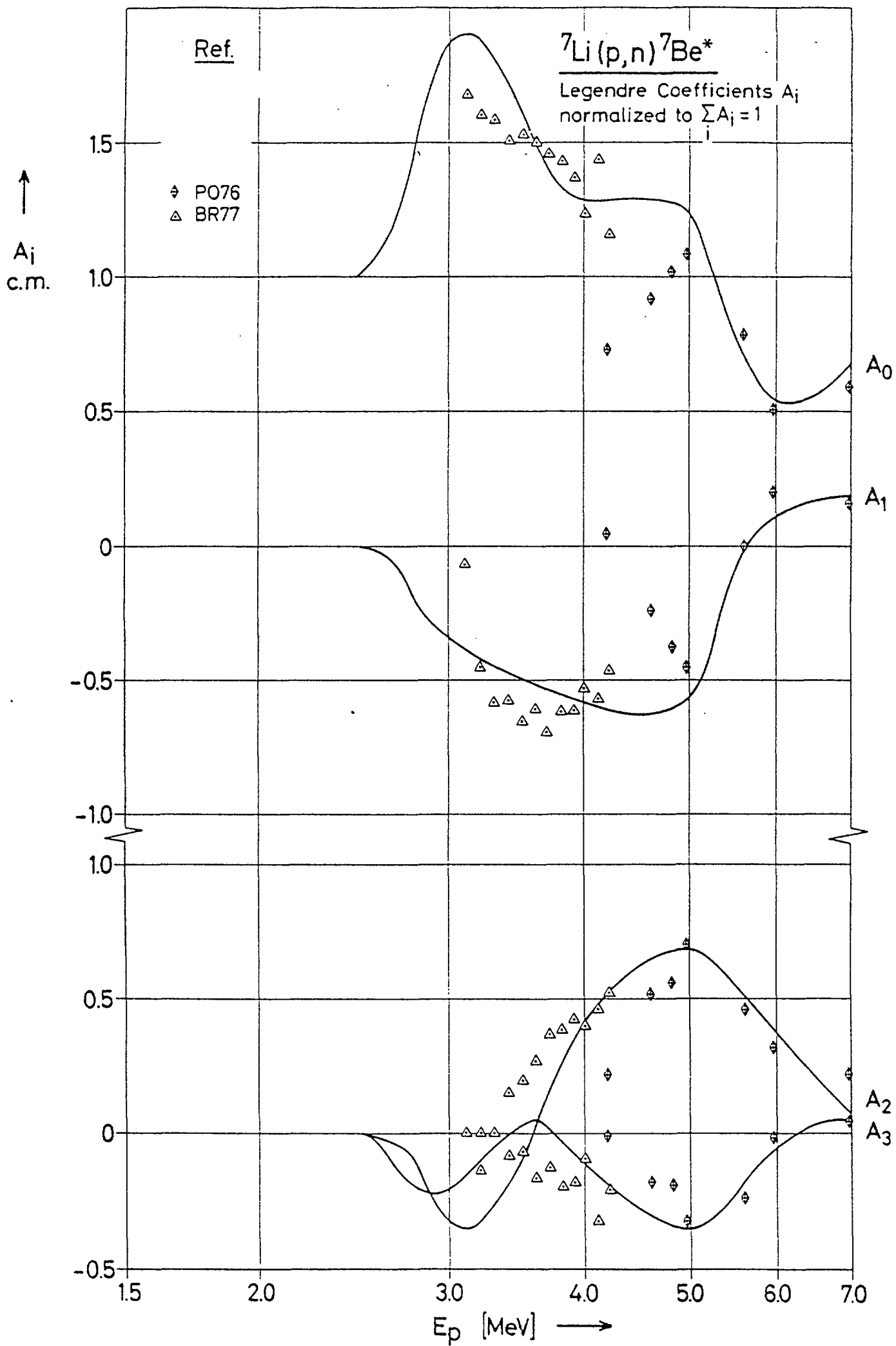
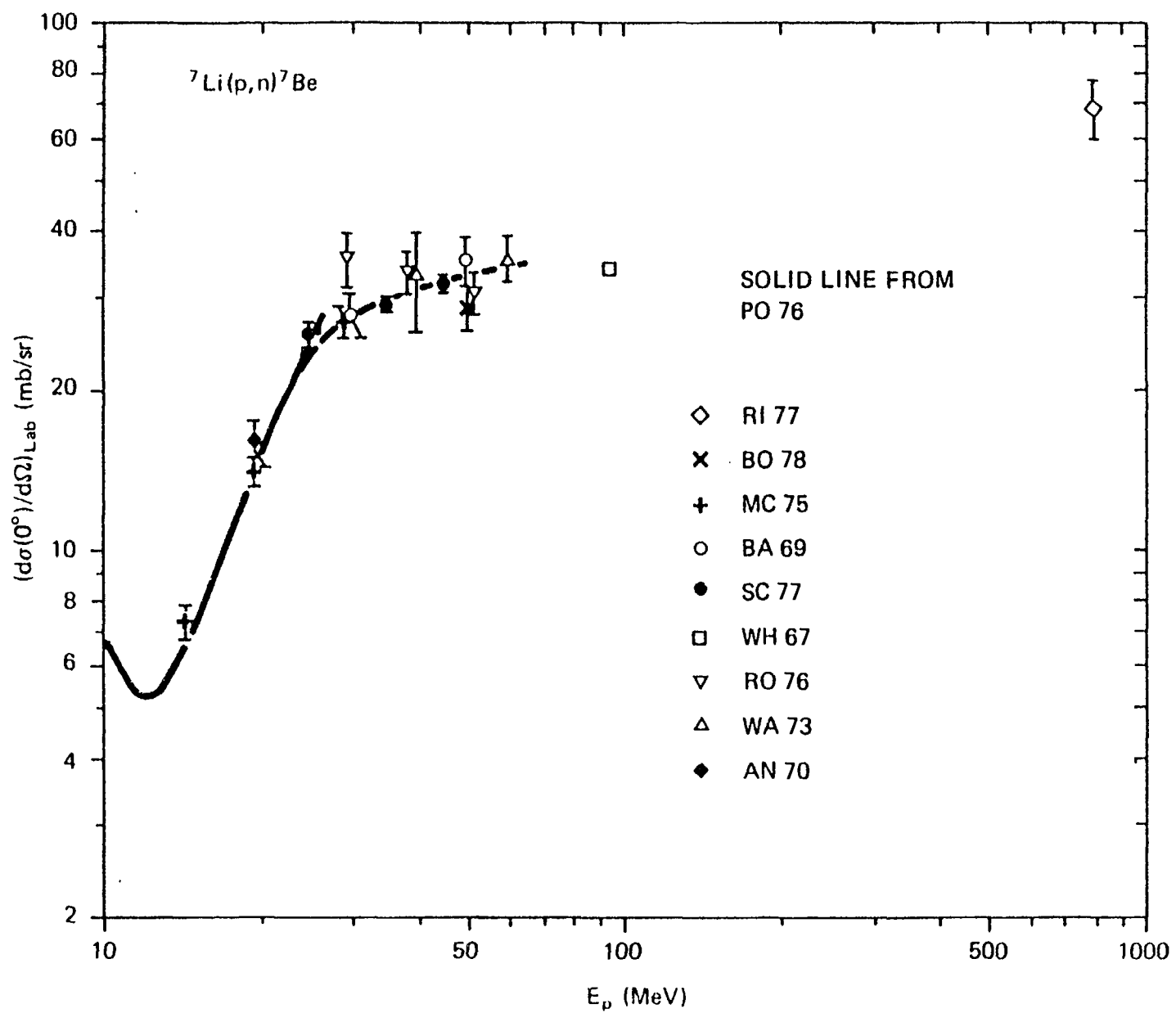


Fig. 5

Fig. 6



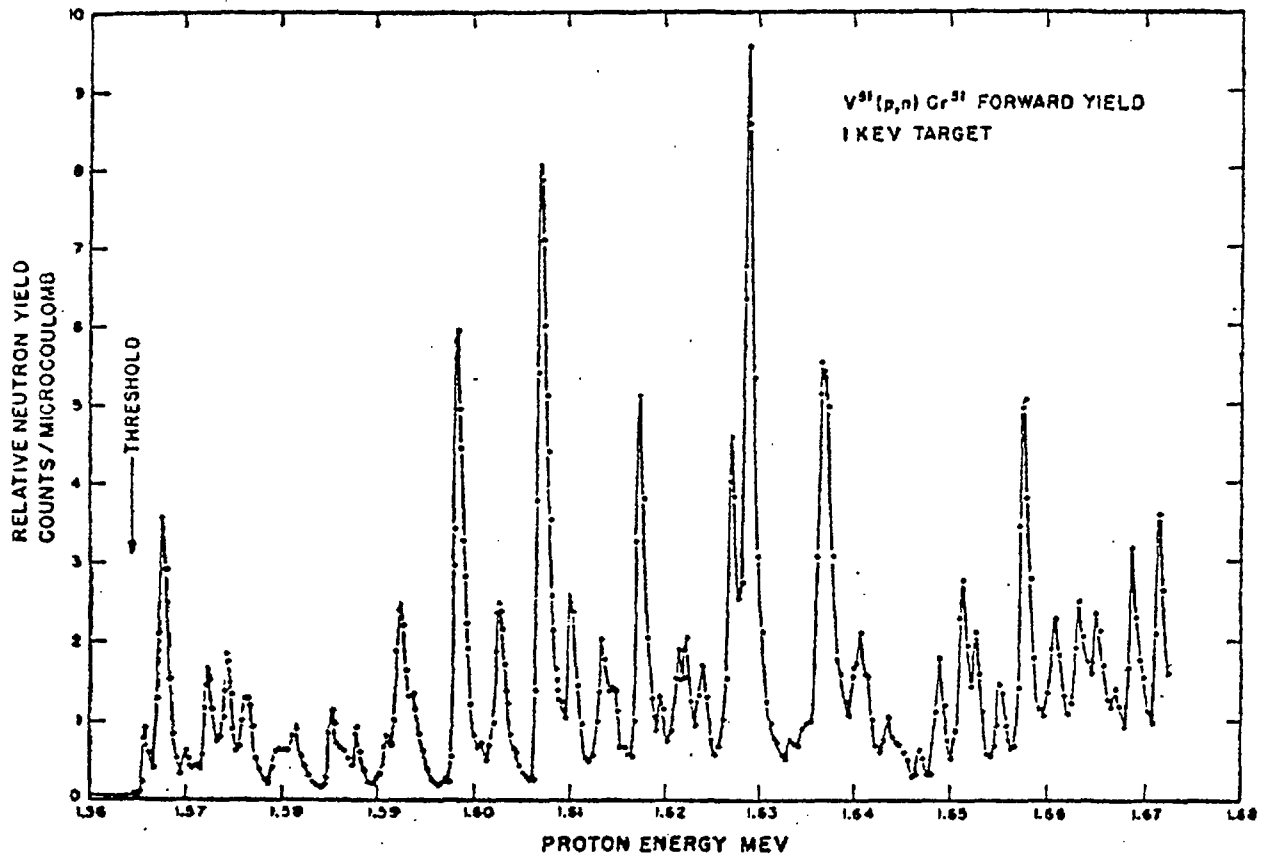


Fig. 7

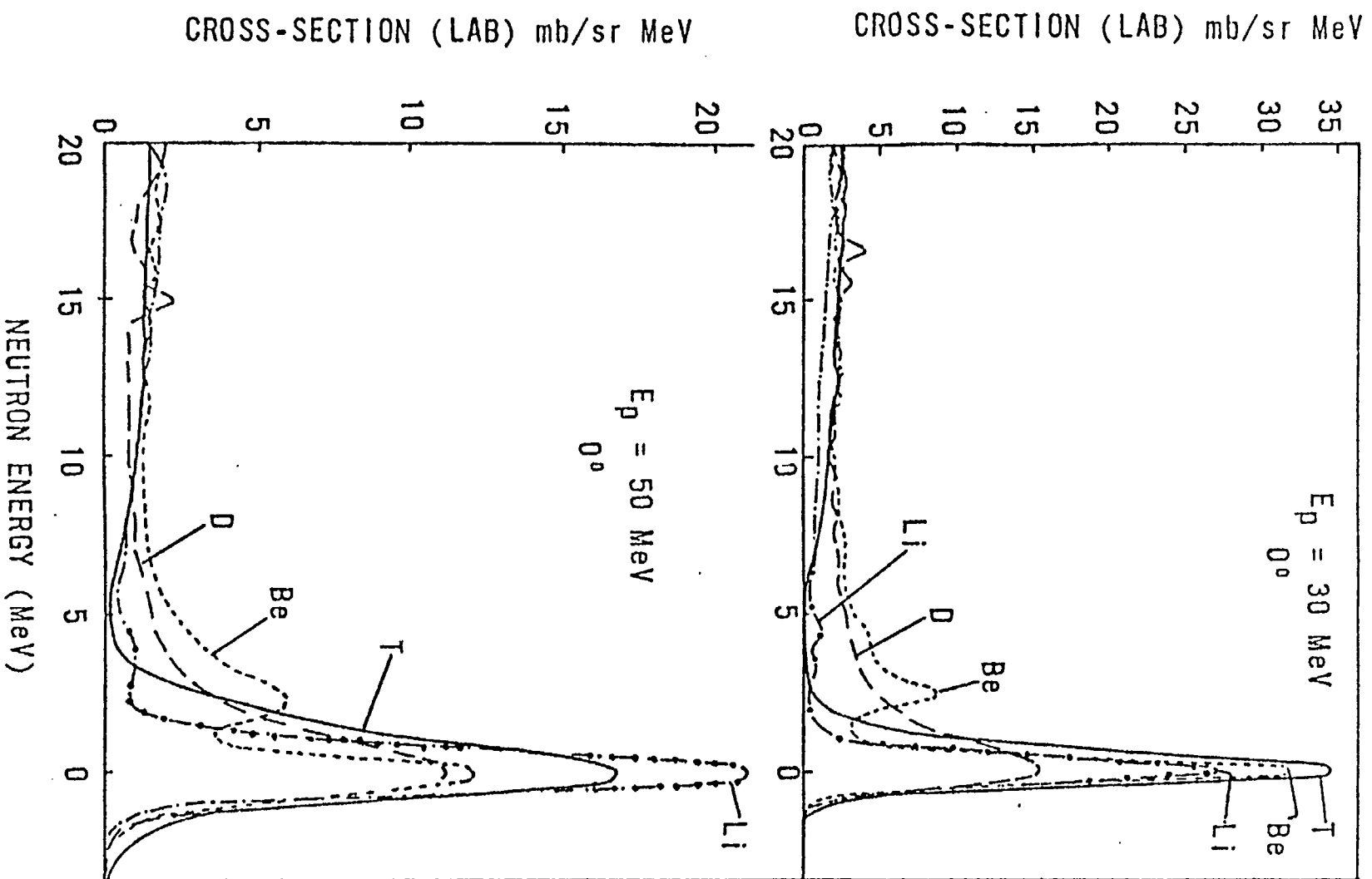


Fig. 8



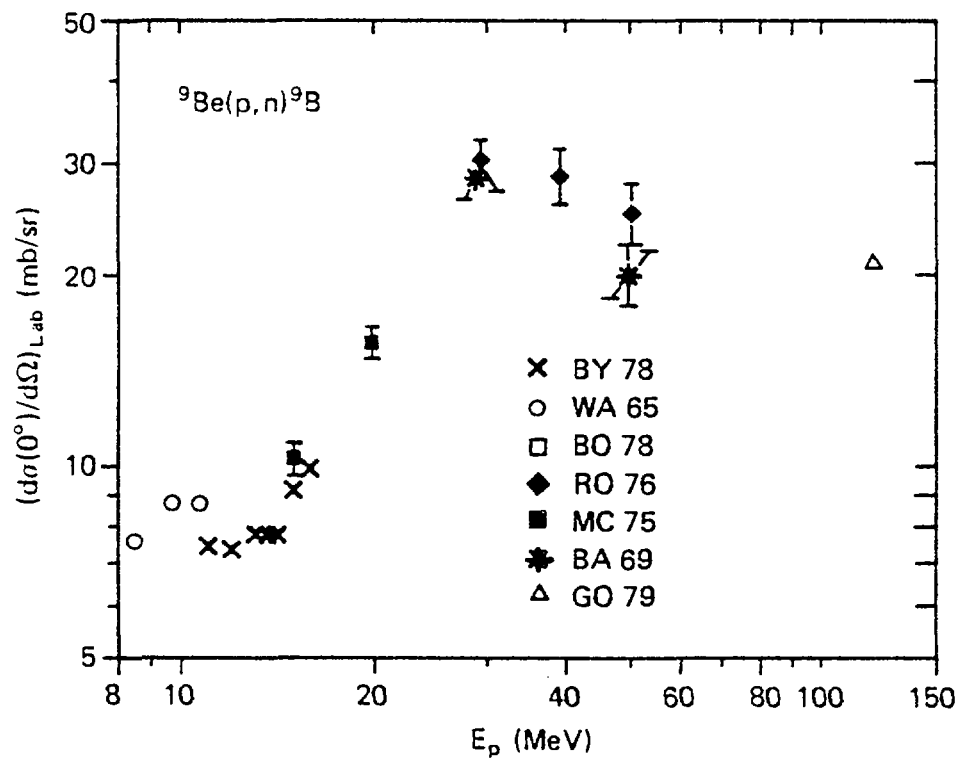


Fig. 9

PRODUCTION OF 14 MeV NEUTRONS BY LOW VOLTAGE  
ACCELERATORS

J. CSIKAI  
Institute of Experimental Physics, Kossuth University,  
Debrecen, Hungary

Abstract. This review outlines the present state of the development of D-T neutron sources based on low voltage accelerators. The following topics are discussed: importance of 14 MeV neutrons in the determination of neutron data and different fields of applications; output characteristics of the D-T reaction; generation and acceleration of ions; targets and neutron yields; characteristics of some neutron generators.

INTRODUCTION

The first device for the acceleration of charged particles has been constructed by Cockcroft and Walton [1] in 1932, the same year when Chadwick [2] discovered the neutron.

On the basis of the pioneering work of Penning and Moubis [3] Graves et al. [4] have developed metal tritide targets in 1949 which were used by Barschall and his co-workers to measure the angular distribution of neutrons scattered by protons [5], deuterons [19] and tritons [20] and to determine the total cross sections [21] for the elements from H to U.

From this time tritium was available as a target material to produce 14 MeV neutrons by the D-T reaction with high intensities, resulting in an extensive development in the use of small accelerators.

It is well known that the large cross section of the  ${}^3\text{H}(d,n){}^4\text{He}$  reaction permits high yields of fast neutrons to be obtained even at low energy, e.g. at 150-200 keV. Such a device is inexpensive, easy to install and operate; therefore, hundreds of small neutron generators are used at present in various institutions, e.g. in research laboratories, universities, industry and medical centres. During the last decade the International Atomic Energy Agency has promoted neutron research in several developing countries by providing neutron generators to be used in pure and applied research service and education.

As indicated in the latest list issued by the Agency [6], there is still a large number of requests for the 14 MeV neutron data, mostly for the design of D-T fusion reactors. Most recently, under the auspices of IAEA, an Interregional Project has been formulated [7] for the measurement of fast neutron nuclear data (with emphasis on 14 MeV) required for peaceful uses of nuclear energy.

The aim of this proposal is to complete the data needed for applications and also for checking nuclear model calculations.

In a number of laboratories much progress has been made in producing intense neutron sources based on the D-T reaction to study the interaction of 14 MeV neutrons with structural materials of fusion reactors, to increase the sensitivity of the activation analysis, to measure the low cross sections and to use them in neutron therapy. From the fifties till now a number of reaction cross sections were determined, mostly by activation method. Recently the intense neutron sources have made possible to measure the energy and angular distributions of emitted charged particles [22] as well as cross sections for rare reactions as  $(n,\gamma)$ ,  $(n,{}^3\text{He})$ ,  $(n,t)$  and  $(n,2p)$  etc.

Using nanosecond pulsed D-T generators both the spectra and angular distributions of neutrons and gamma rays emitted

in  $(n,n')$ ,  $(n,2n)$ ,  $(n,n'ch)$  reactions as well as in secondary processes can be determined.

Pulsed D-T generators in the  $\mu s$  region are used in neutron gas physics, reactor experiments and bore-hole measurements.

Recently the D-T generators are the cheapest source of high energy neutrons which can provide adequate intensity for neutron therapy, permitting isocentric mounting with a source strength of  $5 \times 10^{11} \text{ n s}^{-1} \text{ sr}^{-1}$  so that treatment time does not exceed 5-10 minutes. For the total body in vivo activation analysis the D-T generators with a source strength of about  $5 \times 10^{10} \text{ n/s}$  is satisfactory. In this case only a few minutes irradiation time is needed for the determination of O, N, Na, Mg, P, S, Cl, K, Ca, etc.

The innermost wall of an expected D-T fusion reactor is bombarded by a 14 MeV neutron flux density of about  $10^{14} \text{ n/cm}^2 \text{ s}$ . Intense 14 MeV neutron sources are not available at present for the study of the radiation damage of structural materials for such systems.

This review is based mainly on the excellent papers of Barschall [8] and Sztaricskai [23] regarding to the 14 MeV D-T sources. The details on D-T generators, as well as on their installation, operation and hazards can be found e.g. in Refs. [8, 12, 13]. A survey of commercially available neutron generators is given in Ref. [14].

### 1. OUTPUT CHARACTERISTICS OF D-T REACTION

The cross section of the  $^3\text{H}(d,n)^4\text{He}$  reaction as a function of bombarding deuteron energy has a broad resonance at  $E_d=109 \text{ keV}$ ; therefore, the thick-target neutron yield increases rapidly up to about  $E_d=200 \text{ keV}$ . The excitation function of the  $^3\text{H}(d,n)^4\text{He}$  reaction has been measured by several groups [24] in the energy range of 10 keV to 1 MeV. Accurate cross section data would be

very important below 10 keV especially for the design of fusion reactors. As shown in Fig. 1 the yield increases by a factor of four between 100 and 200 keV and only about 50 % excess can be achieved when the 200 keV deuteron energy is doubled [9].

According to the evaluation of Paulsen and Liskien [10] for the differential cross sections, the yield of neutrons from the D-T reaction depends on the emission angle in the laboratory system, but the anisotropy is less than 15 % between the forward and backward directions at  $E_d=200$  keV. The energy of neutrons in the c.m. system emitted in D-T reaction is 14.1 MeV. In the laboratory system the neutron energy depends on the bombarding deuteron energy and on the emission angle as shown in Fig. 2. If  $E_d=200$  keV, the angular variation of energy is  $E_n \sim 2$  MeV; this variation is especially accentuated around  $90^\circ$ .

It is important to note that at an angle of  $98^\circ$  the neutron energy remains constant at a value of about 14.0 MeV and is independent of the bombarding deuteron energies below 500 keV.

The excitation functions for many threshold reactions vary significantly around 14 MeV (see Fig. 3), thus the cross section depends on the position and the dimension of the sample. This may be one reason of the large spread in the data published by different authors.

As it can be seen in Fig. 4 the differences between the (n,2n) activation cross sections relating to the same nuclide, considerable exceed the errors given in the references. The deadline date for the literature survey for points was 1969, while the crosses represent the modern data. The spreads are significant both for points and crosses.

To decrease the inconsistencies of the data caused by the unnormalized neutron energy the sample should be placed in the angular interval from  $93^\circ$  to  $103^\circ$ , in which the energy spread of neutrons does not exceed a few ten keV, resulting in negligible errors in the cross sections [11]. The energy spread

of neutrons at a definite angle arises mainly from the stopping and scattering of deuterons in the target. The spread caused by stopping is indicated in Fig. 2 in function of the angle, for different deuteron energies. The large energy spread ( $\Delta E \approx 0.45$  MeV) in forward and backward directions raises several problems in measuring rapidly varying excitation functions [11]. This is the reason why physicists should take into consideration the target arrangements - and through it the spectra - of emitted neutrons, before measuring the cross sections.

Recently Raics [58] has given the following simple formula (based on the reaction kinematics) for the calculation of the laboratory neutron energy ( $E_n$ ) versus deuteron energy ( $E_d$ ) and emission angle ( $\vartheta$ ) for thick Ti-T target:

$$E_n(E_d, \vartheta) = 1.94 \cdot 10^{-4} E_d^{3/2} \cos^3 \vartheta + 0.162 E_d \cos^2 \vartheta + (9.52 \cdot 10^{-4} E_d^{3/2} + 67.42 E_d^{1/2}) \cos \vartheta + 0.397 E_d + 14049.51 \quad (1)$$

were  $E_n$  and  $E_d$  are in keV. Using this formula, such quantities as  $\sigma' E_n / \sigma' E_d$  and  $\sigma' E_n / \sigma' \vartheta$  as well as the anisotropy factor can be given in a simple way. In the knowledge of the stopping cross section  $\xi(E_d) = (dE_d/dx)/N$  and the D-T reaction cross section  $\sigma(E_d)$ , the energy distribution of emitted neutrons  $S(E_n, E_d)$  at a given angle can be calculated. Fig. 5/a shows the "stopping spectra" of neutrons for five different angles at  $E_d = 175$  keV. The resultant spectrum  $S(E_n)$  that will reach the sample, depends on the source-sample geometry, too. If the dimension of the sample covers a  $\vartheta^0 \pm \Delta \vartheta$  angle interval which corresponds to a change in neutron energy  $E_n^0 \pm \Delta E_n$ , then the average energy  $\langle E_n \rangle$  for the surface of the sample far from a point source is:

$$\langle E_n \rangle = \frac{\int_{E_n^0 - \Delta E_n}^{E_n^0 + \Delta E_n} N(E_n) \Phi(E_n) E_n dE_n}{\int_{E_n^0 - \Delta E_n}^{E_n^0 + \Delta E_n} N(E_n) \Phi(E_n) dE_n} \quad (2)$$

where  $N(E_n)$  is the number of target atoms in the unit angle interval at  $\theta^\circ$  direction. The spectrum of the impinging neutrons on the sample is  $S(E_n) = S(E_n, E_d) N(E_n) \Phi(E_n)$ , where  $\Phi(E_n)$  is the flux density. Curves of  $S(E_n)$  are given in Fig. 5/b for the following geometrical arrangement: the diameter of the sample is 19 mm; the distance from the source is 7 cm; the diameter of the beam is 14 mm. In Table I. neutron energies and the relative yields as a function of angle as well as the energy spreads, including the effect of multiple scattering of deuterons, are summarized for the geometrical conditions mentioned above. The relatively large spread at  $90^\circ$  is caused by the effect of finite angular interval used for the irradiation.

Table I.

Neutron energies vs. emission angle for D-T reaction  
at  $E_d = 175$  keV.

Angle	Average energy (MeV)	Relative intensity
0	$14.80 \pm 0.17$	1.07
30	$14.70 \pm 0.15$	1.06
60	$14.45 \pm 0.12$	1.03
90	$14.12 \pm 0.08$	1.00
120	$13.75 \pm 0.10$	0.97
150	$13.52 \pm 0.12$	0.95
180	$13.41 \pm 0.13$	0.94

The energy spread of neutrons depends also on the ratio of atomic and molecular ions. The energy of the latter is half of the former; therefore, they produce much less neutrons. According to the problems mentioned above in the nuclear data measurements the neutron energy must be specified more definitely that "14 MeV" and it is advisable to determine the

spectrum experimentally for the given source-sample arrangement. One should pay special attention to the role of secondary neutrons produced in the target holder or in the surrounding materials if cross sections for low threshold reactions are measured; e.g.  $(n,\gamma)$ ,  $(n,n'\gamma)$ ,  $(n,p)$ , etc. Because of the large amount of structural materials around the target the sealed-tube generator and the intense D-T sources [8] have serious limitations in the cross section measurements but not in the field of applications. By these equipments, however, the primary neutron spectrum to be expected from a D-T plasma of a few ten keV temperature can be simulated. Liskien [15] has pointed out that the 14.1 MeV line is strongly broadened and has a width of about 2 MeV if neutrons with at least 5 % of the maximum intensity are included (see Fig. 6).

## 2. GENERATION AND ACCELERATION OF DEUTERIUM IONS

### a) High voltage power supply

There are two basic types of power supplies to produce accelerating voltages up to a few hundred kV, namely the electrostatic (the Van de Graaff or Felici [37] design) and the Cockcroft-Walton voltage-doubler systems.

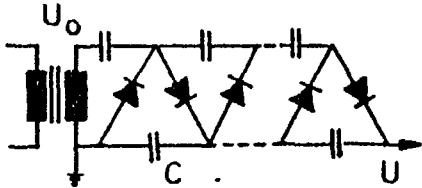
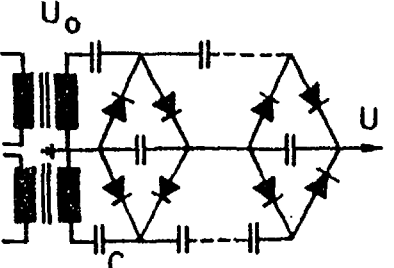
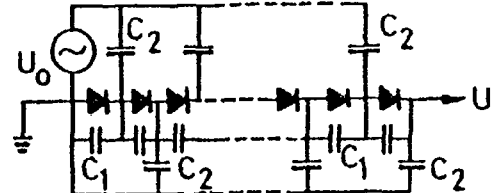
The Van de Graaff and Felici power supplies have good voltage stability and low ripple which are required to produce a stable beam for analysis and long transport. Most commercially available D-T generators do not have beam analysis and their power supplies can provide current up to 50 mA, below 300 kV. The C-W system has various versions: cascade [25, 26], symmetrical cascade [27-29] and dynamitron [30-32]. The principles and main parameters of these circuits are summarized in Table II. [38].

The advantage of the symmetrical cascade and dynamitron systems in comparison with the original C-W doubler is the lower voltage drop against increasing of cascade steps  $N$ .



Table II.

Main parameters of cascade circuits.

CIRCUIT	CASCADE	SYMMETRICAL CASCADE	DYNAMITRON
			
IDEAL OUTPUT VOLTAGE	$U = 2NU_0$ $N = \text{number of doublers}$ $U_0 = \text{input voltage}$	$U = 2NU_0$	$U = U_0 \frac{N}{1 + \frac{4C_1}{C_2}}$
RIPPLE	$\delta U = \frac{I}{2fC} N(N+1)$ $f = \text{frequency}$ $I = \text{loading current}$	$\delta U = \frac{I}{2fC} N$	$\delta U = \frac{I}{2fC_2}$
VOLTAGE DROP	$\Delta U = \frac{I}{fC} \left( \frac{2}{3} N^3 + \frac{N}{3} \right)$	$\Delta U = \frac{I}{fC} \left( \frac{N^3}{6} + \frac{N}{3} \right)$	$\Delta U = \frac{I}{fC_2} \frac{N}{1 + \frac{4C_1}{C_2}}$
WORKING VOLTAGE	0,1 - 1 MV	0,1 - 2,5 MV	0,7 - 5,7 MV
MAXIMUM CURRENT	~ 1 A	~ 200 mA	~ 20 mA

The selenium rectifiers have been replaced with high-speed Si diodes to increase the frequency range. A 600 kV, 10 mA C-W voltage supply using Si diodes at 100 kc was described by Reginato and Smith [25].

For neutron generators and sealed-off neutron tubes not only cascade and electrostatic systems are used as voltage supplies but also insulated core transformers (ICT) [33], pulse transformers (PTA) and transformer accelerators (TA) [34-36]. In the PTA and TA systems the accelerating tube is used as rectifier. In high yield neutron generators the acceleration field is produced often with a single electrode pair placed at a distance of 10 to 100 mm from each other.

Rectifiers are manufactured by the High Voltage Engineering Corporation, Tunzini-Sames, E. Haefely and Co. with voltages up to 500 kV and current ratings up to 500 mA. These supplies are available with medium and high stability, e.g. at 250 kV and 7 mA the voltage drop with load is between 400 V/mA and 2 V/mA with a ripple less than 0.5 %.

#### b) Ion Sources

Low-voltage D-T generators employ three types of ion sources: radiofrequency (RF) [39-43], Penning (PIG) [44-46] and duoplasmatron (DP) [23, 47, 51]. The advantage of RF sources is their high monatomic ratio (~ 90 %), while PIG and DP have high currents. After several hundred hours of operation, a thin metallic layer is deposited on the inner walls of the RF source bottle and this leads to a reduction in the atomic ion ratio to 40-50 %.

In the case of PIG and DP sources the extracted beam contains only about 40-60 % of atomic ions. The neutron

yield [52, 53] and the target life-time [54] can be drastically increased by using analysed atomic beam. Nevertheless, PIG ion sources are often applied in neutron generators, even for deuteron energies lower than 200 keV, because of their simple construction, power supply system and long operating life-time.

While the ion current of RF sources is generally a few mA, PIG sources can produce 30 mA at a pressure of  $10^{-2}$  mm Hg [55].

Gurtovoy et al. [56] and Anufrienko et al. [57] have described ion sources for fast neutron time-of-flight spectrometry. The duoplasmatron ion source is able to produce currents of a few amperes [59-62] which can satisfy the requirements of intense D-T sources. The characteristics of high intensity ion sources applicable for particle accelerators have been surveyed by van Steenberg [63].

#### c) Beam accelerating and analysing systems

There are various simple designs for accelerating tubes with homogeneous or inhomogeneous field of low voltage accelerators [64-67]. The transport of the beam over long distances is simple if the currents do not exceed a few 10 mA.

The defocussing effect of the space charge cannot be neglected for a few 10 mA beam of 5-10 mm diameter at 100-200 keV.

The multi-electrode lens structure is a weak focussing system, the major amount of focussing of the ion beam being generally performed by the extraction lens. The Einsel lens system contains only a few gaps and it is therefore easy to change the focal point over a wide range. In the case of high currents a Pierce geometry column is used for the acceleration of the ions [17, 68].

Fig. 7 shows an accelerating tube designed in Debrecen [69] for a 200 kV and 30 mA D-T generator. The voltage difference along the glass insulator rings is divided by electrodes connected to a bank of resistors. The shape and arrangement of electrodes can shield the insulator surfaces from the secondary electrons, scattered ions and other contaminations.

Recently accelerator tubes both with a single-gap [50, 70, 71] and special multi-gap arrangements [48, 72] are used.

After acceleration focussing lenses should be used to transport the beam through the analysing magnet to the target placed at long distance from the accelerating gap. To avoid the large amount of structural material near to the target the analysing or deflecting magnets can be replaced by a Wien filter [77].

### 3. TARGETS AND NEUTRON YIELDS

There is a growing need to design tritium targets with long life time at high neutron yields.

In addition to the solid targets, tritium gas [74] as well as an implanted mixed beam [73, 79] of  $^2\text{H}$  and  $^3\text{H}$  have been used as targets to produce 14 MeV neutrons. Figure 8 plots the neutron yields of various targets against the deuteron energy [17, 18]. Using gas target more than  $10^{14}$  n/s can be expected but there are many technical difficulties of building such sources [8, 74].

In low-voltage generators the most common target is tritium absorbed in thin metal layers. Besides titanium and zirconium, Er, Sc, Y and U are also used to produce inter-metallic compounds <sup>with</sup> tritium. A thin layer of Ti or Zr is evaporated onto Al, Cu, Ag and W backing metal. Theoretically, the ratio of tritium to titanium atoms is about 1.9:1, but in the case of commercial targets it is about 1.5:1. Rare

earth targets have a much higher thermal stability than Ti (see Fig. 9, Ref. [81]). Under the bombardment with deuterons tritium is removed from the Ti-T layer resulting in a change in the ratio of T/Ti atoms with the time and depth. The targets of hundreds Ci can release high amount of tritium into the vacuum system and special precautions are needed to avoid the contamination of the environment. The life-time of a target can be represented by the following ratio [16]:

$$\text{Target life-time} = \frac{\text{Ion current (mA)} \times \text{Hours to half yield}}{\text{Target area (cm}^2\text{)}}$$

The average target life for Ti-T is about  $2.7 \text{ mA}\cdot\text{h}/\text{cm}^2$ , the maximum being  $4 \text{ mA}\cdot\text{h}/\text{cm}^2$  for stationary targets. In a recent paper [54] it was shown that the half-lives of TiT targets of  $10\text{-}20 \text{ mAh}/\text{cm}^2$  can be obtained if analyzed beam is used. For Ti-T targets, by the time the 14 MeV neutron yield reaches one half of its initial value, the deuteron build-up achieves saturation and the yield of 3 MeV neutrons is about 1 % of the D-T output. Nowadays various suppliers (Amersham UK, ORNL USA, CEA France, IRE Belgium, SORIN Italy, Techsnabexport USSR, Metronex Poland, International Engineering Service Austria) sell metal tritide target for DT generators, mostly with Ti layers from  $0.2$  to  $4 \text{ mg}/\text{cm}^2$  thickness with different backing materials. Targets with dimension up to 50 cm diameter and thickness from micrograms to milligrams per  $\text{cm}^2$  can be manufactured. In addition to disks, rectangular strips, annuli and other geometrical shapes of targets are commercially available. In the case of large target surface strong backing materials are needed to withstand of pressure differences.

These backings are prepared from copper alloys (Amzirk: 0.15 % Zr in Cu, Glid-Cop:  $\text{Al}_2\text{O}_3$  in Cu).

Targets should be stored for short periods only, in dry and inert atmosphere, to ensure that the titanium layer remains adherent.

According to the yield curve shown in Fig. 1, 1 mA of 200 keV atomic deuteron beam on a fresh tritium target produces about  $2 \times 10^{11}$  n/s. Typical D-ion currents both for home-made and commercially available D-T generators are a few mA, producing neutrons in the order of  $10^{11}$  n/s.

Yields much above  $10^{11}$  n/s need high beam currents, dissipating about 100 kW power in the target. Using 0.5 A ion current a neutron source strength of  $8 \times 10^{12}$  n/s was achieved in D-T reaction at 80 kW power (see Ref. [8]). Various methods to obtain high source strengths have been described by Barschall [8].

The maximum yield from neutron generators, in addition to the beam current, is determined by the target construction and a number of different stationary and rotary target systems have been developed. The type and geometry of structural materials around the target and the design of a target with a long life time are playing very important role in the neutron data measurements.

Using a 22 cm diameter rotating target, 16 mA of 400 keV deuterons produced a neutron yield of  $4 \times 10^{12}$  n/s that decreased 10-20 % in 50 hours for a 1 cm diameter spot [76] which correspond to about 1600 mA.h/cm<sup>2</sup> life-time.

Rotating target neutron generators (RTNS) have been investigated in detail by Booth et al. [48]. A target 23 cm in diameter was rotated at 1100 rpm. The cooling water was distributed over the back of the target using channels as shown in Fig. 10 to produce turbulent flow [48]. Air bearing vacuum seal which rotates at 5000 rpm has been constructed for a 21 diameter target using two stages of differential pumping system between the air cushion and the vacuum [75]. Rotating target developed by Cossutta [78] seems to be promising for intense D-T sources. As it can be seen in Fig. 12 magnetic fluid seal is used in the system.

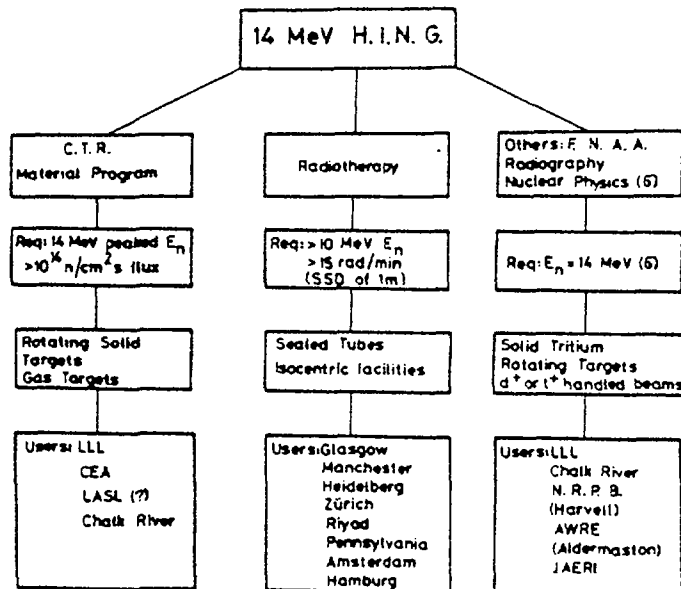
Many details on the production and properties of tritium targets have been discussed by Pivaric [80].

#### 4. CHARACTERISTICS OF SOME D-T GENERATORS

Various types of pumped and sealed tube D-T generators have been developed for continuous and pulsed operations. Schematic diagram of a nanosecond generator constructed in Obninsk and Debrecen [82] for the neutron time-of-flight measurements is shown in Fig. 11. Lehman et al. [83] and Roche [86] have published excellent papers about the possibilities of nanosecond pulsing of direct current accelerators. Target and sample arrangement recommended for the cross section measurements by activation method around 14 MeV is shown in Fig. 13 [84]. Scheme of a generator developed by Schmidt and Dohrmann [85] that produces  $5 \times 10^{12}$  n/s in continuous operation using mixed beam of D and T to bombard a central conical target in a radial magnetic field is presented in Fig. 14. Some typical applications of intense D-T generators are given in Table III. [23].

Table III.

Typical applications of intense D-T generators.



General characteristics of some D-T generators are summarized in Table. IV., without making an effort for the completeness.

Table IV.  
Some characteristics of D-T generators

MODEL	Voltage (kV)	Current (mA)	Pulse width ( $\mu$ s)	Beam diam. (mm)	Yield (n/s)
SAMES : T	400	2	$10-8 \times 10^3$	10-30	$5 \times 10^{11}$
J	150	2.5	$10-8 \times 10^3$	10-30	$10^{11}$
HVE : LN-S	300	2	-	<10	$4 \times 10^{11}$
Accelerator Inc.	150	3.5	$0.5-10^5$		$3.5 \times 10^{11}$
Texas Nuclear	280	7	-	20	$6 \times 10^{11}$
Kaman Nuclear	200		$1-2 \times 10^5$		$2.5 \times 10^{11}$
Marconi Avionics } <sup>ST</sup>			10 ns		
SAMES TB-8	300	8	-	30-50	$10^{12}$
Chalk River	300	25		10	$4 \times 10^{12}$
Dynagen	500	12		20	$3.5 \times 10^{12}$
RTNS-II(LLL)	400	150		10	$4 \times 10^{13}$
LANCELOT	160	200		50	$6 \times 10^{12}$
Cyclotron Corpor.	175	450			$8 \times 10^{12}$
Philips	250	18			$10^{12}$
Marconi Avionics } <sup>ST</sup>					$10^{12}$



# REFERENCES

- [1] COCKCROFT, J.D., WALTON, E.T.S., Proc. Roy. Soc. ( London )  
A136 (1932) 619.
- [2] CHADWICK, J., Nature 129 (1932) 312.
- [3] PENNING, F.M., MOUBIS, J.H.A., Physica 4 (1937) 1190.
- [4] GRAVES, E.R., RODRIGUES, A.A., GOLDBLATT, M., MEYER, D.I.,  
Rev. Sci. Instr. 20 (1949) 579.
- [5] BARSCHALL, H.H., TASCHEK, R.F., Phys. Rev. 75 (1949) 1819.
- [6] MUIR, D.W., WRENDA 79/80, INDC SEC-73/URSF, IAEA, Vienna  
(1979)
- [7] Proposal for an IAEA sponsored Interregional Project for  
the determination of 14 MeV neutron data, Course on Nuclear  
Theory for Applications, ICTP, Trieste (1980)
- [8] BARSCHALL, H.H., 14 MeV d,t Sources, UWFD-331 University  
of Wisconsin (1979)
- [9] SHOPE, L.A., Sandia Corp. Report SC-TM-66-247 (1966)
- [10] PAULSEN, A., LISKIEN, H., Rep. EANDC E-144 "L" CBNM (1972);  
Rep. EANDC E-143 "L" CBNM (1971)  
Nuclear Data Tables 11 (1973) 569.
- [11] CSIKAI, J., BUCZKÓ, M., BÖDY, Z., DEMÉNY, A., Atomic Energy  
Review 7 (1969) 93.
- [12] NARGOLWALLA, S.S., PRZYBYLOWICZ, E.P., Activation Analysis  
with Neutron Generators, Wiley, New York (1973)
- [13] CSIKAI, J., Atomic Energy Review 11 (1973) 415.
- [14] Nucleonics 23 4 (1965) 60 J.
- [15] LISKIEN, H., Advisory Group Meeting on Nuclear Data for  
Fusion Reactor Technology, Vienna 11 to 15 December (1978)  
p. AG-159/B4.
- [16] SMITH, D.L.E., Accelerator Targets Designed for the  
Production of Neutrons, Rep. EUR-3895 d-f-e (1968) 5.
- [17] KELSEY, C.A., SPALEK, C.G., DELUCA, P.M., CHENEVERT, G.M.,  
McCULLOUGH, E.C., NICKLES, R.J., Proc. Symp. Neutron  
Dosimetry in Biology and Medicine, Neuhergerg/München (1972) 818.

- [18] HILLIER, M., LOMER, P.D., STARK, D.S., WOOD, J.D.L.H.,  
Accelerator Targets, Designed for the Production of  
Neutrons, Rep. EUR-3895 d-f-e (1968) 125.
- [19] COON, J.H., TASCHEK, R.F., Phys. Rev. 76 (1949) 710.
- [20] COON, J.H., BOCKELMAN, C.K., BARSCHALL, H.H., Phys. Rev.  
81 (1951) 33.
- [21] COON, J.H., GRAVES, E.R., BARSCHALL, H.H., Phys. Rev.  
88 (1952) 562.
- [22] ALVAR, K.R., BARSCHALL, H.H., BORCHERS, R.R., GRIMES, S.M.,  
HAIGHT, R.C., Nucl. Instrum. Methods 148 (1978) 303.
- [23] SZTARICKAI, T., Technical solutions for high intensity  
solid target neutron generators, ATOMKI Közlemények,  
(to be published)
- [24] STEWART, L., HALE, G.M., USNDC-CTR-2, (1974)
- [25] REGINATO, L.L., SMITH, B.H., IEEE (Inst. Electr. Electron.  
Eng.) Trans. Nucl. Sci. 12 (1965) 274.
- [26] REINHOLD, G., TRÜMPY, K., GLEYVOD, R., IEEE (Inst. Electr.  
Electron. Eng.) Trans. Nucl. Sci. 18 (1971) 92.
- [27] SEITZ, J. REINHOLD, G., MINKNER, R., Helv. Phys. Acta 33  
(1960) 977.
- [28] ALBERTINSKY, B.I., KURICYN, I.V., NYKONOV, O.F.,  
OVTSINNYKOV, O.B., Prib. Tekh. Ehksp. 3 (1971) 43.
- [29] REINHOLD, G., BILL, J., IEEE (Inst. Electr. Electron. Eng.)  
Trans. Nucl. Sci. 14 (1967) 145.
- [30] CLELAND, M.R., MORGANSTERN, K.H., Nucleonics 18 8 (1960) 52.
- [31] CLELAND, M.R., FARRELL, P., IEEE (Inst. Electr. Electron.  
Eng.) Trans. Nucl. Sci. 12 (1965) 227.
- [32] CLELAND, M.R., HANLEY, P.R., THOMPSON, C.C., IEEE (Inst.  
Electr. Electron. Eng.) Trans. Nucl. Sci. 16 (1969) 113.
- [33] HVEC-ARP, Nucleonics 18 (1960) 56.
- [34] KIRYANOV, G.I., Radiacion. Tekh. 1 (1967) 177.
- [35] ABRAMYAN, E.A., BROVIN, M.M., VETSESLAVOV, V.V., GORBUNOV, V.A.,  
KONONOV, V.I., TSERTOK, I.L., At. Ehnerg. 29 (1970) 346.

- [36] ABRAMYAN, E.A., IEEE (Inst. Electr. Electron. Eng.) Trans. Nucl. Sci. 18 (1971) 447.
- [37] FELICI, H.J., Elektrostatische Hochspannungsgeneratoren und ihre industrielle Anwendungen, Verlag G. Braun, Karlsruhe (1957)
- [38] PETŐ, G., Izotóptechnika Budapest 16 (1973) 561.
- [39] MOAK, C.D., REESE, H., GOOD, W.M., Nucleonics 9 (1951) 18.
- [40] STRIZHAK, V.I., NAZAROV, N.S., Prib. Tekh. Ehksp. 2 (1961) 72.
- [41] NAGY, J.L., GOMBOS, P., ATOMKI Közlemények 4 (1962) 19; 5 (1963) 39.
- [42] SZABÓ, Z., Nucl. Instrum. Methods 78 (1970) 199.
- [43] PÁSZTOR, E., Isotopenpraxis 3 (1967) 259.
- [44] PENNING, F.M., MOUBIS, J.H., Physica 4 (1937) 1190.
- [45] EHLERS, K.W., GAVIN, B.F., HUBBARD, E.L., Nucl. Instrum. Methods 22 (1963) 87.
- [46] NAGY, J.L., Nucl. Instrum. Methods 32 (1965) 229.
- [47] ARMSTRONG, D.D., EMIGH, C.R., MEIER, K.L., MEYER, E.A., SCHNEIDER, J.D., Nucl. Instrum. Methods 145 (1977) 127.
- [48] BOOTH, R., DAVIS, J.C., HANSON, C.L., HELD, J.L., LOGAN, C.M., OSHER, J.E., NICKERSON, R.A., POHL, B.A., SCHUMACHER, B.J., Nucl. Instrum. Methods 145 (1977) 25.
- [49] BOOTH, R., BARSCHALL, H.H., Nucl. Instrum. Methods 99 (1972) 1.
- [50] HOURST, J.B., ROCHE, M., MORIN, J., Nucl. Instrum. Methods 145 (1977) 19.
- [51] OSHER, J.E., HAMILTON, G.W., Report LBL-3399 (1974)
- [52] KELSEY, C.A., SPALEK, G.C., DELUCA, P.M., CHENEVERT, G.M., McCULLOUGH, E.C., NICKLES, R.J., Proc. Symp. Neutron Dosimetry in Biology and Medicine, Neuherberg/München (1972) 818.

- [53] HILLIER, M., LOMER, P.D., STARK, D.S., WOOD, J.D.L.H.,  
Accelerator Targets, Designed for the Production of  
Neutrons, Rep. EUR-3895 d-f-e (1968) 125.
- [54] STENGL, G., VONACH, H., Nucl. Instrum. Methods 140  
(1977) 197.
- [55] REIFENSCHWEILER, O., Proc. Symp. Neutron Dosimetry in  
Biology and Medicine, Neuherberg/München (1972) 40.
- [56] GURTOVOY, M.E., KUKHLENKO, A.S., LESHCHENKO, B.E.,  
STRIZHAK, V.I., Prib. Tekh. Ehksp. 4 (1970) 24.
- [57] ANUFRIENKO, V.B., DEBKIN, B.V., MOROKA, V.I., SALNIKOV, O.A.,  
Prib. Tekh. Ehksp. 3 (1971) 46.
- [58] RAICS, P., Thesis, Kossuth University Debrecen (1978).
- [59] MOAK, C.D., BANTA, H.E., THURSTON, J.N., JOHNSON, J.W.,  
KING, R.F., Rev. Sci. Instrum. 30 (1959) 694.
- [60] DUNN, E.D., Rep. LA-4753-MS, UC-28 (1971)
- [61] PLESHIVCEV, N.V., TOMASHEV, G.G., GRIGOROVITS, F.F.,  
NIZHEGORODCEV, V.V., MATVEENKO, O.G., SHEMBEL, B.K.,  
Prib. Tekh. Ehksp. 6 (1967) 23.
- [62] GREEN, T.S., MOSSON, G.A.G., ATOMKI Közlemények (Debrecen)  
18 (1976) 391.
- [63] VAN STEENBERGEN, A., IEEE (Inst. Electr. Electron.) Trans.  
Nucl. Sci. 12 (1965) 746.
- [64] GALEJS, A., ROSE, P.H., "Optics of electrostatic accelerator  
tubes" Focusing of Charged Particles SEPTIER, A., Ed. ,  
Academic Press New York 2 (1967) 297.
- [65] KOLTAY, E., Nucl. Instrum. Methods 6 (1960) 45.
- [66] GYARMATI, B., KOLTAY, E., ATOMKI Közlemények (Debrecen)  
9 (1967) 319.
- [67] BOAG, J.W., IEEE (Inst. Electr. Electron.) Trans. Nucl. Sci.  
51 (1953) 63.
- [68] EMIGH, C.R., MEYER, E.A., MUELLER, D.W., IEEE (Inst. Electr.  
Electron.) Trans. Nucl. Sci. 16 (1969) 46.

- [69] SZABÓ, G., KOLTAY, E., Contract Report Debrecen (1979)
- [70] HEPBURN, J.D., ORMROD, J.H., CHIDLEY, B.G., IEEE (Inst. Electr. Electron.) Trans. Nucl. Sci. NS-22 (1975) 1809.
- [71] ALGER, D.L., STEINBERG, R., IEEE (Inst. Electr. Electron.) Trans. Nucl. Sci. NS-20 (1973) 420.
- [72] EVANS, L.R., WARNER, D.J., IEEE (Inst. Electr. Electron.) Trans. Nucl. Sci. NS-18 (1971) 1068.
- [73] KIM, J., Nucl. Instrum. Methods 145 (1977) 9.
- [74] CHENEVERT, G.M., DELUCA, P.M., KELSEY, C.A., TORTI, R.P., Nucl. Instrum. Methods 145 (1977) 149.
- [75] BOOTH, R., LOGAN, C.M., Nucl. Instrum. Methods 142 (1977) 471.
- [76] BOOTH, R., GOLDBERG, E., BARSCHALL, H.H., Br. J. Radiol. 47 (1974) 737.
- [77] JENSEN, K., VEJE, E., Nucl. Instrum. Methods 122 (1974) 511.
- [78] COSSUTTA, D.D., Multivolt Ltd. of Crawley, private communication [23]
- [79] CLOTH, P., DARVAS, J., FILGES, D., HAUBOLD, H.B., HEMMERICH, J., IHLE, H.R., KIRCH, N., KUPSCHUS, P., MEIXNER, C., ATOMKI Közlemények (Debrecen) 18 (1976) 439.
- [80] PIVARC, J., ATOMKI Közlemények (Debrecen) 18 (1976) 463.
- [81] CRAWFORD, J.C., BAUER, W., ANL-CTR-75-4 (1975) 227.
- [82] SZTARICKS KAI, T., VASVÁRY, L., PETŐ, G., Proc. of the V. Int. Symp. on the Interaction of Fast Neutrons with Nuclei, November 17-21, Gaussig (1975) 218.
- [83] LEHMANN, D., SEELIGER, D., SGONINA, A., Zfk-268 Dresden (1974)
- [84] CSIKAI, J., Nuclear Data for Fusion Reactor Technology, IAEA-TECDOC-223 (1979) 199.
- [85] SCHMIDT, K.A., DOHRMANN, H., Atomkernenergie 27 (1976) 158.
- [86] ROCHE, M., Rapport CEA-R-3796, C.E.N.-Saclay (1969)

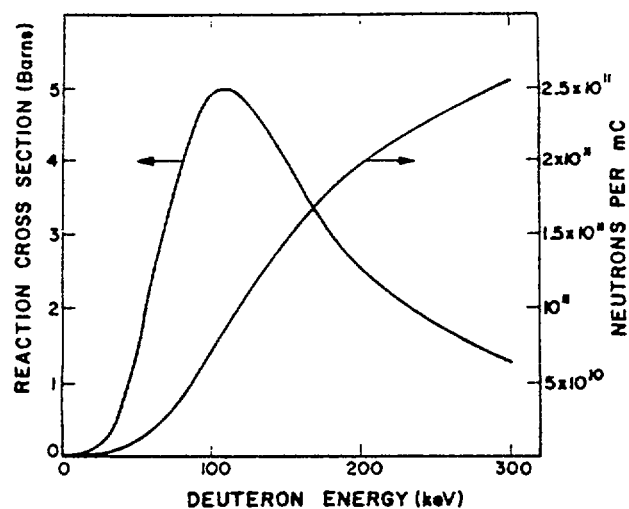


Fig. 1 Cross section of the  $^3\text{H}(\text{d},\text{n})^4\text{He}$  reaction and the total neutron yield as a function of deuteron energy

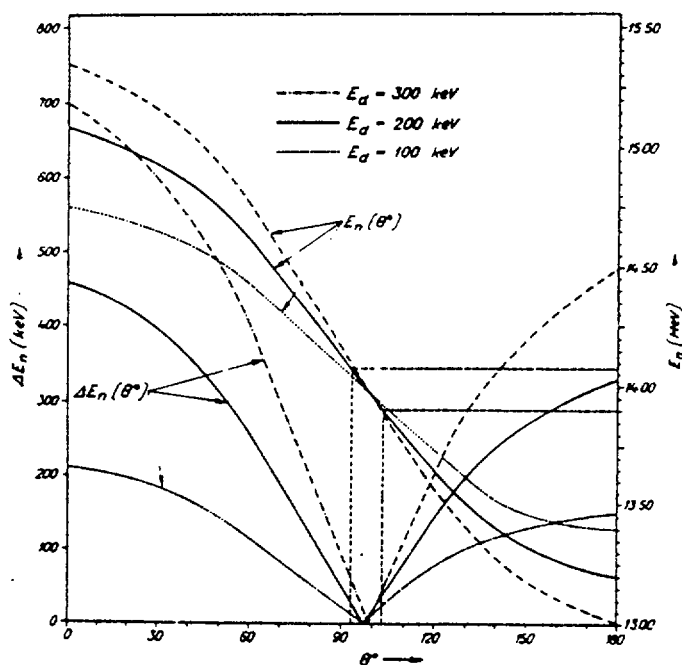


Fig. 2 The energy and energy spread of neutrons versus angle for D-T reaction

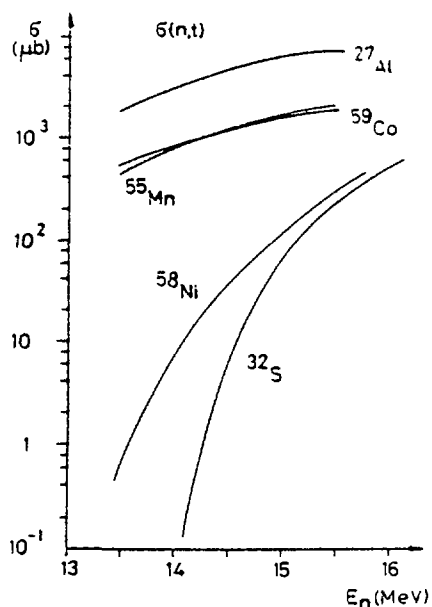


Fig. 3 Excitation functions of some (n,t) reactions

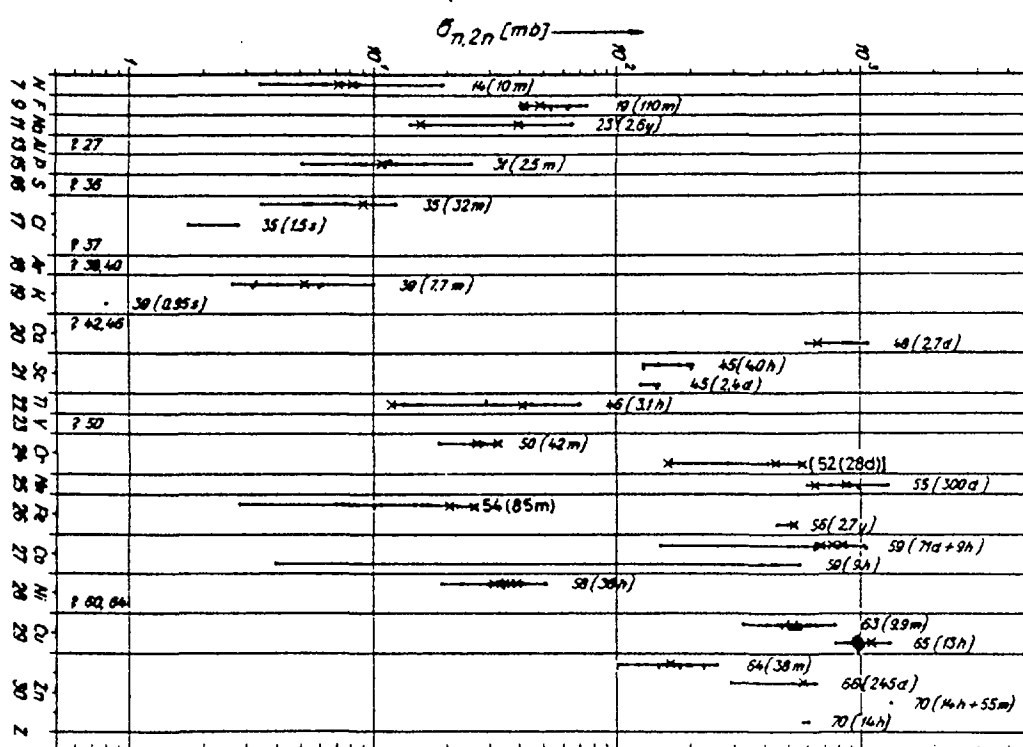


Fig. 4 Activation cross sections for (n,2n) reactions at 14 MeV

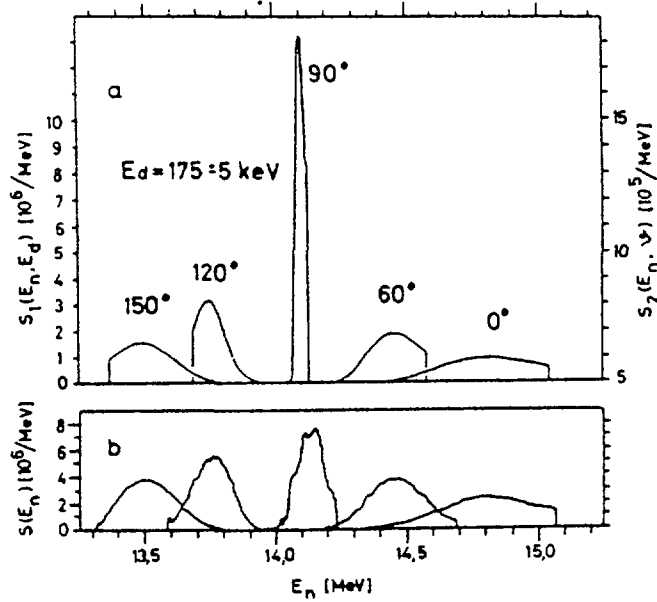


Fig. 5 Energy spectra of neutrons for five different angles at  $E_d=175$  keV

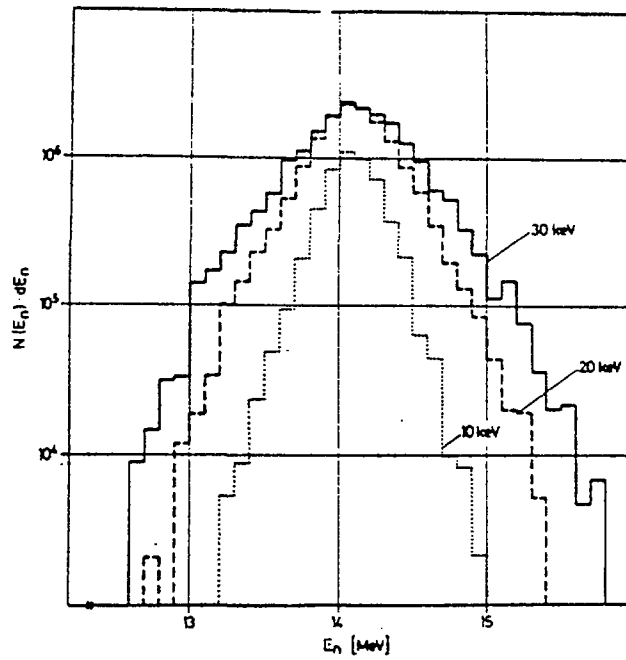


Fig. 6 Energy spectra of neutrons from a D-T plasma of temperature  $T=10, 20$  and  $30$  keV



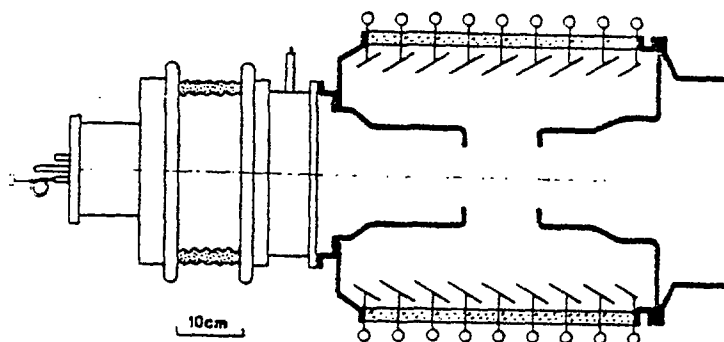


Fig. 7 Scheme of a single gap accelerator tube

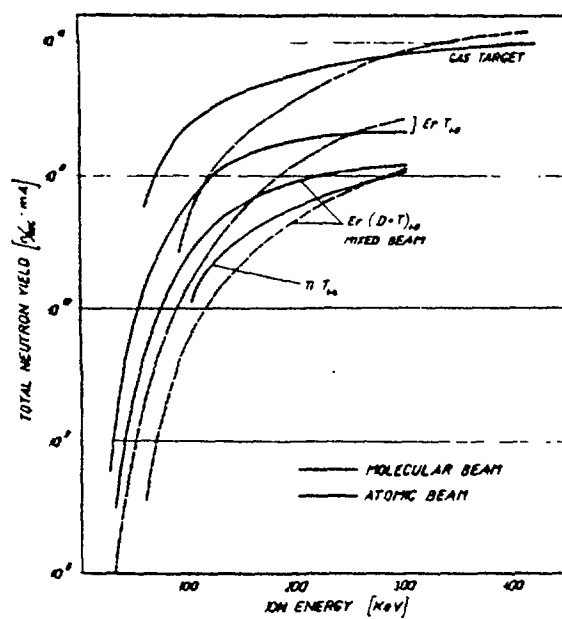


Fig. 8 Total neutron yields for various target compositions

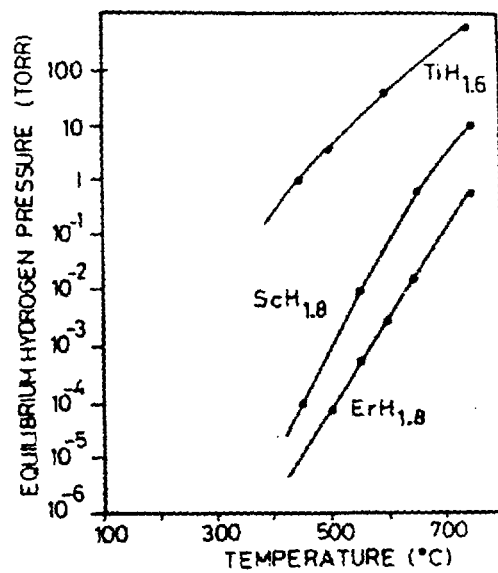


Fig. 9 Thermal stability of various solid tritium targets

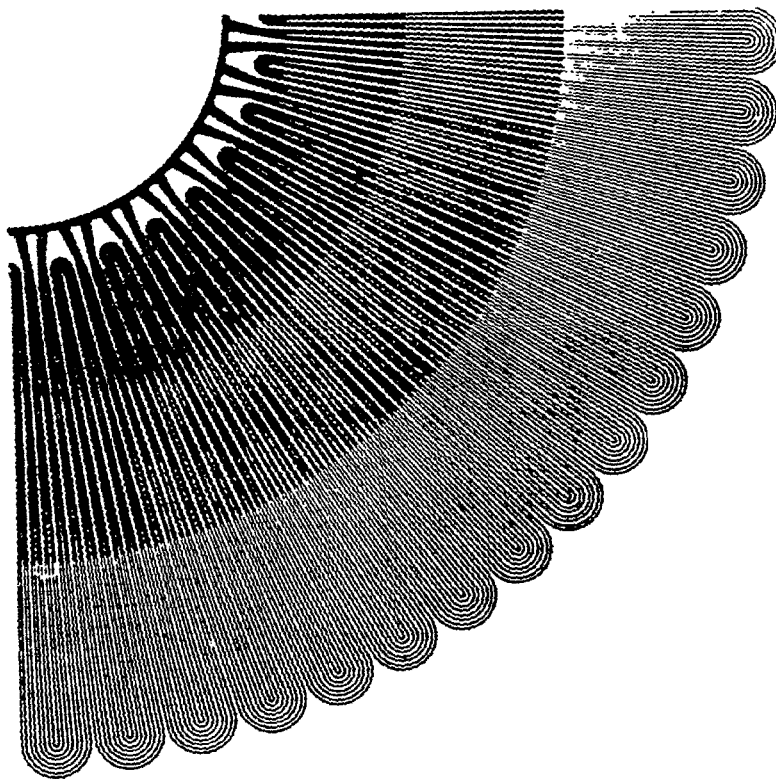


Fig. 10 Etching mask used to produce water-cooling channels within the rotating target



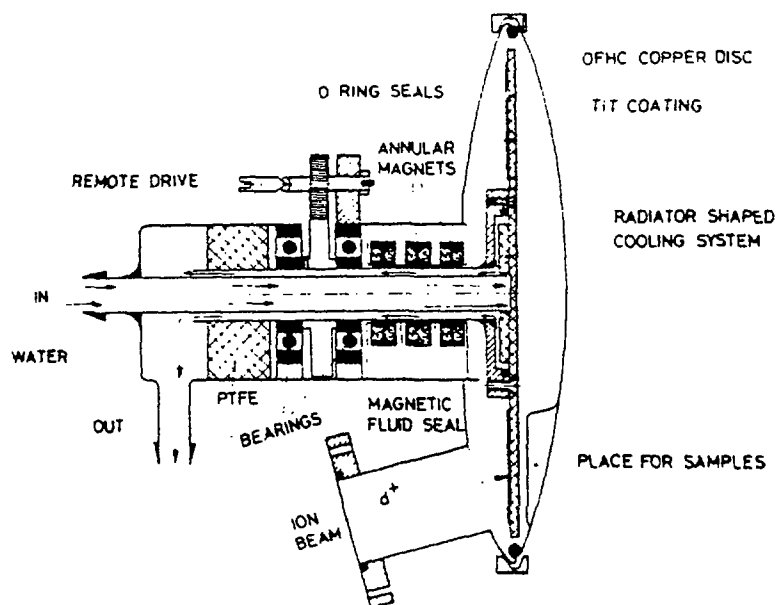


Fig. 12 Scheme of a high speed rotating target

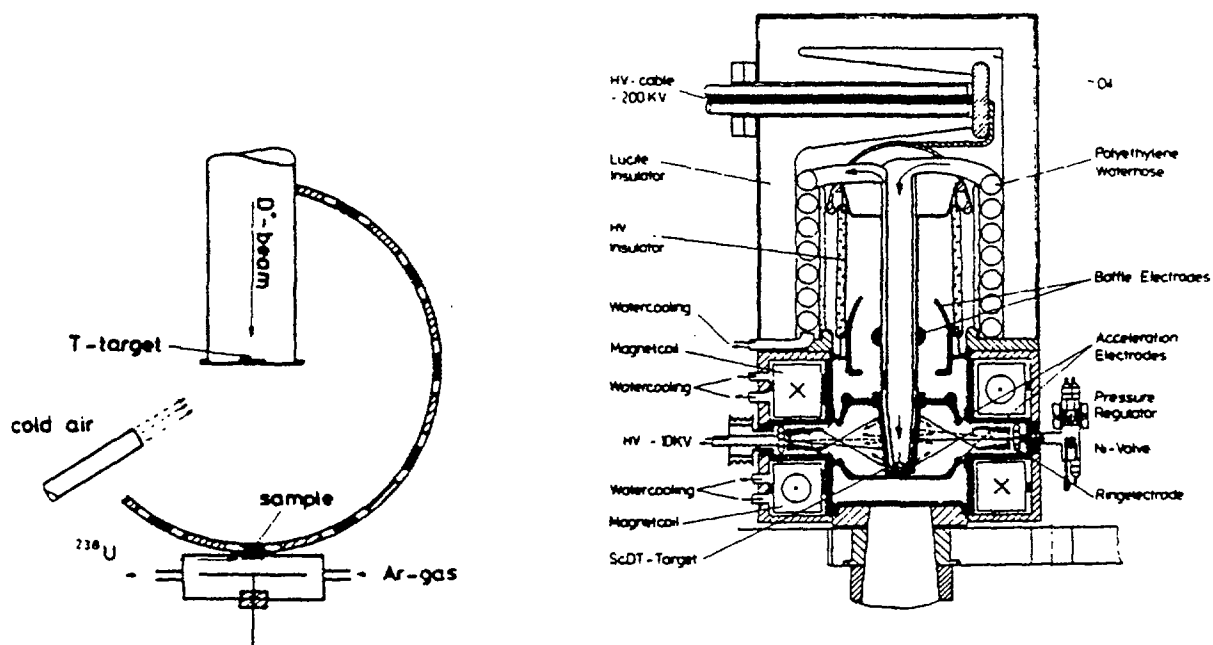


Fig. 13 Scattering free arrangement for irradiation around 14 MeV

Fig. 14 Scheme of an intense neutron generator based on mixed beam of T and D



# ***CONTRIBUTED PAPERS***

( abstracts only )

Full papers can be requested directly from the authors



Emission rate and neutron spectrum measurements  
for Be( $\alpha$ ,n) sources

H. Kluge, H.W. Zill

Physikalisch-Technische Bundesanstalt, Braunschweig  
(presented by W.G. Alberts)

Be ( $\alpha$ ,n) sources are investigated at the PTB to serve as calibration sources for radiation protection purposes. The spectral distributions of neutrons from these sources are measured to calculate mean conversion factors for fluence to dose equivalent and to investigate their dependence on the spectral shape. A facility has been developed to allow easy and fast relative source strength determinations by means of a precision long counter. It can be used for neutron sources showing similar energy spectra and an emission of rotational symmetry.

---

Final expanded version to be published in the Nuclear Instr. and Methods.



## Radioisotope Neutron Sources

Glenn F. Knoll  
The University of Michigan  
Ann Arbor, Michigan USA

Sources of neutrons that are based on the decay of radioactive nuclides date back to the very discovery of the neutron. Their simplicity, small size, and predictable yield offer substantial advantage in many applications. Most, however, are limited to relatively low neutron yield. They also are characterized by a fixed neutron energy spectrum that often is broadly distributed. Despite these shortcomings, radioactive neutron sources continue to find many applications in various aspects of neutron physics.

There are three main categories of such sources. Radioactive ( $\alpha, n$ ) sources are based on a combination of an alpha emitting isotope with a suitable target material. Beryllium is by far the most common choice for target, and results in the largest neutron yield per alpha particle. Other useful targets include boron, fluorine, lithium, and separated C-13. Common alpha particles sources are Pu-239, Po-210, Pu-238, Am-241, Cm-242, Cm-244, and Ra-226.

Neutrons can also be produced by the photonuclear reaction using radioactive isotopes as a source of gamma rays. Only two target materials are of any consequence: beryllium and deuterium. Gamma ray sources must have at least one photon line above the respective photonuclear disintegration energies of 1.666 and 2.226 MeV. Common sources are Na-24, Ga-72, La-140, and Sb-124. Photon-neutron sources are characterized by nearly monoenergetic neutron yields. However, a very large gamma ray background is always present with these neutrons and can hamper their use in many applications.

The third general category of radioisotope neutron sources are those based on spontaneous fission. There is only one nuclide of any practical consequence: Cf-252. Its half-life of 2.65 years, combined with a nu-bar value of 3.75, yields  $2.3 \times 10^6$  neutrons per second per microgram of the isotope. These neutrons are broadly distributed across a Maxwellian-shaped fission spectrum.

---

The revised version of the contributed paper is to be published as part of the "Neutron Physics and Nuclear Data in Science and Technology" (NEANDC monograph series) by Pergamon Press.

Radioactive Neutron Source Measurements at the  
National Physical Laboratory, England

A. G. Bardell

National Physical Laboratory  
Div. of Radiation Science and Acoustics  
Teddington, Middlesex, TW11 LOW, United Kingdom

A description of the methods used at the National Physical Laboratory England for the absolute measurement of the emission rate of radioactive neutron sources is presented. The detection of significant amounts of impurity in the manganese sulphate solution and the availability of improved methods of data analysis has led to a re-evaluation of the national standard source emission rate and a new value for the ratio of the hydrogen to manganese thermal neutron capture cross section. The previously used manganese sulphate has been replaced with a purer grade containing a low impurity level and work is proceeding to verify the re-evaluation. The desirable properties of neutron sources for use as standard or reference sources are briefly described.

Properties and Applications of  
Radioactive Photoneutron Sources

Friedrich Bensch

Atominstitut der Österreichischen Universitäten  
Schüttelstraße 115, A-1020 Vienna, Austria

Some spherical photoneutron sources have been investigated in the "Atominstitut der Österreichischen Universitäten" ( $^{124}\text{Sb}-\text{Be}$ ,  $^{72}\text{Ga}-\text{Be}$ ,  $^{72}\text{Ga}-\text{D}_2\text{O}$ ,  $^{228}\text{Th}-\text{Be}$ ,  $^{228}\text{Th}-\text{D}_2\text{O}$ ,  $^{24}\text{Na}-\text{Be}$ ,  $^{24}\text{Na}-\text{D}_2\text{O}$ ,  $^{140}\text{La}-\text{Be}$ ,  $^{116}\text{In}-\text{Be}$ ,  $^{56}\text{Mn}-\text{Be}$ ) by experiments ( $\text{MnSO}_4$ -bath for source strength determination, proton-recoil proportional counter tubes for the measurement of the neutron distribution) and/or by Monte-Carlo calculations to find data on intensity and emission spectra of the sources. Preliminary results are presented.

---

The full report is available as Atominstitut Report AIAU 80202 (Feb. 1980)

Absolute calibration of  $^{252}\text{Cf}$  sources and effective  
half-life

W.G. Alberts, W. Mannhart, M. Matzke

Physikalisch-Technische Bundesanstalt, Braunschweig

Strong californium sources are used at the PTB to provide neutron reference radiations for the measurement of spectrum-averaged cross sections and for the calibration of neutron detectors. The neutron source strength is determined by means of gold-foil activation in a water bath.

The reproducibility of this method is demonstrated by comparing a series of six absolute calibrations during a period of almost seven years (i.e. 2.5 half-lives). From such a comparison an effective half-life for Cf-252 can be extracted with a relative standard deviation of the mean from the least squares evaluation method. A preliminary value of  $(2.650 \pm 0.002)$  years was derived.

Measurement of the Neutron Activity of a  $^{252}\text{Cf}$  Source Relative to  $\bar{\nu}_p$   
for the Spontaneous Fission

J. Frehaut, M. Beau

Service de Physique Neutronique et Nucléaire

Centre d'Etudes de Bruyères-le-Châtel

B.P. No. 561

92542 Montrouge Cédex, France

We have developed a method for measuring the absolute neutron activity of a large  $^{252}\text{Cf}$  source. The neutron counting assembly is composed of eight  $\text{BF}_3$  counters mounted in a large tank filled with water which is used as a moderator. The detection efficiency is determined using a low activity  $^{252}\text{Cf}$  source. The method is based on the identification of every fission event, followed by the counting of the fission neutrons detected by the  $\text{BF}_3$  counters during a time interval equal to the maximum neutron lifetime in the moderator. The efficiency is thus obtained relative to the average number of prompt neutrons emitted per  $^{252}\text{Cf}$  spontaneous fission which is commonly used as a standard. The measurement accuracy is estimated to be of the order of 1%.

$^{235}\text{U}$  Cavity Fission Neutron Field Calibration via the  
 $^{252}\text{Cf}$  Spontaneous Fission Neutron Field

V. Spiegel, C. M. Eisenhauer, D. M. Gilliam, J. A. Grundl  
E. D. McGarry, I. G. Schröder, W. E. Slater, and R. S. Schwartz  
National Bureau of Standards  
Washington, D. C. 20234

The NBS-I primary standard neutron source has been recalibrated against  $\bar{v}$  of  $3.766 \pm 0.008$  for  $^{252}\text{Cf}$ . The emission rate was determined to be  $1.245 \times 10^6 \pm 0.8\%$  as of September 1978, which is within 0.25% of that expected from the calibration of June 1961. This source is the neutron flux measurement base for the  $^{252}\text{Cf}$  irradiation facilities at the National Bureau of Standards. The method of flux transfer from the  $^{252}\text{Cf}$  neutron field is used to determine the flux in many of our other neutron fields. A brief description is given of this latest calibration of NBS-I, the relative calibration of our intense  $^{252}\text{Cf}$  sources to NBS-I in the manganous sulfate bath, and the fluence transfer method from the  $^{252}\text{Cf}$  field to the  $^{235}\text{U}$  cavity fission neutron field. An appendix gives a brief description of neutron sources and fields at the NBS with some of their applications.

The Fast Neutron Emission Spectrum of  $^{252}\text{Cf}$

Friedrich Bensch and Hans Jasicek

Atominstitut der Österreichischen Universitäten  
Schüttelstraße 115, A-1020 Vienna, Austria

The fast neutron emission spectrum of  $^{252}\text{Cf}$  has been investigated by means of two proton-recoil spectrometers. By means of a large counter tube of 900 mm length the neutron distribution between 0.9 MeV and 10 MeV was determined. Monte-Carlo calculated response functions were applied to unfold the measured proton-recoil distributions. Using a smaller, 466 mm long counter tube the energy interval between 1 MeV and 3 MeV was examined in a search for neutron fine-structure groups. No such groups could be established. The numerical results are presented in a preliminary form.

---

This work has been performed under the IAEA Research Contract No. 1909/RI/RB. The preliminary report is available as both Atominstitut Report AIAU 80201 and INDC(AUS)-4.

Final results have been submitted for publication to "The Journal of Nuclear Science and Engineering".

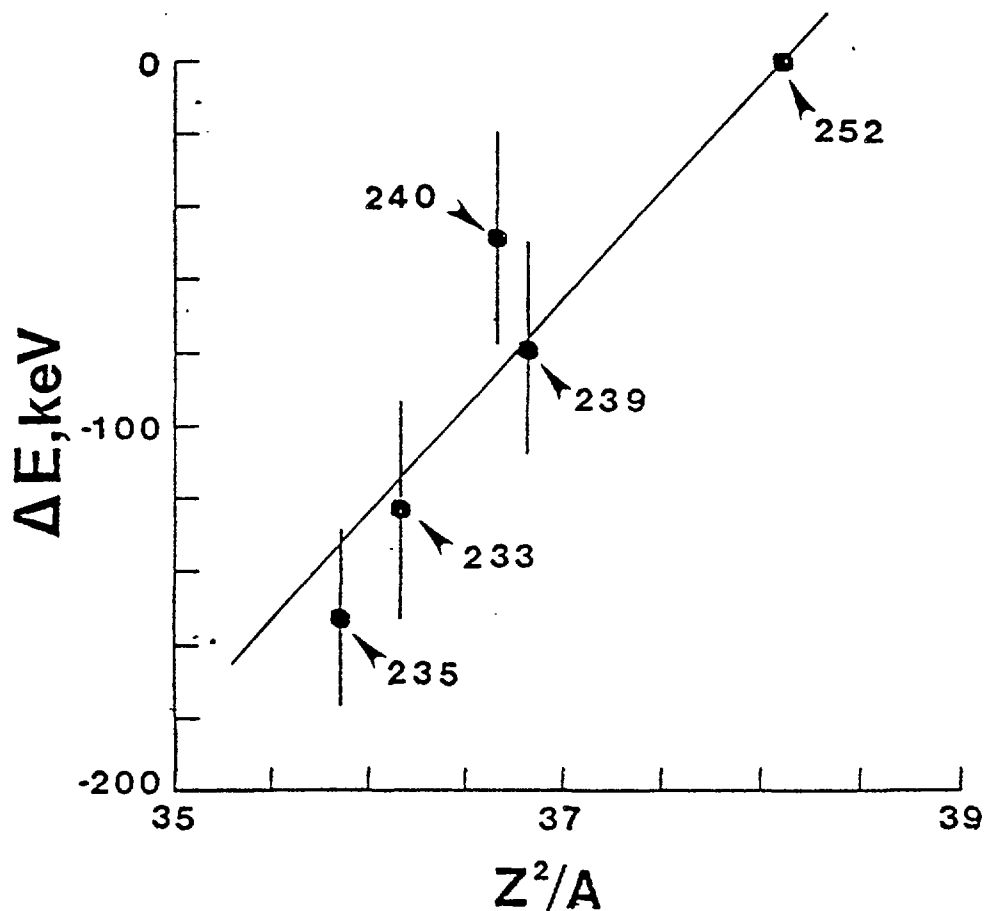
NOTE ON THE PROMPT-FISSION-NEUTRON SPECTRA OF  $^{233}\text{U}$ ,  $^{235}\text{U}$ ,  $^{239}\text{Pu}$   
AND  $^{240}\text{Pu}$  RELATIVE TO THAT OF  $^{252}\text{Cf}$ \*

A. Smith, P. Guenther, G. Winkler<sup>†</sup> and R. McKnight

Applied Physics Division  
Argonne National Laboratory  
Argonne, Illinois 60439 U.S.A.

ABSTRACT

The prompt-neutron-induced-fission spectra of  $^{233}\text{U}$ ,  $^{235}\text{U}$ ,  $^{239}\text{Pu}$  and  $^{240}\text{Pu}$  are measured relative to the prompt-spontaneous-fission-neutron spectrum of  $^{252}\text{Cf}$ . Analysis of the measured values indicates that the average-fission-neutron energies are  $-123 \pm 30$  ( $^{233}\text{U}$ ),  $-157 \pm 24$  ( $^{235}\text{U}$ ),  $-76 \pm 29$  ( $^{239}\text{Pu}$ ) and  $-46 \pm 29$  ( $^{240}\text{Pu}$ ) keV relative to that of  $^{252}\text{Cf}$ . These relative values are indicated in the following figure.



\*This work supported by the U.S. Department of Energy.

<sup>†</sup>Permanent address: Institut fuer Radiumforschung und Kernphysik, Vienna.



## A Radioactive Neutron Source with an Effective Energy of 500 eV

J. R. Harvey and A. J. Mill

Central Electricity Generating Board,  
Berkeley Nuclear Laboratories,  
Berkeley, Glos., GL13 9PB EnglandAbstract

There are many areas in working environments around reactors and other neutron generating locations where the neutron dose-rate is important and furthermore, surveys have shown that a significant fraction of the neutron dose-equivalent rate is often in the intermediate energy range from 0.5 eV to 500 keV. However, surprisingly little is known about the response of health physics instruments in this range or about the ways in which these neutrons affect biological systems.

In order to provide some information on the response of instruments at intermediate energies a simple and inexpensive system for producing neutrons around 0.5 keV has been developed. In such a source, to be used for health physics instrument calibrations, it is essential to keep high energy neutrons to a minimum: this is because the dose-equivalent per unit neutron fluence for neutrons above  $\sim 1$  MeV is  $\sim 30$  times that for neutrons below  $\sim 10$  keV. Hence an intermediate energy neutron source based on americium-beryllium, for example, is no good for this purpose.

The 0.5 keV neutron source consists of an antimony-beryllium ( $\gamma, n$ ) source surrounded by a sphere of water contained in a boron-carbide loaded plastic shell. The original energy of the neutrons from the antimony-beryllium source is 23 keV. This system has been used to calibrate several instruments and several of these have been shown to be oversensitive by a factor of three at this energy.

The source has considerable scope for development. For example, a build-in shield would reduce the accompanying gamma dose-rate, and a polythene moderator would be handier and more hydrogenous than water.

References

- J. R. Harvey and S. Beynon. In: Proceedings of the First Symposium on Neutron Dosimetry in Biology and Medicine. Munich 1972. EUR-4896 d-f-e.  
J. R. Harvey and R. C. Bending. Physics in Medicine and Biology, 21, 85, 1976.  
J. R. Harvey, et al. Health Physics, 31, 363, 1976.  
K. G. Harrison, et al. Nuclear Instruments and Methods, 148, 511, 1978.

---

\*) Contributed Paper but not presented

The Measurement of the Average Number of Prompt Neutrons and the  
Distribution of Prompt Neutron Numbers for  $^{252}\text{Cf}$  Spontaneous Fission

Zhang Huan-Qiao     Liu Zu-Hua

Institute of Atomic Energy, Academia Sinica, Beijing (Peking)

The average number of prompt neutrons  $\bar{\nu}_p$  and the distribution of prompt neutron numbers  $P_\nu$  for the spontaneous fission of  $^{252}\text{Cf}$  have been measured absolutely by use of a spherical gadolinium-loaded liquid scintillation counter. The efficiency curve of neutron detection in liquid scintillation counter was calibrated on the basis of occurring (n,p) scattering as the collimated monochromatic fast neutron beam bombarded on the stilbene crystal. The fission events have been detected by use of current pulse ionization chamber. Finally, it has been obtained that the average number of prompt neutrons for spontaneous fission of  $^{252}\text{Cf}$ ,  $\bar{\nu}_p = 3.743 \pm 0.018$ .

---

The full paper (in Chinese) was published in the Chinese Journal of Nuclear Physics Vol. 1, No. 1 (1979) 9. The English translation (translated by the authors) can be obtained from the IAEA Nuclear Data Section.

\*) Contributed paper but not presented

Measurement of Prompt Neutron Energy Spectrum  
for Spontaneous Fission of  $^{252}\text{Cf}$  +)

Mon Jiang-shen, Bai Xi-xiang, Zhang Bai-shen, Hwang Sheng-nian  
Institute of Atomic Energy, Academia Sinica, Beijing (Peking)

Energy spectrum of prompt neutrons from  $^{252}\text{Cf}$  spontaneous fission was measured for energy range 0.3 - 15 MeV using the time-of-flight technique. O-time signal was obtained from fission fragment; Neutron timing signal was obtained from a fast response neutron detector. The data was fitted to a Maxwellian distribution and the preliminary result of  $E = 2.12 \text{ MeV}$  ( $T = 1.413 \text{ MeV}$ ) was obtained.

---

\*) Contributed paper but not presented

+) to be published

The Current Status of Accelerator Produced Neutron Fluence Standards  
at the National Physical Laboratory, England

A. G. Bardell

National Physical Laboratory  
Div. of Radiation Science and Acoustics  
Teddington, Middlesex, TW11 OLW, United Kingdom

The accelerator produced fast and thermal neutron fluence standards available at the National Physical Laboratory, England are described together with details of some recent developments and an outline of the current program of measurements.

NEUTRON YIELDS FROM PROTON, DEUTERON AND ALPHA BOMBARDMENT OF  
BERYLLIUM

M.A. Lone

Atomic Energy of Canada Limited, Chalk River Nuclear Labora-  
tories, Chalk River, Ontario, Canada K0J 1J0

and

B.C. Robertson

Queen's University, Kingston, Ontario, Canada

Abstract

For cancer therapy neutrons produced by the bombardment of Be with deuterons or protons have been commonly used. A comparative study of these neutron source reactions is useful for determining the most cost-effective means of producing neutrons for radiotherapy. In the present paper we give yields, average energies, and spectral distributions of neutrons from bombardment of Be targets of various thicknesses with protons and deuterons at energies below 50 MeV and alphas at energies below 30 MeV. Characteristics of neutrons from bombardment of Li targets with protons are also discussed. The minimum projectile energy and current needed to satisfy the requirements of neutron sources for cancer therapy are determined.

Flux density measurements in the FMRB filtered neutron beams

W.G. Alberts, K. Knauf, H. Lesiecki

Physikalisch-Technische Bundesanstalt, Braunschweig

At the research and measuring reactor of the PTB two neutron filtered beam facilities have been installed for 24 keV (iron/aluminium) and 2 keV (scandium) neutrons with the aim of getting reference neutron fields for the investigation and calibration of neutron detectors, especially neutron dosimeters used in radiation protection.

Neutron flux density in the filtered beams is measured using several proton recoil proportional counters of both cylindrical and spherical form.  $\gamma$ -ray pulse-shape discrimination systems are applied. Neutron flux densities are derived from the pulse-height spectra for the nominal energies as well as for the high-energy neutrons in the beams.

Examples of Theoretical and Experimental Determinations of  
Neutron Yield From ( $\alpha$ ,n) Reactions in the Light Elements

A. Capgras

Laboratoire de Métrologie des Rayonnements Ionisants  
Centre d'Etudes Nucléaires de Saclay  
91190 - Gif sur Yvette - France

In fuel reprocessing solutions, primary neutrons are to a large extent issued from ( $\alpha$ ,n) reactions on the light nuclei of the organic and aqueous mediums.

In the present work, determinations of ( $\alpha$ ,n) reaction yields in solid phase for oxygen, fluorine, beryllium, carbon 13, in liquid phase for oxygen, are achieved. The theoretical yields are calculated with stopping powers and cross sections data from literature and with the assumption of an homogeneous medium.

For experimental determinations manganese bath neutron emission and calorimetric  $\alpha$  emission measurements are made.

Both results are in good agreement when the composition is well known, i.e.  $\text{Am}^{13}\text{C}$  or solution of americium.

An important difference between theory and experiment for  $\text{Am,F}$  source is explained by the lack of knowledge of the granulometry and by composition and cross section data uncertainties.

Few comparisons with other results of literature have been possible to do on account of experimental conditions either different or unknown. Nevertheless a fair agreement has been showed for ( $\alpha$ ,n) neutron yield in oxygen.

---

To be published as Note CEA-N series

\*) Contributed paper but not presented

PRODUCTION OF MONOENERGETIC NEUTRONS  
WITH ENERGIES BETWEEN A FEW HUNDRED KeV AND 40 MeV

G. HAOUAT and M. CANCE

Service de Physique Neutronique et Nucléaire

C.E de Bruyères-Le-Châtel

B.P n° 561

92542 MONTROUGE Cédex FRANCE

ABSTRACT

*Cross section data for neutron-induced reactions are requested in a wide energy range mainly for fission and fusion reactor developments and for medical applications.*

*We review here various modes of production of monoenergetic neutrons for performing cross section measurements in the energy range from a few hundred KeV to 40 MeV.*

*The required characteristics for the neutron sources, the source reactions which can be utilized and some target designs are presented.*



Neutron Production in the Energy Range 7 to 12 MeV  
using a Gas-Target \*)

S. Mittag, W. Pilz, D. Schmidt, D. Seeliger and T. Streil  
Technical University Dresden, German Democratic Republic

A gas-target for operation at a tandem-accelerator is described. Using the DD-reaction, an energy range of neutrons between 7 and 12 MeV can be realised. Construction and operation are described in detail. For neutron energies below 9 MeV the neutron source is almost mono-energetic; above this energy the deuteron break-up limits the mono-energetic behaviour.

---

The full paper has been published as INDC(GDR)-11/L+ Special (May 1980).

\*) Presented by H. Helfer

# Limitations in the Use of Deuterium Gas Targets<sup>+</sup>

H. Klein, H.J. Brede

Physikalisch-Technische Bundesanstalt, D-3300 Braunschweig  
Fed. Rep. Germany

Deuterium gas targets are often used to produce 'monoenergetic' neutrons in the energy range from 5 MeV to 15 MeV via the reaction  $D(d,n)^3\text{He}$ . Even if the setup of the gas targets is optimized with respect to the entrance foil as well as the beam stop material and thickness, the applicability of this neutron source is limited:

- (1) The energy resolution is mainly determined by the energy loss within the gas. The straggling due to the energy loss in the entrance foil, the nonuniformity of the foil and the properties of the incoming beam have to be considered.
- (2) The angular spread is caused by the multiple scattering in the entrance foil. In addition the beam divergence and the detector geometry have to be included in estimating the angular resolution.
- (3) Besides the main neutron energy undesired background neutrons are produced in the entrance foil and the beam stop. These contributions can be determined by 'gas out' runs, if the production of neutrons due to deuterium-selftarget buildup in the backing is avoided. Finally the rapidly increasing amount of neutrons from deuterium breakup reactions limits the use of this neutron source in scattering experiments.

<sup>+</sup>to be published

to be submitted to the Nuclear Instr. and Methods

Multipurpose Intense 14 MeV Neutron Source at Bratislava:

Design Concept

J. Pivarč, S. Hlaváč, J. Král, P. Obložinský, I. Ribanský and I. Turzo  
Institute of Physics, Slovak Academy of Sciences  
899 30 Bratislava, Czechoslovakia

and

H. Helfer  
Technical University, 8027 Dresden, German Democratic Republic

The present state of design of the multipurpose intense 14 MeV neutron source based on a  $D^+$  ion beam and a metal tritide target is reported. It is essentially a 300 keV electrostatic air insulated accelerator capable to accelerate a deuterium ion beam up to 10 mA. With such a beam and a beam spot of  $1 \text{ cm}^2$ , a neutron yield typically  $10^{12} \text{ n/s}$  and a useful target lifetime of around 10 h are expected. Various users requirements are met by means of three beam lines: an intense, low current dc and a low current fast pulsed.

The key components of the intense source section are the rotating target and the ion source. The rotating target is proposed, with respect of the heat dissipation and the removal of  $3 \text{ kW/cm}^2$ , in continuous operation. A rotation speed up to 1100 rpm is considered. The ion source should deliver about 0.5 kW of extracted  $D^+$  ion beam power. A duoplasmatron source with an electrostatic beam focusing system has been selected.

Low current sections of the neutron source may operate with a high frequency ion source as well. The dc section for maximum yields around  $10^{10} \text{ n/s}$  is designed with special regard to beam monitoring. The fast pulsed section should produce up to 1 ns compressible pulsed  $D^+$  ion beam on a target spot with 5 MHz repetition rate.

The report includes information about other components of the neutron source as a high voltage power supply, a vacuum system, beam transport, a diagnostic and control system and basic information about neutron source cells and radiation protection.

Monoenergetic neutron sources in the energy range  
from 10 keV to 20 MeV for dosimetry experiments

M. Cosack, S. Guldbakke<sup>+</sup>

Physikalisch-Technische Bundesanstalt, D-3300 Braunschweig  
Fed. Rep. Germany

The response of radiation protection detectors is investigated at the PTB ion accelerators for neutron energies from 10 keV to 20 MeV. 'Monoenergetic' neutrons are produced by means of the reactions  $\text{Sc}(p,n)$ ;  $\text{Li}(p,n)$ ;  $\text{T}(p,n)$ ;  $\text{D}(d,n)$  and  $\text{T}(d,n)$  using a 3.75 MV v.d. Graaff accelerator. The background of photons or undesired neutrons produced in the target backings had to be minimized.

The following details are discussed:

- a.) The preparation and handling of the targets (Sc, Li) as well as the longtime stability of the neutron yield ( $\text{Ti}(D)$ ,  $\text{Ti}(T)$ ).
- b.) The photon spectra produced by bombarding different backings (Ag, Al, Cu, Ta, W) with protons and deuterons.
- c.) The contamination of the neutron fields by spurious neutrons from D-selftarget buildup within cooled Ag-backings.

<sup>+</sup>presented by H. Klein

Neutron Sources for the Medical Use.

K. Tsukada

Atomic Energy Research Institute

Nihon University

1-6-14, Kanda-Surugadai, Chiyoda-ku

Tokyo, Japan

Recently encouraging results of the neutron radiation therapy have been obtained in clinical trials. In addition to the therapy, the neutrons are applied to the diagnosis besides the production of radioisotopes, that is, in-vivo activation analysis and neutron radiograph.

In the medicine, high energy neutrons are effectively used. The necessary conditions, especially neutron source reactions, angular distributions, etc., and the neutron dosimetry including neutron kerma factors are discussed.

Finally the requirements for neutron sources, their related problems and nuclear data are enumerated.

---

The full paper has been published as INDC(JAP)-45/L+ Special, May 1980

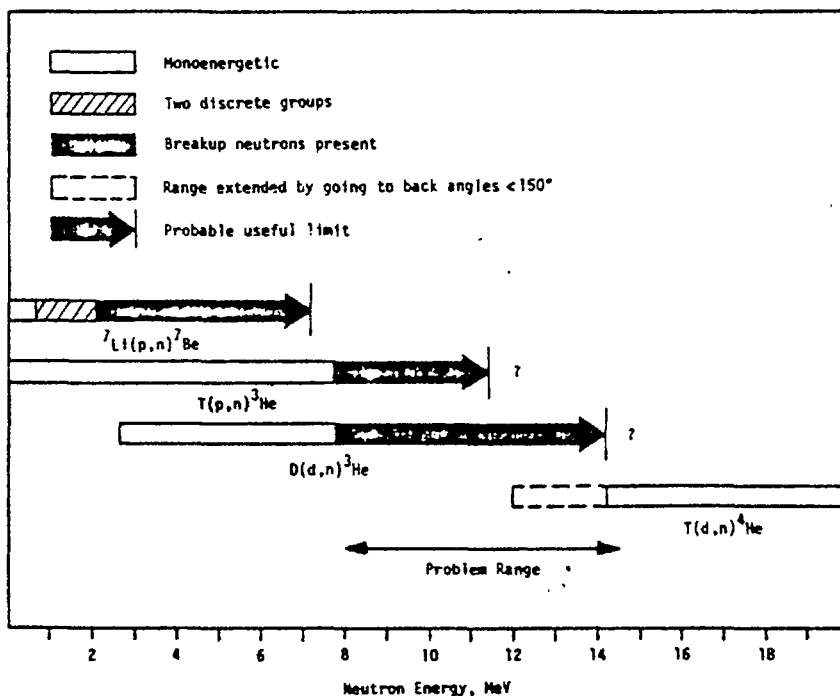
NEUTRON SOURCE INVESTIGATIONS IN SUPPORT OF THE  
CROSS SECTION PROGRAM AT THE ARGONNE FAST-NEUTRON GENERATOR\*

James W. Meadows and Donald L. Smith +)

Applied Physics Division  
Argonne National Laboratory  
Argonne, Illinois 60439 U.S.A.

ABSTRACT

Experimental methods related to the production of neutrons for cross section studies at the Argonne Fast-Neutron Generator are reviewed with emphasis on the  ${}^7\text{Li}(p,n){}^7\text{Be}$ ,  $\text{T}(p,n){}^3\text{He}$ ,  $\text{D}(d,n){}^3\text{He}$  and  $\text{T}(d,n){}^4\text{He}$  reactions. Ranges of applicability are indicated in the figure.



Target assemblies commonly employed in these measurements are described, and some of the relevant physical properties of the neutron source reactions are discussed. Various measurements have been performed to ascertain knowledge about these source reactions which is required for cross section data analysis purposes. Some results from these studies are presented and a few specific examples of neutron-source related corrections to cross section data are provided.

\*This work has been supported by the U.S. Department of Energy.

+ ) presented by A. B. Smith

The full paper will be issued as Argonne National Laboratory Report, ANL/NDM-53

Limits of Application of the Method of Recoil Protons  
in Neutron Spectrometry Using a NE 213 Organic Scintillator

A. Capgras

Laboratoire de Métrologie des Rayonnements Ionisants  
Centre d'Etudes Nucléaires de Saclay  
91190 - Gif sur Yvette - France

In part one, the difficulties which have occurred in achieving an experimental matrix used in neutron spectrometry are described. Unaccuracy depends mainly of:

- . Uncertainty of the flux density given by the reference detector
- . Uncertainty of the calibration by gamma sources

Moreover the number of monoenergetic neutron lines investigated being limited, interpolation between them has to be achieved to get the response function. The great sensibility of the method to the accuracy of the neutron-electron equivalent light-yield has been demonstrated with two examples.

The experimental efficiencies have been compared to theoretical values calculated with Monte Carlo O5S code. Agreement is not very good, specially for energies of maxima of carbon scattering cross section curve. A better one is obtained when this cross section is averaged over energy intervals of 0.2 MeV.

In the second part the LMRI matrix obtained is introduced in FERDO code and used for deconvolution of protons vectors get with AmBe and  $^{252}\text{Cf}$  sources, and with a 14 MeV generator.

In conclusion is pointed out that the quality of the results for this method depends of the four parameters:

- accuracy of the electron-proton relationship
- accuracy of the efficiency
- position of the lower threshold
- spread of the spectrum

Recommendations are made for achieving an experimental matrix and suggestion is set for the use of smaller detectors in all cases of less than 15 MeV neutrons measurements.

---

To be published as Note CEA-N series

\*) Contributed paper but not presented

Performance of Gas TargetUsing D(d,n) Reaction as a Fast Neutron Source

Lian Tun-chi, Ye Jine-ping, Sa Dren

Institute of Atomic Energy, Academia Sinica, Beijing (Peking)

A gas target using the  $D(d,n)^3\text{He}$  reaction as a pulsing fast neutron source in the Isochronous Cyclotron is described. The characteristics of this neutron source are the high yield of neutron ( $10^8 - 10^9$  n/sec), wide energy range, and the small stray neutron background. It was designed for the studies of neutron scattering, neutron-induced charged particle reactions, and direct neutron-capture reactions. The target cell is a Pt-lined stainless-steel cylinder ( $\phi$  2- x 3- x .03 cm), isolated from the vacuum system by a 5  $\mu\text{m}$  thick Mo foil, and filled to a pressure of 3 atm deuterium. In the target cell system, a culdesac tube filled with activated charcoal as a trap of high purity deuterium was incorporated. Low background neutron time-of-flight (TOF) spectrum of D(d,n) reaction and the TOF spectrum of neutron scattered from  $^{12}\text{C}$  at  $30^\circ$  with deuteron energy 9 MeV are presented.

---

\*) Contributed paper but not presented

To be published





## *Appendices*



The following papers were circulated at the Meeting  
during the Working Group sessions

MEASUREMENTS AND CALCULATIONS OF NEUTRON SPECTRA FROM 35 MeV DEUTERONS ON THICK LITHIUM FOR THE FMIT FACILITY

D. L. JOHNSON and F. M. MANN

Hanford Engineering Development Laboratory\*, Richland, Washington, 99352 USA

J. W. WATSON<sup>†</sup>, J. ULLMANN and W. G. WYCKOFF

University of California at Davis, Davis, California, 95616 USA

Neutron yields and energy spectra were measured for 35 MeV deuterons on a thick target of natural lithium. Data were obtained using the time-of-flight technique over an angular range of 0° to 150° and for neutron energies from about 1 to 50 MeV. A simple nuclear model that describes the differential cross sections of neutron production was adjusted to agree with these new thick target data. Different model parameters were obtained when the model was adjusted to agree with previous ORNL thick target data for 40 MeV deuterons. Our experimental data are in good agreement with model predictions based upon the ORNL time-of-flight data but are somewhat lower than predictions based upon the ORNL dosimetry data. Finally the model was used to predict the neutron spectrum at the position of highest flux in the FMIT test cell.

- 0-1 Presented at the first topical meeting on Fusion Reactor Materials Jan. 1979, Miami Beach, Florida, USA. The full paper is available as Journal Nuclear Materials 85+86 (1979) 467-471.

MEASUREMENTS OF NEUTRON SPECTRA FROM 35 MeV DEUTERONS  
ON THICK LITHIUM FOR THE FMIT FACILITY

D. L. Johnson and F. M. Mann  
Hanford Engineering Development Laboratory\*  
Richland, Washington 99352. U.S.A.

J. W. Watson,† J. Ullmann and W. G. Wyckoff  
University of California at Davis  
Davis, California 95616. U.S.A.

Neutron yield spectra were measured for 35 MeV deuterons on thick natural lithium. The time of flight technique was used and data were obtained for laboratory emission angles of 0° to 150°. The yield of neutrons greater than 1 MeV was determined at each angle and was integrated to find the total yield.

- 0-2 To be published in the proceedings of the International Conference on Nuclear Cross Sections for Technology, Oct. 22-26 1979, Knoxville, Tennessee, USA. This is an updated version of 0-1.

RADIOACTIVE NEUTRON SOURCE SPECTRA FROM <sup>9</sup>Be(α,n) CROSS SECTION DATA

K. W. GEIGER and L. VAN DER ZWAN

*Division of Physics, National Research Council of Canada, Ottawa, Ontario, Canada*

Cross sections and angular distributions for the <sup>9</sup>Be(α,n)<sup>12</sup>C reaction were evaluated from the existing literature. These cross sections as well as the published neutron spectra from the Be+α break-up reaction were used to calculate the neutron yield and the spectra emitted by radioactive Be(α,n) sources. Seven

different source types containing <sup>239</sup>Pu, <sup>210</sup>Po, <sup>241</sup>Am, <sup>244</sup>Cm, <sup>242</sup>Cm, <sup>226</sup>Ra or <sup>227</sup>Ac as α-emitters were considered. The predicted spectra should aid in clarifying the differences which are found between the many published experimental spectra.

- 0-3 Appeared in the Nuclear Instruments and Methods 131 (1975) 315.

Résumé on neutron yields from α-particle bombardment of light elements

K.W. Geiger, Division of Physics, National Research Council, Ottawa,  
Canada K1A 0R6

1. Introduction

The thick target neutron yield which results from α-particle bombardment of light elements is important for environmental considerations in the spent fuel technology. The yield can also serve as an additional parameter in chemical analysis. Actinide α-emitters are produced by successive neutron capture when burning the fuel in a reactor. Inevitably these α-emitters come into contact with light elements, either by chemical processing or because the fuel itself has a light element component when, for instance, it consists of UO<sub>2</sub> or UC. The spent fuel will, in addition to spontaneous fission neutrons, exhibit neutron emission through (α,n) reactions. To evaluate such complex actinide plus light element system one needs to know the thick target (α,n) yields as a function of incident α-energy.



List of Participants

Alberts, W.G.	Physikalisch Technische Bundesanstalt Abteilung 6, Bundesallee 100 D-3300 Braunschweig, Fed. Rep. of Germany
Andersson, P.	Lunds Universitet Fysiska Institutionen Sölvegatan S-223 62 Lund, Sweden
Bardell, A.G.	National Physical Laboratory Div. Radiation Science and Acoustics Teddington, Middlesex, TW11 0LW United Kingdom
Bensch, F.	Atominstitut der Österreichischen Universitäten Schüttelstrasse 115 A-1020 Wien, Austria
Blinov, M. V.	Radiemij Institut V.G. Khlopina Ul. Rentgena 1 Leningrad, P-22, U.S.S.R.
Bowman, C. D.	National Bureau of Standards Center for Radiation Research Nuclear Radiation Division Washington, D.C. 20234, U.S.A.
Cierjacks, S.	Institut für Kernphysik Kernforschungszentrum Karlsruhe Postfach 3640 D-7500 Karlsruhe, Fed. Rep. of Germany
Csikai, J. (Local Secretary)	Institute of Experimental Physics Kossuth Lajos University P.O. Box 105 H-4001 Debrecen, Hungary
Dezsoe, Z.	Institute of Experimental Physics Kossuth Lajos University P.O. Box 105 H-4001 Debrecen, Hungary

- Drosg, M.                    Institut für Experimentalphysik  
                             Universität Wien  
                             Strudlhofgasse 4  
                             A-1090 Wien, Austria
- Fréhaut, J.                Centre d'Etudes Nucléaires de  
                             Bruyères-le-Châtel  
                             B.P. No. 561  
                             F-92542 Montrouge Cédex, France
- Geiger, K.W.              National Research Council  
                             Division of Physics  
                             Ottawa, Ontario K1A 0R6, Canada
- Haouat, G.                Centre d'Etudes Nucléaires de  
                             Bruyères-le-Châtel  
                             B.P. No. 561  
                             F-92542 Montrouge Cédex, France
- Helfer, H.                Technische Universität Dresden  
                             Sektion Physik  
                             Mommsenstrasse 13  
                             DDR-8027 Dresden  
                             German Democratic Republic
- Klein, H.                Physikalisch Technische Bundesanstalt  
                             Abteilung 6, Bundesallee 100  
                             D-3300 Braunschweig, Fed. Rep. of Germany
- Knoll, G.F.              The University of Michigan  
                             Department of Nuclear Engineering  
                             Cooley Building, North Campus  
                             Ann Arbor, Michigan 48109, U.S.A.
- Kwiecinski, S.            Institute of Nuclear Physics and Techniques  
                             The University of Mining and Metallurgy  
                             Ul. Radzikowskiego 152  
                             PL-31-342 Krakow, Poland
- Lone, A.M.                Atomic Energy of Canada Limited  
                             Neutron and Solid State Physics Branch  
                             Chalk River, Ontario K0J 1J0, Canada
- Mill, A.                Central Electricity Generating Board  
                             Berkeley Nuclear Laboratory  
                             Berkeley, Gloucestershire GL13 9PB  
                             United Kingdom

K. Okamoto (Scientific Secretary)	Nuclear Data Section International Atomic Energy Agency P.O. Box 100 A-1400 Vienna, Austria
Pivarč, J.	Institute of Physics of SAS Dúbravská cesta CS-699 36 Bratislava, Czechoslovakia
Seeliger, D.	Technische Universität Dresden Sektion Physik Mommsenstrasse 13 DDR-8027 Dresden German Democratic Republic
Schmidt, J.J.	Nuclear Data Section International Atomic Energy Agency P.O. Box 100 A-1400 Vienna, Austria
Smith, A.B. (Chairman)	Argonne National Laboratory 9700 South Cass Avenue Argonne, Illinois 60439, U.S.A.
Spiegel, V.	National Bureau of Standards Neutron Field Standards Nuclear Radiation Division Washington, D.C. 20234, U.S.A.
Tsukada, K.	Atomic Energy Research Institute Nihon University Kanda-Surugadai, Chiyoda-ku Tokyo-101, Japan
Turkiewicz, J.	Instytut Badaw Jadrowych Hoza 69 PL-00-681 Warsaw, Poland



Observers

- |      |                                                                                                              |                                                                                                                    |
|------|--------------------------------------------------------------------------------------------------------------|--------------------------------------------------------------------------------------------------------------------|
| I.   | Berenyi, D.<br>Bornemissza-Pauspertl, P.<br>Medveczky, L.<br>Török, I.<br>Uray, I.                           | ATOMKI (Institute of Nuclear<br>Research of the Hungarian Academy<br>of Sciences<br>P.O. Box 51<br>H-4001 Debrecen |
| II.  | Angeli, I.<br>Daróczy, S.<br>Juhász, S.<br>Nagy, S.<br>Pető, G.<br>Raics, P.<br>Sudár, S.<br>Sztaricskai, T. | Institute of Experimental Physics<br>Kossuth Lajos University<br>P.O. Box 105<br>H-4001 Debrecen                   |
| III. | Csuth, S.<br>Pongrácz, Cs.                                                                                   | Eötvös Lorand University<br>Fuskin Utca 5-7<br>H-1088 Budapest                                                     |